Sudan University of Science and Technology
College of graduate studies

Ultrasound Findings of Livers with Abnormal Function

نتائج فحص الموجات فوق الصوتية للكبد ذات الخلل الوظيفى

A thesis submitted in partial fulfillment for the requirements of M.Sc Degree in Medical Diagnostic Ultrasound

By

Mazza Isameldeen Eltyb Mahran

Supervisor

Associate Prof, Dr. Mohamed Elfadil Mohamed

2013

الآيـة

قال تعالى :

أقرأ وربك الأكرم الذي علم بالقلم علم الإنسان ما لم يعلم)

صدق الله العظيم

Dedication

I dedicate this work to **the soul of my father, my mother, my**

sisters, my brothers, my teachers and my friends.

Always you are sitting in mine and encouraging me to do the best in my life.

Best regards for all.

Acknowledgment

I thank God for enabling me to complete this thesis. I sincerely thank Dr. Mohammed Elfadil, the supervisor of my thesis for his continuous help, supervision and guidance.

I greatly thank all those who supported and helped me to complete this thesis. I am very grateful to all my teachers in all educational levels.
Very much thanks to the staff of military Hospital, especially the staff of X. Ray and Ultrasound Department for their help and co.operation to achieve my work.

Abstract

This study deals with the ultrasound finding of abnormal liver function test. The main objective of this study is to evaluate the sonographic appearance of the liver in case of abnormal LFT to collaborate sonographic appearance of the liver with the defect in the LFT, determine the cause of unexplained abnormal liver function tests, and characterize the ultrasound findings as (normal, descriptive and definitive). The study carried out on 50 patients with abnormal LFT at the military Hospital. During The period from October 2011 up to April 2012. The US mobile machines used this study were GE logic5 with probe frequency 3.5 MHz and Mandarin machine with probe frequency

3.5 MHz, probes was convex with frequencies ranging from 3.4MHz. All patient were prepared by full bladder and using trans.abdominal probe. All patients scanned with supine position technique. After the detailed literary work the study comes to conclusion that A normal ultrasound does not exclude the presence of fatty liver or cirrhosis. The study reveal that the liver echogenicity were isoechoic in (31) patients and hypoechoic in (19) patients, the liver texture was fine in (33) patients and coarse in (17) patients. LFT was high in 41(82%) and low in 9(18%). The study shows that RT lobe mean size was 12.4±1.8, LT lobe was (6.5±1.8) and caudate lobe was (2.3±0.6). The mean portal vein diameter was (1.4±0.3). Most causes of abnormal LFT were associated with Alcoholic liver disease, Non.alcoholic steatohepatitis, Chronic hepatitis C or B, Drug ,induced hepatotoxicity, Haemochromatosis ,Wilson's disease , Primary biliary cirrhosis, Autoimmune hepatitis, Acute hepatitis A or E , Primary sclerosing cholangitis .The main objective to proceed this study is evaluation the liver by US .

ملخص البحث

هذا البحث اهتم بدراسة نتائج الموجات فوق الصوتية لحالات فحص وظائف الكبد الغير طبيعي

في مستشفى السلاح الطبي. إن الهدف من هذه الدراسة هو تقيم الكبد بواسطة الموجات فوق

الصوتية والربط بين ظهور الكبد في الموجات الصوتيه والخلل في وظيفته وتحديد سبب الخلل

وتشخيص صورة الموجات لطبيعيه وقاطعه في التشخيص. عدد المرضى الذين أجريت عليهم الدراسة خمسين مريض يعانون من خللفى وظائف الكبد في مستشفى السلاح الطبي بامدرمان. هذه الدراسةِ أجريتْ في الفترة من أكتوبر 2011 إلى ابريل 2012م . الاجهاز التى أستعملي في هذه الدراسةِ جنيرال إلكترك لوجك فايف ومندارى وأما المسبار كَان محدّب بتردد يتراوح مِن 3.4 ميغاهيرتز. جميع المرضى تم تحضيرهم بملء المثانة وباستخدام المسبار البطني . كُلّ المرضى مَسحوا بتقنيةِ الوضع المنبطح. خلصت الدراسة إلى أن الظهور الطبيعي للكبد في المسح بالموجات الصوتيه لا ينفي وجود تغيير دهني او تليف بالكبد. وتوصلت الدراسة إلى أن الصدى الصوتي كان متناسق عند 31 من المرضى وكان منخفض عند 19 من المرضى.وكان فحص وظائف الكبد مرتفع عند 41 (82%) ومنخفض عند 9 (18%). وأظهرت الدراسة أن متوسط قياس الكبد كان عي النحو الاتي: الفص الايمن 12.4±1.8 و الفص الايسر(6.5±1.8) وفص الكوديت (2.3± 0.6) وكان اتساع شريان البورتال(1.4±0.3). أغلب حالات وظائف الكبد غير الطبيعي ارتبطت بأمراض لكبد الكحوليه والالتهابات الفيروسيه. الهدف الرئيسى لاجراء هذه الدراسة تقيم الكبد بواسطة الموجات فوق الصوتية.

List of abbreviations

CBD	common Bile Duct.
IVC	Inferior Vena Cava.
CCC	cholangiocellular carcinoma.
GI	gastrointestinal.
LTH	ligamentum teres hepatis.
SSOTM	(Size, Shape, Outline, Texture and Measurement).
USCA	Ultrasound contrast agents.
FLL	focal liver lesions.
FHA	focal hypoechoeic areas.
AIH	autoimmune hepatitis.
PSC	primary sclerosing cholangitis.
PBC	primary biliary cirrhosis.
HCV	chronic viral hepatitis C.
ASH	alcoholic steatohepatitis.
NASH	non.alcoholic steatohepatitis
CDI	Colour Doppler imaging.
VOD	veno.occlusive disease.
TIPSS	transjugular intrahepatic portosystemic shunts.
DPI	Doppler perfusion index.
PVCI	portal vein congestive index.
TC	celiac trunk.
AMS	mesenteric superior artery.
AHC	common hepatic artery.
AHP	proper hepatic artery.
PSV	peak systolic velocity.
EDV	end diastolic velocity.

RI	resistance index.
PI	pulsatility index.
TAVmax	time averaged maximum velocity.
TAVmean	time averaged mean velocity.
D	diameter.
BF	blood flow volume.
FFT	fast Fourier transformation.
FNH	Focal nodular hyperplasia.
HCA	Hepatocellular adenoma.
HCC	Hepatocellular carcinoma.
NET	neuroendocrine tumours.
NRH	Nodular regenerative hyperplasia.

List of figures

:List of tables

- Table 4.9 the mean size and SD of the liver lobes and portal vein in respect to liver function test level and the difference in means using t.test with the critical p.value shown.
- Table 4.10 a cross tabulation table of gender versus liver function test
- Table 4.11 cross.tabulation of patient habit versus liver function test for 50 patients
- Table 4.12 a cross.tabulation of echogenicity versus liver function test for 50 patients
- Table 4.13 a cross.tabulation of texture versus liver function test for 50 patients

Table of Contents

Chapter three

Chapter four

Chapter five

Chapter one

Introduction

Ultrasound are diagnostic, noninvasive, and relatively inexpensive to evaluate the structure, size, and position of the liver in the right upper quadrant (RUQ) of the abdomen and allows visualization of the gallbladder and bile ducts when the patient may have impaired liver function, Symptoms occur only in end-stage liver disease, so many cases of liver disease are now identified in individuals incidentally found to have abnormal liver function tests (LFTs) as part of routine automated laboratory testing. Abnormal LFTs cannot be ignored because a subgroup of these patients will have progressive and potentially life-threatening liver disease for which therapeutic interventions are often available.

Physical examination is often normal unless hepatomegaly is present – the finding of which lowers the threshold for investigation – or signs indicative of cirrhosis with portal hypertension (splenomegaly, ascites or spider naevi). An appropriate response to abnormal LFTs requires an assessment of: pattern (hepatocellular or cholestatic), magnitude of elevation, duration of abnormality, associated symptoms, and Clinical evidence of cirrhosis. Therefore LFT abnormalities fall into several patterns which help in differentiating the underlying liver disease, included: Hepatocellular damage (high serum transaminase), cholestasis (high alkaline phosphatase (ALP)), and Poor synthetic function.

Although a liver biopsy is the gold standard for assessing both aetiology and the degree of fibrosis, it is associated with some morbidity and should be undertaken only after assessing the risk benefit. The clinical setting, together with the specific pattern of LFT abnormality and

appropriate additional tests, can narrow the differential diagnosis and provide a cost-effective approach to identifying those patients who need a liver biopsy.

1.1. Problem of the study

Ability of ultrasound to differential diagnosis, visualize and assess liver with abnormal LFT.

1.2. Objectives:

The main objective of this study was to evaluate the sonographic appearance of the liver in case of abnormal LFT

1.3. Specific Objectives:

- To correlate between sonographic appearances of the normal liver with the one of abnormal function test.
- To compare the size of Rt, Lt and caudate lobe of the normal liver to the abnormal LFT including the portal vein size.
- To determine the cause of unexplained abnormal liver function tests.
- To characterize the ultrasound findings in respect to echogenecity and texture.
- To find the effect of age, gender and habit in liver size and appearances.

1.4. significant of the study

This study will provide a quantitative analysis of liver having abnormal function test in respect to normal one, as well as the qualitative characterization of both categories in term of echogenecity and texture. Also the study will investigate the impact of gender, age and habit on the appearance of the liver as confounding factors.

1.5. Overview of the study

This study consisted of five chapters; with chapter one is an introduction, which includes statement of the problem, objective, significant of the study and overview. Chapter two includes theoretical background and scholarly studies review concerning the problem under the study, while chapter three includes material used to collect the data as well as method and techniques of data acquisition. Chapter four consisted of data presentation using graphs and figures and finally chapter five consisted of discussion of the portrayed data as well as conclusion and recommendations.

Chapter two

Theoretical background and previous study

2.1. Topographic remarks

The liver is located inside the intraperitoneal cavity and under the right hemidiaphragm, but can also extend across the midline reach to the left hemidiaphragm and to the spleen in some cases. The liver is fixed to the diaphragm by the pars affixa and to the ventral abdominal wall by the ligamentum falciforme (falciform ligament) and its strong margin, the ligamentum teres hepatis. The minor omentum consists of the ligamentum hepatogastricum and the ligamentum hepatoduodenal. The hepatoduodenal ligament carries three vessels – two containing blood (the portal vein and hepatic artery) and one carrying bile (common bile duct (CBD). The further course of these three vessels (known as Glisson's triad) is mainly parallel (Christoph F. Dietrich.2011).

The structures of the liver hilum are accompanied by a number of ventrally and dorsally (in relation to the portal vein) located lymph nodes, which can be routinely demonstrated by ultrasound; however, lymphatic vessels are too small to be visualised on ultrasound. The liver has three main (hepatic) veins – left, middle and right – that drain the liver blood to the inferior vena cava (IVC) located in the retroperitoneum. The IVC is variably surrounded by liver parenchyma (Christoph F. Dietrich.2011).

The organs and structures of the peritoneal cavity surround the liver, as well as pleural and pericardial structures. Neighbouring structures adjacent to the liver are numerous and include (clockwise) basal lung portions separated by the muscular layers of the right diaphragm (and more or less the left diaphragm as well), heart, stomach, intestine (e.g. upper duodenal loop and

right colonic flexure), abdominal aorta, IVC, right adrenal gland and right kidney. The interposition of the colon between the liver and the anterior abdominal wall can prevent sonographic approach to the right liver lobe in cases of Chilaiditi's syndrome. Finally, in the case of complete or incomplete situs in versus, topographic relations are inverted (Christoph F. Dietrich.2011).

2.2 Liver anatomy

2.2.1. Anatomical orientation

Liver anatomy is defined by ligaments and fissures as well as by vascular architecture i.e. the branches of the hepatic artery, portal vein and bile ducts define the centers of liver segment anatomy by their parallel course.

2.2.2. Liver segment anatomy

A simplified anatomy divides the liver into the larger right lobe (including segment V, VI, VII and VIII); the left lobe with its medial (IVa, b) and lateral segments (II, III); and the caudate lobe, (Christoph F. Dietrich.2011)

2.2.3. Couinaud classification

The widely accepted Couinaud system describes liver segment anatomy. This classification, modified by Bismuth (segment IVa, b), is based on eight segments, each of which has its own arterial and portal venous vessel architecture (Glisson's triad) for vascular inflow, outflow and biliary drainage. As a result of this division into self-contained

units, each can be resected (alone or in groups) without damaging the remaining segments because the vascular inflow, outflow and biliary drainage is preserved. Depending on the three-dimensional volume orientation of the liver (longitudinal or oblique), the interpretation of the Couinaud classification can be inconsistent in the literature. While the portal vein plane has often been described as transverse, it may also be oblique because the left branch runs superiorly and the right runs inferiorly. In addition to forming an oblique transverse plane between segments, the left and right portal veins branch superiorly and inferiorly to project into the centre of each segment. (Christoph F. Dietrich.2011).

2.2.4. Liver segment nomenclature

In a clockwise fashion starting with the caudate lobe as segment I [video caudate lobe], the left posterolateral segment is number II, followed by the left anterolateral, segment III; left super medial, segment IV a; left inferomedial, segment IVb; right anteroinferior, segment V; right posteroinferior, segment VI; right posterosuperior, segment VII; and right anterosuperior, segment VIII. This appears more complicated than it actually is. (Christoph F. Dietrich .2011)

2.2.5. Right liver lobe

Anterior segments V and VI are separated from the posterior segments VII and VIII in the plane of the right hepatic and portal veins. The anterior and posterior divisions are further sub-divided by a plane defined by the right main branch of the portal vein. Segments IVa (superior) and IVb (inferior) are situated to the left of the plane separating the right and left liver lobes. Segments V and VIII are to the right and segment VIII is more superior and dorsal to segment V. In the

Couinaud classification, the plane defined by the middle hepatic vein sub-divides the liver into the true right and left lobes. A standard right or left lobectomy requires division along the plane of the middle hepatic vein. Segments IVa and IVb lie to the left of the plane, while a segment V and VIII lies to the right; VIII being more superior to V. In Couinaud nomenclature, the plane defined by the right branch of the portal vein divides the anterior and posterior portions of the right liver superiorly and inferiorly, thus dividing the right lobe into four segments (Joseph, et al 1979).

2.2.6. Left liver lobe

The “umbilical level” separates segments IVa and IVb from the lateral segments II and III. Remarkably, this level is the only plane with a vertical orientation not defined by a hepatic vein. The left liver lobe can be defined on the surface of the liver by its associated landmarks. It extends from the umbilical fissure anteriorly through the ligamentum venosum along the lateral aspect of the caudate lobe. Structures within the plane of the umbilical fissure include the falciform ligament, ligamentum venosum (remnant of the ductus venosus) and the ligamentum teres (remnant of the umbilical vein). The left hepatic vein plane is somewhat controversial. The left hepatic vein courses laterally to the umbilical fissure. Most investigators believe that the plane defined by the left hepatic vein is a true intersegmental boundary and is not the same as the plane of the umbilical fissure. However, others claim the true division between segments II and III is formed by the transverse plane of the left portal vein. We will define the plane of the left hepatic vein as the boundary between segments II and III. The medial segment of the left lobe can be divided into two segments by the plane of the portal vein (IVa and IVb).

2.2.7. Caudate lobe (segment I)

The most unique of the Couinaud segments is segment I, which is part of the caudate lobe (sometimes called the Spiegel lobe). This segment is located posteriorly and adjacent to segment IV. Its medial and lateral boundaries are defined by the IVC and ligamentum venosum, respectively. The caudate lobe has a variable vessel anatomy that differs from the rest of the liver; its portal inflow is derived from both the left and right branches of the portal vein, and it has its own short (and usually small) hepatic veins that connect directly to the IVC. Owing to the variable and extensive crossing of vessels, and its position relative to the liver hilum and IVC, segment I is frequently not resected, unless absolutely necessary.

2.2.8. Surgical resection

Surgical resections proceed along the vessels that define the peripheries of the segments. In general, this means resection lines are parallel to the hepatic veins to preserve the hepatic arteries, portal veins and bile ducts that provide vascular inflow and biliary drainage through the centre of the segment. When a lesion occurs within the lateral segment of the left lobe, usually both Couinaud segments II and III are removed together based on the plane formed by the umbilical fissure (known as left lateral segmentectomy). Note that because the plane of the left hepatic vein is oblique, it forms a division between segments III anteriorly and segment II posteriorly.

2.2.9. Additional anatomical structures

The falciforme ligament runs between the ventral abdominal wall and the liver, ending with its free caudal margin as the ligamentum teres containing the obliterated umbilical vein. It can be

identified at the left lateral border of segment IVb (in the quadrate lobe), and it is often mistaken to form the anatomical border between the left and right liver lobe, which is not the case. This border follows a plane along the middle hepatic vein between the IVC and the longitudinal gallbladder axis. It is identified by ultrasound only in patients with one-sided biliary obstruction and a subsequent different fluid content between the right and left liver lobe in cholangiocellular carcinoma (CCC) in the Klatskin's position. The ventral border of segment I is delineated by the ligamentum venosum (remnant of duct of Aranti in the foetus), which runs caudally to the hepatic artery and can be identified in this way. (Christoph F. Dietrich.2011).

2.3. Ultrasound examination technique

2.3.1. Patient preparation

It is recommended that patients undergo a period of fasting prior to upper abdominal imaging to maximise the distension of the gall bladder and reduce food residue and gas in the upper gastrointestinal (GI) tract, which may reduce image quality or preclude liver imaging. This is essential for full imaging of the liver and related biliary tree, but may not be required in an acute situation, such as trauma where immediate imaging of the gall bladder is not essential. A patient may have small amounts of still water by mouth prior to the scan, e.g. for medication. There is some evidence that smoking can reduce image quality when scanning the upper abdominal structures and it is good practice to encourage the patient not to smoke for 6-8h prior to an ultrasound scan. This is because smoking increases the gas intake into the upper GI tract, which can reduce image quality, and some chemicals in tobacco are known to cause contraction of the smooth muscle of the GI tract, which can cause contraction of the gall bladder, even after fasting (Christoph F. Dietrich.2011).

2.3.2. Examination

The liver is a large, pyramidal shaped organ and liver sectional anatomy may be best described, imaged and defined using real-time ultrasound imaging (see “Liver segment anatomy” and the examination technique videos). Conventional real-time ultrasound produces images of thin slices of the liver on screen, therefore it is essential that the operator always scans the entire organ systematically in at least two anatomical planes to ensure the entire volume of the liver tissue and structures have been imaged. The operator must then use this two-dimensional information to

visualise a three-dimensional map of the individual patient's liver anatomy and pathology. This requires good hand-eye-brain coordination. (Christoph F. Dietrich.2011).

For orientation, the central portion of the liver can be differentiated into three levels: level of the confluences of the hepatic veins (Figure 2-1) Level of the pars umbilicalis of the (left) portal vein branch (Figure 2-2), and level of the gall bladder (Figure 2-3).

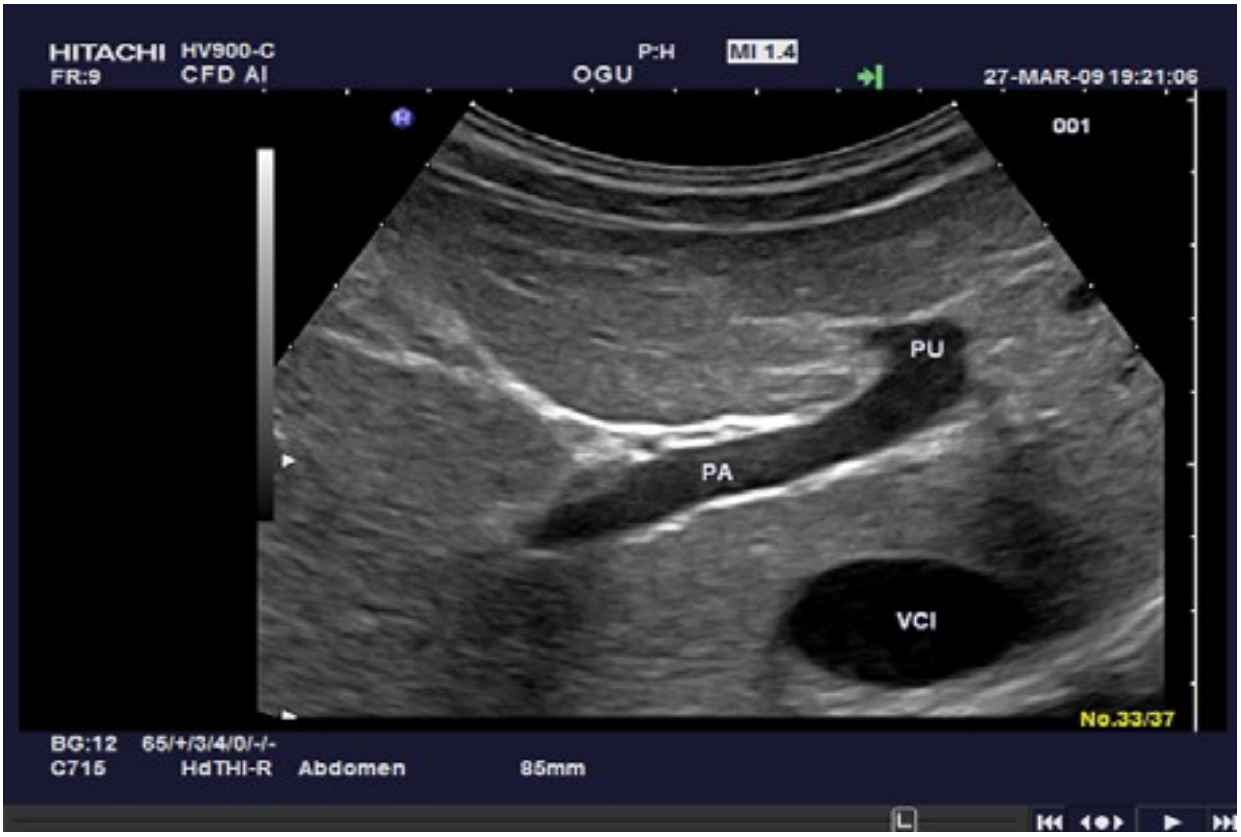

(Figure 2-1) Confluences of the hepatic veins. This "junction" level is the first in ultrasound examination of the right liver lobe by sub-costal scanning sections steeply "looking" upwards, preferably in deep inspiration [video]. VCI, inferior vena cava; LLV, left liver vein; MLV, middle liver vein; C, confluence of the LLV and MLV; RLV, right liver vein. The RLV often separately joins the inferior vena cava, whereas the LLV and MLV often reveal a common trunk c.

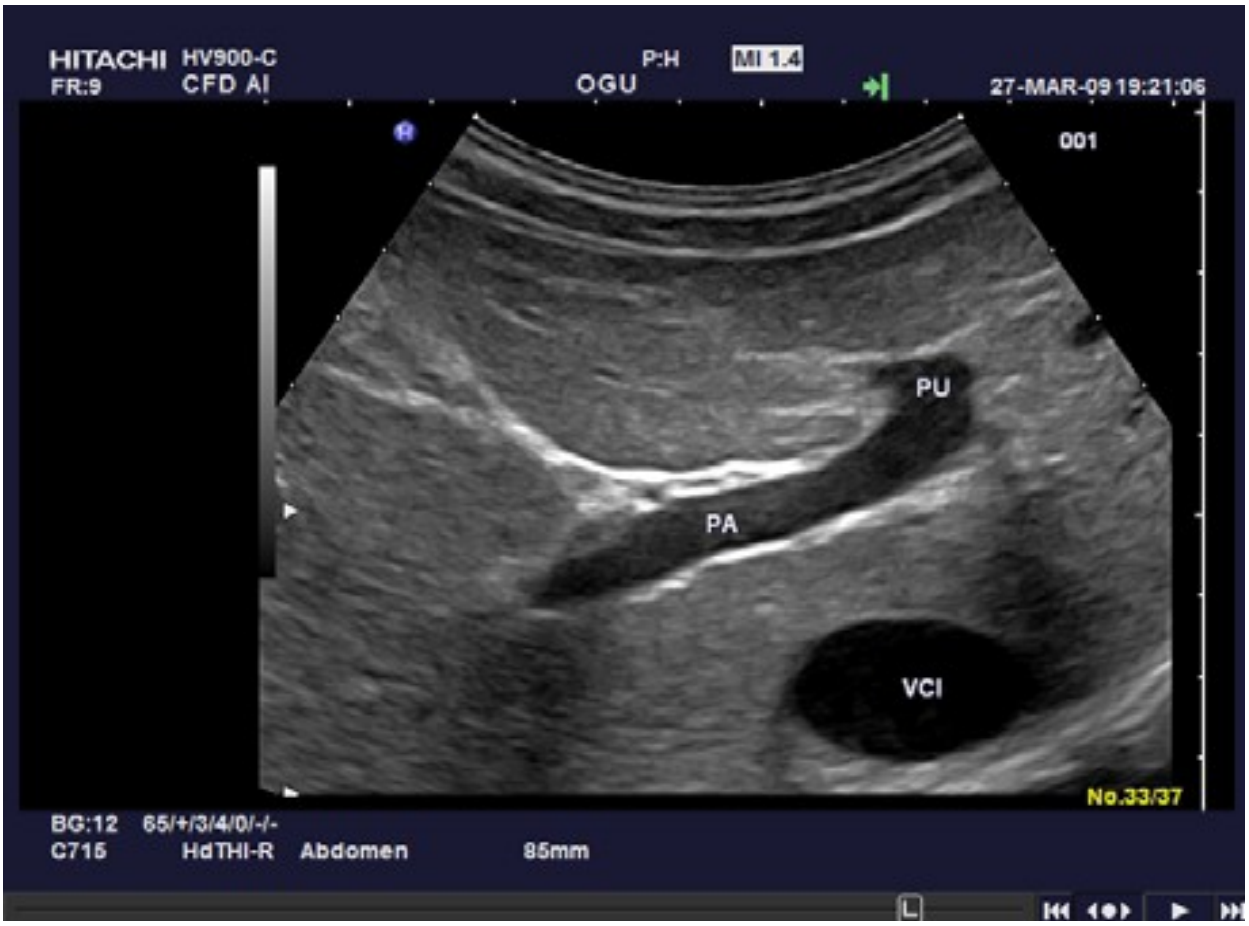

(Figure 2-2) Pars umbilical is of the portal vein. Scanning planes display the left and right liver lobes in a more downwards orientated view into the right liver lobe as compared with the level of the confluence of the hepatic veins [video]. PA, portal vein; PU, pars umbilicalis of the portal vein; VCI, inferior vena cava.

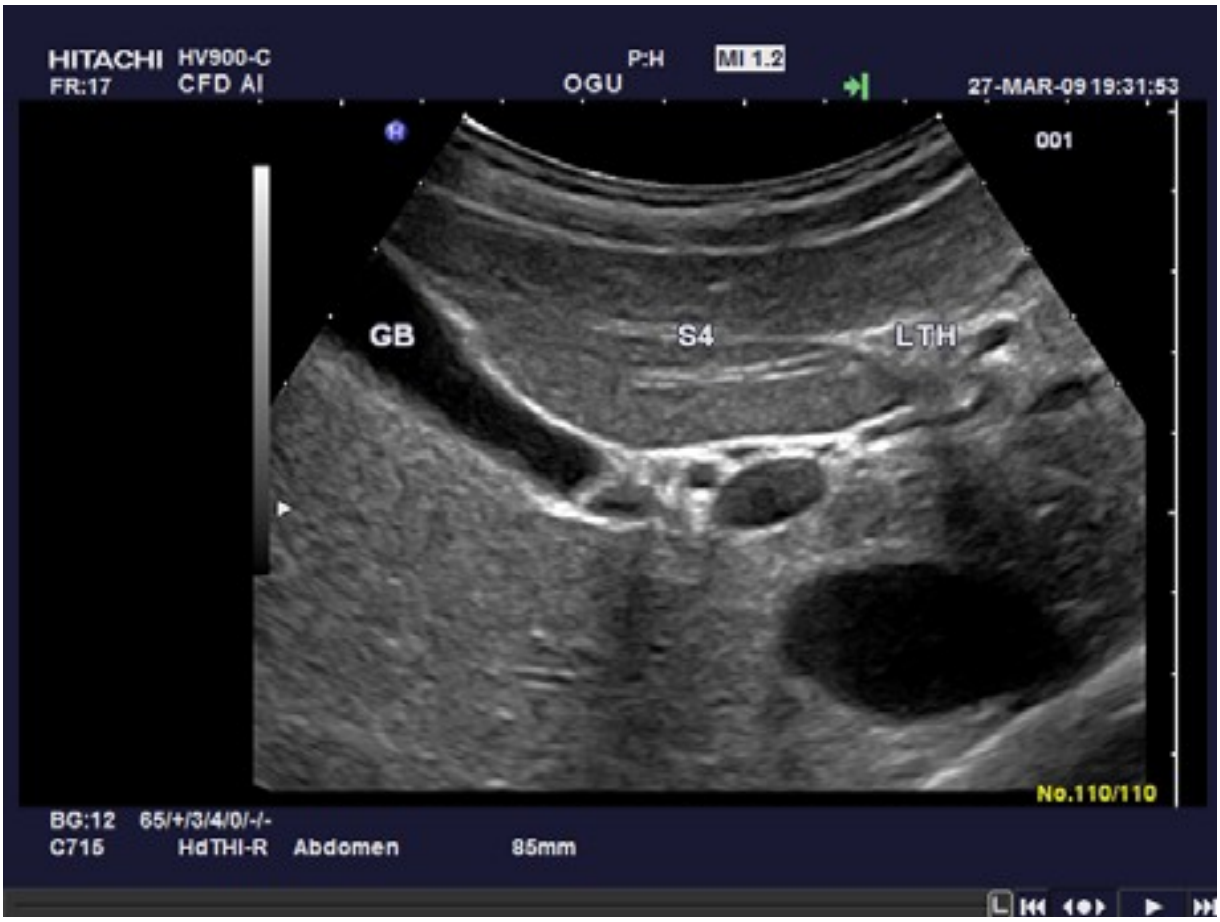

(Figure 2-3) Gallbladder level as the most caudate scanning plane. GB, gallbladder; LTH, ligament terse hepatis, S4, segment IV of the liver (quadrate lobe).

Using these levels as, more or less, parallel scanning sections allows the examiner to visualise a real-time three-dimensional ("4D") image of the patient's individual anatomy and pathology. Standardized scanning in a systematic sequence of probe- and patient–positions, and of scanning planes is mandatory to cover all segments and the complete liver surface. The patient should be examined from the sub- to the intercostals in the decubitus position as well in the modified, slightly oblique, positions with the right arm above the head and the right leg stretched during all respiration cycles to identify the best approach and to avoid artifacts caused by the thorax. Examination in the standing position is also helpful owing the liver moving caudally with gravity. Scanning from the sub- or intercostals probe positions (depending on the individual

anatomy) avoids interposed lung, which can occur in the right poster lateral (superficial) parts of the liver when using the intercostals approach. There are other examination techniques that can also be used, but these will not be mentioned here in detail. There are a number of variations from the norm that will be encountered (e.g. with respect to accessory lobules, vascular branching, shape and configuration).

2.3.3. Examination criteria

The acronym SSOTM (Size, Shape, Outline, Texture and Measurement) is a useful way to recall the examination criteria (Christoph F. Dietrich.2011).

2.3.4. Size, Shape, Outline

The size of the liver has had many methods of measurement, including three-dimensional-reconstructions. However, liver size measurement does not form part of current clinical practice because there is no established reliable or reproducible ultrasound method at present. Shape; the shape is normally described as pyramidal. Outline***;*** the normal liver surface should be smooth with no protruding lumps or indentations. The inferior liver border in the normal patient should have an acute angled edge. Liver surface border delineation and other ultrasound criteria are described in the respective chapters.

2.3.5. Texture and echogenicity

The normal liver parenchyma is of medium homogenous echogenicity. It is usually slightly darker than the spleen and slightly brighter than the renal cortex, independent of age except in childhood. It is essential when comparing the liver with the spleen and renal cortex that comparison is done at the same depth. Liver surface and vessel borders are smooth and vascular

architecture with its classic branching dichotomy is perceived as a harmonic and detailed aspect. The normal parenchyma image varies very little between individuals (Christoph F. Dietrich.2011).

2.3.5.1. Hepatic veins

The three hepatic veins are positioned in between the liver segments. Their course, in addition to the Glasson's triad, is helpful in defining liver lobes and liver segments. The number and course of the hepatic veins are somewhat variable (Figure 2-1) (Christoph F. Dietrich.2011).

2.3.5.2. Portal veins

Formed by the confluens of the splenic and superior mesenteric vein, the portal vein can be displayed sonographically by scanning more or less perpendicular to the lower costal margin (orientation can be achieved by reference to the right shoulder to the umbilicus), preferably in a left decubitus position and on variably deep inspiration. Intrahepatically, the portal vein bifurcates into a main left and right branch. The first (right) portal vein branch splits into an anterior and a posterior branch, which itself leads to the segments V to VIII. The latter (left) main portal branch bifurcates into segments II and III and, into the left medial branches for segments I (caudate lobe), IVa and IVb (Figure 2-2). *Hepatic artery:* The common hepatic artery originates from the coeliac axis, branching into the gastroduodenal artery and the proper hepatic artery (arteria hepatica propria). Anatomical variations are frequent (in up to 50% of the population), and include the origin of the left proper hepatic artery from the left gastric artery, as well as the variable arterial supply to the liver by superior mesenteric arterial branches. The hepatic artery runs with the portal vein, the right main arterial branch frequently meandes around the portal vein and is displayed sonographically as short segments medially (or less often laterally) of the

portal vein. The normal and pathological flow patterns are described in the Doppler chapter. *Bile ducts*: Bile ducts accompany the portal vein and hepatic artery branches from the liver hilum into the liver lobules. Intrahepatically, they form the ductus principals dexter and the ductus principals sinister, which join as the CBD. The extrahepatic course of the CBD is cranially (prepancreatic), often ventral to the portal vein and caudally (intrapancreatic) more dorsolateral. The respective course of the hepatic artery is more variable (Figure 2-4) (Christoph F. Dietrich.2011).

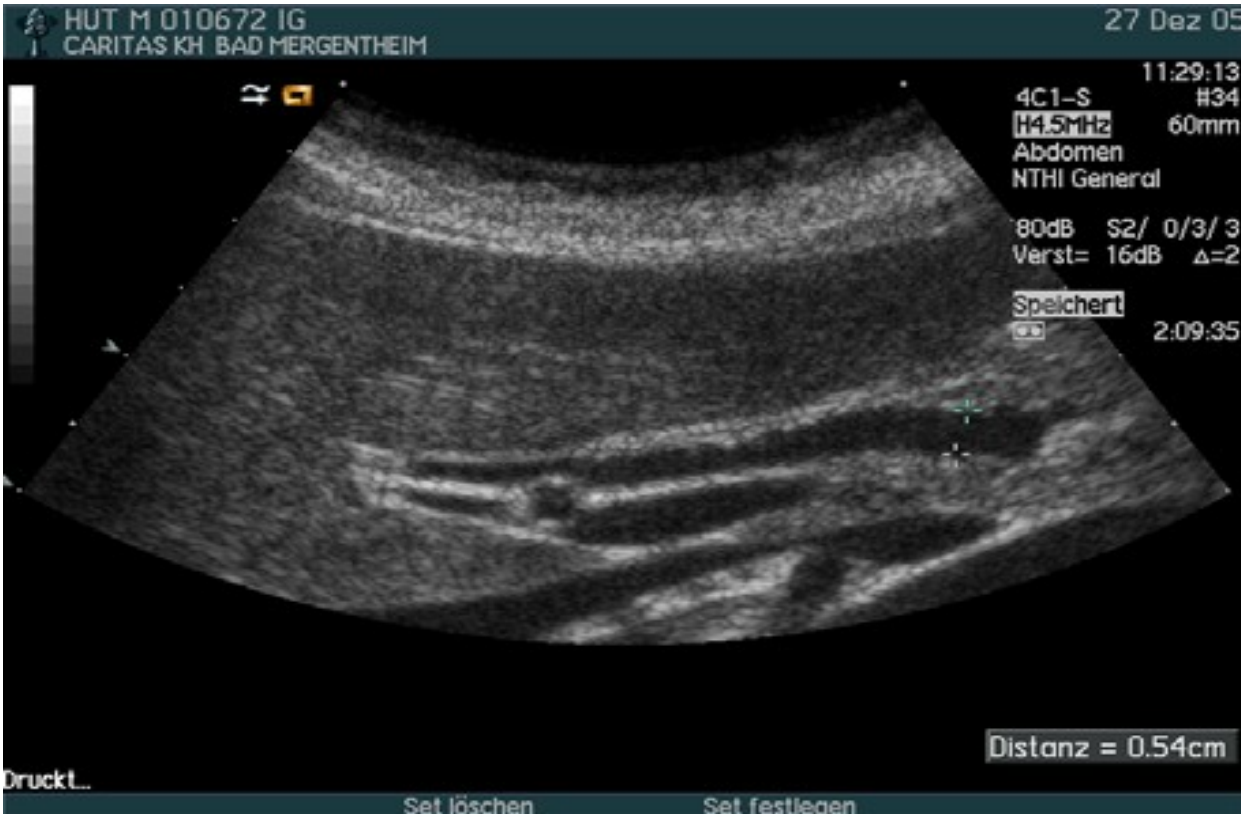

(Figure 2-4) Common bile duct (CBD), and therefore the liver hilum, is often best examined in a left lateral decubitus position using a sub-costal approach in slight inspiration. In a typical view the CBD (in between markers (+)), portal vein (PV), hepatic artery (HA), inferior vena cava (IVC) and right renal artery (RRA) (sometimes the aorta (AO)) can also be seen; the papilla region (PAP) is indicated.

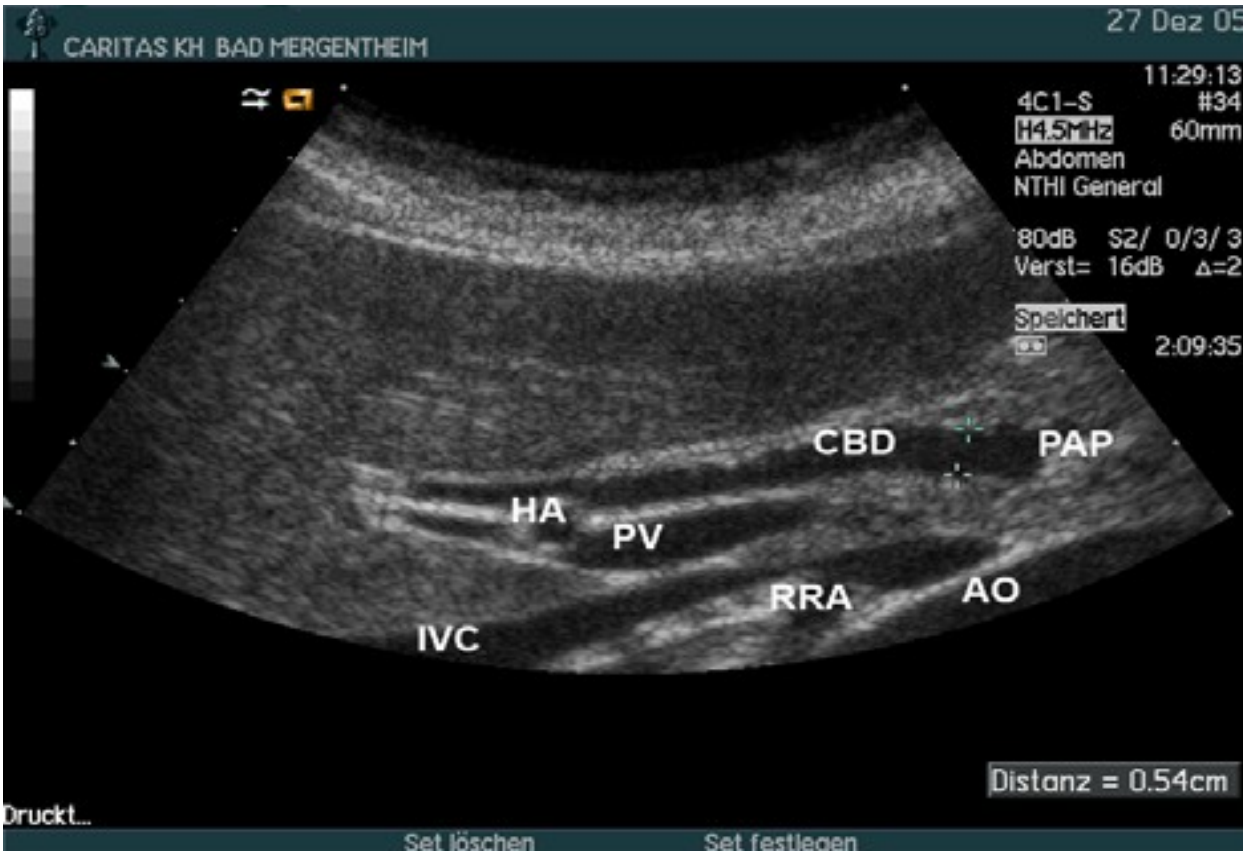

(Figure 2.5) Perihepatic lymph nodes Perihepatic lymph nodes in the hepatoduodenal ligament are commonly found next to the cystic duct are therefore called cystic duct lymph nodes .

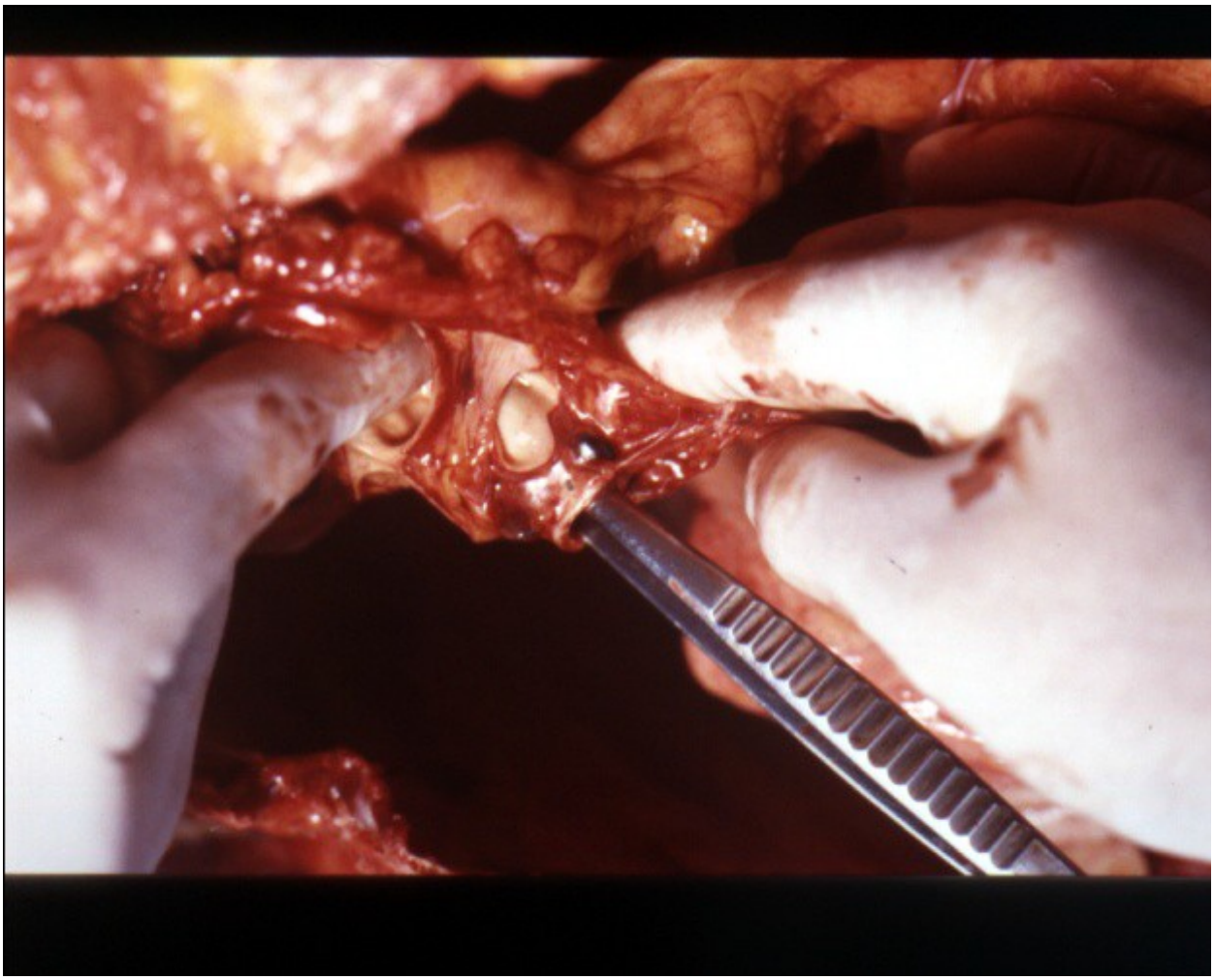

(Figure 2.6) Per hepatic lymph nodes in the hepatoduodenal ligament (LK) are commonly found next to the cystic duct and are therefore known as cystic duct lymph node. They are shown here in a post-mortem examination on (a) ultrasound and (b) macroscopically. VCI, inferior vena cava.

2.3.6. Liver pathology

Diffuse liver disease Criteria for analyzing diffuse liver disease include the evaluation of:

- Liver parenchyma (echo-texture, ultrasound attenuation, vascular architecture, etc.) as well as the liver surface (a high frequency transducer can be helpful to detect details of superficially located structures) (Christoph F. Dietrich .2011) .
- liver hilum structures including perihepatic lymph nodes in the hepatoduodenal ligament, lymph nodes in inflammatory liver disease or neoplastic infiltration;
- hepatic vessel flow patterns using colour and pulsed wave Doppler imaging (CDI) (Christoph F. Dietrich .2011) .
- Ultrasound contrast agents (USCA) have improved the detection/exclusion rate of focal liver lesions (FLL) in diffuse liver disease. (Christoph F. Dietrich .2011).

2.3.7. Hepatic steatosis

Hepatic steatosis (fatty liver) is the most common liver pathology. Sensitivity and specificity of the detection of hepatic steatosis by B-mode ultrasound examination can be very high in the hands of an expert investigator, who consistently applies specific criteria in patients with significant fatty liver disease. In transabdominal ultrasound, hepatic steatosis is characterized by increased echogenicity, which is often compared with spleen or kidney parenchyma at the same depth (Figure 6); supporting findings include ultrasound attenuation (the decrease in intensity as sound travels through a material, caused by absorption, scattering and beam divergence). Attenuation decreases the detail of vascular architecture, and it can cause a loss of visibility deeper within the liver and impeded imaging of the diaphragm.(Christophe F. Dietrich.2011).

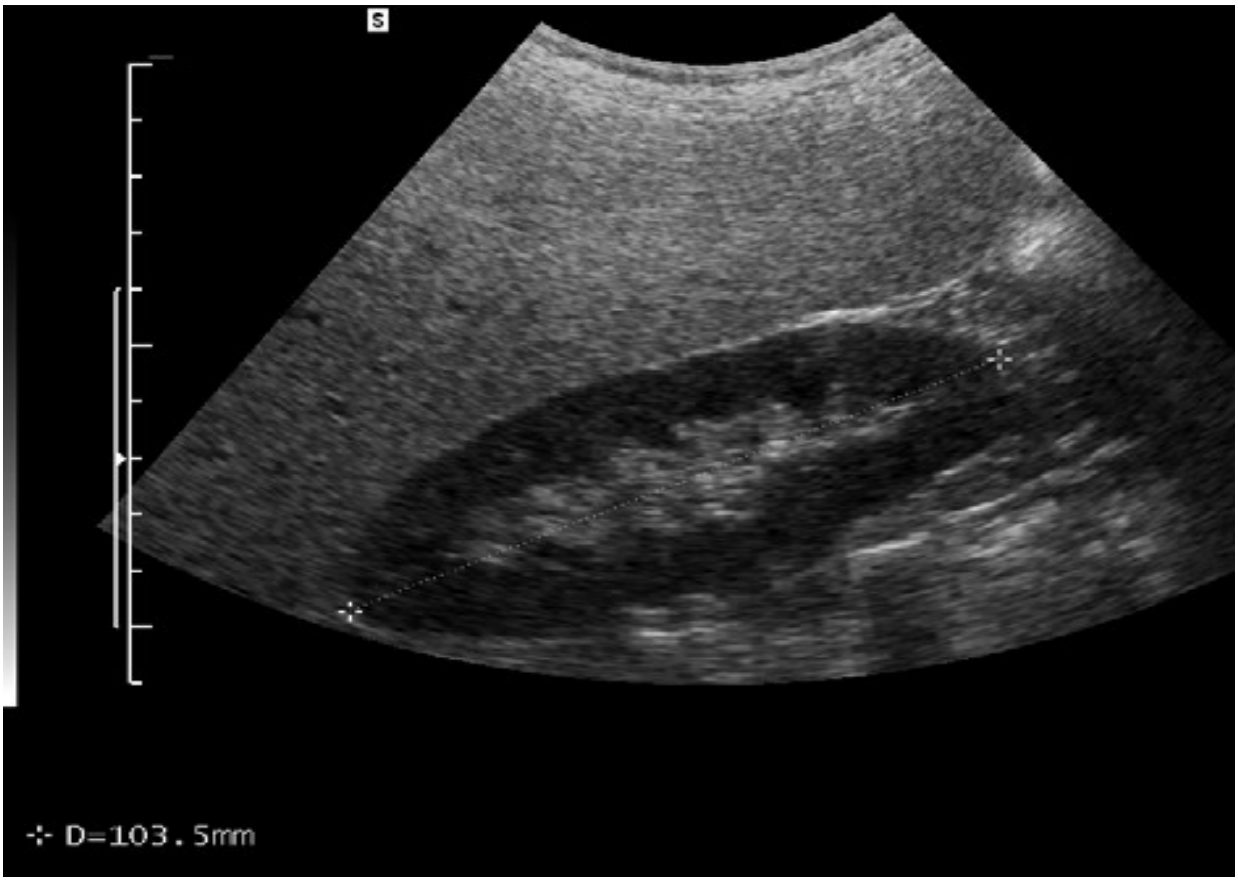

(Figure 2.7) Sonographic signs of hepatic steatosis (fatty liver) include hepatomegaly with rounded borders, increased echogenicity, ultrasound attenuation caused by absorption, scattering and beam divergence, and decreased detail display of intrahepatic vascular architecture. There is an exaggeration of the difference between the kidney parenchyma and liver echogenicity. The right kidney is shown between callipers (+).

In the majority of patients with hepatic steatosis, distinctive hypoechoic areas in the liver hilum can be demonstrated by ultrasound examination (Figure 7). It is believed that the presence of focal hypoechoeic areas (FHA) within the liver hilum (and elsewhere in the liver) corresponds to parenchymal islands, with, or close to, normal fat content (owing to a locally different blood supply), which are surrounded and contrasted by bright echogenic parenchyma with fatty infiltration. Sub-capsular FHA and FHA close to hepatic veins are other typical locations; these

“pseudolesions” are polycyclic and non-round in shape. The FHAs are relatively specific to hepatic steatosis and may be helpful in differentiating fatty from fibrotic liver disease.

Similar FHA were demonstrated in patients with liver steatosis owing to systemic corticosteroid therapy, even though the more important focal lesions in this condition are hyperechoic Pathophysiologically, areas of different fat content might be caused by the different arterial and portal venous blood supply in comparison with the surrounding liver parenchyma, which is mainly portal venous and therefore contains a higher fat and insulin concentration in focal fatty infiltration (Christophe F. Dietrich.2011).

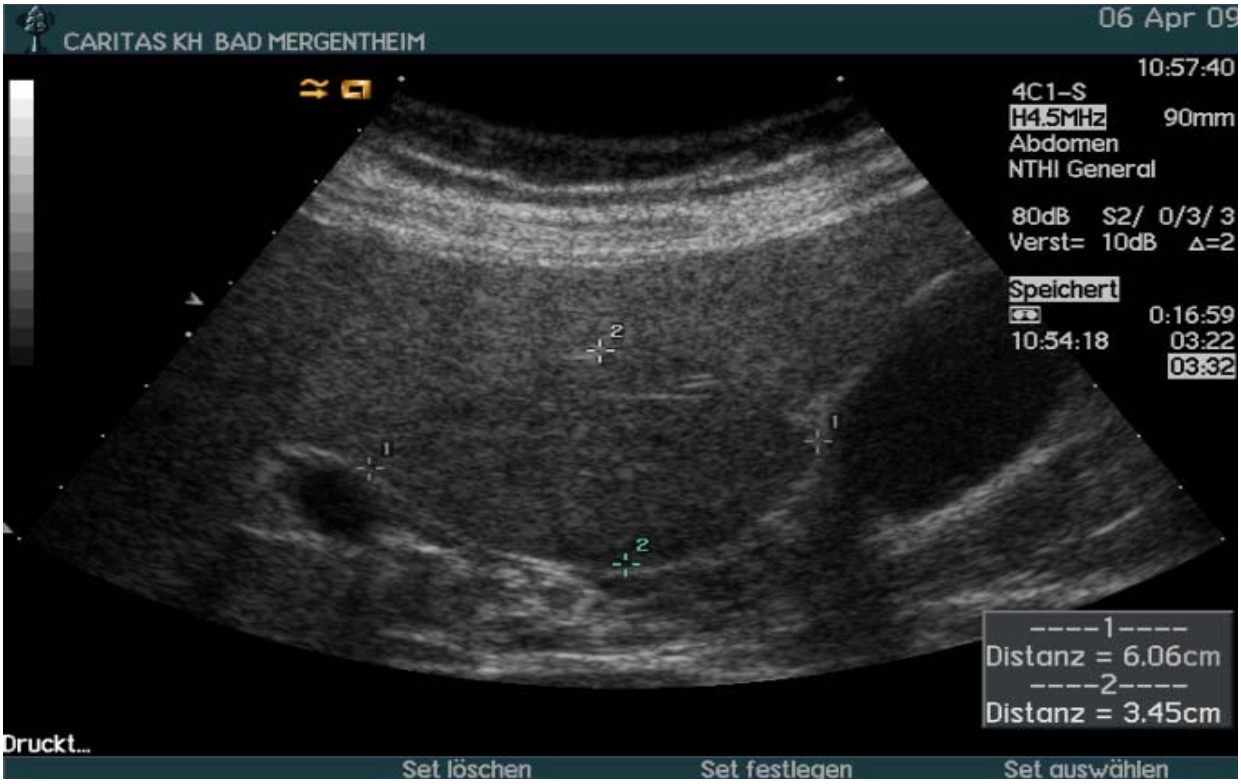

(a)

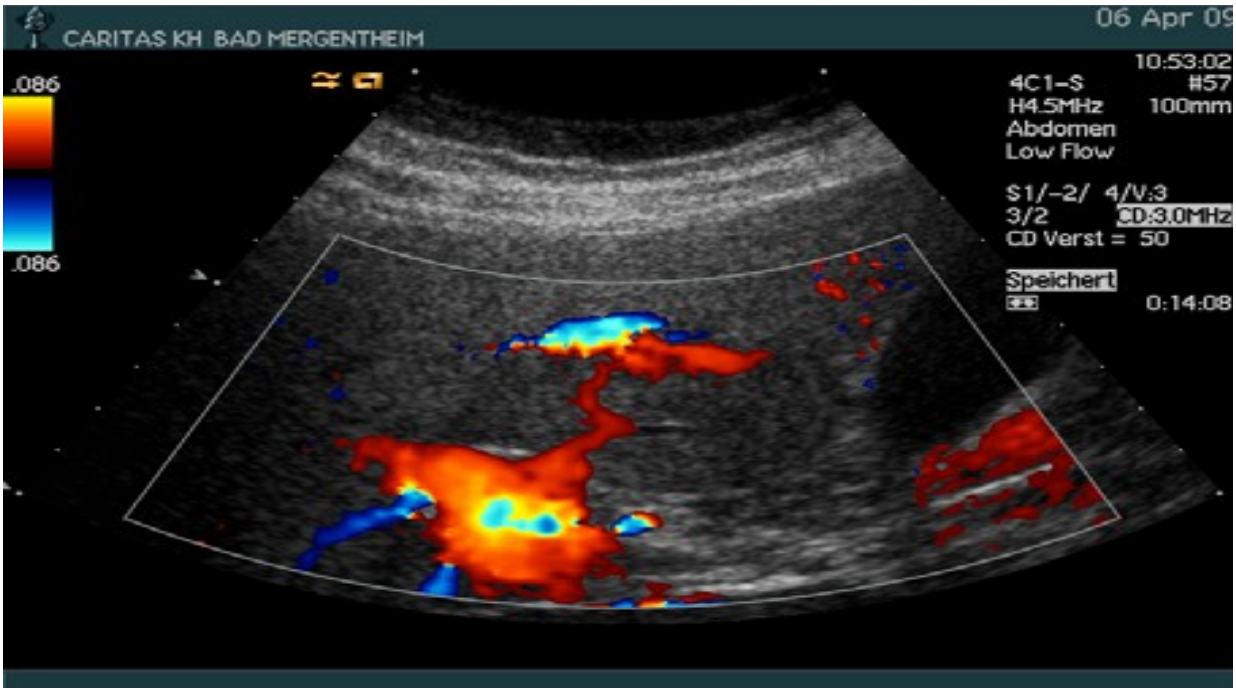
CARITAS KH BAD MERGENTHEIM
06 Apr 09
10:53:02
.086
4C1-S
#57
H4.5MHz
100mm
Abdomen
Low Flow
S1/-2/ 4/V:3
3/2
CD:3.0MHz
CD Verst = 50
Speichert
0:14:08
.086

(b)

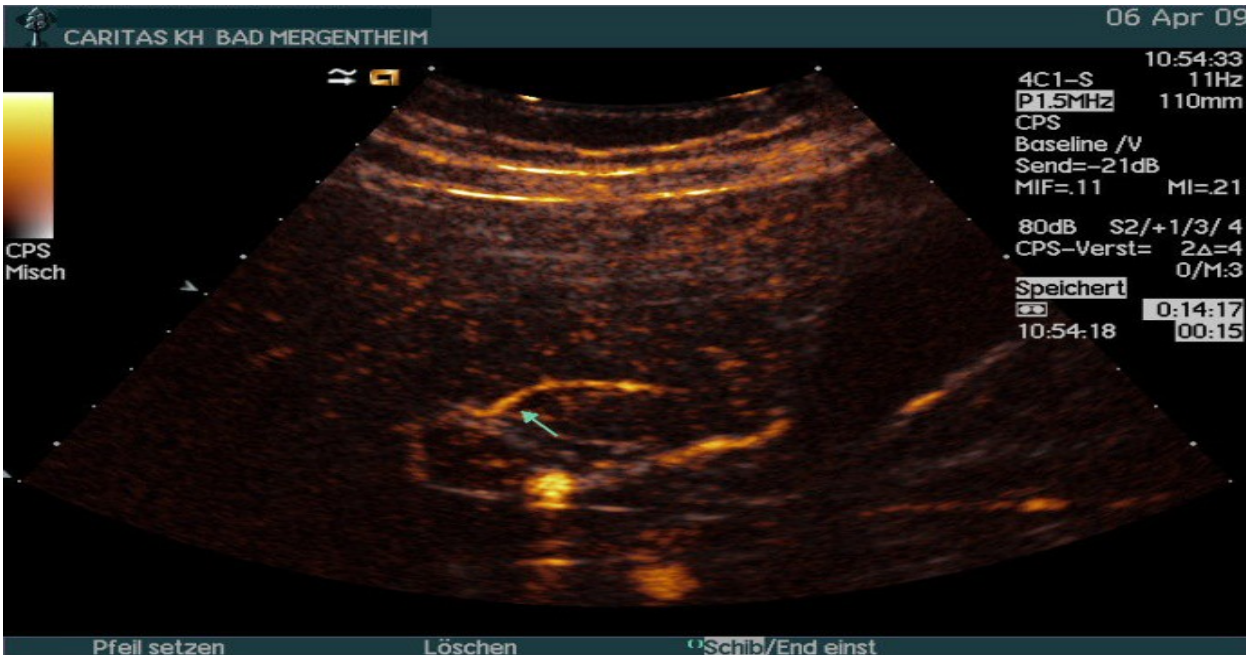
CARITAS KH BAD MERGENTHEIM
06 Apr 09
10:54:33
4C1-S
11Hz
P1.5MHz
110mm
CPS
Baseline /V
Send=-21dB
MIF=.11
MI=.21
80dB
S2/+1/3/ 4
CPS-Verst=
2Δ=4
0/M:3
Speichert
0:14:17
10:54:18
00:15
CPS
Misch
Pfeil setzen
Löschen
Schib/End einst

(c)

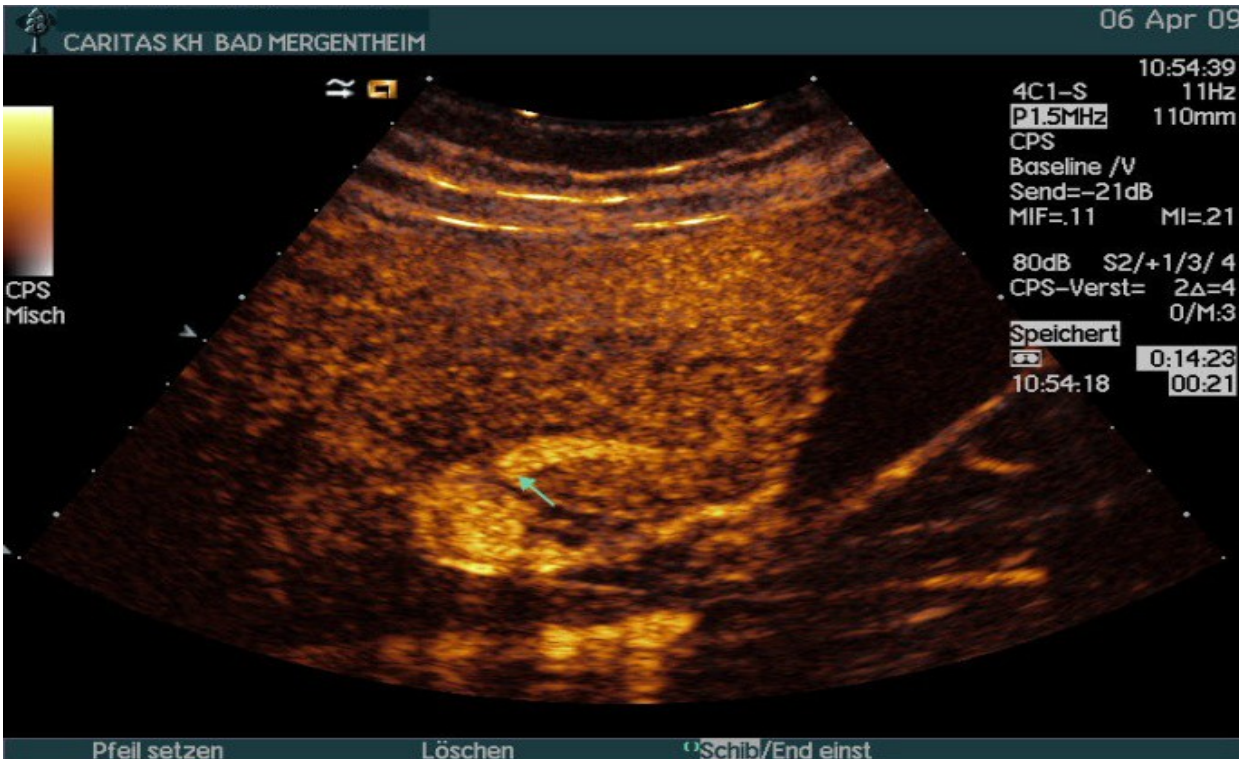

(d)

(Figure 2.8) Hepatic steatosis. Perhaps the most objective, and therefore the most important, sign of hepatic steatosis is the circumscribed focal hypoechoic areas in the liver hilum examined in a left posterior oblique position. (a) B-mode ultrasound demonstrates a focal liver lesion in between callipers (+). (b) Colour Doppler imaging indicates a centrally located vessel of undetermined origin. (c) Contrast-enhanced ultrasound shows the typical enhancement pattern. Typically a centrally located arterial vessel can be displayed in the arterial phase (arrow) and (d) a portal vein branch in the portal venous phase (arrow) and homogenous enhancement in the late phase.

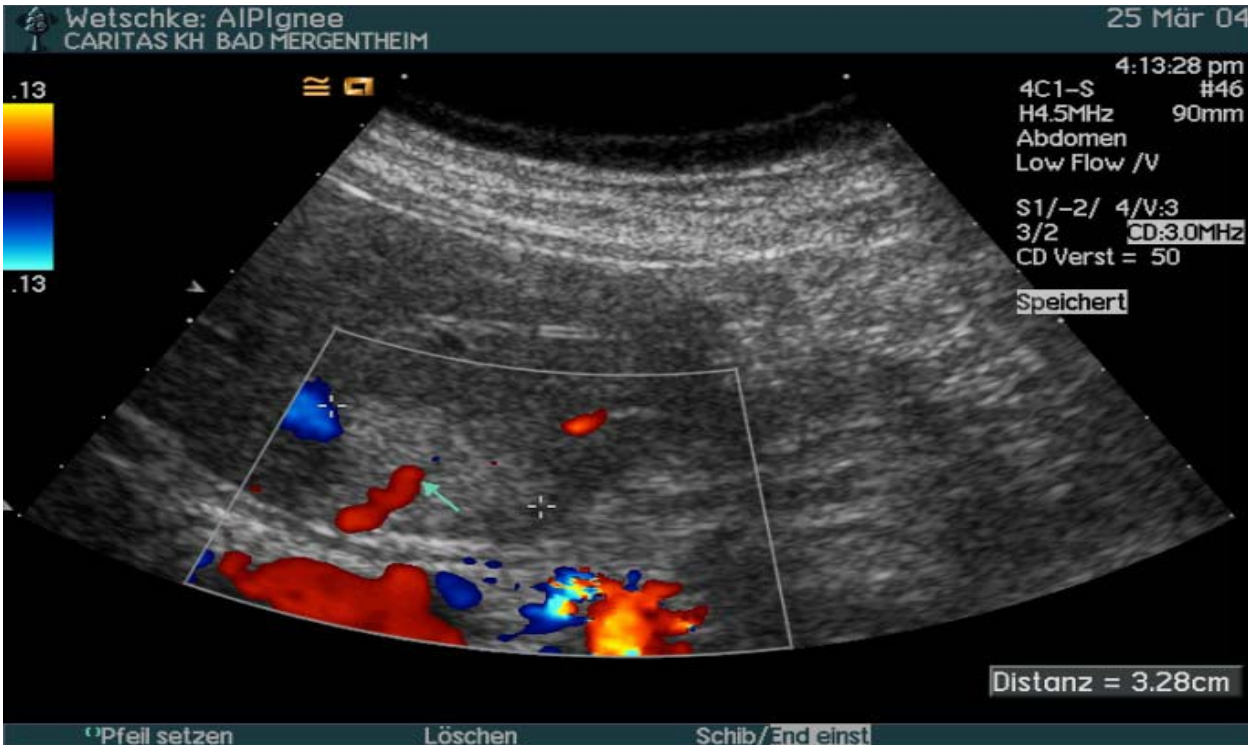
Wetschke: AIPIgnee
CARITAS KH BAD MERGENTHEIM
25 Mär 04
4:13:28 pm
4C1-S #46
H4.5MHz 90mm
Abdomen
Low Flow /V
S1/-2/ 4/V:3
3/2 CD:3.0MHz
CD Verst = 50
Speichert
.13
.13
Distanz = 3.28cm
Pfeil setzen
Löschen
Schib/End einst

(a)

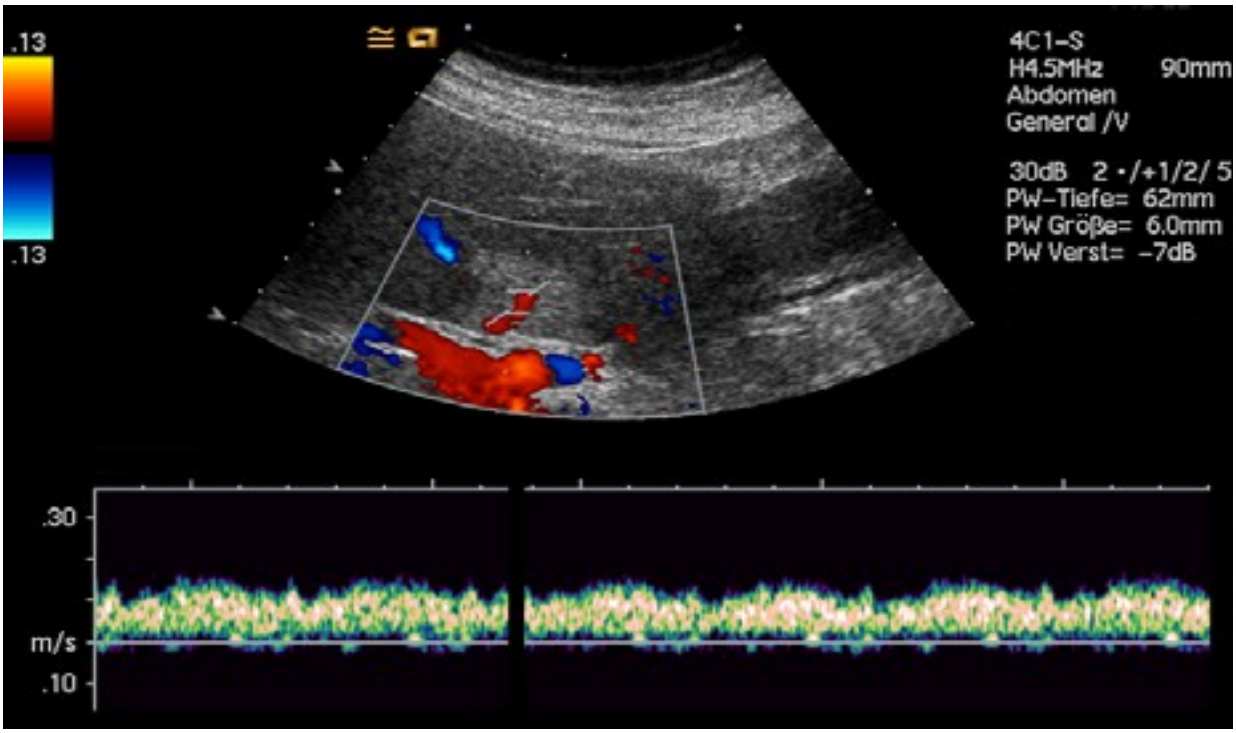
4C1-S
H4.5MHz 90mm
Abdomen
General /V
30dB 2 •/+1/2/ 5
PW-Tiefe= 62mm
PW Größe= 6.0mm
PW Verst= -7dB
.13
.13
.30
m/s
.10

(b)

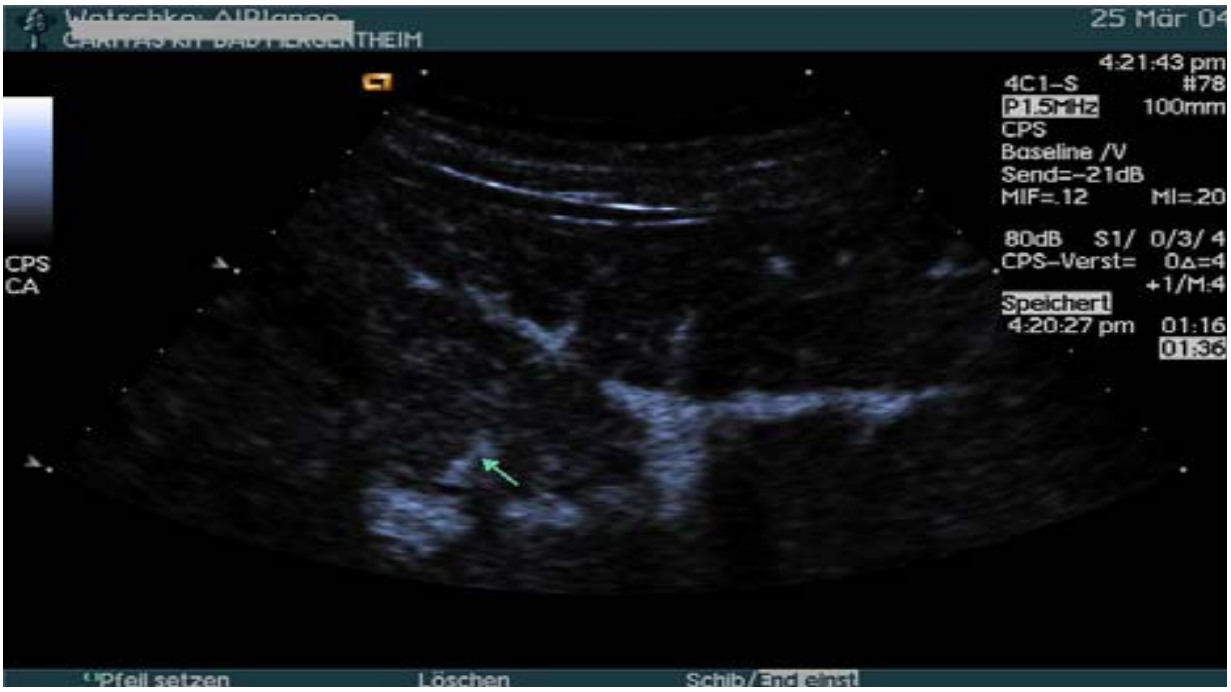

(c)

(Figure 2.9) Hepatic steatosis indicated by focal hyper echoic areas in the liver hilum. They are characterized by centrally located (portal) vein branches identified by colour Doppler imaging (a), spectral analysis (b) and contrast-enhanced ultrasound (c). Such lesions are typically found sub-capsular next to the terse ligament.

2.3.8. Liver cirrhosis

The accuracy of ultrasound in the correct diagnosis of liver cirrhosis in patients with complications (ascites, splenomegaly and collaterals) is high (>90%). In the initial stages and in micronodular cirrhosis, it may be overlooked in up to 30% of cases. Sonographic signs of liver cirrhosis include inhomogenous echo-texture and irregular-nodular liver surface delineation, and a variety of other possible findings, including destroyed vascular architecture, dependent on the

aetiology of the disease (Figure 2.11). Disproportional segment atrophy (and hypertrophy) has also been observed (Figure 2.10)(Christophe F. Dietrich.2011).

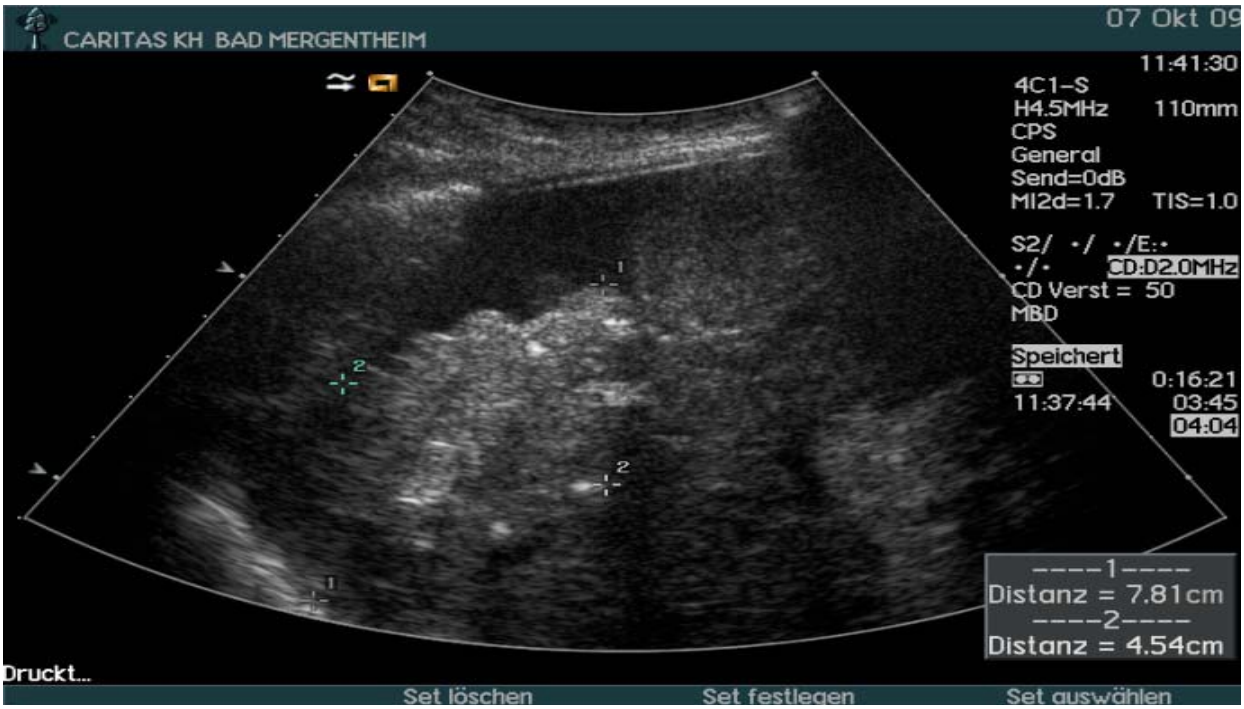

(Figure 2.10) Liver lobes and segments may behave differently during the course of a disease, as shown in this patient with systemic sclerodermy and gradual shrinkage of the right liver lobe (between +). The changes to the liver evolved gradually over 10 years.

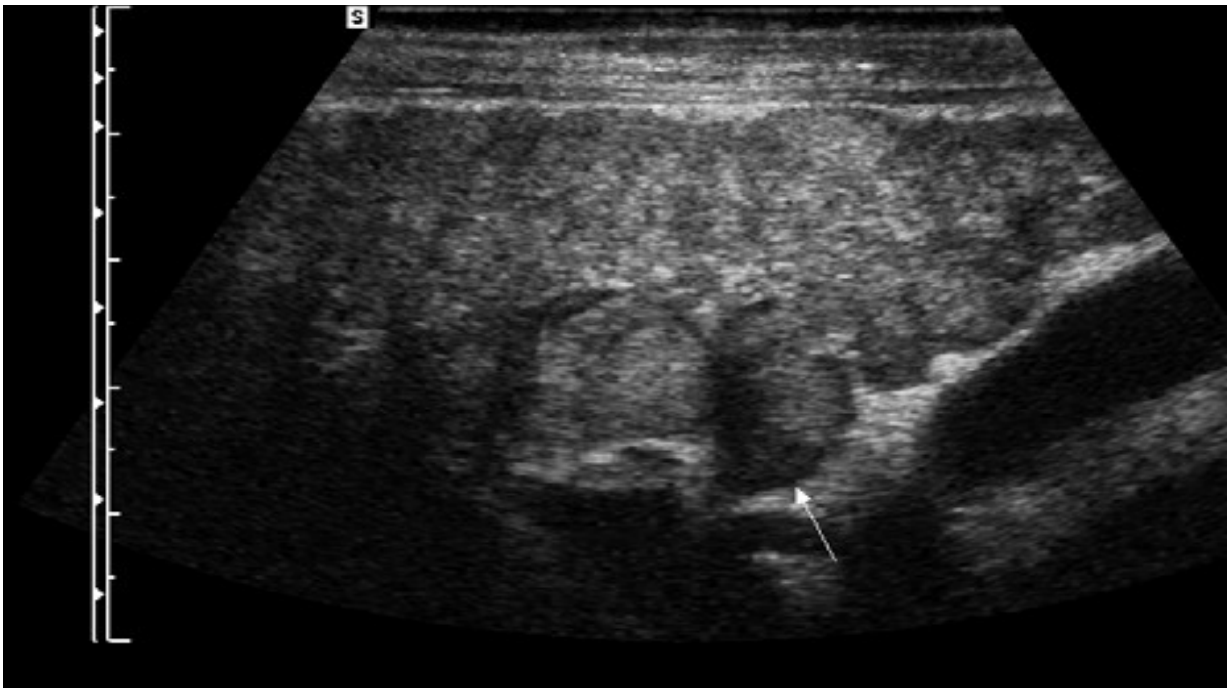

(a)

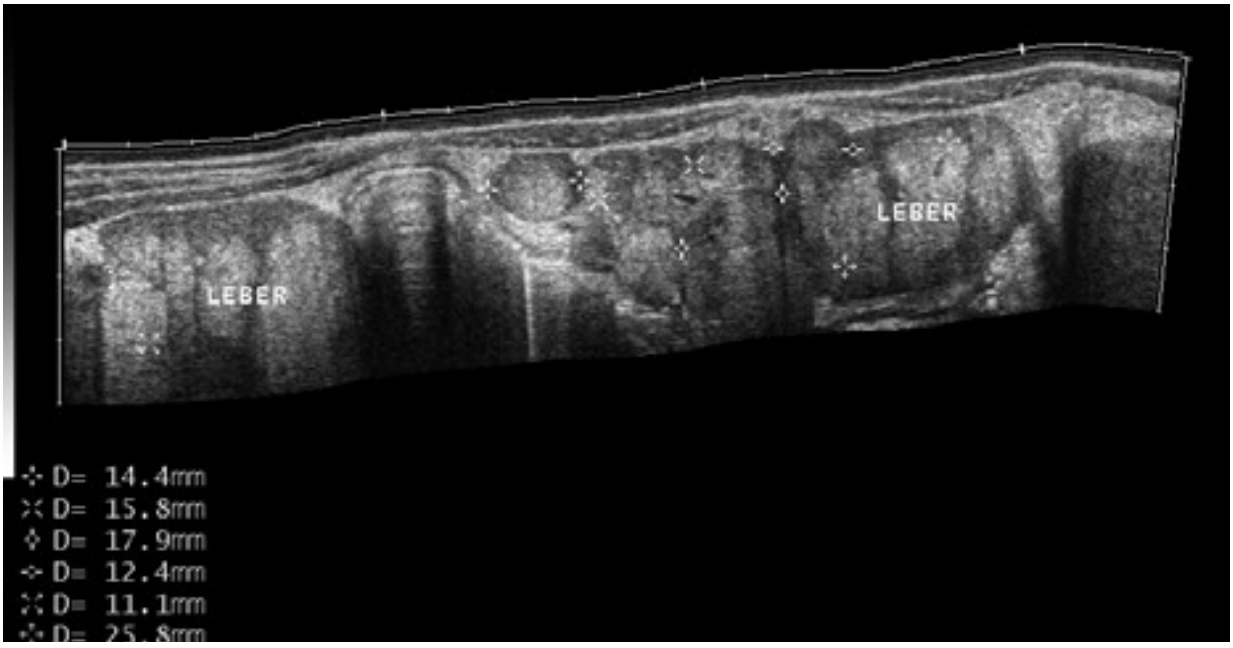

(b)

(Figure 2.11) typical signs of liver cirrhosis include (a) inhomogeneous echo-texture and irregular liver surface delineation (arrow); (b) distinctive nodules are also suggestive. Sometimes

it may be difficult to identify the liver parenchyma, in these cases the organ is indicated as well: Leber: liver.

Nodular liver surface (especially when using high frequency transducers) has an excellent positive predictive value (close to 100%) for cirrhosis. A disproportional volume enlargement of the caudate lobe in relation to the right and left lobe can be indicative of liver cirrhosis, but this sign is of limited value in daily clinical practice (Christophe F. Dietrich.2011).

Coarse liver parenchyma and a disturbed or destroyed vascular architecture as a sign of portal hypertension, such as reversed portal flow and collateral vessels, are other indicators of liver cirrhosis. In Doppler studies, a rise in the arterioportal peak velocity ratio (maximum velocity of the hepatic artery divided by the maximum velocity of the vena portae) of more than 3.5 is predictive of cirrhosis. The positive predictive value for the detection of portal hypertension is excellent, the signs include reversed portal flow and the detection of collateral vessels. The negative predictive value is not as high; the overall accuracy is only 60%. An enlarged portal vein diameter greater than 1.25cm or a reduced portal vein flow velocity indicates cirrhosis with a sensitivity and specificity of approximately 80%. However, all these parameters are of limited value in daily clinical practice (Christophe F. Dietrich.2011)

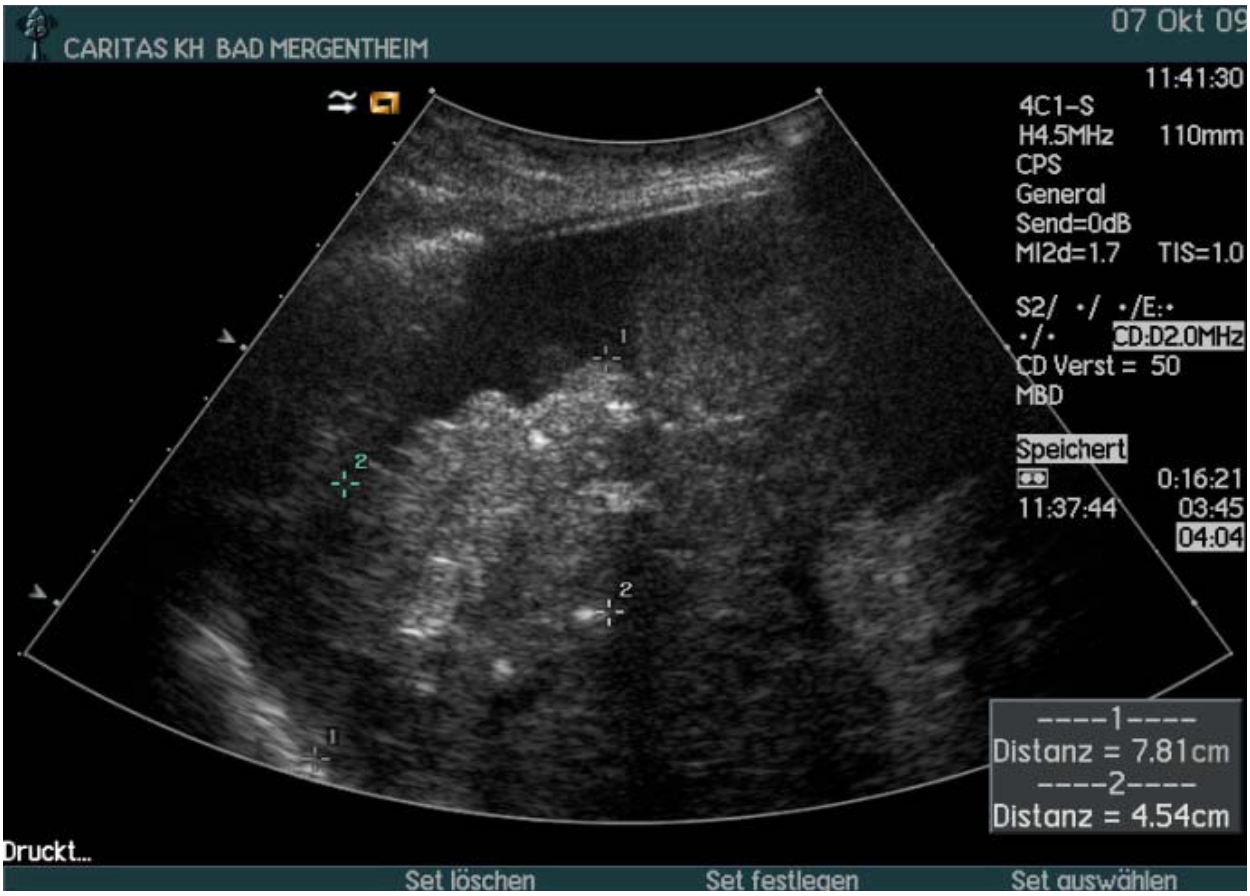

(Figure 2.12) Liver lobes and segments may behave differently during the course of a disease, as shown in this patient with systemic sclerodermy and gradual shrinkage of the right liver lobe (between +). The changes to the liver evolved gradually over 10 years.

2.3.9. Detection of lymph nodes in the hepatoduodenal ligament (perihepatic lymphadenopathy)

Improvement of sonographic technology, techniques and knowledge of well-defined anatomical sites of perihepatic lymph nodes (between the inferior cava and portal vein next to the right renal artery) have led to improved identification of, not only, enlarged, but also normal sized lymph nodes in the liver hilum by ultrasound. Normal lymph node size is up to 19 mm. Two groups of lymph nodes can normally be detected: the dorsal in the hepatoduodenal ligament adjacent to the

cystic duct (”cystic duct nodes”) and ventral in the hepatoduodenal ligament adjacent to the orifice of the foramen epiploicum next to the common hepatic artery (Figure 11). The liver hilum should be examined in a slight left lateral oblique patient position (15-30o) with the right arm elevated, thus improving the detection rate from 25% to 75% compared with the decubitus position (Christoph F. Dietrich.2011).

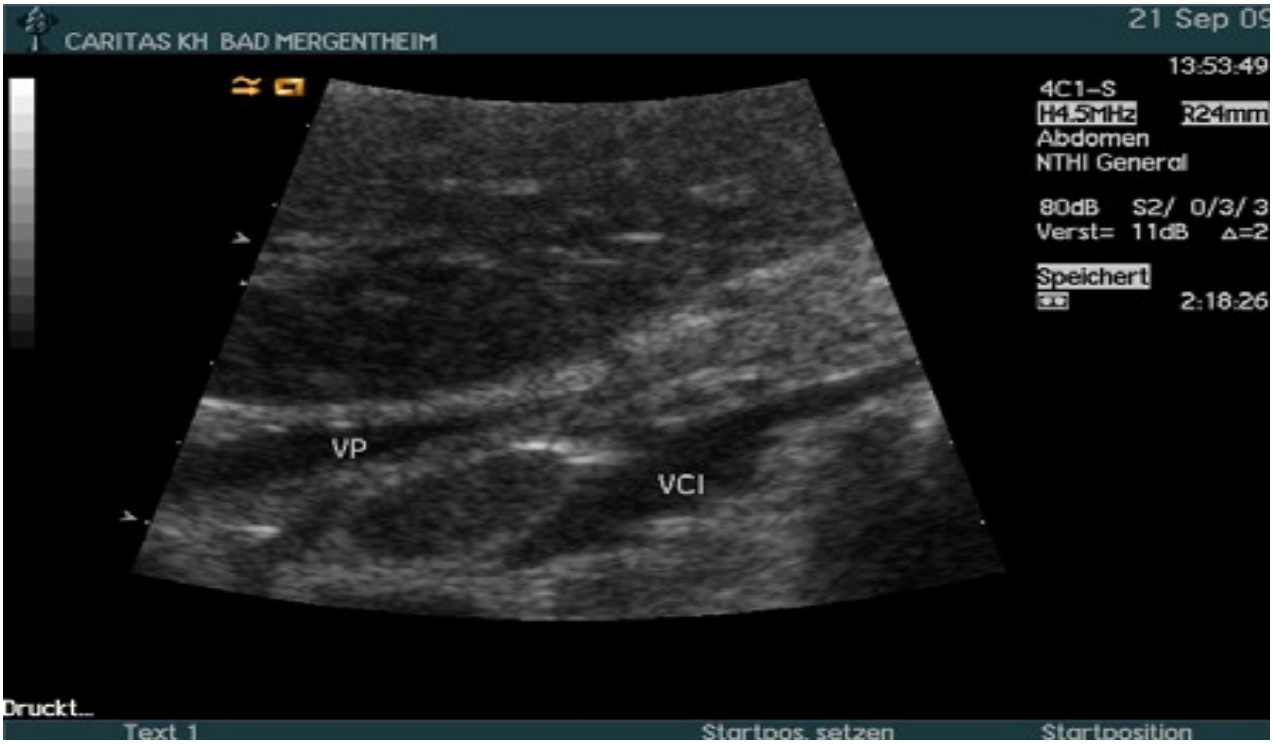

(a)

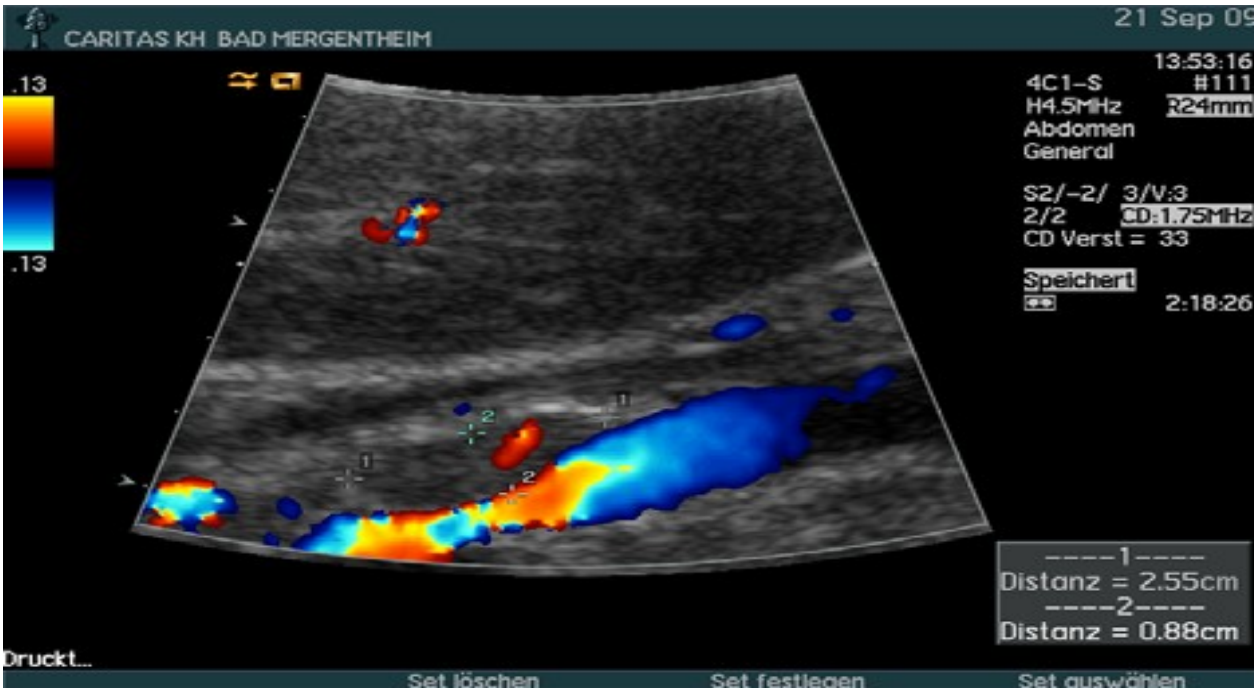

(b)

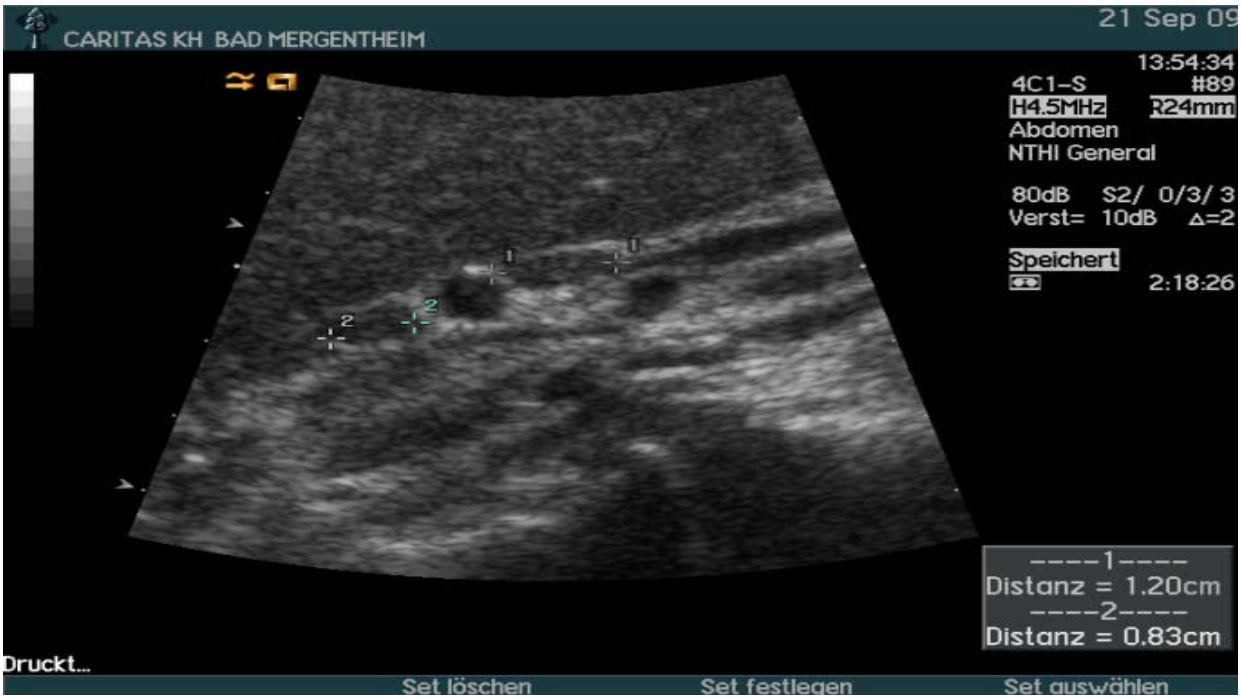

(c)

(Figure 2.13) Two groups of lymph nodes can normally be detected in anatomical examinations:

the dorsal group in the hepatoduodenal ligament adjacent to the common hepatic bile duct and cystic duct (“cystic duct nodes”, seen in (a) and (b) between markers (+). VCI, inferior vena cava; VP, portal vein; and (c) ventral in the hepatoduodenal ligament adjacent to the orifice of the foramen epiploicum next to the common hepatic artery (between markers).

2.3.10. Acute viral hepatitis

There are no significant changes in liver echo-texture in acute viral hepatitis. However, enlarged perihepatic lymph nodes are a fairly constant feature, which is also present in chronic hepatitis, conditions such as viral and autoimmune hepatitis (AIH) (including primary sclerosing cholangitis (PSC)), but not in toxic inflammatory liver disease or haemochromatosis. One study of 40 patients with acute hepatitis found enlarged perihepatic lymph nodes could be identified by transabdominal ultrasound in all patients with adequate visualisation of the liver hilum (a sensitivity of 100%), which is helpful to differentiate between toxic and viral genesis. Additionally, in chronic liver disease, perihepatic lymphadenopathy was present in 86% of patients with viral hepatitis, in 90% with AIH, in 100% with PSC, in 97% with primary biliary cirrhosis (PBC), but in only 6% with haemochromatosis, in 1% with fatty liver disease and in 4% with cholecystolithiasis (Christoph F. Dietrich.2011).

Doppler techniques can be used to exclude complications (e.g. portal vein thrombosis) and reveal an unspecific hyperdynamic state in hepatic vessels with a higher diastolic arterial blood flow when compared with healthy individuals. Portal venous blood flow is increased and, perhaps owing to oedema and narrowing of the hepatic veins, the flow pattern is often monophasic.

Gallbladder wall thickening (Figure 12) is a short-life sonographic phenomenon of early phase acute hepatitis in approximately 50% of patients. This must not be confused with acute

cholecystitis where there is no circumscript pain under ultrasound visualized palpation. (Christoph F. Dietrich.2011).

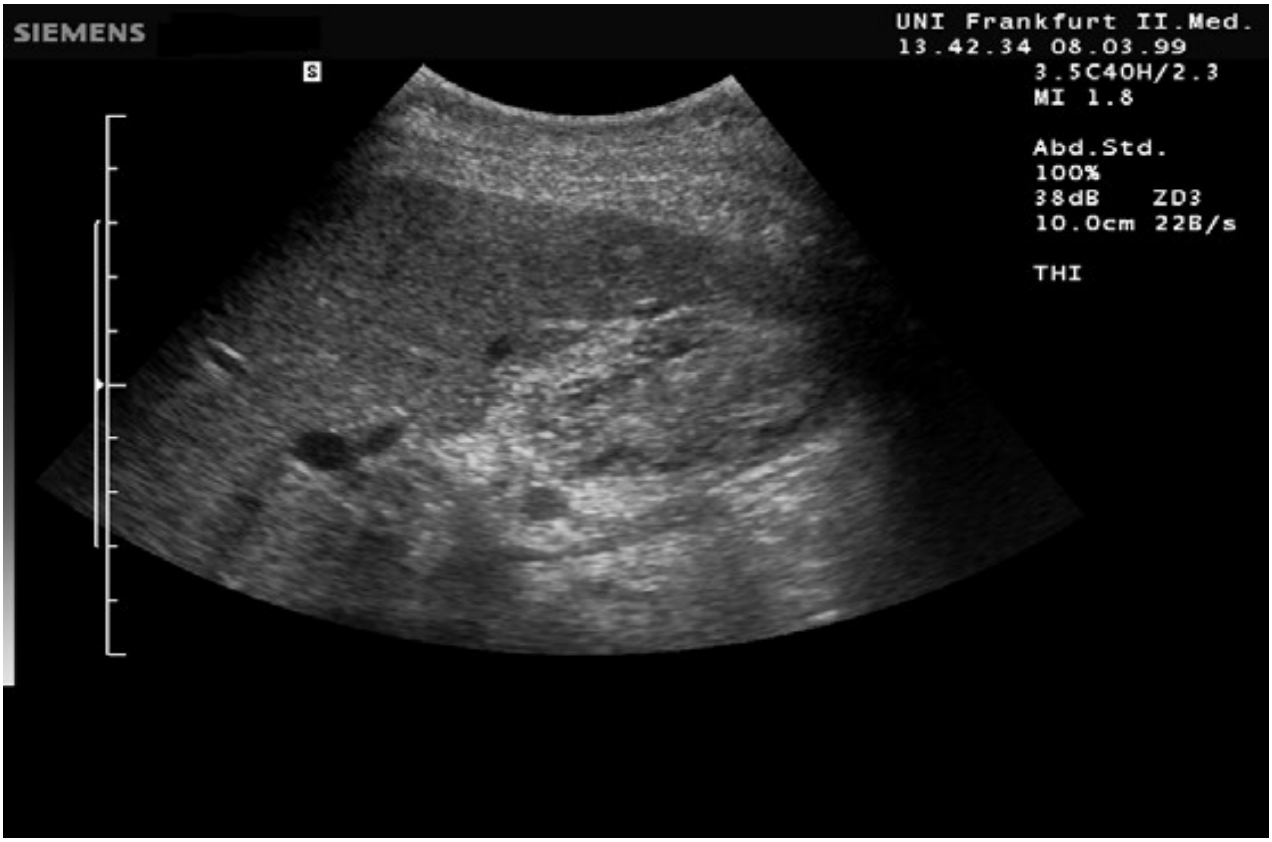

(Figure 2.14) Gallbladder wall thickening in acute hepatitis is a short-life sonographic phenomenon of early phase acute hepatitis in approximately 50% of patients, which can be confused with acute cholecystitis.

2.3.11. Chronic viral hepatitis C

In patients with chronic viral hepatitis C (HCV) infection, hepatic steatosis is a frequent histological finding and occurs in more than 50% of cases. The reason for this remains poorly understood; even when the most common causes of steatosis are excluded, a significant

proportion of patients with chronic HCV infection show signs of liver steatosis (Christoph F. Dietrich.2011).

2.3.12. Perihepatic lymphadenopathy

Lymph nodes are detectable within the hepatoduodenal ligament in almost all patients with chronic HCV. The total perihepatic lymph node volume changes according to the antiviral response and leads to progressive normalization of the perihepatic lymph node volume in those with a sustained virological response. A decrease in perihepatic lymph node volume is associated with an improvement in liver histology. Mediastinal lymphadenopathy has also been described in patients with chronic HCV using mediastinal ultrasound, whereas other abdominal lymph node locations are not significantly altered in patients with the infection (Christoph F. Dietrich.2011).

2.3.13. Primary biliary cirrhosis

The echo-texture of the liver parenchyma in patients with PBC in Stage I and II is often unremarkable. In Stage IV typical signs of liver cirrhosis are detectable. The liver parenchyma of patients with Stage III PBC show advanced sonomorphological modifications such as inhomogenous parenchyma, but no indicative signs of liver cirrhosis. The extent of perihepatic lymphadenopathy reflects the progression of the disease with a larger lymph node size in more advanced stages.

2.3.14. Primary sclerosing cholangitis

Neither the clinical symptoms nor the biochemical evidence of cholestasis are specific to PSC and they lack sensitivity, particularly in the early course of the disease. Ultrasound is useful in the detection and follow-up of extrahepatic bile duct lesions, but it should be noted that

alterations of the intrahepatic duct system are not displayed under all circumstances. Asymmetric mural thickening is a typical ultrasound finding in advanced PSC (Figure 13), but it is important to mention that symmetric mural thickening by itself is a rather unspecific marker for cholangitis. Finally, enlarged hilum lymph nodes are detectable in almost all patients with PSC (Christoph F. Dietrich.2011).

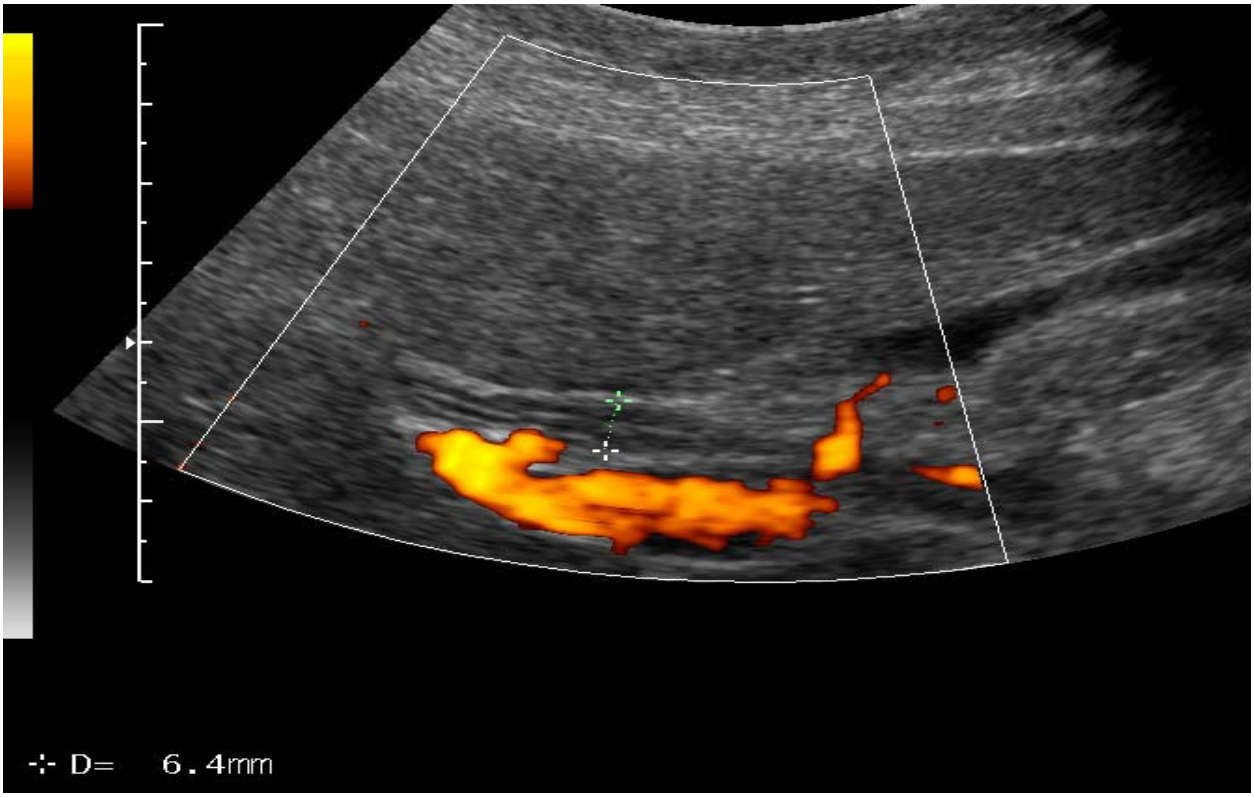

(Figure2.15) Asymmetrical mural thickening of the common bile duct (between markers, +) is a sensitive sign of primary sclerosing cholangitis.

2.3.15. Other diffuse liver diseases

Patients with autoimmune hepatitis (AIH) generally show perihepatic lymphadenopathy with lymph nodes over 19mm in size. There are no other typical ultrasound features of liver texture or

the hepatobiliary tract in patients with AIH. Changes in the liver parenchyma and echo-texture in patients with sarcoidosis are unspecific, but occasionally circumscribed (isoechoic) sarcoid infiltrations can be observed, which mimic malignancies even with contrast-enhanced techniques. Perihepatic lymphadenopathy in these patients is sometimes impressive with lymph nodes of up to 60mm noted. Perihepatic lymphadenopathy is indicative of hepatic involvement. In patients with advanced disease, signs of liver cirrhosis and portal hypertension are common with the respective flow changes of the hepatic vessels. Similar to PBC, the flow pattern in the portal and hepatic veins is increased in contrast with other forms of liver cirrhosis (Christoph F. Dietrich.2011).

In the recently published literature none of the cystic fibrosis patients showed enlarged perihepatic lymph nodes (with the exception of patients with CBD stones and cholangitis). There are no typical liver echo-texture sonographic findings. One study reported a micro-gallbladder as a typical sign of cystic fibrosis. The authors found a frequency of 18 in 72 (25%) patients compared with 0 in the control group (Christoph F. Dietrich.2011).

In patients with alcoholic steatohepatitis (ASH) and non-alcoholic steatohepatitis (NASH) the attenuation of the ultrasound beam makes it difficult to examine the liver hilum. Adequate visualisation is possible in only 80% of patients. In a series of 60 patients no enlarged perihepatic lymph nodes could be found (unpublished data by the author). Toxic liver disease is frequently encountered, but sonographic features in patients are unspecific. In a currently unpublished series of 100 patients, no enlarged perihepatic lymph nodes could be found (personal communication).

Changes to liver parenchyma in patients with human immunodeficiency virus infection are dependent on opportunistic infections or neoplastic infiltration. Many causes have to be considered [e.g. bacillary angiomatosis]. In a consecutive series, 82 of 100 patients with acquired immune deficiency syndrome showed enlarged perihepatic lymph nodes (unpublished data by

the author). Coinfection with hepatitis B and C virus and mycobacteriosis is common. There was no significant correlation with viraemia. Hepatobiliary infection as a cause of perihepatic lymphadenopathy should also be considered, e.g. cytomegaly virus infection. Enlarged perihepatic lymph nodes have been found in almost all patients with end-stage liver disease.

Wilson's disease is a rare autosomal-recessive inherited disorder of copper metabolism, which results in the accumulation of copper in the liver and many other organs. Liver disease varies depending on the severity of the disease at time of diagnosis. Histopathological findings include (focal) fatty changes, signs of acute (including hepatic necrosis) or chronic hepatitis, fibrosis and cirrhosis. Liver imaging findings reflect a wide range of physiopathological processes of the disease and demonstrate the associated findings of cirrhosis in cases with advanced disease.

Ultrasound findings in end-stage Wilson’s disease resemble liver cirrhosis caused by other aetiologies. In early stages multiple intrahepatic small (<20mm) hypoechoic nodules were observed in 8 out of 10 consecutive patients with Wilson’s disease (unpublished data by the author). In these lesions biopsy and histological examination revealed prominent copper accumulation in comparison with the surrounding liver parenchyma (Figure 14). In two patients additional dysplastic nodules were observed (Christoph F. Dietrich.2011).

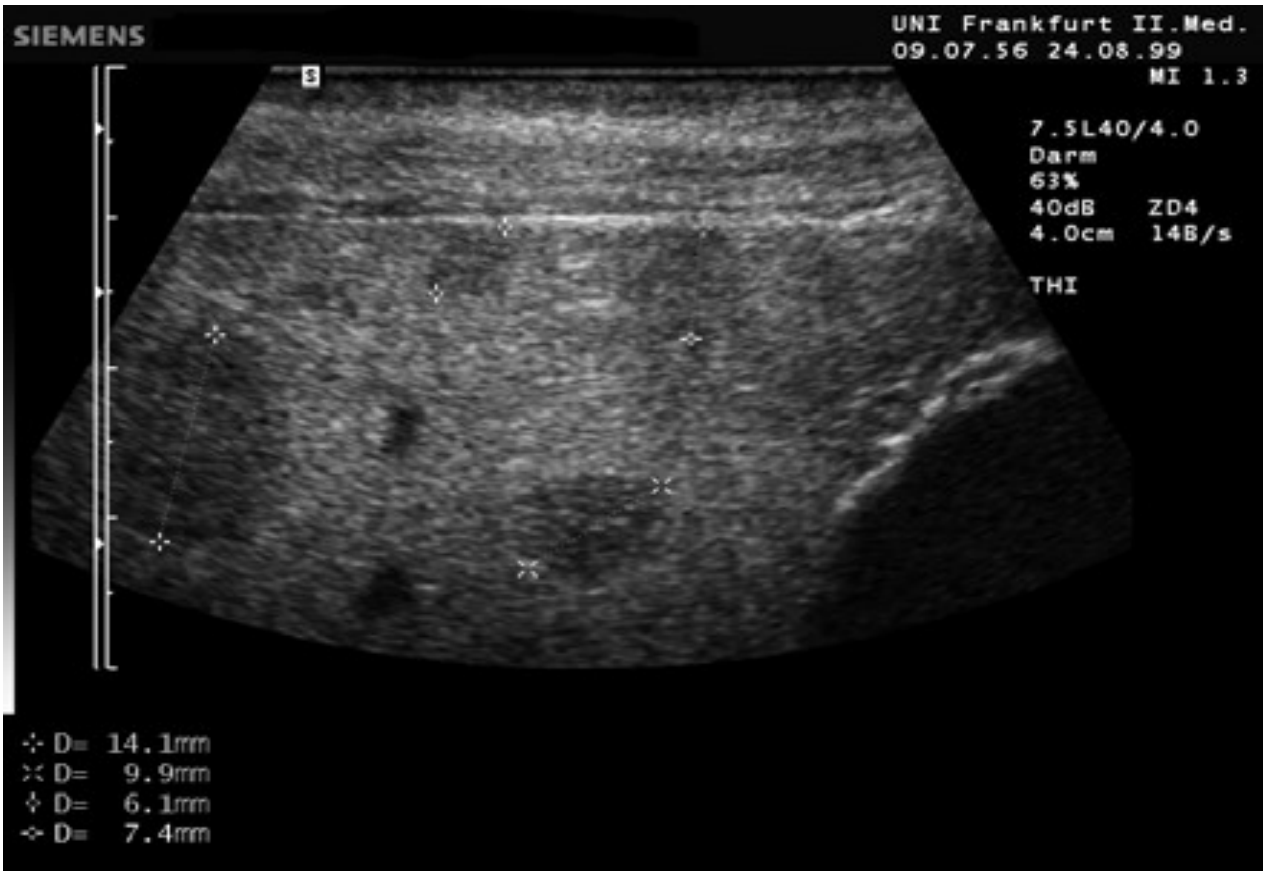

(Figure 2.16) Wilson disease. The parenchymal echo pattern has typical increased echogenicity with abundant round or oval foci of decreased echogenicity (shown between the callipers) resembling metastatic liver disease. Biopsy and histology revealed prominent copper accumulation.

There are many liver diseases with specific and unspecific ultrasound changes that are not described here. We have focused on the common diseases of the Western world; however, examples with striking ultrasound features from elsewhere in the world include patients with hepatobiliary schistosomiasis and portal hypertension who show typical fibrotic strands as sequelae of fibrous portal venous obliteration (Figure 2.16)

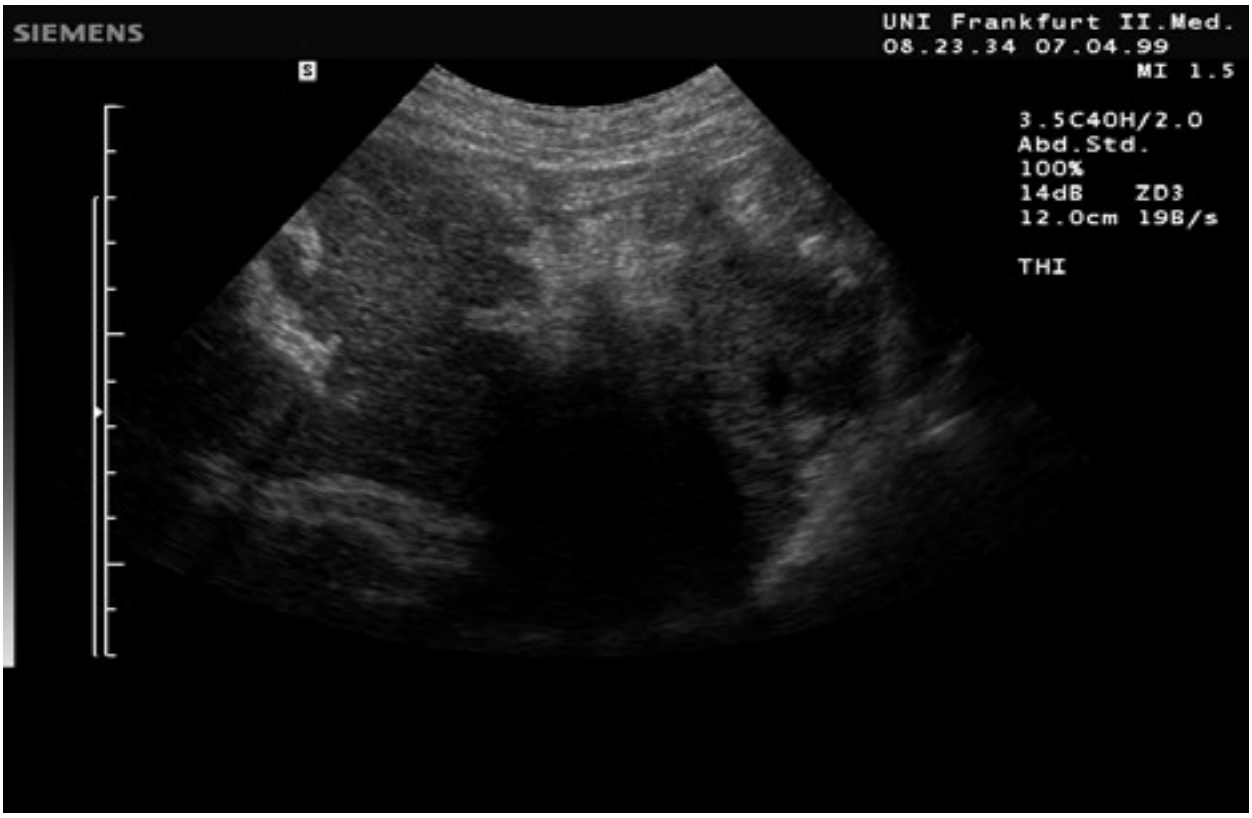

(Figure 2.17) Schistosomiasis shows hyperechoic typical fibrotic strands as sequelae of fibrous portal venous obliteration.

2.3.16. Doppler ultrasound techniques in the evaluation of liver disease

2.3.16.1. Anatomy and blood supply

Hepatic perfusion is characterized by two vascular systems with completely different hemodynamic and one outflow system:

- Arterial inflow (high pressure, low flow resistance) (Figures 2.17)
- Portal-venous inflow (low pressure, low flow resistance) (Figure 2.18)
- Venous outflow (low pressure and low flow resistance) (Figure 2.19)

Vascular hepatopathies include the abnormal vascular course, aneurysms, stenoses and occlusions of the vessels in these systems (Christoph F. Dietrich.2011).

2.3.16.2. Arterial flow

Arterial liver perfusion disorders are rare for both hypo- and hyperperfusion. A diminished arterial blood flow can be caused by congenital malformations as well as by acquired embolic, thrombotic, inflammatory, vascular-tumourous, vasculitic or arteriosclerotic-degenerative changes, or, in acute myocardial, by forward failure and shock. Hyperperfusion is observed even less frequently and is due to arteriovenous shunts, of congenital (e.g. Osler's disease), traumatic or septic-embolic origin. Pathological sonographic findings of arterial vessels are summarised, examples include:

- Hypoplasia and aplasia of the common hepatic artery and/or its branches with atrophy of related liver segments,
- Aneurysms of the common hepatic artery and its branches,
- Atypical vascular courses (e.g. with impression of the hepatic choledochal duct),
- Arteriovenous and arterioportovenous shunts (e.g. Osler's disease)

Abnormal hepatic vascular malformations occur more frequently in connection with vascular changes in other organs (heart, lungs, brain and kidneys), which tend to determine the clinical course and prognosis (Christoph F. Dietrich.2011)

.

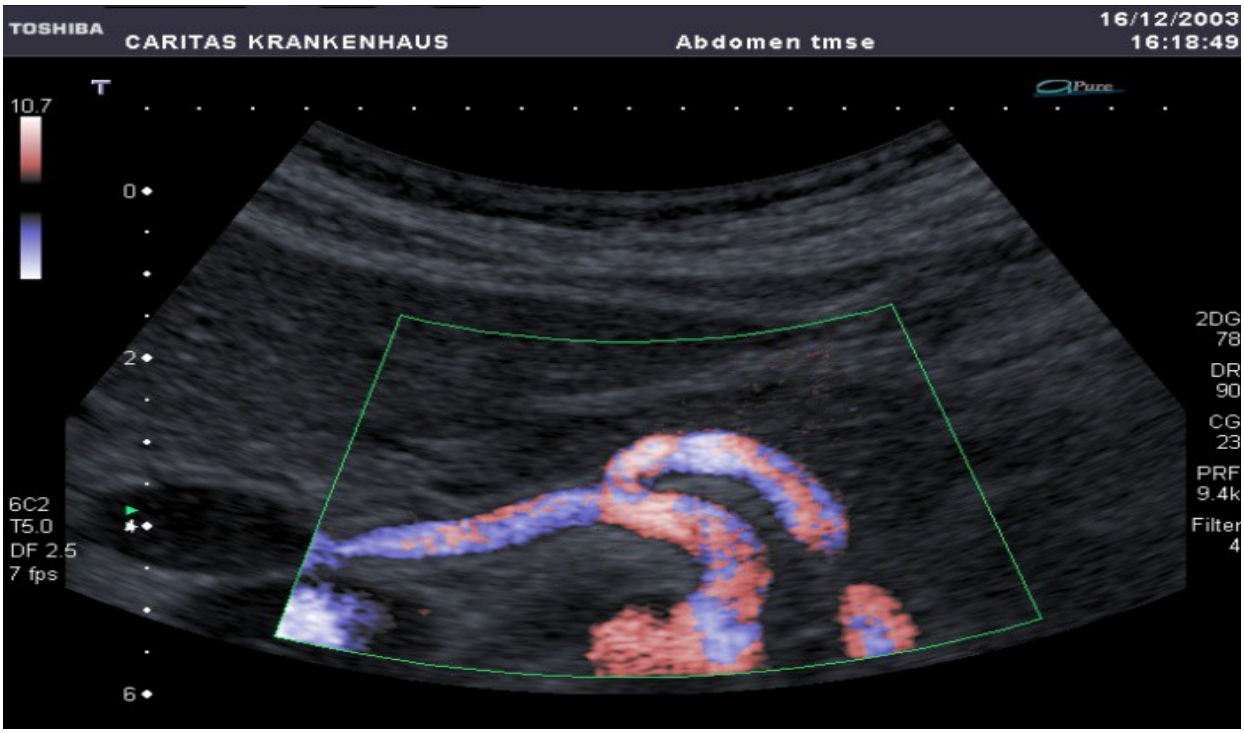

(Figure 2.18) colour Doppler imaging of the coeliac trunk, which supplies the arterial blood for the liver and the perihepatic structures. The liver hilum is often best examined in a left lateral decubitus position.

2.3.16.3. Portal venous system

Signs of portal hypertension (splenomegaly, ascites and collateral vessels) with continued liver function impairment can be shown on ultrasound. The most important disorder to identify is portal vein thrombosis (collier, j.et al, 2002).

2.3.16.4. Venous outflow

In disorders of venous outflow, firstly liver function is substantially restricted and secondly, signs of high portal vein pressure are detected. Right-ventricular heart failure is the most common venous outflow disorder. The increase in post-hepatic resistance reduces portal hepatic perfusion

and can lead to a pendular or retrograde flow in the portal vein, especially in cases with an additional intra-hepatic increase in resistance (collier, j.et al, 2002).

2.3.16.5. Colour Doppler imaging for analysis of hepatic vessel flow pattern – an introduction

Colour Doppler imaging (CDI) is an accurate and well-established technique in evaluating portal hypertension, portal vein thrombosis, Budd-Chiari-syndrome and other forms of veno-occlusive disease (VOD). CDI is routinely used to evaluate patients prior to liver transplantation to determine portal vein patency, signs of portal hypertension and hepatic artery patency post-operatively. CDI is also important to monitor flow direction and patency of spontaneous and artificial portosystemic shunts, e.g. transjugular intrahepatic portosystemic shunts (TIPSS). Post-liver transplantation patients are monitored by analysing the hepatic artery profile; stenosis and rejection are indicated by changes in the resistance flow pattern (e.g. pulsus parvus et tardus).
Chronic heart failure reveals tetra-phasic flow in the right liver vein and highly undulating flow patterns in the portal vein, which reverses during intensified therapy. Analysis of the flow pattern in the hepatic veins is helpful to characterise diffuse parenchymal liver disease (Christoph F. Dietrich.2011).

2.3.16.6. Vascular (Doppler) indices

Vascular indices, (e.g. Doppler perfusion index (DPI)), hepatic transit time and various ratios analysing different vessels have been used for liver tumour detection and characterisation, but are currently only used in experimental settings. The portal vein congestive index (PVCI) is defined as the ratio of cross-sectional area of the extra-hepatic portal vein to the time averaged mean velocity of blood flow in the portal vein. The PVCI is elevated in liver cirrhosis at an early

stage with a constant portal vein blood flow (cross-sectional area multiplied by the time averaged mean velocity), which can be reached by an increased portal vein pressure with consecutive dilatation of the latter vessel. The method, which, after some training, is more difficult in its wording than in its application, has still not achieved general acceptance.

The DPI is the ratio of hepatic arterial blood flow (normally below 20%) to the total liver blood flow (hepatic arterial and portal venous blood flow). DPI is reported to be elevated in the presence of intra-hepatic tumours as well as in patients with liver cirrhosis, and has been used to screen patients with suspected metastases; however, the promising data could not be reproduced (Christoph F. Dietrich.2011)

2.3.17. Examination of the hepatic artery in patients with diffuse liver disease

2.3.17.1. Examination technique

There are only limited data analyzing hepatic arterial vessels in diffuse hepatic disease compared with portal venous studies. The reason for this is clear: the common anatomical variations of the coeliac trunk in up to 50% of the population do not allow reproducible and standardized examinations. Resistance and pulsatility indices represent the parenchymal influence distal to the measurement point. These indices can therefore represent hepatic parenchymal influence with a certain degree of confidence. Interobserver variability when analysing hepatic arterial blood flow at this measurement point is less than 12%, but much higher for peak systolic, end diastolic and time averaged mean velocity, and for blood flow volume (approximately 30%). Hepatic blood flow can also depend on food intake, posture, activity and is influenced by drugs. (Christoph F. Dietrich ..2011).

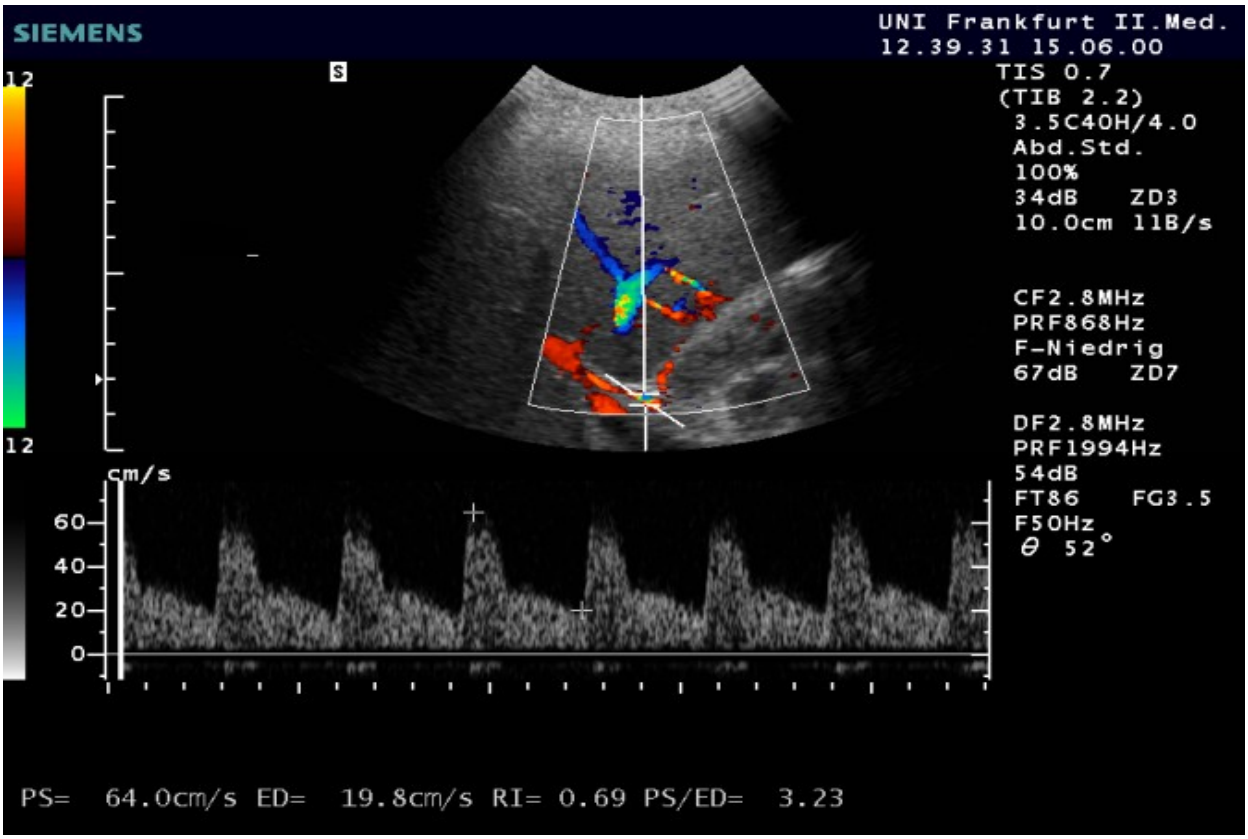

(Figure2.19) The hepatic artery in its typical topographic next to the common bile duct and portal vein .A low resistance flow pattern is typical with significant diastolic flow.

Table 1; Table of normal flow parameters analyzed in 47 healthy probands.

Vessel	TC	AMS	AHC	AHP
PSV (cm/s)	137±45 (53-260)	145±42 (47-228)	102±46 (31-202)	58±34 (23-193)
EDV (cm/s)	39±15 (17-90)	18±9 (5-40)	27±11 (10-56)	20±12 (8-60)
RI	0.7±0.06 (0.59-0.88)	0.87±0.05 (0.74-0.96)	0.71±0.09 (0.5-0.83)	0.65±0.07 (0.52-0.78)
PI	1.86±0.9 (1.03-4.77)	3.74±1.39 (177-7.75)	1.68±0.59 (0.72-2.93)	1.16±0.25 (0.73-1.75)
TAVmax (cm/s)	59±21 (22-115)	37±15 (15.6-73)	45±20 (15-108)	34±20 (13-102)

TAVmean (cm/s)	33±12 (10-70)	22±9 (9-40.66)	25±13 (10–72)	20±12 (9-68)
D (mm)	6±1 (4.2-8.8)	6±1 (4-10)	4±1 (3-7)	3±1 2-6)
BF (ml/min)	630±250 (184-1239)	395±206 (159-1061)	250±220 (88-1163)	105±89 (24-503)
Angle (°)	26±19 (1-60)	42±16 (7-63)	59±14 (22-81)	42±19 (7-73)

TC, celiac trunk; AMS, mesenteric superior artery; AHC, common hepatic artery; AHP, proper hepatic artery; PSV, peak systolic velocity; EDV, end diastolic velocity; RI, resistance index; PI, pulsatility index; TAV max, time averaged maximum velocity; TAV mean, time averaged mean velocity; D, diameter; BF, blood flow volume. Values are mean ± standard deviation (range)
(Christoph F. Dietrich ..2011).

2.3.18. Examination of the portal vein in patients with diffuse liver disease

2.3.18.1. Examination technique

Portal vein diameter and flow pattern is measured using an intercostal approach at an angle close to 0o, just before the portal vein splits into the right and left branches. Biphasic fast Fourier transformation (FFT) Doppler spectrum of the portal vein should be documented during a 5-8s suspended respiration at a mid-respiration level, avoiding respiratory and thoracic pressure influences. The sample gate is adjusted to the inner diameter of thevessel and the FFT spectral

analysis is recorded. The maximum (Vmax) and minimum (Vmin) velocity in centimetres per second of an undulational circle are set automatically or manually. The differences in Vmax and Vmin are calculated as a parameter of biphasic oscillations as well as the portal vein resistance index ((Vmax–Vmin)/Vmax) in a similar way to the resistance index of arterial vessels. The reproducibility of the method was investigated by repeated sonographic examinations of the portal vein flow in 10 healthy individuals over 7 consecutive days. The mean coefficient of variation for intra-individual assessment of the flow velocity (Vmax and Vmin) was 12% and 10%, respectively. (Christoph F. Dietrich.2011)

2.3.18.2. Normal and pathological portal venous blood flow

Normal portal venous blood flow undulates slightly (normal values, 12–24cm/s using the intercostals approach with a mean resistance index of 0.36). Different pathological flow patterns of the portal venous system have also been described.

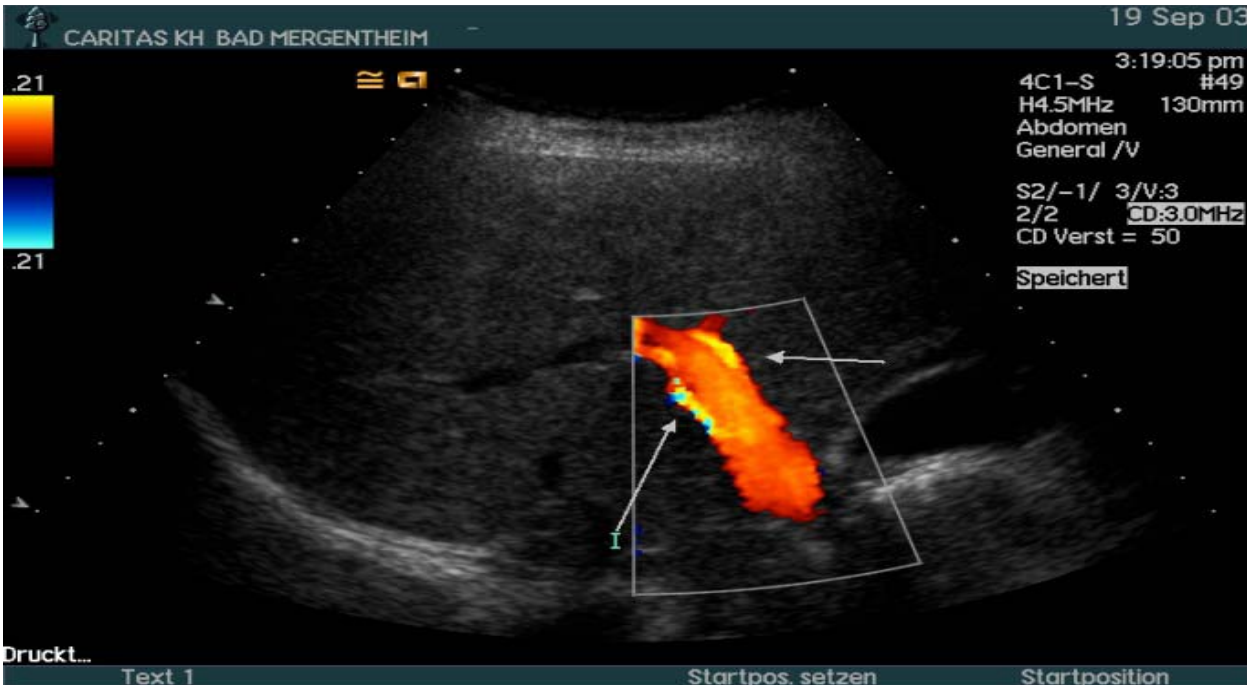

(a)

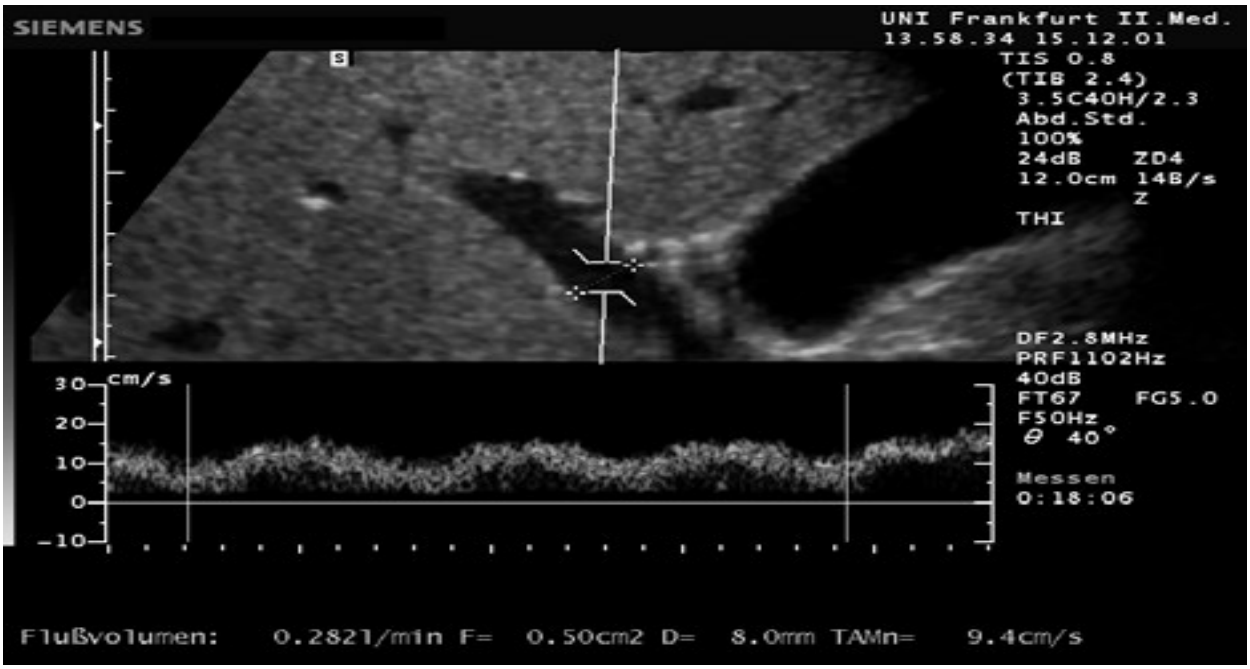

(b)

(Figure 2.20) the portal vein (arrows) is scanned using a transcostal approach on (a) colour

Doppler imaging and (b) continuous duplex scanning with a normal flow pattern range of 12–24cm/s.

2.3.18.3. Portal hypertension

Colour Doppler ultrasound examination is recommended in patients with suspected portal hypertension because CDI is helpful in the detection of the presence and direction of blood flow within the portal venous system. Hepatofugal flow in the portal vein is found in approximately 10% of patients with liver cirrhosis. Prevalence does not differ in relation to the aetiology of liver cirrhosis, but it is stage dependent and is often found more frequently in Child B and C cirrhosis compared with Child A cirrhosis. The clinical significance of this Doppler phenomenon is still unclear, especially in relation to repeat variceal bleeding. Increased pulsatile flow (high resistance index) in the portal vein has predominantly been found in patients with severe right heart failure, demonstrating that right atrial pressure is negatively correlated with portal vein pulsatility ratio (Figure 19). In patients with steatosis the flow is flattened and is demonstrated by a low resistance index (Christoph F. Dietrich.2011)

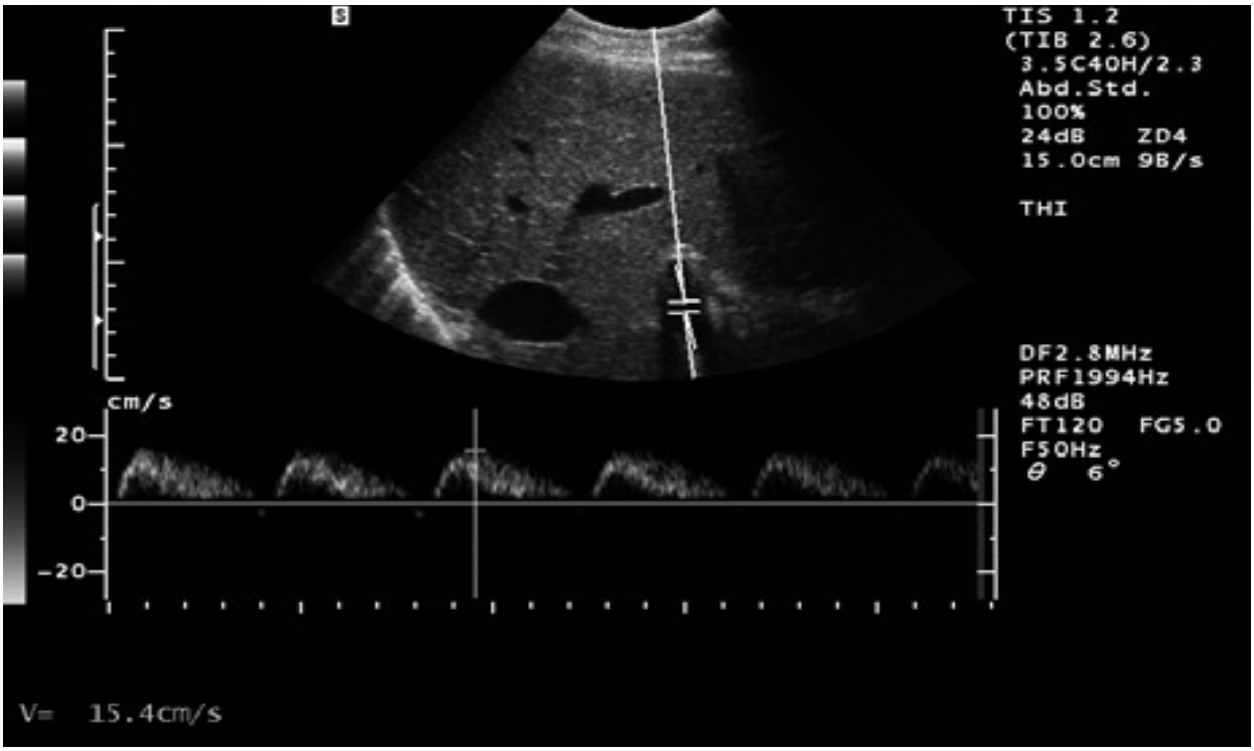

(Figure 2.21) Increased pulsatile flow in the portal vein, which is predominantly found in patients with severe right heart failure and demonstrates that right atrial pressure is negatively correlated with the portal vein pulsatility ratio.

2.3.18.4. No portal venous blood flow

Very slow portal vein velocities of less than 2cm/s are difficult to detect because the Doppler signal is lower than the threshold of the ultrasound equipment and additional respiratory modulation of the patient. A stagnant or portal venous "0" flow is seen mainly in patients with advanced liver cirrhosis. In patients with stagnant portal vein flow the use of ultrasound contrast enhancing agents may be helpful in the exclusion of portal vein (appositional) thrombosis (Christoph F. Dietrich.2011).

2.3.18.5. Retrograde portal venous blood flow

Reversed portal venous blood flow can be observed when intrahepatic resistance is greater than the resistance of portosystemic collaterals (Figure 20). An association has been found between portal venous flow patterns (e.g. abnormal flow direction) and the presence of, mainly spontaneous, portosystemic shunts as well as esophageal varices and ascites. The increase of intrahepatic resistance may be explained by structural abnormalities, e.g. hepatocyte enlargement, space of Disse collagenisation and hepatic vein sclerosis. Retrograde portal venous flow has mainly been observed in patients with portal hypertension. Respiration dependent hepatofugal portal flow is a rare finding associated with periodic portal hypertension in patients with right heart insufficiency and/or liver disease; the clinical significance is unclear (Christoph F. Dietrich.2011).

Pulmonary hypertension, pericardial effusion, constrictive pericarditis, pericardial tumours, right atrial tumour and other causes that lead to an increased right atrial pressure are responsible for pressure-related hepatic venous out-flow block with subsequent trans-sinusoidal hepatoportal shunting, similar to the mechanical outflow block that causes reversed pulsatile flow in liver cirrhosis. Portal vein–hepatic vein shunts and portocaval (portosystemic) shunts may also cause pulsatile portal flow. (Christoph F. Dietrich.2011).

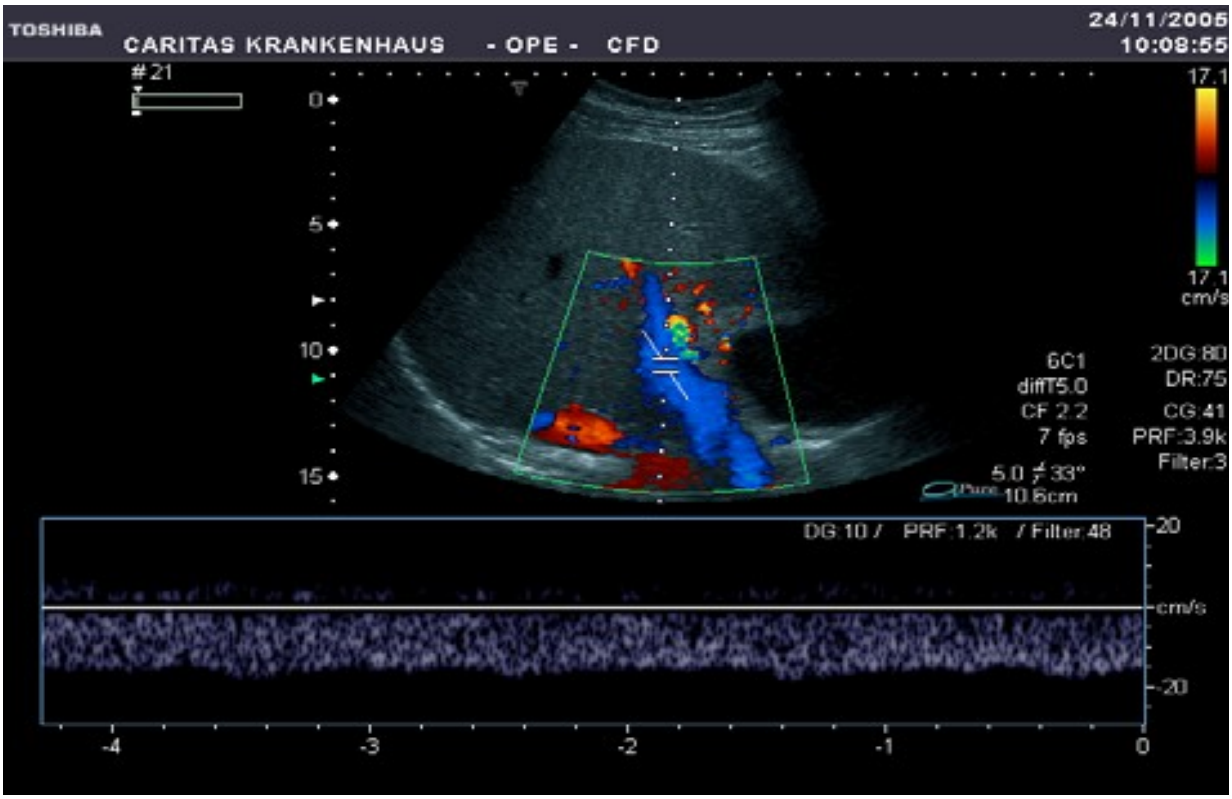

(Figure 2.22) Retrograde portal venous blood flow as a typical sign of severe portal hypertension.

2.3.18.6. Portal vein thrombosis

Portal vein occlusion with an increase in pre-hepatic portal vein pressure may have a variety of causes including coagulation defects with thrombocystosis, an increase in fibrogen concentration owing to inflammation have to be encountered.

Periportal venous collaterals, as a cavernous transformation, may at least partially compensate the portal venous hepatic inflow. Reduced portal venous blood supply may be compensated by an increased arterial perfusion so that liver function appears only slightly impaired. However, portosystemic collaterals lead to a reduced “first-pass” deteriorating effect (e.g. encephalopathy). This is especially important when portal vein thrombosis is caused by cirrhosis with a reduction

of flow, because of this, encephalopathy may manifest and liver-dependent medication metabolism may be disturbed. Colour-coded duplex sonography is the method of choice for detection. It has a high degree of sensitivity (>90%) for the detection of localised segmental or complete portal venous thrombosis (Figure 2.23) (Christoph F. Dietrich.2011).

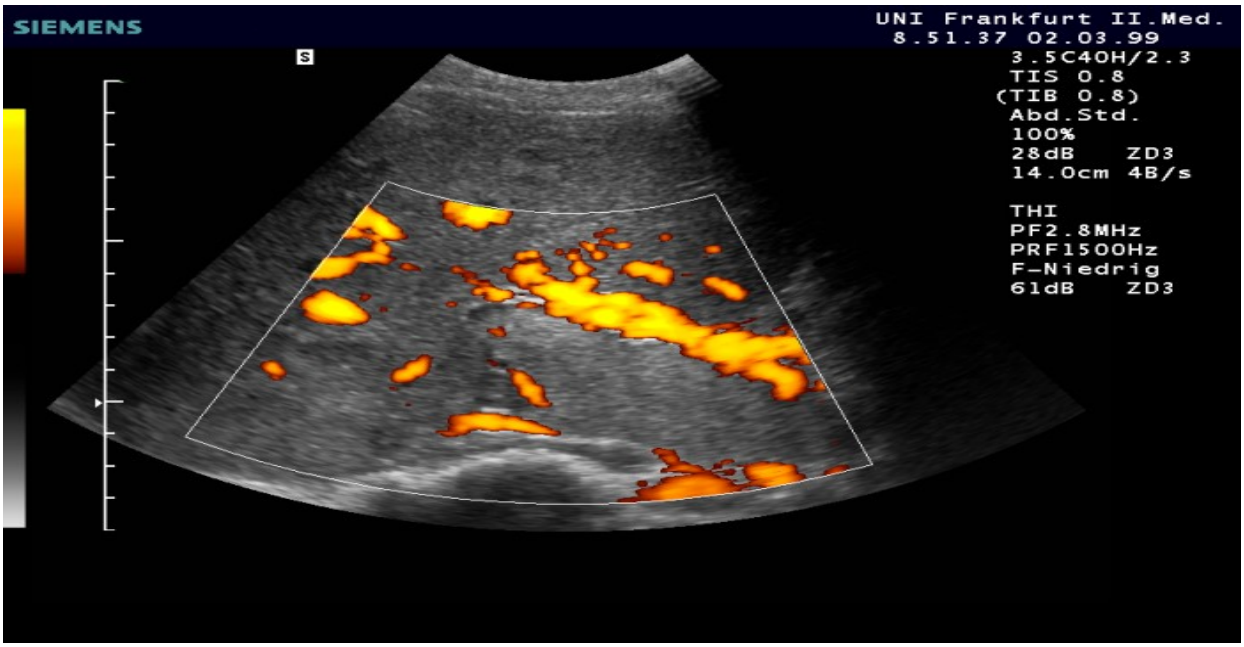

(a)

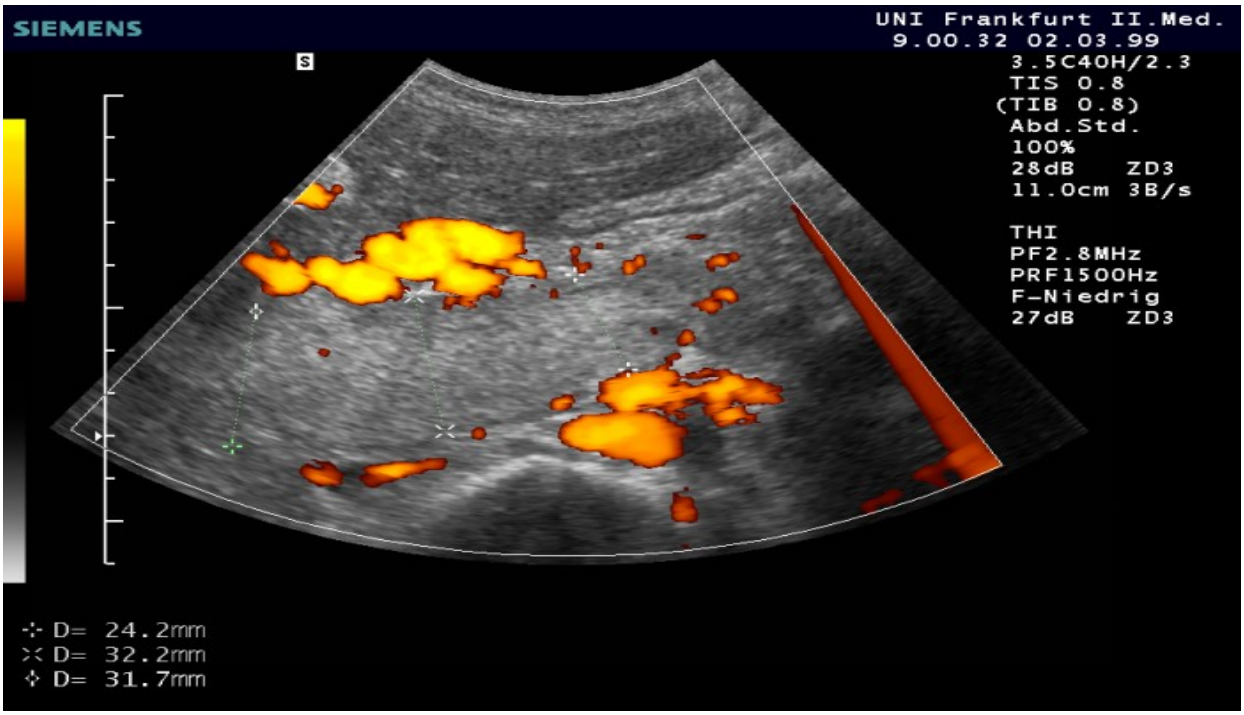
SIEMENS
UNI Frankfurt II.Med.
9.00.32 02.03.99
3.5C40H/2.3
TIS 0.8
(TIB 0.8)
Abd.Std.
100%
28dB ZD3
11.0cm 3B/s
THI
PF2.8MHz
PRF1500Hz
F-Niedrig
27dB ZD3
D= 24.2mm
D= 32.2mm
D= 31.7mm

(b)

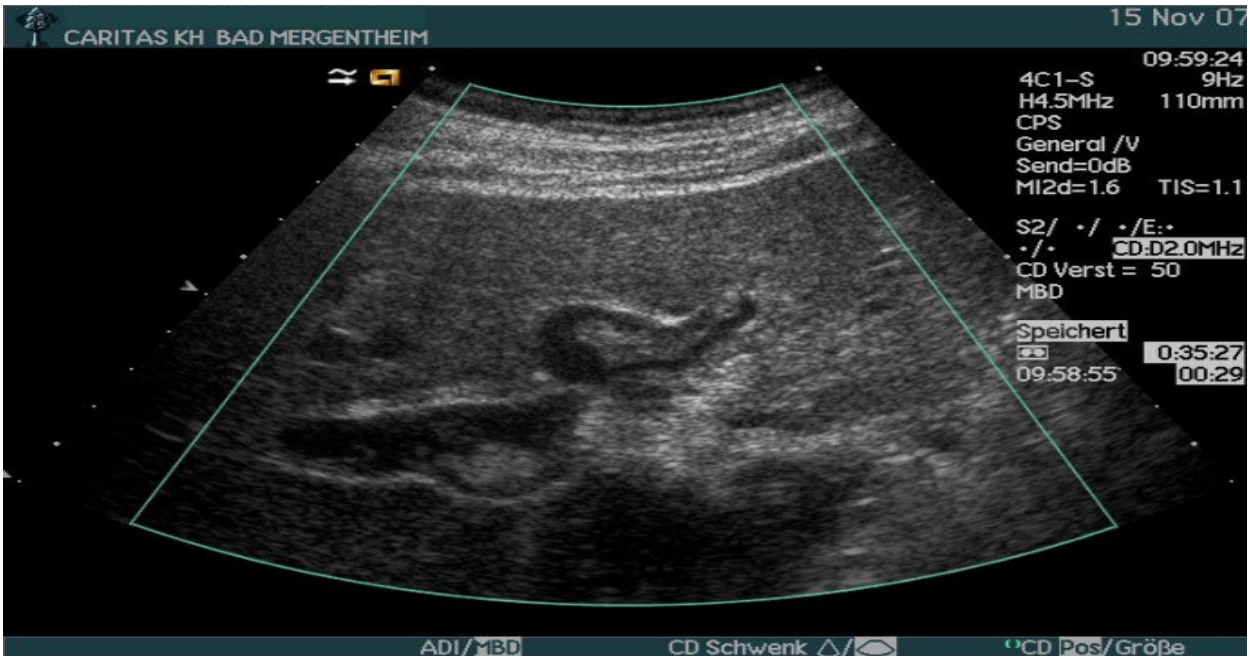
CARITAS KH BAD MERGENTHEIM
15 Nov 07
09:59:24
4C1-S 9Hz
H4.5MHz 110mm
CPS
General /V
Send=0dB
MI2d=1.6 TIS=1.1
CD:D2.0MHz
CD Verst = 50
MBD
Speichert
0:35:27
09:58:55 00:29
ADI/MBD
CD Schwenk
CD Pos/Größe

(c)

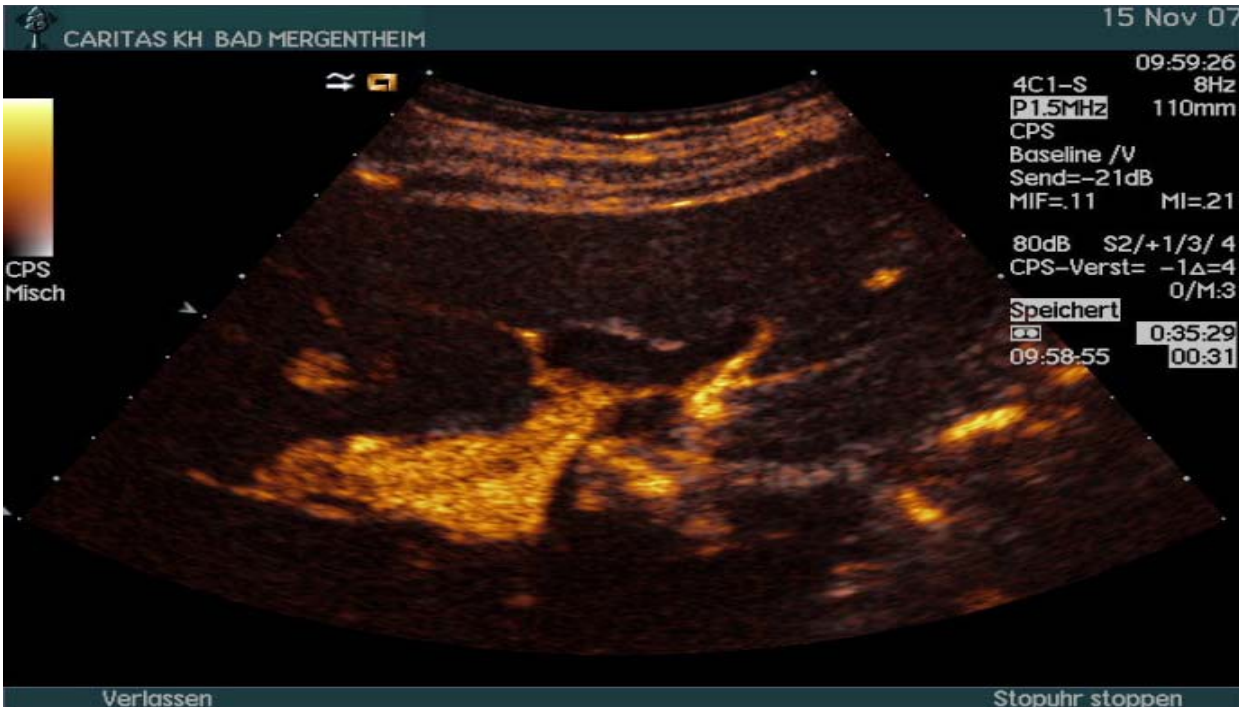

(d)

(Figure 2.23) Portal vein thrombosis. (a) hyperechoic total portal vein thrombosis intrahepatically and (b) extrahepatically. Circumscript portal vein thrombosis is shown in (c) B-mode ultrasound and (d) using contrast-enhanced ultrasound.

2.3.19. Examination of the hepatic veins in patients with diffuse liver disease

The normal flow pattern in the right hepatic vein is triphasic (Figure 2.23). The FFT-Doppler ultrasound spectrum of the right hepatic vein next to the IVC reflects mainly cardiovascular and respiratory changes in pressure and flow pattern. In contrast, the FFT-Doppler ultrasound spectrum of the right hepatic vein, 6-8cm distal to the confluence of the hepatic veins, reflects histological changes of the liver parenchyma and can be classified into a triphasic waveform with a short-reversed flow, a biphasic waveform with no reversed flow with a fluttering of more than 10% of the mean phasic amplitude, or a monophasic flat waveform with a fluttering of less than

10% of the mean phasic amplitude. In patients with heart insufficiency the flow can be tetraphasic, which means there is a significant amount of hepatopetal flow showing a pendular flow (backward and forward). The maximum, medium and minimum (reversed flow) velocity in centimeters per second could also be recorded. Owing to changes in the vessel diameter of up to 2mm per cycle during systole and diastole, and different directions of the normal triphasic hepatic vein flow, it is not useful to calculate the blood flow (in milliliters per minute) in the hepatic veins. (Christoph F. Dietrich.2011).

2.3.19.1. Exaination technique

The right hepatic vein is identified via the right intercostal approach, displayed longitudinally by a counter-clockwise turn, the sample gate is positioned 6-8cm distal to the confluence of hepatic veins and adjusted according to the inner diameter of the vessel (typically 3-7mm). FFT spectral analysis is recorded for at least 5s. The Doppler ultrasound spectrum can be recorded within a short breathing pause of 5-8s without relevant intra-abdominal or intra-thoracic pressure related artefacts. To avoid artefacts as a result of different respiratory positions and different abdominal and intra-thoracic pressures, the evaluation of the right hepatic vein via the 10th or 11th intercostal space 6-8cm distal to the confluence of the hepatic veins offers a standardised procedure and provided reproducible results with an acceptable insonation angle in all patients and healthy individuals (Christoph F. Dietrich.2011).

2.3.19.2. Which hepatic vein should be examined

The close anatomical relationship between the left liver lobe and the heart frequently leads to Doppler signal artefacts in any signal obtained from the left hepatic vein. Owing to these artefacts, which are mainly due to heart movements, the left hepatic vein cannot always be reliably evaluated. Adequate sonographic visualisation of the middle hepatic vein and evaluation of the FFT-spectrum is best accomplished during slight inspiration and via the sub-costal route. However, in 35 out of 135 patients evaluation of the middle hepatic vein this was only possible during deep inspiration with respiration related artefacts of the Doppler ultrasound spectrum with an initial monophasic waveform changing to a bi- and triphasic waveform during the examination. The most reproducible Doppler ultrasound spectrum can be obtained from the right hepatic vein via the right intercostal approach (Christoph F. Dietrich.2011).

The reproducibility of the method was investigated by repeated sonographic examinations of the flow pattern in the right hepatic vein in 10 healthy individuals over 7 consecutive days. The mean coefficient of variation for intra-individual assessment of flow velocity was 13% for the hepatofugal flow and 19% for the reversed flow. The flow pattern in the 10 individuals investigated was always triphasic. The reproducibility for the middle hepatic vein was less favourable with a mean coefficient of variation for intra-individual assessment of the flow velocity of 25% for the hepatofugal flow and of 76% for the reversed flow (Christoph F. Dietrich.2011).

2.3.19.3. Clinical application

It has been previously shown that a non-triphasic hepatic vein flow (HVF) is mainly associated with the degree of fat deposition within the liver and less related to inflammatory parameters and the extent of liver fibrosis. Recently, a large scale study on patients with chronic HCV infection confirmed that hepatic steatosis can be excluded by normal liver haemodynamics; however,

some operative characteristics (specificity and positive predictive values) were rated insufficient. Non-triphasic HVF and FHA within the liver hilum are both parameters that can be easily measured and quantified by ultrasound. The recorded values are reproducible and less dependent on the investigators interpretation than conventional grey scale imaging.

In general more than 90% of healthy probands have a triphasic flow pattern, whereas only 60–70% of patients with a hepatopathy show a non-triphasic pattern. So, for non-triphasic flow and the diagnosis “liver disease”, the positive predictive value is high but the negative predictive value is low (Christoph F. Dietrich.2011).

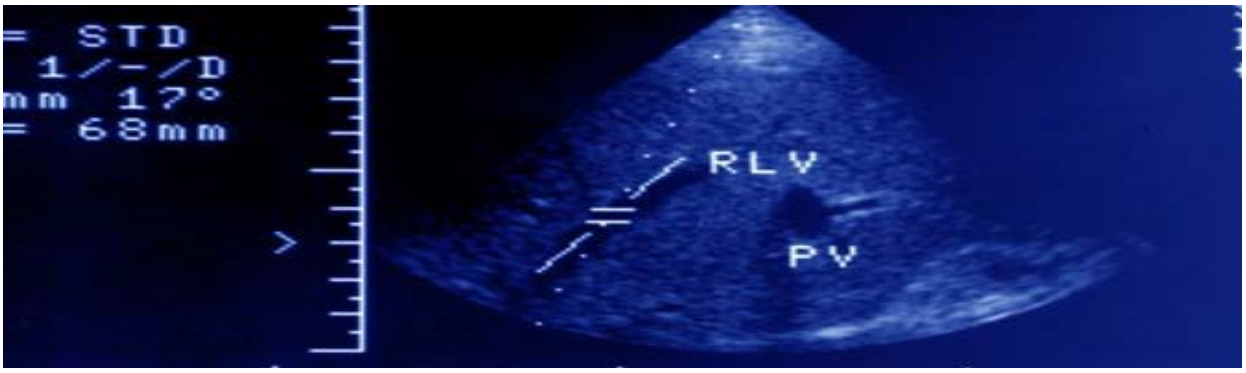

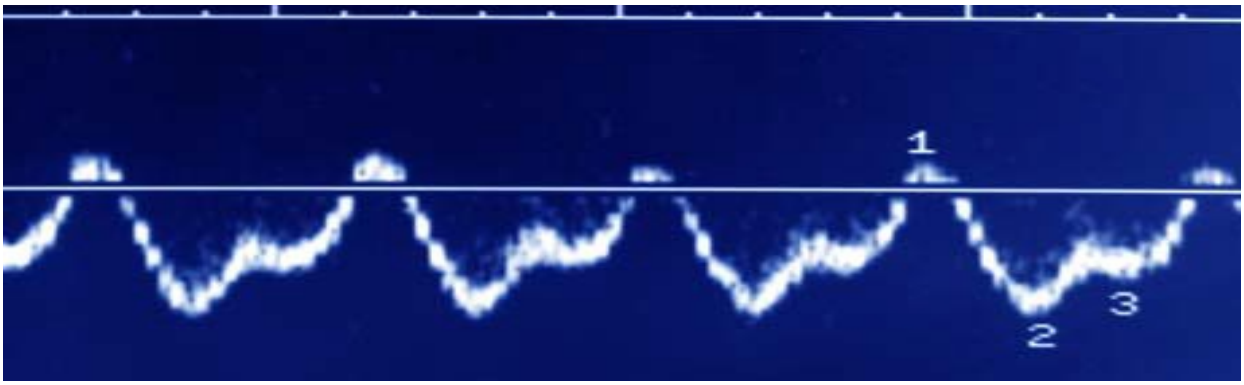

(a)

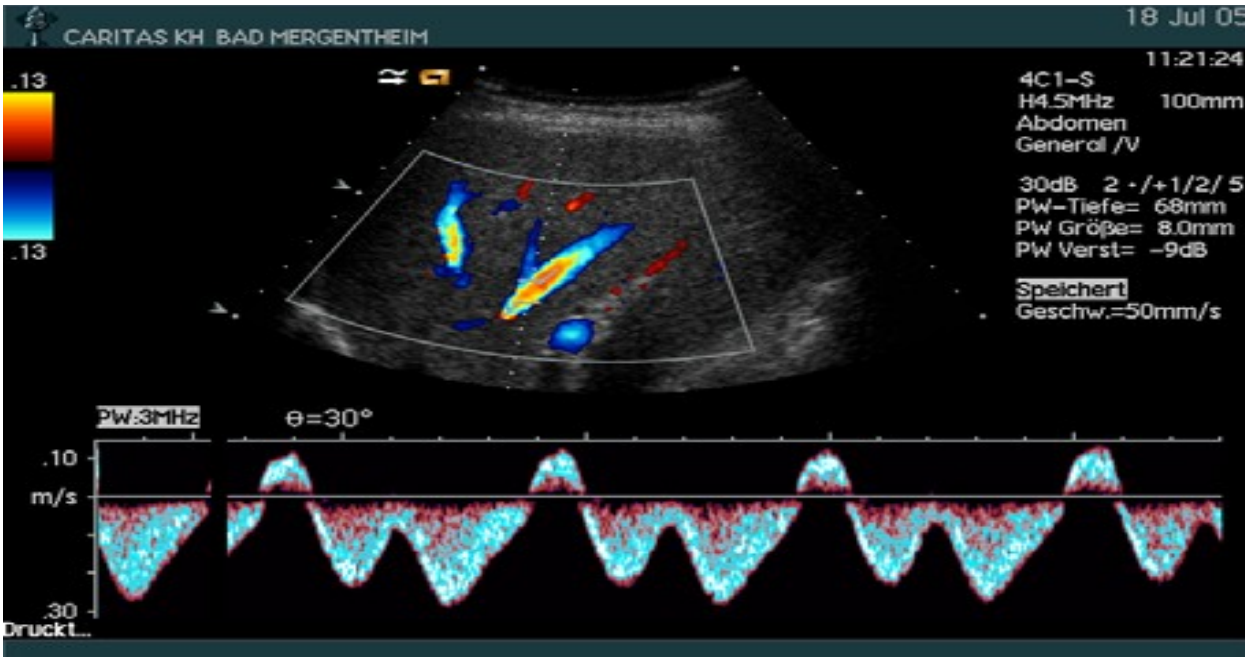

(b)

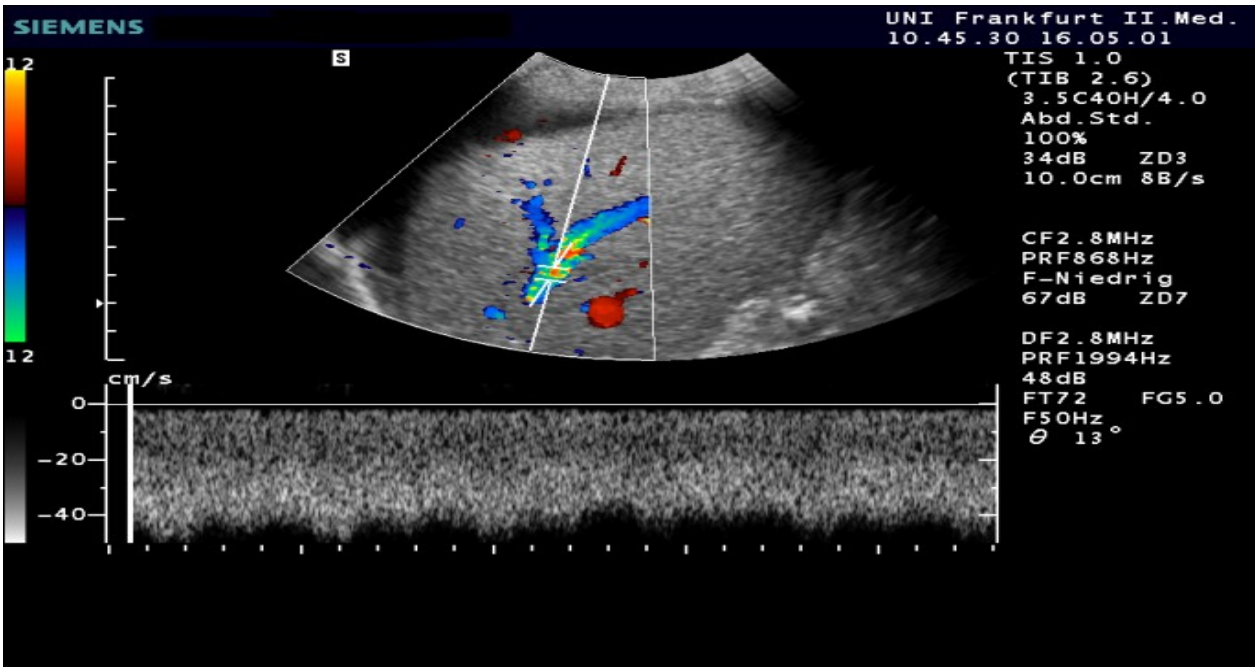

(c)

(Figure 2.24) Hepatic vein blood profile. (a,b) The normal hepatic flow profile is triphasic in the right liver vein (RLV); the portal vein is also indicated (PV). (c) Monophasic flow deformation is

mainly due to hepatic fat infiltration, as shown in this patient with steatohepatitis. (Christoph F. Dietrich.2011).

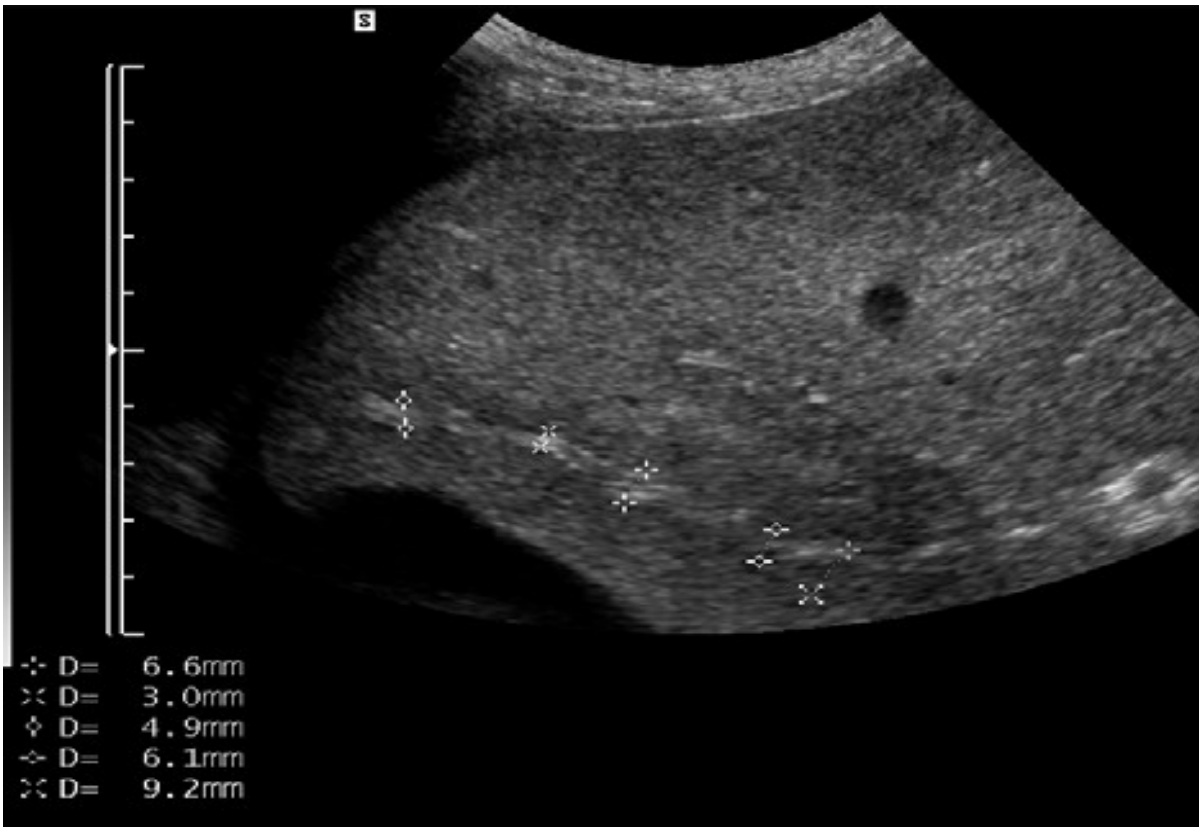

(a)

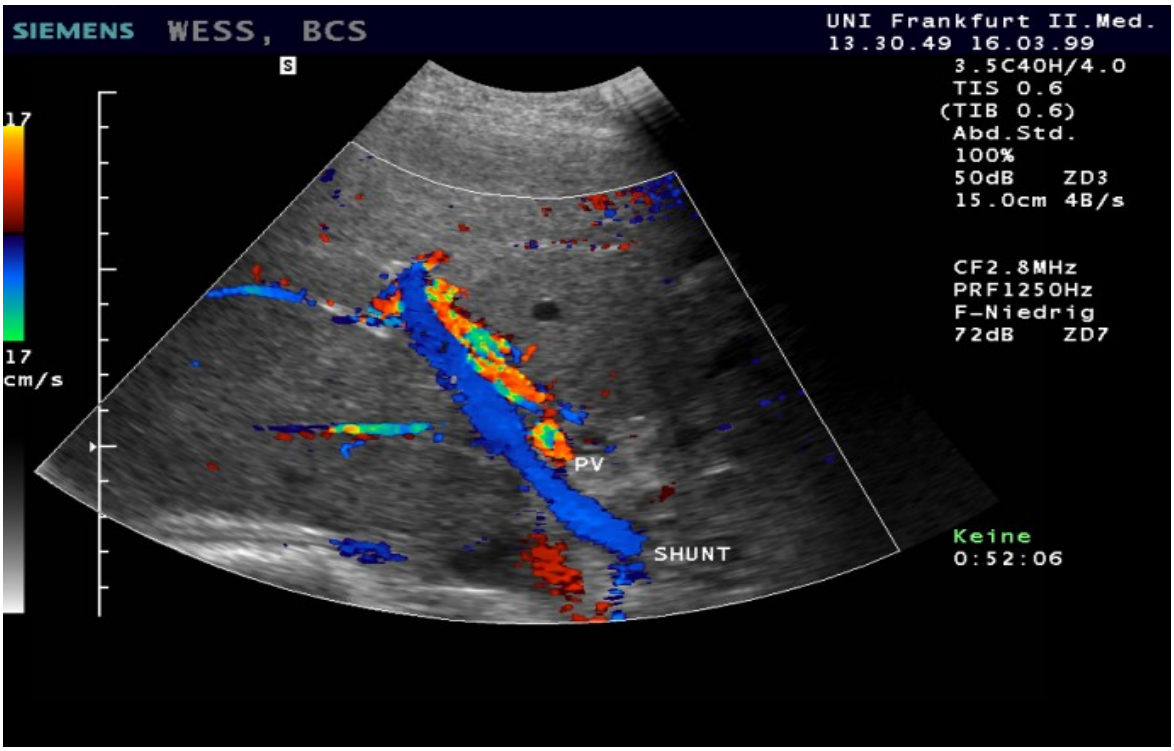

(b)

(Figure 2.25) Budd-Chiari syndrome. Approximately, one-third of patients present with acute disease with sonographically detectable thrombosis. Approximately, two-thirds have chronic presentation songraphically with (a) occluded hepatic veins (between markers), (b) retrograde portal venous outflow, and intrahepatic collaterals with or without extrahepatic shunts. PV, portal vein.

2.3.19.4. Veno-occlusive disease

Duplex sonography of the portal vein system and the hepatic veins may show typical changes, but may display only a relatively low sensitivity and specificity. Sonographic signs of VOD are ascites, thickening of the gall bladder wall, increase of the resistance index in the hepatic artery as well as retrograde flow in the portal vein and changes in the portal vein flow profile. CDI in the diagnosis of 12 patients with VOD after bone marrow (or stem-cell) transplantation reveals

low (<10cm/s) or reversed portal venous flow, high resistance arterial flow pattern (resistance index >0.85) and flattened monophasic flow pattern in the right hepatic vein of less than 8cm/s. Published data is sparse in patients with VOD (Christoph F. Dietrich.2011)

2.3.19.5. Osler's disease

Liver involvement occurs in 30–70% of cases and can lead to a specific form of liver cirrhosis, as a result of sclerosis formed around the multiple vascular malformations that can be easily detected on ultrasound. Doppler ultrasound helps to identify the nature of shunts (arterio-portal, arterio-systemic, arterio-porto-systemic) (Figure 24). When using conventional B-mode ultrasound, especially in the supply area of the superior mesenteric artery dense network of vessels, oval cystic lesions with corresponding malformations are found to represent shunts (Christoph F. Dietrich.2011).

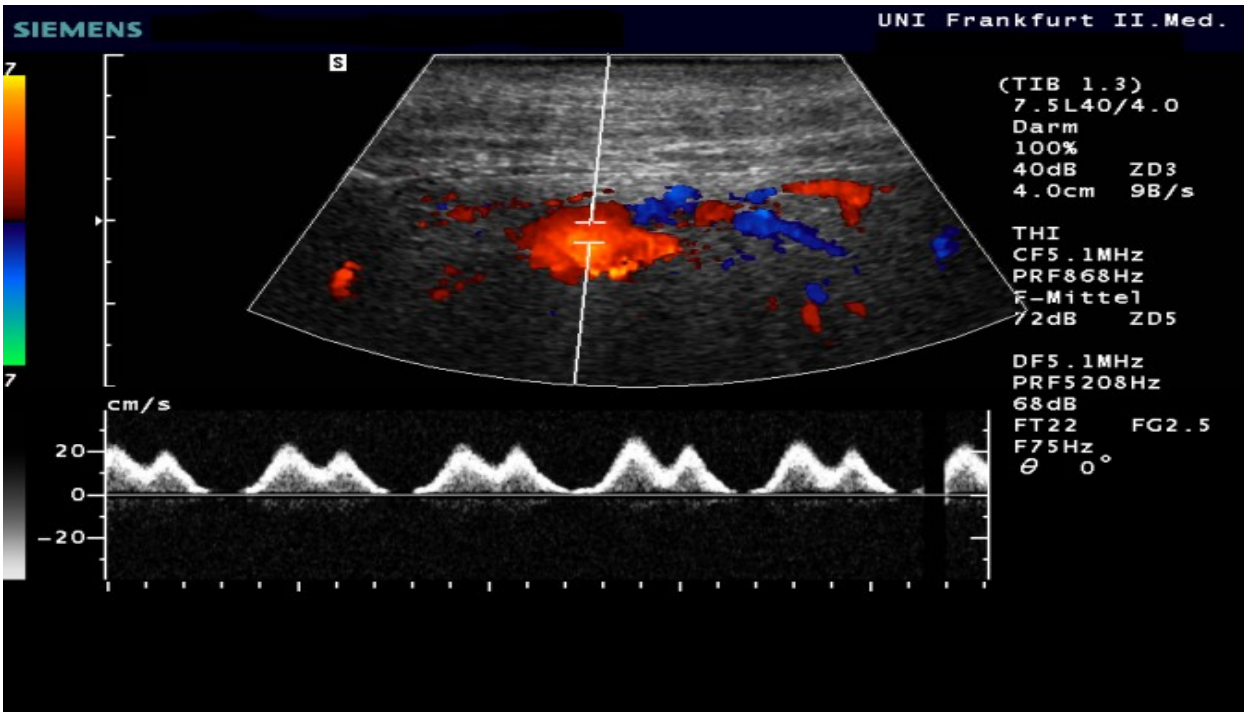

(Figure 2.26) Osler’s disease showing intrahepatic arterio-porto-venous shunts with typical Doppler spectrum for shunts.

2.3.19.6. Liver pathology - detection and characterization of focal liver lesions (FLL)

The definition of a FLL is the difference in echogenicity between a circumscribed area and the surrounding liver tissue. A differences in ultrasound echogenicity usually, although not necessarily, shows a pronounced difference in X-ray attenuation and MR as well. Consequently, most FLL are visualised by all three sectional imaging modalities, whereas a few are shown by only one or two of these modalities (Christoph F. Dietrich.2011).

FLL are detected and characterised sonographically by echogenicity differences from the surrounding liver tissue, as well as by the detection of hyper- or hypovascularisation (on colour Doppler ultrasound). Conventional B-mode ultrasound makes it possible to unequivocally detect the frequently of typical liver cysts and calcifications. However, detection and characterisation of liver tumours still represents a challenge to all imaging modalities despite the advances in imaging techniques (i.e. ultrasound, CT and MRI scanning) (Christoph F. Dietrich.2011).

More recently, CEUS has been able to provide important additional information on FLL perfusion kinetics and vascularisation pattern. Circumscribed lesions of foreign-liver-tissue (e.g. metastases) can be detected by the absence of uptake of contrast media Such lesions appear in the post-vascular late-phase image as storage defects, although this late-phase effect is neither absolutely specific nor absolutely sensitive. As a result of their doubled blood supply via the portal vein and the hepatic artery, focal lesions in the liver often exhibit no general hyper- or hypoperfusion, but depending on the flow phase and the histology, present a complex temporal

and spatial picture of increased and reduced contrast. Certain lesions can give a characteristic vascular picture (e.g. the wheel-spoke phenomenon) or a distinctive perfusion pattern (e.g. halo contrasting or iris diaphragm phenomenon), allowing the lesions to be characterised, but contrast patterns do not always take this typical form. Similar arterial, parenchymatous and venous characteristics are exhibited by the spleen and lymph nodes.

2.3.19.7. Contrast agents are used in the liver for different purposes including

- Detection of liver tumors.
- Characterization of liver tumors (benign vs. malignant).
- Monitoring of local ablative treatment.
- Imaging hepatic vessels.

2.3.19.8. Liver tumor detection

CEUS increases the detection rate of metastases as compared with conventional B-mode ultrasound, which has been demonstrated by multicentre trials. Comparative studies have shown that the detection rate has the same accuracy as the detection rate for contrast-enhanced CT and MRI scans. CEUS allows the same detection rate for benign FLL compared with the occurrence in normal liver parenchyma (10% of all livers), which is important for differential diagnosis (Christoph F. Dietrich.2011).

2.3.19.9. Differentiation of benign and malignant lesions

Characterization of a liver lesion begins once an abnormality is found. An imaging procedure used to detect liver masses should also enable the examiner to differentiate between benign and

malignant lesions. CEUS in the portal venous and late phase after injection of SonoVue® (Bracco, Italy) considerably improves the characterization of liver tumours compared with conventional B-mode ultrasound, leading to differentiation of benign and malignant liver lesions in most patients, if cysts and calcifications are excluded by conventional B-mode ultrasound. CEUS facilitates the clinical decision regarding whether a sonographically detected liver lesion will need further investigation or not. This new technique may help to reduce unnecessary or invasive examinations in certain cases (e.g. invasive liver biopsy, CT scan and MRI). Only a few false positive findings have been observed so far, mainly owing to abscesses or necrosis, old fibrous focal nodular hyperplasia (FNH) predominantly with scar tissue, sarcoidosis lesions, and inflammatory pseudotumours of the liver. (Christoph F. Dietrich.2011).

2.3.19.10. Focal liver lesion characterization

2.3.19.10.1. Liver cyst

Liver cysts are a frequent finding (Figure 25-27) and are easily diagnosed using conventional B-mode ultrasound. Liver cysts are characterised, as are other cysts, as typically round, anechoic, smoothly delineated structures with refraction shadows at the edges; a strong posterior wall echo and post-cystic enhancement owing to an intensity difference between the beam intensity deep to the cyst and in the cysts. Cysts displaying all these sonographic signs are defined as typical (Figure2. 25), whereas cysts showing only some of the signs are defined as atypical (Figure2. 26). Very early echinococcosis can be confused with atypical liver cysts. Cystadenoma can also be another differential diagnosis (Figure 2.27).

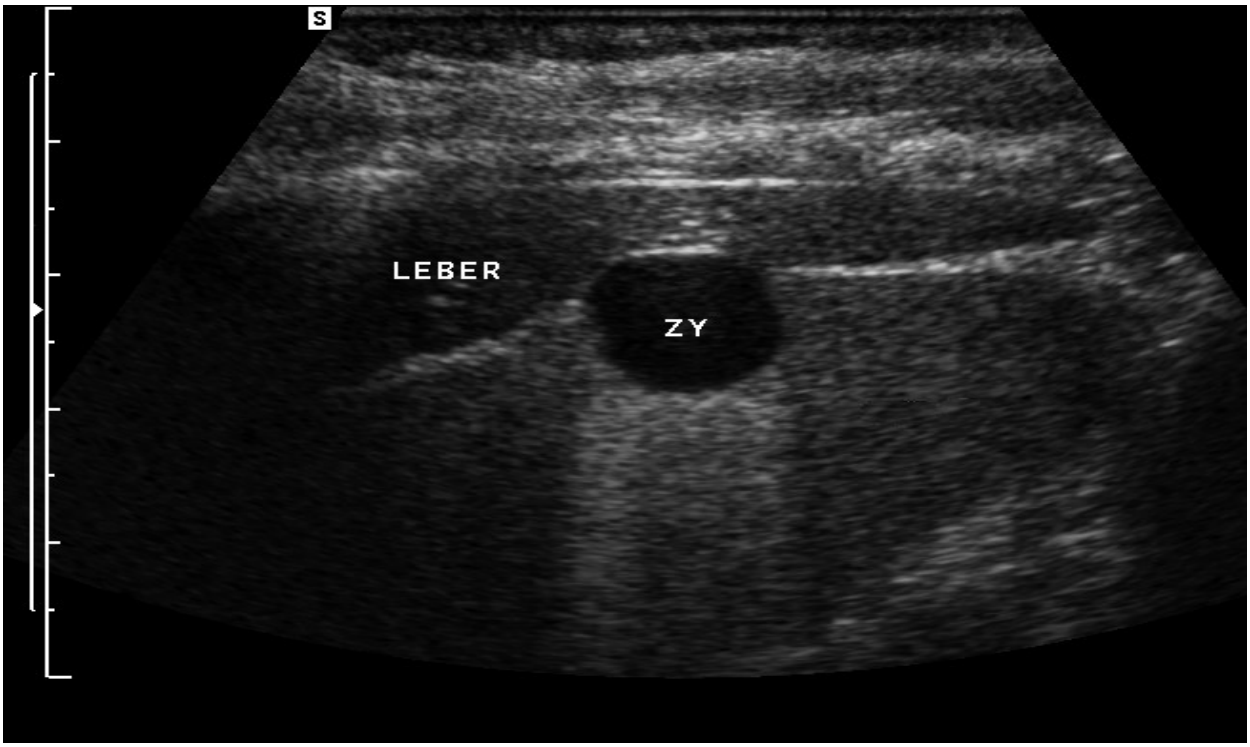

(Figure 2.27) Typical liver cyst. The exophytic liver cyst is next to the spleen. Typical liver cysts display all the morphological criteria (echo-free, round-oval, well-defined borders with lateral shadowing and transducer distal (posterior) echo enhancement), while atypical liver cysts do not. Leber: liver.

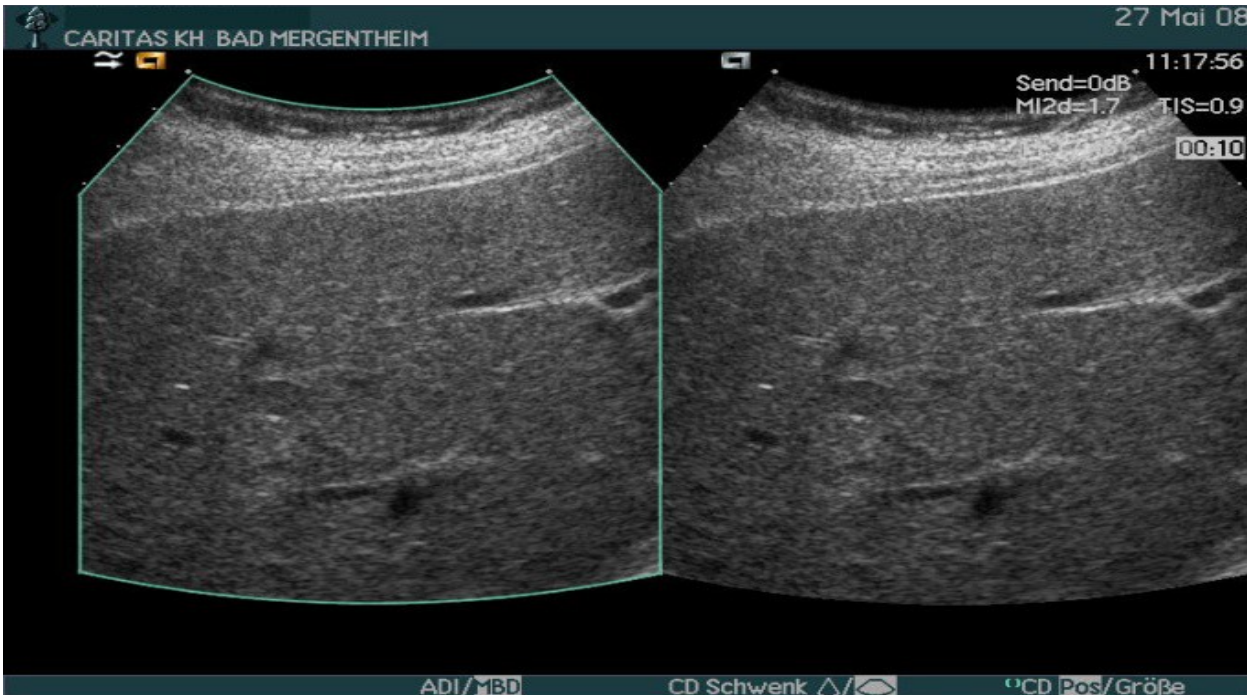
CARITAS KH BAD MERGENTHEIM
27 Mai 08
11:17:56
Send=0dB
MI2d=1.7
TIS=0.9
00:10
ADI/MBD
CD Schwenk
CD Pos/Größe

(a)

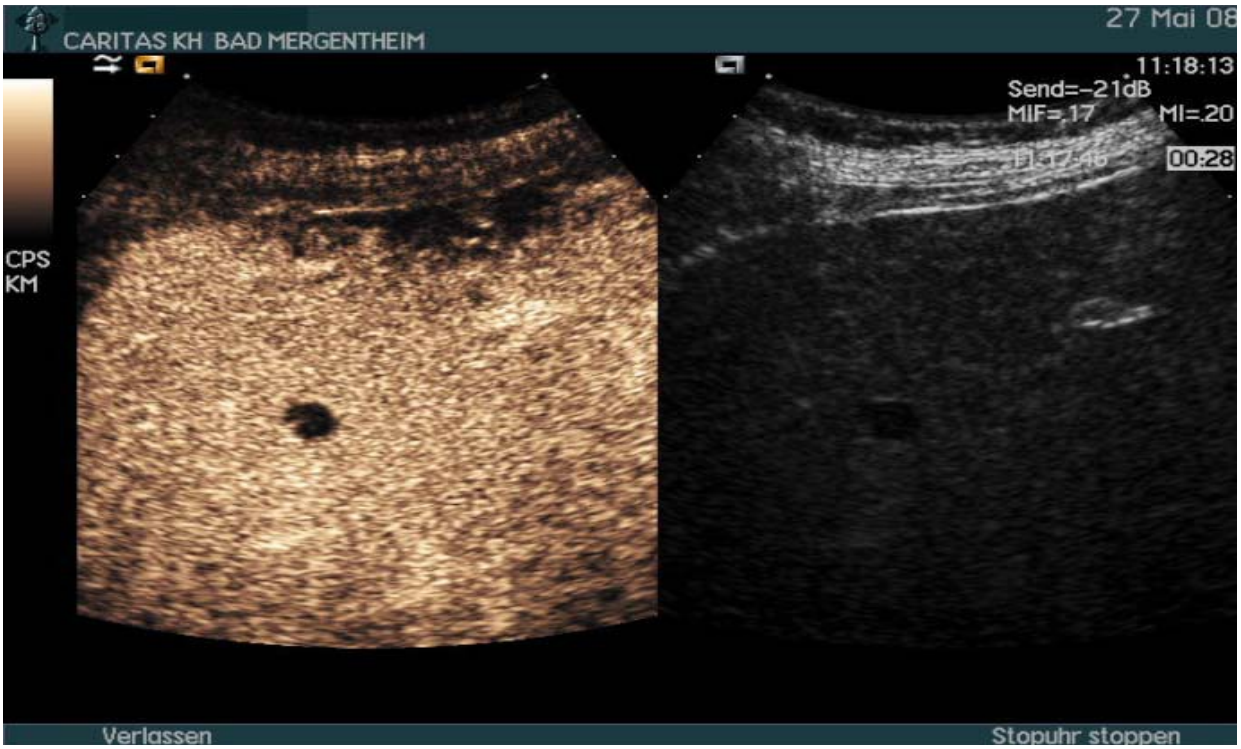
CARITAS KH BAD MERGENTHEIM
27 Mai 08
11:18:13
Send=-21dB
MIF=.17
MI=.20
00:28
CPS
KM
Verlassen
Stopuhr stoppen

(b)

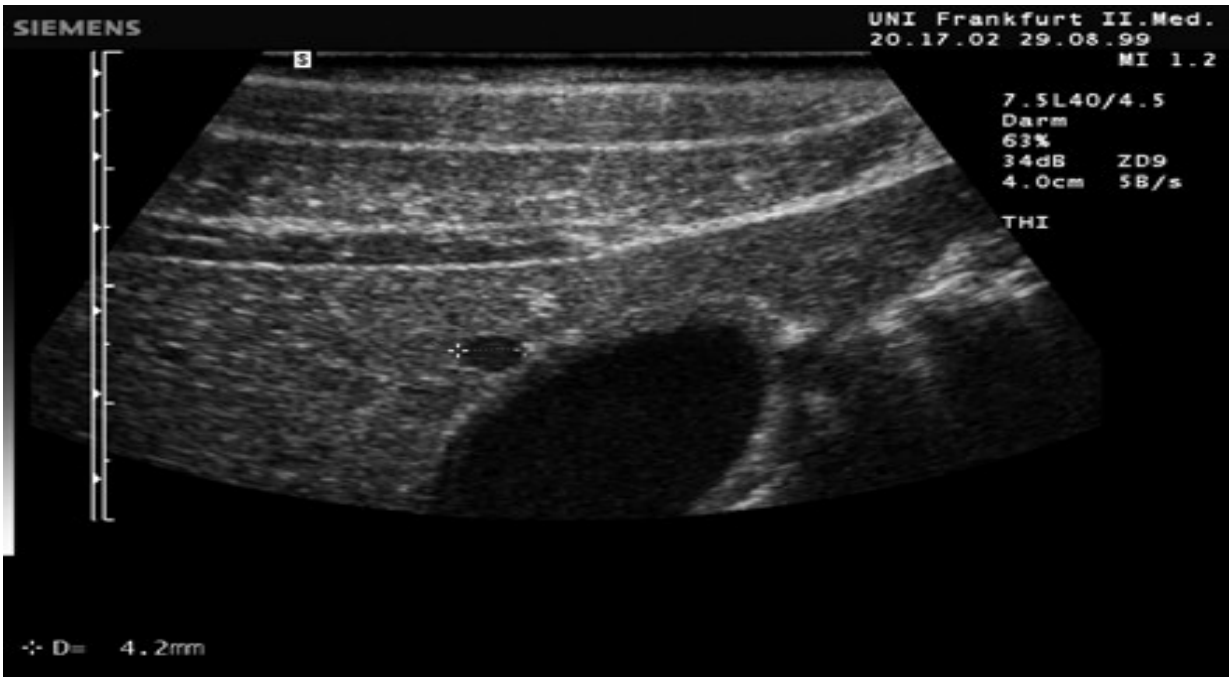

(c)

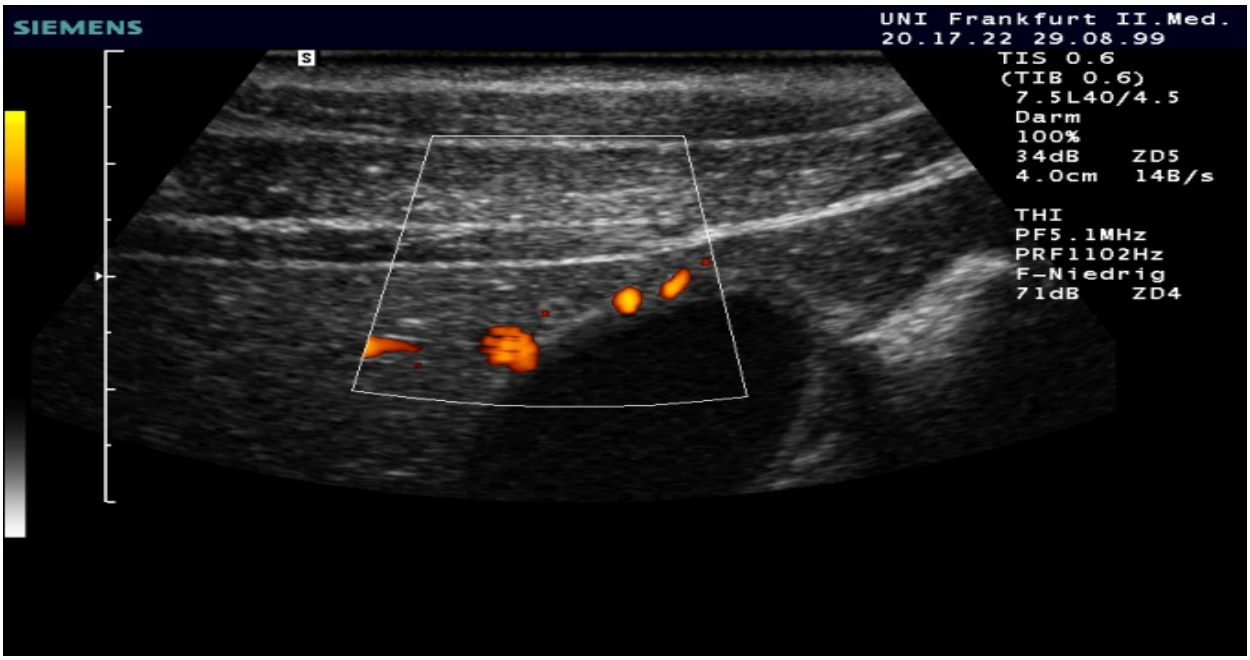

(d)

Figure (2.28) Atypical liver cyst. These cysts do not display all the morphological criteria of typical liver cysts (echo-free, round-oval, thin-walled, well-defined borders with lateral

refraction shadowing and post-cystic echo enhancement). (a) Owing to the small diameter and slice thickness artefacts the cyst is not echo-free, but (b) contrast-enhanced ultrasound shows the cyst. (c,d) In another example the cyst-like structure is a hepatic vessel, which can be difficult to recognize using conventional B-mode ultrasound.

Blood vessels mimicking a simple cyst have to be excluded by CDI to rule out arterioportal venous malformations (Figure 26). On CEUS, cysts show no contrast enhancement at all. As small cysts may be confused with metastases on CEUS, conventional B-mode ultrasound has to precede CEUS. Cystadenoma are rare neoplastic differential diagnoses of atypical cysts. (Figure 2.28).

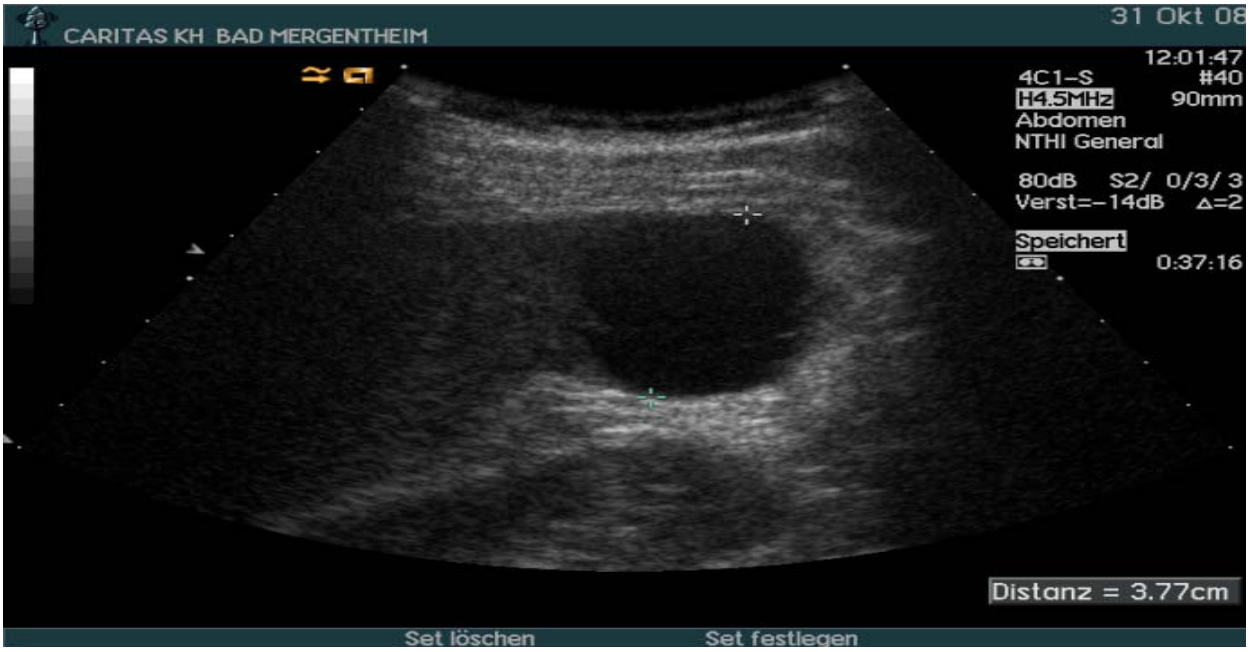

(a)

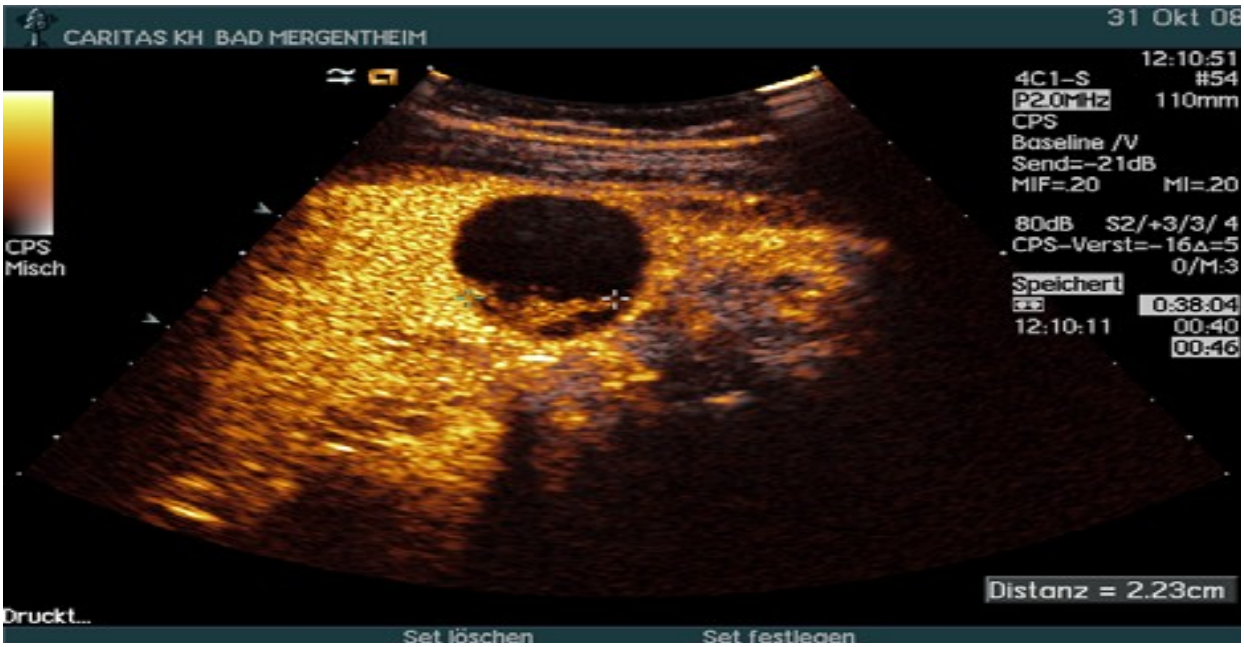

(b)

(Figure 2.29) (a,b) Cyst adenoma are rare neoplastic differential diagnoses of atypical cysts. Contrast enhancing nodules are indicative for this diagnosis.

2.3.19.10.2. Echinococcosis, Echinococcus cysticus:

Gharbi et al (1981) first introduced the widely used and most cited classification of hydatid disease, which has been modified many times. Gharbi Type I cysts consist of pure fluid; Type II have a fluid collection with a split wall; Type III cysts contain daughter cysts (with or without degenerated solid material); Type IV have a heterogeneous echo pattern; and Type V have a calcified wall. It is important to note that lesions may show different stages of hydatid evolution (Christoph F. Dietrich.2011).

Ultrasound and CEUS are helpful in recognising echinococcosis in all stages. Most useful is the combination of morphological criteria and biological behaviour e.g. fertile cysts with viable protoscoleces (Gharbi Type I, II), transitional phase (Gharbi Type III) and inactive cysts that have lost their fertility (Gharbi Type IV, V). Characteristics on ultrasound that are suggestive of

an inactive lesion include a collapsing, flattened elliptical cyst (corresponds to low pressure within the cyst), detachment of the germinal layer from the cyst wall ("water lily sign"), coarse echoes within the cyst and calcification of the cyst wall.

The use of a combined classification including imaging criteria and biological evidence of viable parasites will enable clinicians to perform the correct clinical procedures for the different cyst types.

Type I the most common Type I lesion (50–80%) represents an anechoic smooth, round pure fluid collection without hydatid sand and septa. Containing usually fertile cysts with viable protoscoleces, which can be difficult to distinguish from a benign cyst. The roundish lesion with well-defined borders is characterized by an irregular localized thickened wall (the initial stage of splitting the wall), which should be carefully sought by high frequency, and therefore high resolution probes (7–15MHz), and CEUS, which delineates the nodular appearance very early in the course of the disease.

Type II: Splitting of the wall (in folding of the inner cyst wall resulting in floating membrane, the so-called water lily sign) is typical for Type II fluid-filled lesions also containing fertile cysts, and appears to be the most important and pathognomonic sign of echinococcosis. It is of interest that splitting of the wall to the outer margin (outfolding) is the typical fine nodular appearance with contrast enhancement. When the liver cyst contains membranes and “hydatid sand” mixed echoes will appear, which can be confused with a neoplasm or abscess. The term "hydatid sand" reflects a complex image that consists predominantly of parts of protoscolices (hooklets and scolexes). The finding of mobile sand may be overt and visible when the patient's position is turned, e.g. into the standing position.

Type III: When daughter cysts are present, characteristic internal septation is the result. Type III lesions are characterized by septa, which result in a honeycomb appearance with in folding

membranes. This stage has been described as transitional, when the integrity of the cyst has been compromised either by the host or by medical treatment. The “cyst in the cyst sign” occurs by separation of the hydatid membrane from the wall and the hydatid sand in combination with a fine nodular appearance of contrast enhancement are both pathognomonic of echinococcosis. Neoplasia can be ruled out by the exclusion of contrast enhancement within the lesion. In the very early stages of echinococcosis, without calcifications, ultrasound can depict the specific intralesional morphology in detail much earlier than any other imaging modality (Figure 2.29).

Type IV: Type IV lesions are characterised by a heterogenous echo pattern. The echogenicity of the lesion may be more hypoechoic, but it can also be hyperechoic owing to regressive changes. This stage is unspecific compared with the pathognomonic Stages II and III.

Type V: The Type V pattern reflects a solid heterogeneous mass that is difficult to differentiate from a tumour. An identifiable thickened hyperechoic calcified wall suggests an echinococcal cyst. Cysts with a calcified rim may have a typical "eggshell" appearance. Type IV and V lesions represent inactive cysts with degeneration, which have lost their fertility. Calcification, which usually takes 5 to 10 years to develop, usually occurs with hepatic cysts. Calcifications in pulmonary or bone cysts are more rarely encountered. Total calcification of the cyst wall suggests that the cyst is non-viable [see also the chapter on tropical disease in which the more recently WHO-classification is described] (Christoph F. Dietrich.2011).

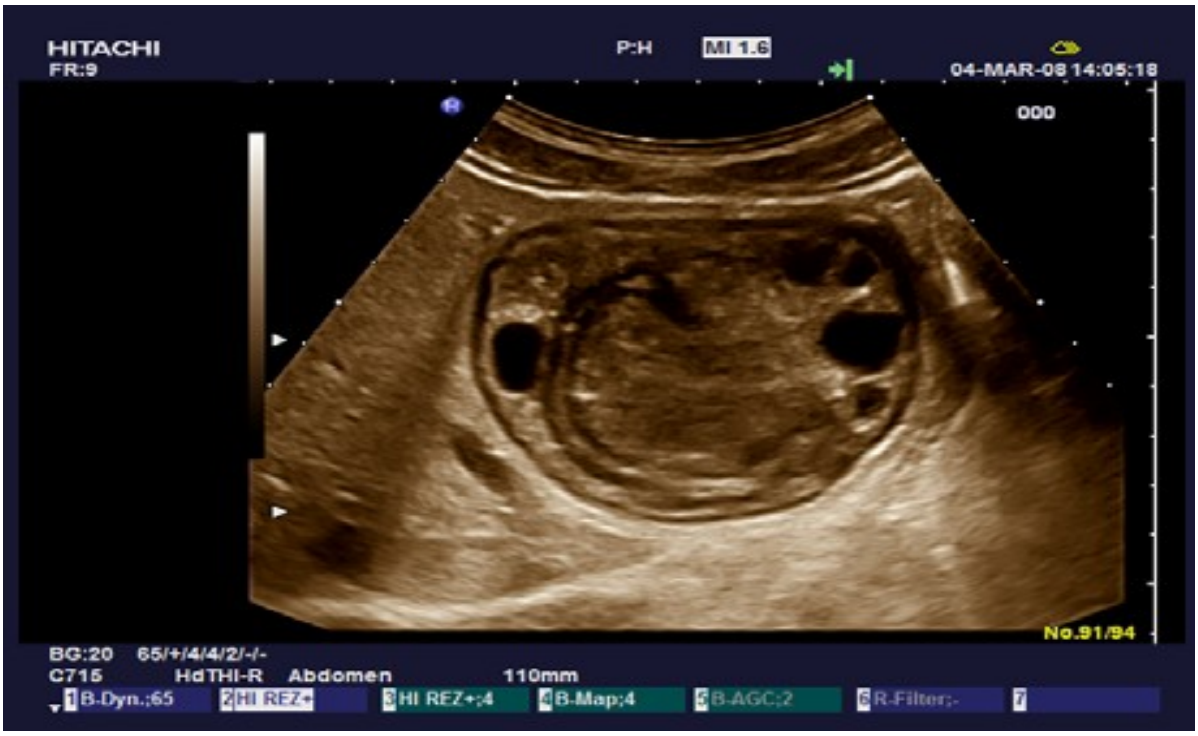
HITACHI
FR:9
P:H
MI 1.6
04-MAR-08 14:05:18
000
No.91/94
BG:20 65/+/4/4/2/-/-
C715 HdTHI-R Abdomen 110mm
1 B-Dyn.;65
2 HI REZ+
3 HI REZ+;4
4 B-Map;4
5 B-AGC;2
6 R-Filter;-
7

(a)

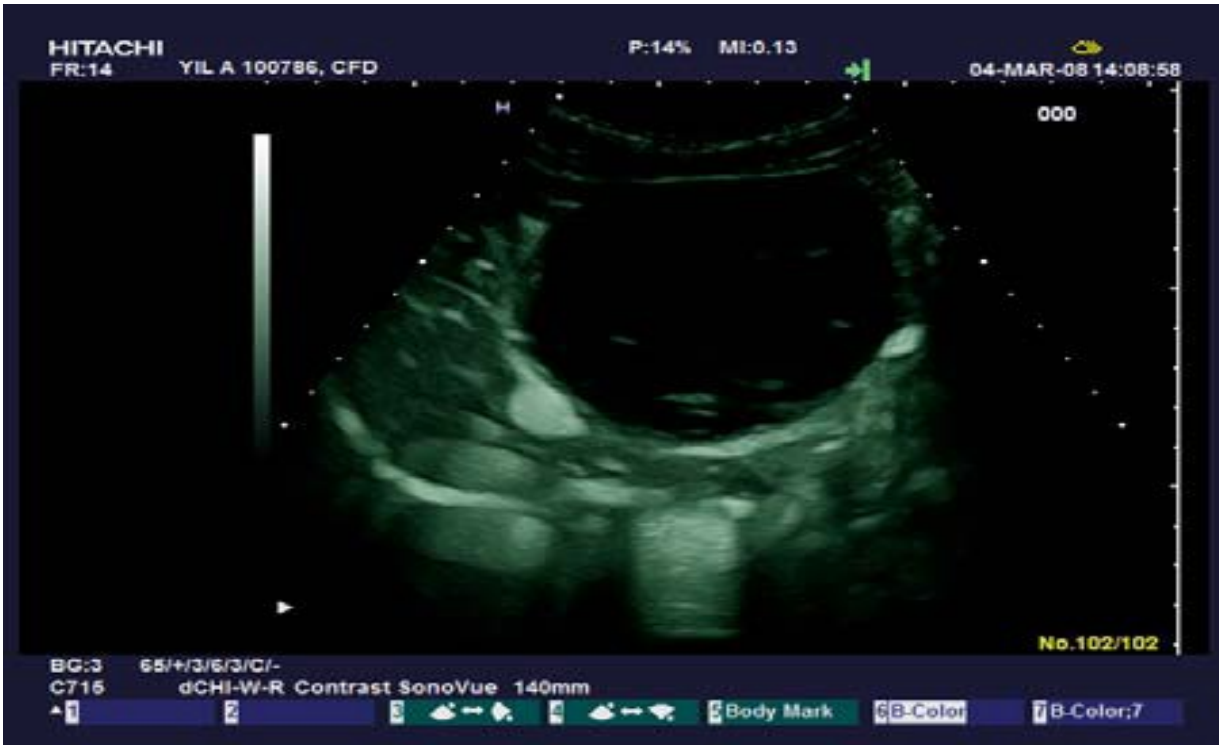
HITACHI
FR:14
YIL A 100786, CFD
P:14% MI:0.13
04-MAR-08 14:08:58
000
No.102/102
BG:3 65/+/3/6/3/C/-
C715 dCHI-W-R Contrast SonoVue 140mm
1
2
3
4
5 Body Mark
6 B-Color
7 B-Color;7

(b)

(Figure 2.30) Echinococcosis stage in this patient is characterised by multiloculated cysts in a honeycomb appearance with infolding membranes (a). Calcifications are difficult to recognise. The contrast enhanced image (b) does not show any enhancement.

2.3.19.10.3. Calcification

Calcifications are characterized as hyper echoic structures, which normally show acoustic shadowing distally owing to reflection/attenuation of the ultrasound (Figure 2.30).

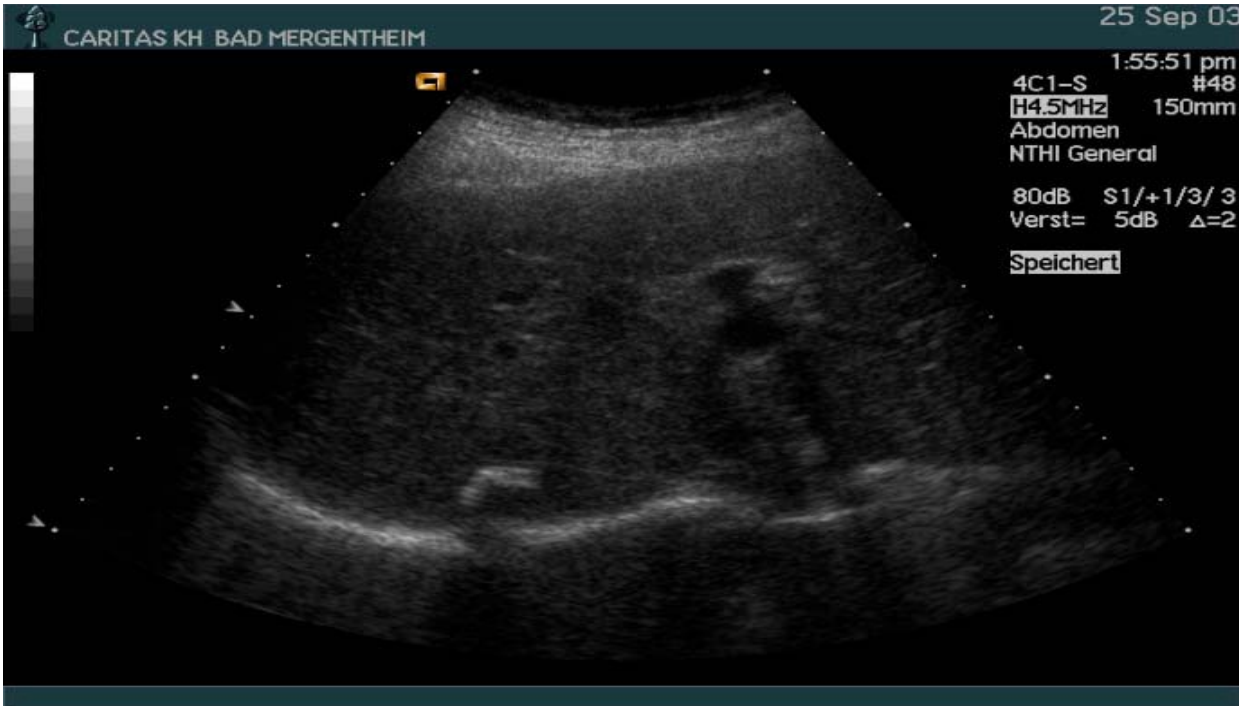

(a)

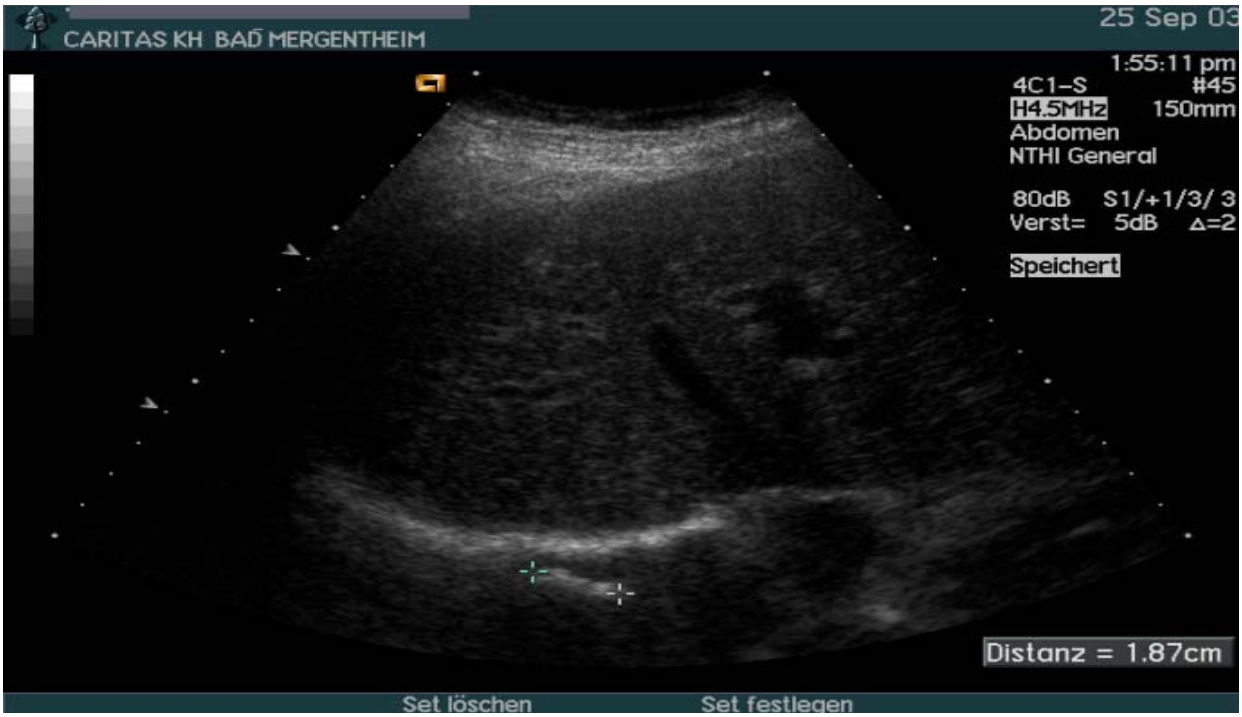
CARITAS KH BAD MERGENTHEIM
25 Sep 03
1:55:11 pm
4C1-S #45
H4.5MHz 150mm
Abdomen
NTHI General
80dB S1/+1/3/ 3
Verst= 5dB Δ=2
Speichert
Distanz = 1.87cm
Set löschen
Set festlegen

(b)

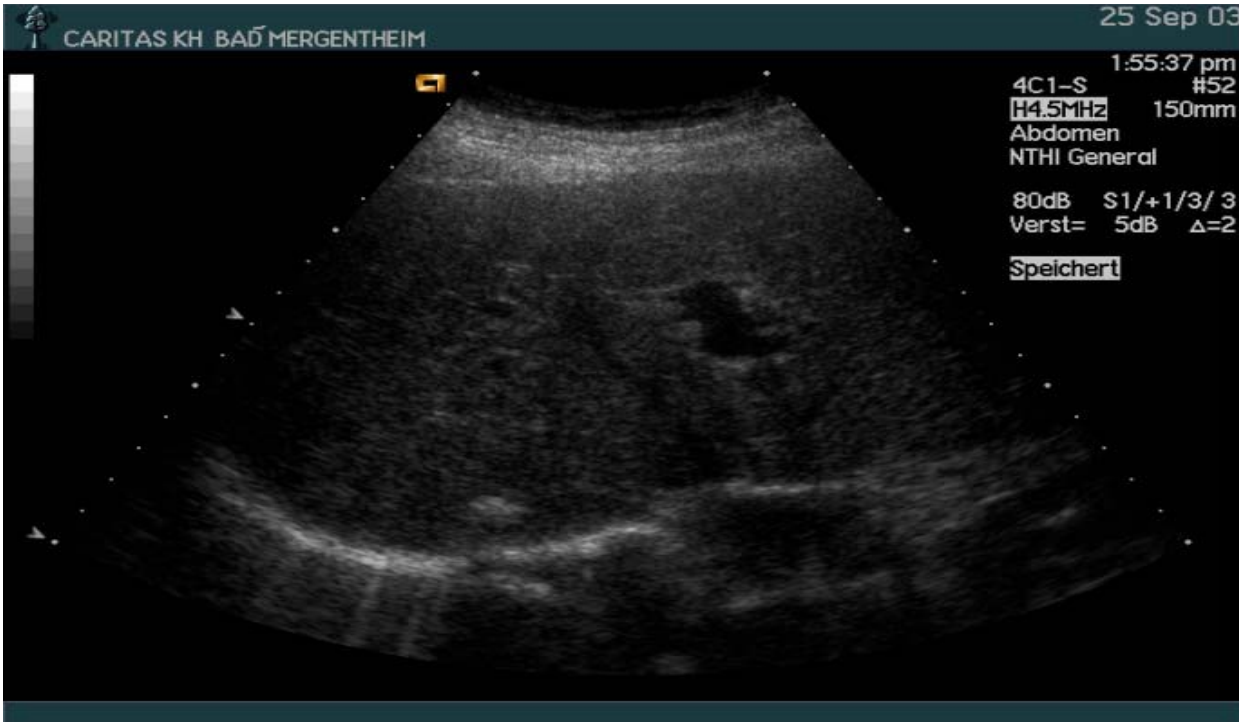
CARITAS KH BAD MERGENTHEIM
25 Sep 03
1:55:37 pm
4C1-S #52
H4.5MHz 150mm
Abdomen
NTHI General
80dB S1/+1/3/ 3
Verst= 5dB Δ=2
Speichert

(c)

(Figure 2.31) Calcifications within the liver. The mirror artifact owing to the acoustic impedance characteristics of the lower lung surface is also shown. Distinct changes of the transducer position shows a different kind of mirror artifact (a-c).

2.3.19.10.4. Haemangioma

Hepatic haemangiomas are known to be the most common benign liver tumour, with an incidence at autopsy and imaging studies of up to 7% (Figure 30-32). Up to 10% of patients with haemangiomas cannot be reliably diagnosed using imaging methods. In these patients only ultrasound guided liver biopsy and examination of the specimen is required for a final diagnosis usually in patients with malignant underlying disease. A retrospective study, of percutaneous biopsies of 38 patients (1cm to 13.5cm; mean 3cm) with suspected haemangioma using 20 gauge needles, reported that it is safe and effective for establishing a diagnosis of haemangioma.

2.3.19.10.4.1. Conventional B-mode ultrasound

Most haemangiomas demonstrate typical sonomorphological features in conventional B-mode ultrasound. They are characterized as less than 3cm in diameter, lobulated with a well-defined outline, located adjacent to liver vessels, demonstrate an hyperechoic texture and occasionally posterior acoustic enhancement owing to blood filled capillaries (Table 2).

Table 2 Typical haemangioma: diagnostic criteria B-mode criteria
Less than 3cm in diameter
Hyperechoic structure
Homogeneous inside
Round or slightly oval shape
Smooth outline
Absence of any halo sign
Possible detection of feeding and draining vessel
Absence of any signs of invasive growth

Posterior acoustic enhancement

2.3.19.10.4.2. Colour Doppler imaging

Although haemangiomas are highly vascularised masses, from a histopathological perspective, they essentially consist of a large number of capillary-sized vessels and so, even with the use of high-end ultrasound systems, conventional colour Doppler ultrasound often detects little or no blood flow inside the haemangioma because the blood flow velocity in the capillary haemangioma is too slow. The supplying and draining vessels (“feedings vessels”) may be visualised (depending on the ultrasound systems performance) at the edge of the lesion.

2.3.19.10.4.3. Contrast-enhanced ultrasound

CEUS has markedly improved the correct diagnosis of haemangioma, which is now possible in approximately 95% of patients. CEUS demonstrates typical haemangioma imaging characteristics, i.e. peripheral nodular contrast enhancement and the iris diaphragm sign in a high percentage of patients with an undetermined lesion. Difficult differential diagnoses include shunt haemangioma (synonymous high-flow haemangioma, which might be confused with FNH when small); HCA; or HCC. A thromboses haemangioma might be confused with a metastasis by demonstrating a contrast sparing in the arterial and portal venous phase.

2.3.19.10.5. Arterioportal shunts

Arterioportal shunts associated with hepatic tumors have been reported primarily in patients with malignant tumors, especially in advanced HCC with portal vein invasion. However, arterioportal shunts have been observed in hepatic haemangiomas not only using CEUS but also on multiphase helical CT and MRI. One possible explanation for rapidly enhancing small haemangiomas is a hyperdynamic status with large arterial inflow, rapid tumoural enhancement,

and consequently, large and rapid outflow, which seems to result in early opacification of the draining portal vein via shunts. Shunt haemangiomas are typically surrounded by focal hypoechoic areas representative of less fat content in comparison with the surrounding liver parenchyma. The metabolic changes are explained by a mainly arterial blood supply of the hypoechoic areas, whereas blood supply of the surrounding liver parenchyma is mainly by portal venous vessels, which contain more lipids possibly due to a higher concentration of insulin (Figure 2-32) (Christoph F. Dietrich.2011)

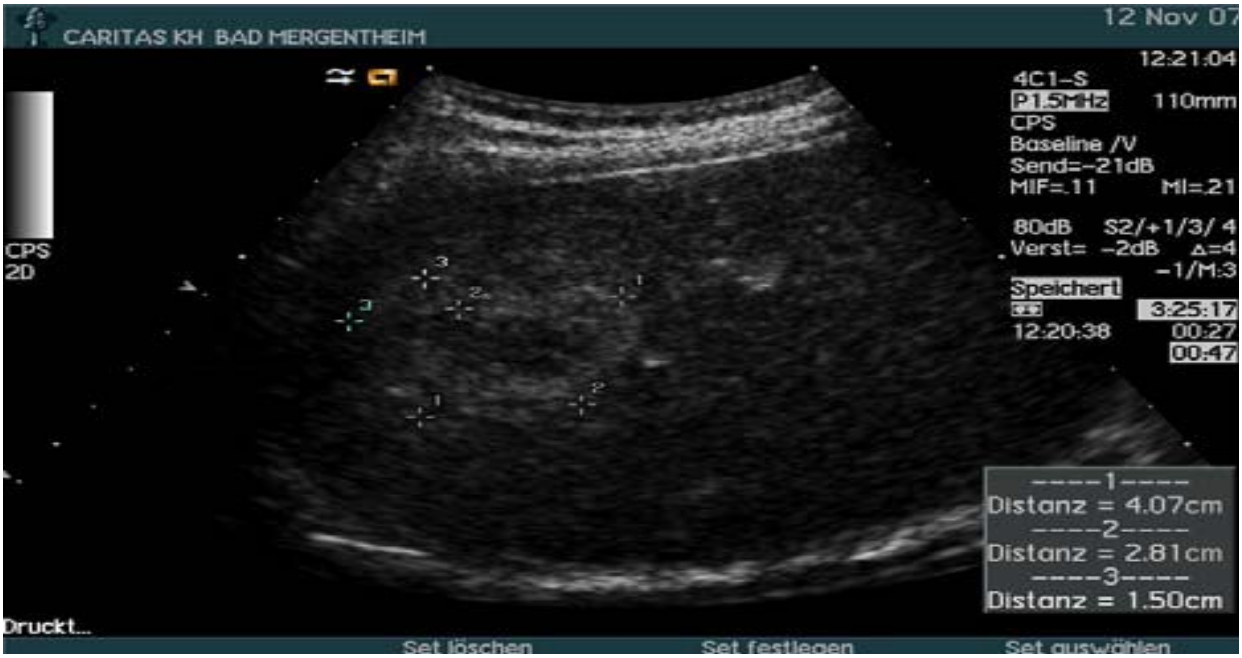

(a)

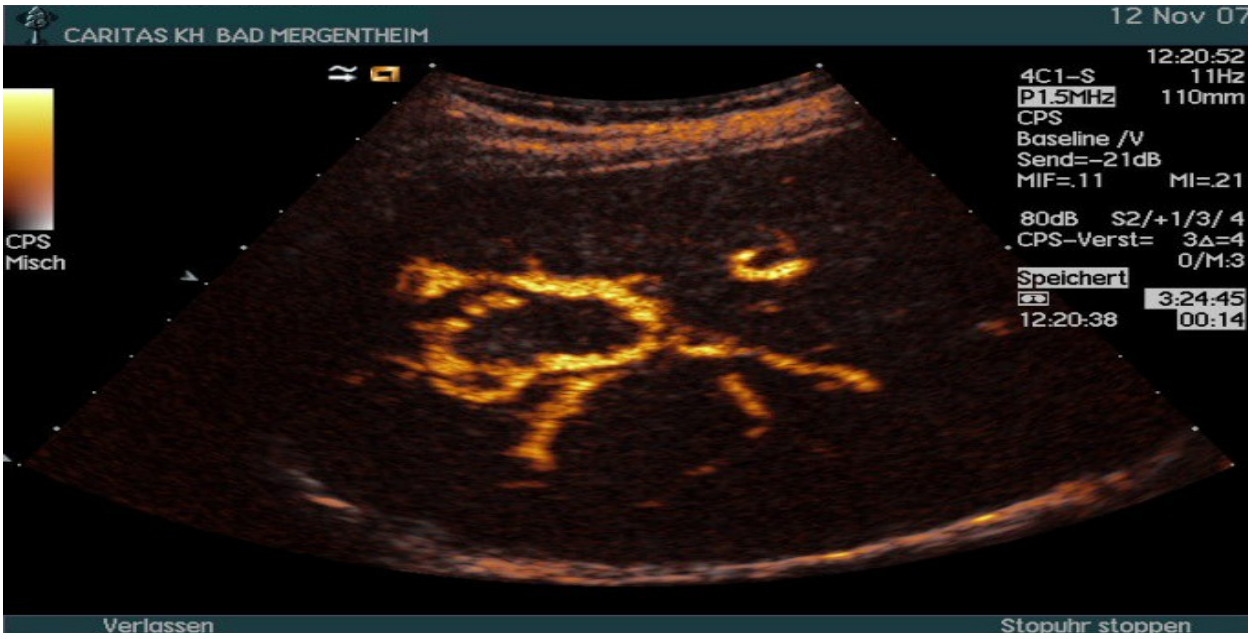
CARITAS KH BAD MERGENTHEIM
12 Nov 07
12:20:52
4C1-S
11Hz
P1.5MHz
110mm
CPS
Baseline /V
Send=-21dB
MIF=.11
MI=.21
80dB
S2/+1/3/ 4
CPS-Verst=
3Δ=4
0/M:3
Speichert
3:24:45
12:20:38
00:14
CPS
Misch
Verlassen
Stopuhr stoppen

(b)

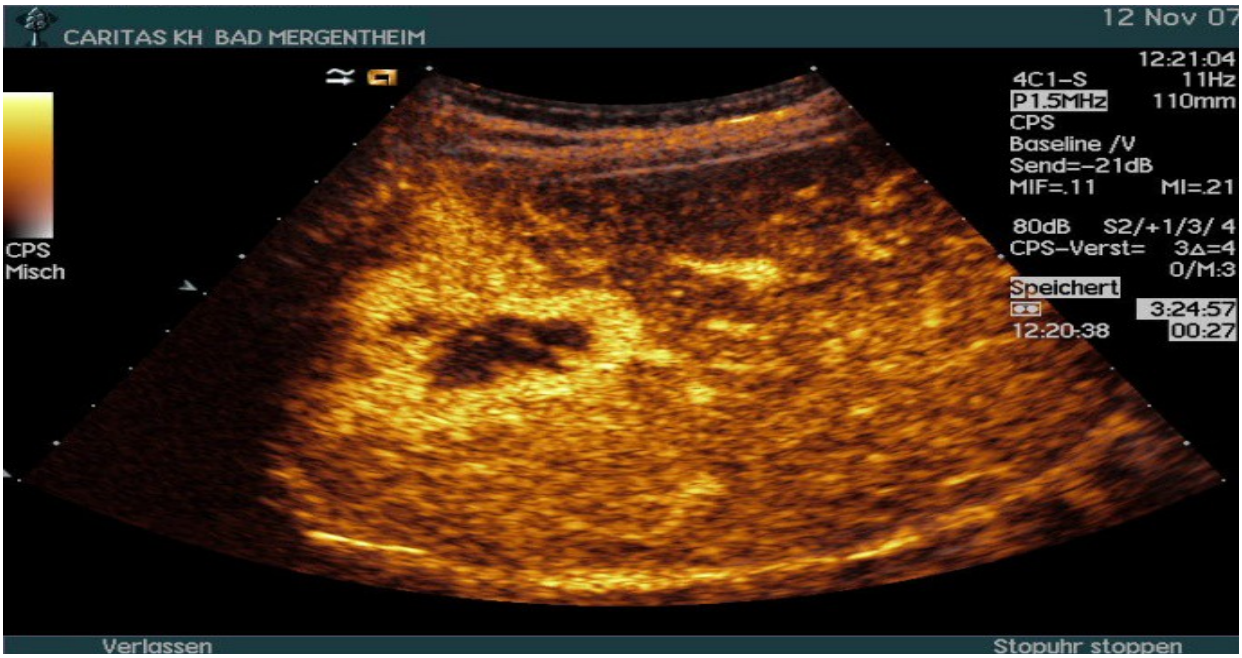
CARITAS KH BAD MERGENTHEIM
12 Nov 07
12:21:04
4C1-S
11Hz
P1.5MHz
110mm
CPS
Baseline /V
Send=-21dB
MIF=.11
MI=.21
80dB
S2/+1/3/ 4
CPS-Verst=
3Δ=4
0/M:3
Speichert
3:24:57
12:20:38
00:27
CPS
Misch
Verlassen
Stopuhr stoppen

(c)

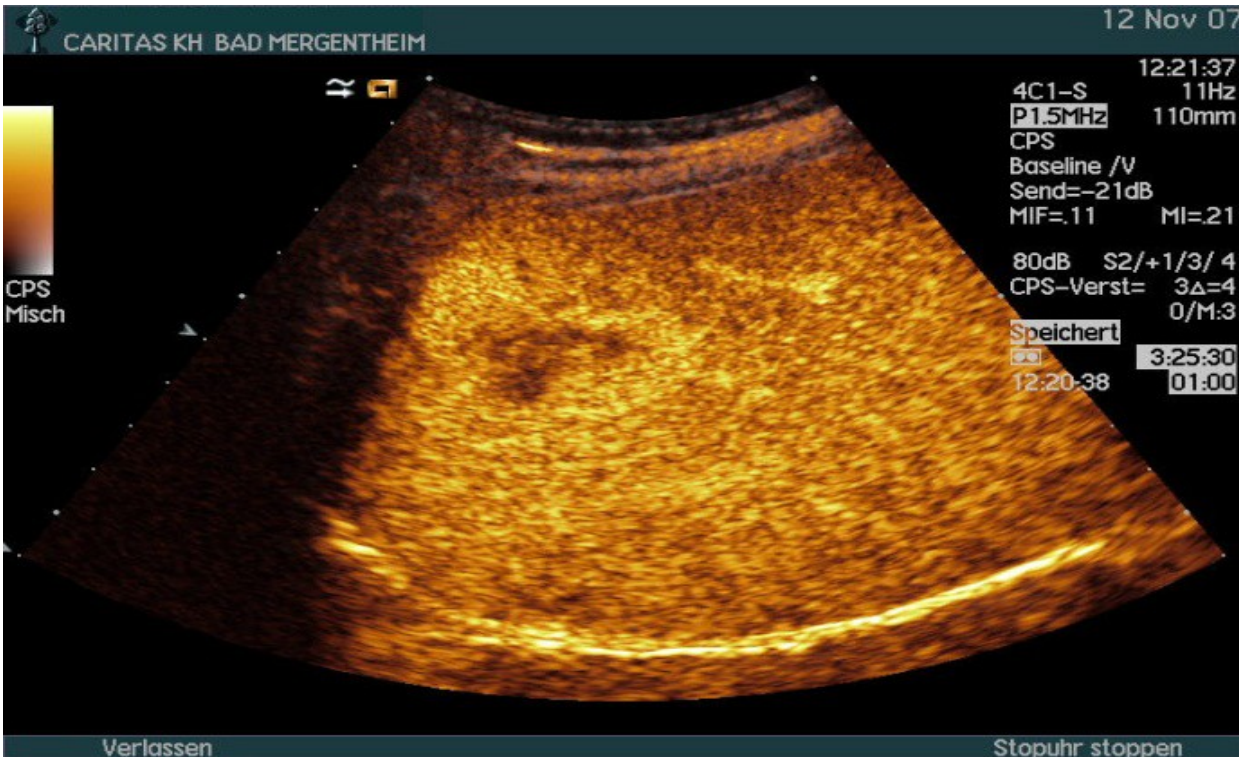

(d)

Figure (2.32) Haemangioma. Haemangioma in B-mode between markers (a). The typical contrast-enhanced ultrasound findings are peripheral nodular contrast-enhancement and centripetal fill-in (“iris diaphragm phenomenon”) with the exception of thrombosed areas and calcifications (shown between callipers (+)) [b-d] (case of the month, EFSUMB.org).

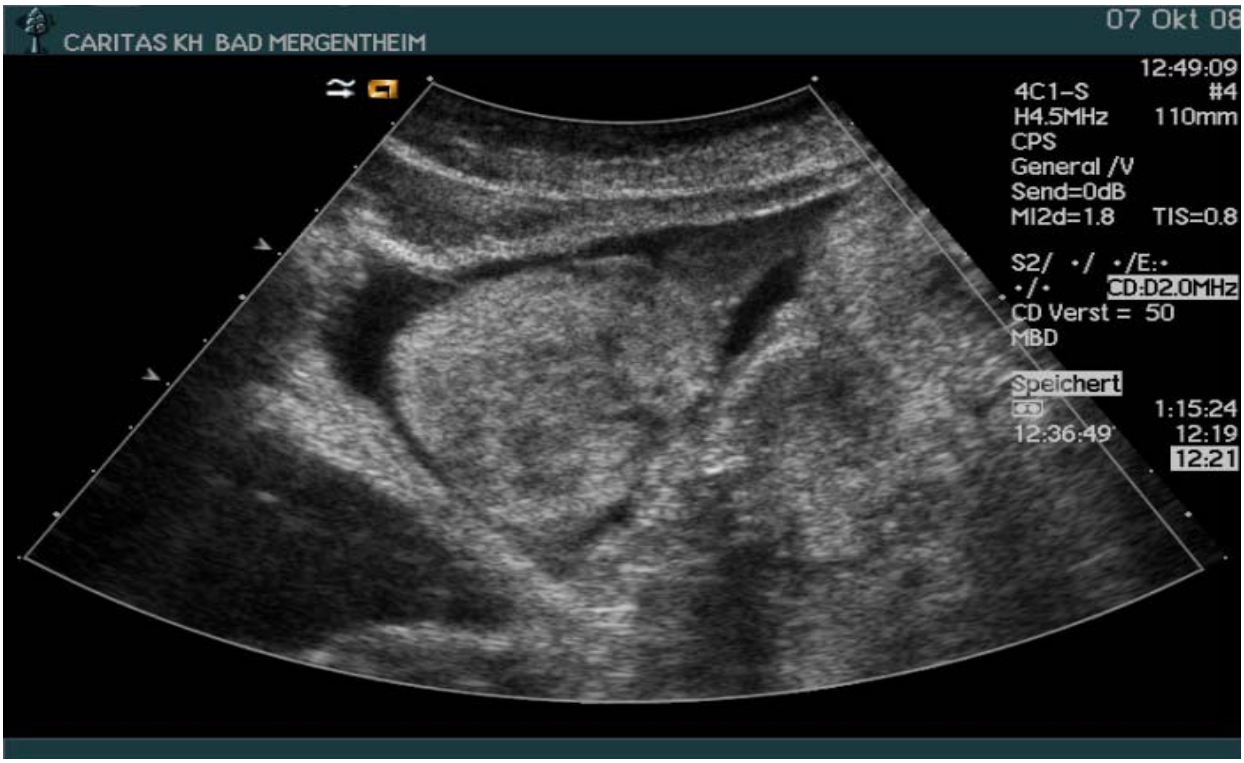
CARITAS KH BAD MERGENTHEIM
07 Okt 08
12:49:09
4C1-S
#4
H4.5MHz
110mm
CPS
General /V
Send=0dB
MI2d=1.8
TIS=0.8
S2/ •/ •/E:•
•/•
CD:D2.0MHz
CD Verst = 50
MBD
Speichert
1:15:24
12:36:49
12:19
12:21

(a)

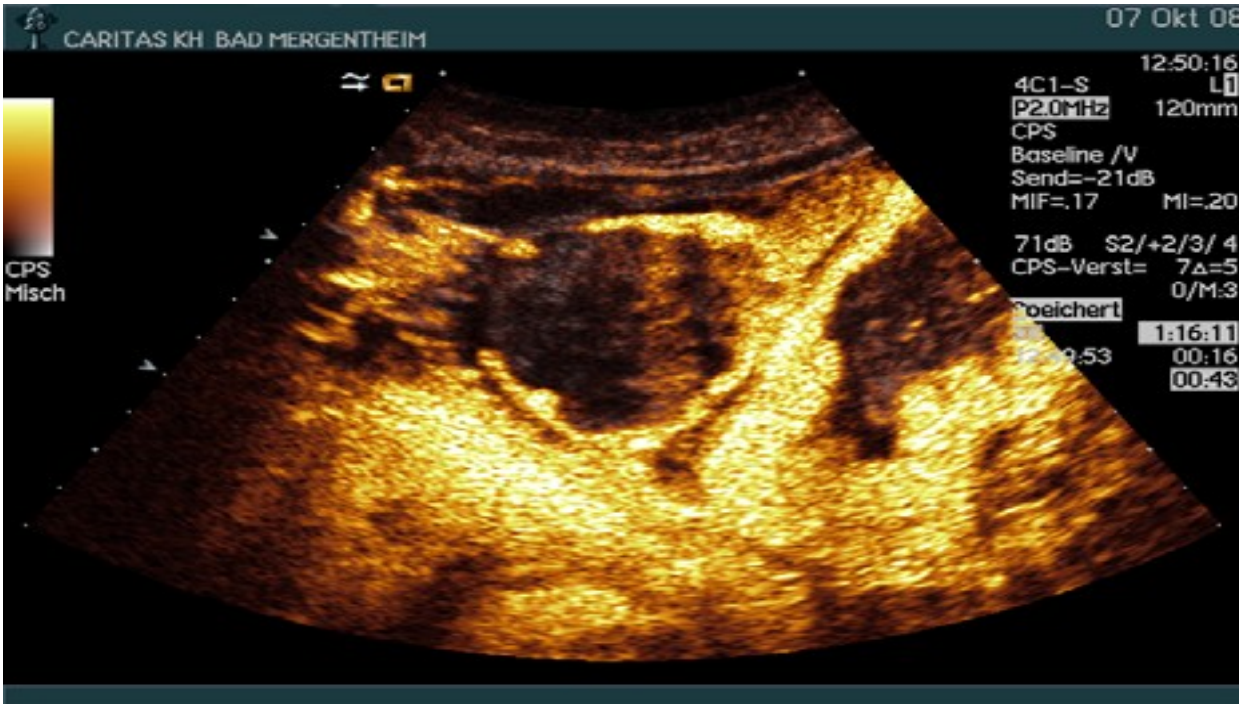
CARITAS KH BAD MERGENTHEIM
07 Okt 08
12:50:16
4C1-S
L1
P2.0MHz
120mm
CPS
Baseline /V
Send=-21dB
MIF=.17
MI=.20
71dB
S2/+2/3/ 4
CPS-Verst=
7Δ=5
0/M:3
Speichert
1:16:11
00:16
00:43
CPS
Misch

(b)

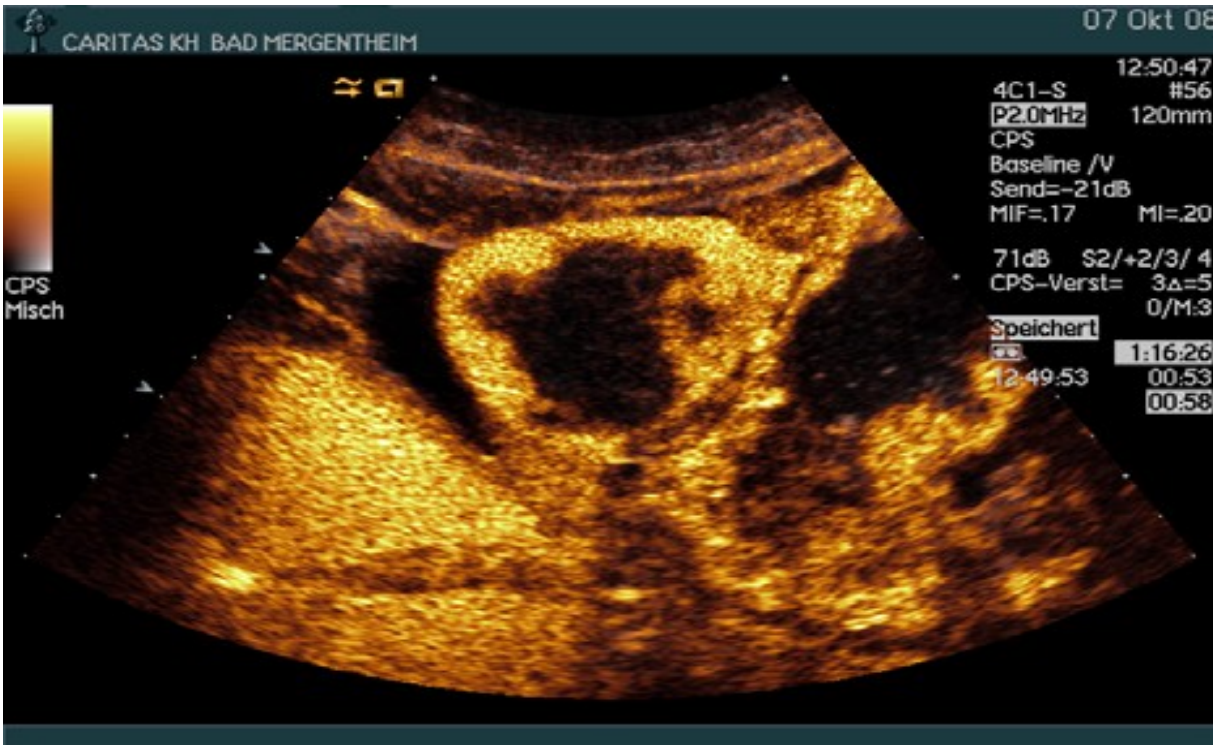

(c)

(Figure 2.33) Haemangioma. (a) The typical B-mode appearance is hyperechoic, which is also seen in liver cirrhosis. Contrast-enhanced ultrasound findings are peripheral nodular contrast-enhancement and centripetal fill in with the exception of thrombosed areas and calcifications (iris diaphragm phenomenon) (b,c).

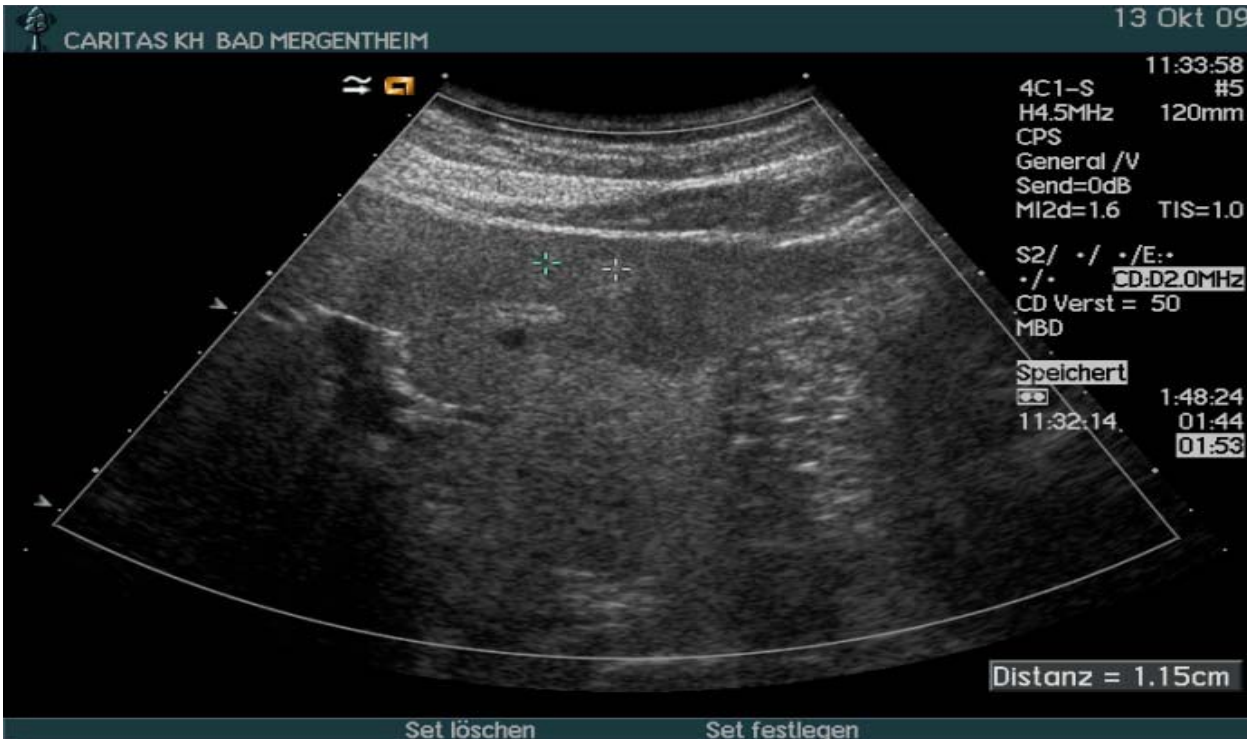
CARITAS KH BAD MERGENTHEIM
13 Okt 09
11:33:58
4C1-S
#5
H4.5MHz
120mm
CPS
General /V
Send=0dB
MI2d=1.6
TIS=1.0
S2/ •/ •/E:•
•/•
CD:D2.0MHz
CD Verst = 50
MBD
Speichert
1:48:24
11:32:14
01:44
01:53
Distanz = 1.15cm
Set löschen
Set festlegen

(a)

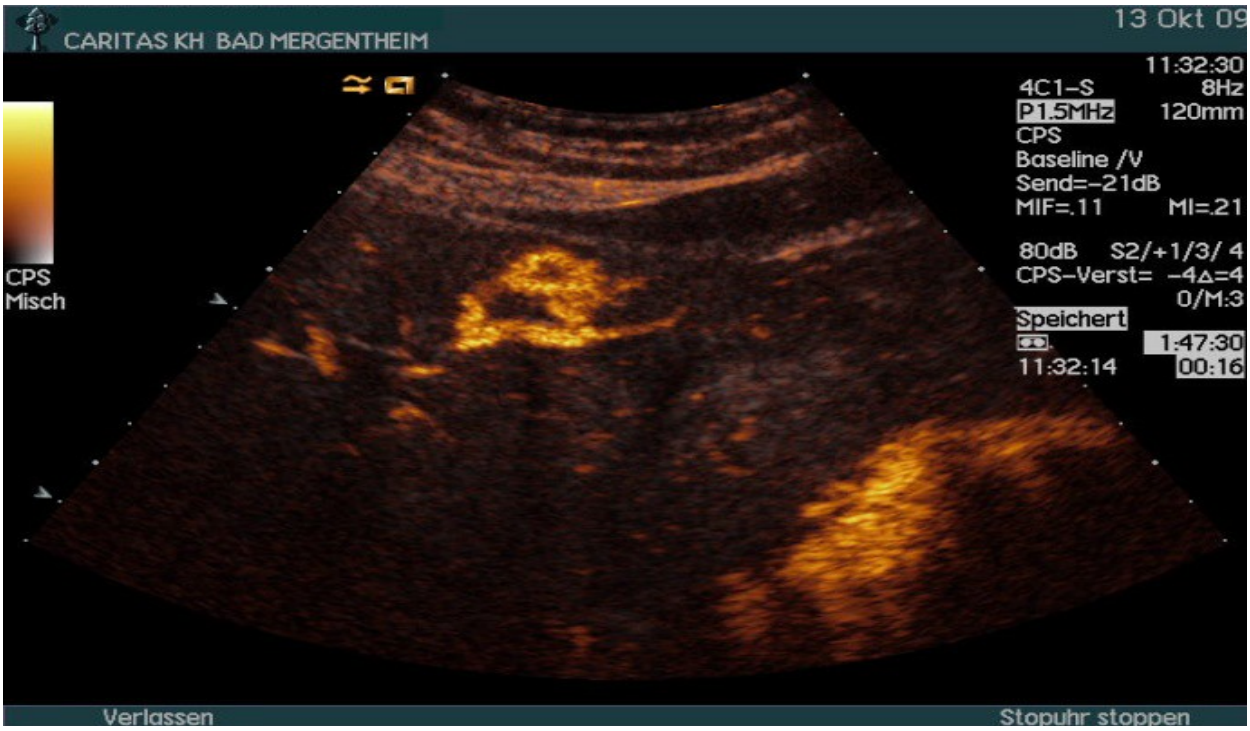
CARITAS KH BAD MERGENTHEIM
13 Okt 09
11:32:30
4C1-S
8Hz
P1.5MHz
120mm
CPS
Baseline /V
Send=-21dB
MIF=.11
MI=.21
80dB
S2/+1/3/ 4
CPS-Verst= -4Δ=4
0/M:3
CPS
Misch
Speichert
1:47:30
11:32:14
00:16
Verlassen
Stopuhr stoppen

(b)

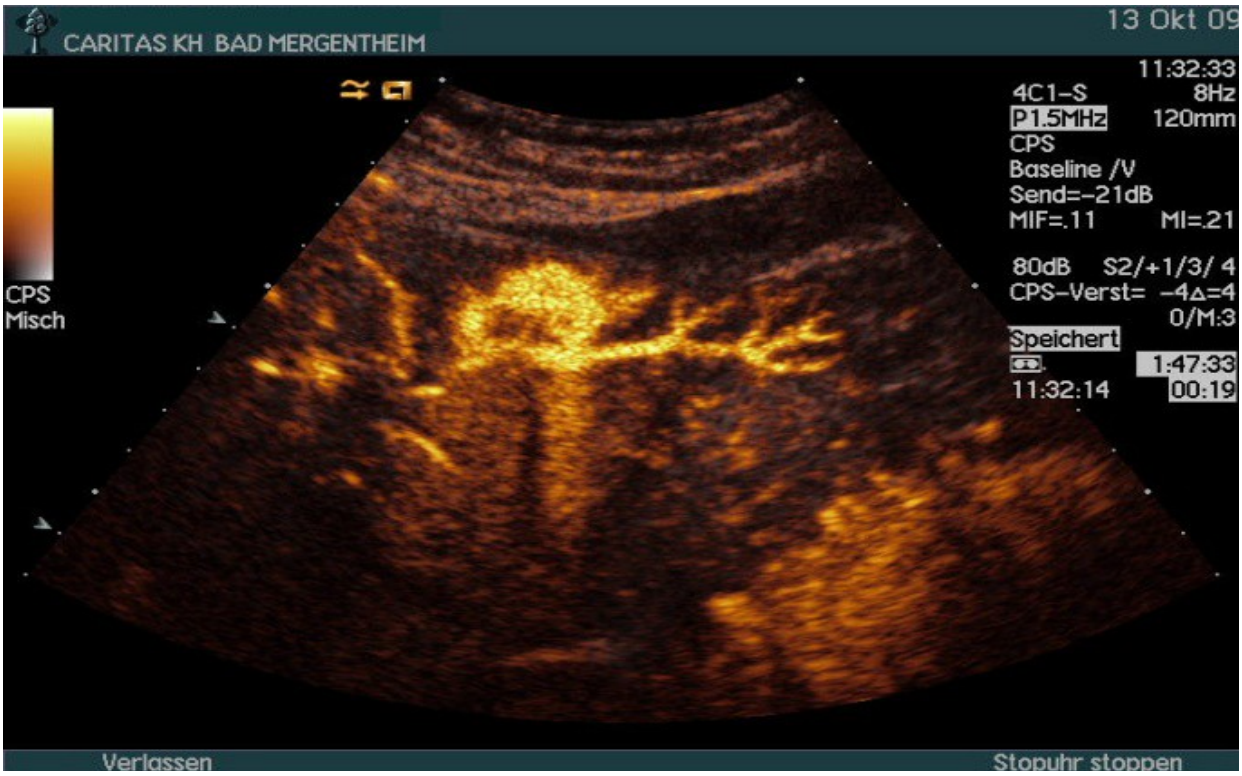

(c)

(Figure 2.34) Shunt haemangioma. (a) Focal hypoechoic and hyperechoic lesions are sub-capsular with inhomogenous echogenicity. Colour and power Doppler imaging were not helpful. The real lesion is shunt-haemangioma (shown between callipers (+)) with arterioportal venous shunts (shunt haemangioma) leading to regional inhomogeneous fat content. (b,c) The typical contrast-enhanced ultrasound finding is centripetal fill-in within seconds and bright appearance in the portal venous phase. The lesions are often missed by CT and MRI because of their small size (typically less than 15mm) and differences in the arterial enhancement pattern in comparison with the surrounding parenchyma for only 1-2s. The final diagnosis is made by histology in patients with malignant underlying disease.

2.3.19.10.6. Focal nodular hyperplasia

FNH and the important differential diagnosis of HCA are two benign, mostly incidental, hepatic neoplasias, which occur predominantly in young and middle-aged women. Differentiation is essential because of the different therapeutic approaches; HCA is an indication for surgery because of the risk of haemorrhage and potential malignant transformation, in contrast FNH can be managed conservatively. Until recently non-invasive differentiation of, especially, atypical FNH from HCA and other benign or malignant neoplasia has remained challenging; there have been no satisfactory tests apart from histological examination of a liver biopsy sample. Histological features of FNH are controversial in the literature. Congenital absence of portal veins has been reported in a few patients, mainly children.

Helical CT and MRI do provide some useful information in the diagnosis of FNH, especially when the lesion depicts typical features, such as a central scar and uniform hypervascularity. Typical features are only reported in approximately 50% of patients. In a series of 305 macroscopically studied FNH, a central scar was found in only approximately 50% (Christoph F. Dietrich.2011).

2.3.19.11. Conventional B-mode ultrasound

FNH is typically an isoechoic tumour of variable size, with a central scar and calcifications (in 50–80%).

2.3.19.11.1. Colour Doppler imaging

Typically, CDI reveals an arterially hypervascularised tumor (in >90%) with characteristic (para-) central arterial blood supply. In many patients, increased blood flow compared with the surrounding liver tissue can be detected even in colour Doppler mode, which causes a so-called wheel-spoke phenomenon. Hyper perfusion can be identified in native imaging and is by no

means obligatory; it is reported in only approximately 50-70% of patients. Inter-observer reliability in recognizing the wheel-spoke appearance is very low.

2.3.19.11.2. Contrast-enhanced ultrasound

The examination of the hepatic arterial and portal venous/sinusoidal phase by contrast-enhanced phase inversion ultrasound allows for a reliable differentiation between FNH and HCA. This important finding can be explained by the lack of portal veins in contrast with FNH, which presents (atypical) portal veins in many but not all patients.

In contrast-enhanced examination, FNH typically appears as a hyperperfused tumour-like lesion relative to the surrounding liver tissue in the early arterial phase. The lesion’s hyperperfusion is easily visible with contrast enhancement during continuous scanning, compared with the surrounding hepatic arteries. Depending on the patient’s cardiac output, some 8 to 20s after injection of the echo-signal enhancer into the cubital vein there is a rapid take-up of the substance with demonstration of the arterial vascular pattern and enhancement from the centre outwards. During the portal venous phase FNH is isoechogenic with the portal vein, and, therefore, slightly hyper-perfused in comparison with the surrounding liver parenchyma (Figure 2.34) (Christoph F. Dietrich.2011).

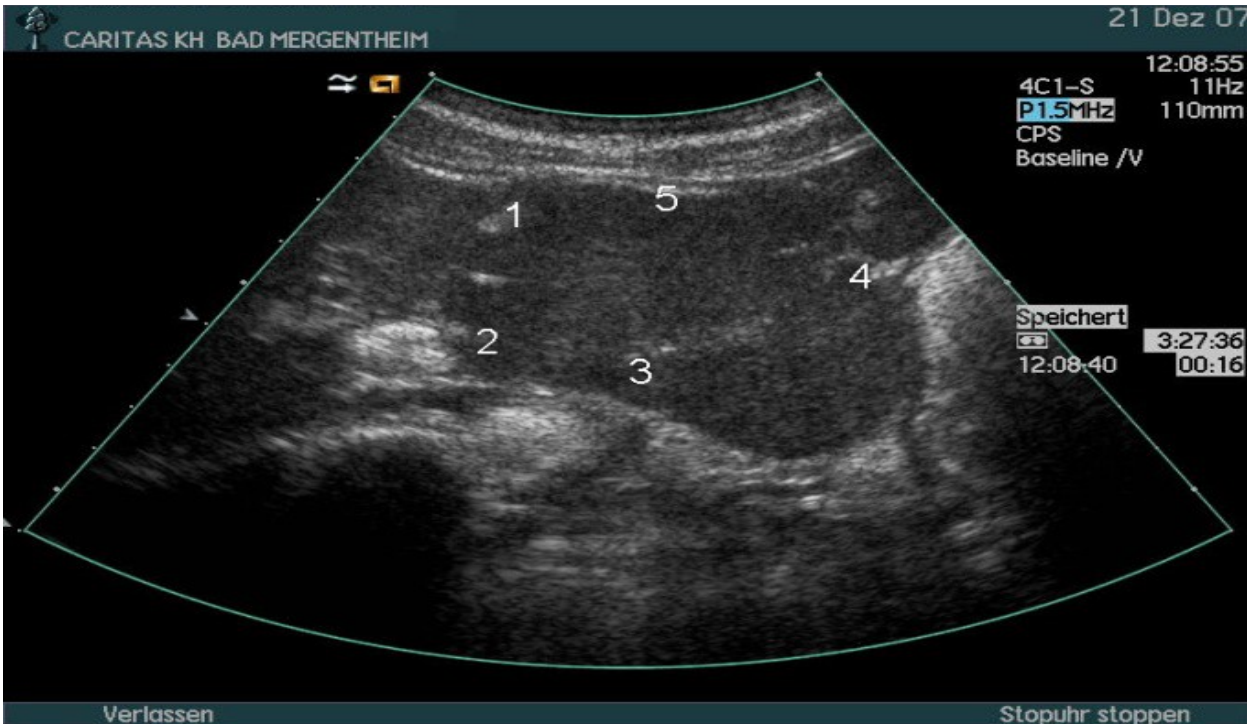
CARITAS KH BAD MERGENTHEIM
21 Dez 07
12:08:55
4C1-S
11Hz
P1.5MHz
110mm
CPS
Baseline /V
1
5
4
2
3
Speichert
3:27:36
12:08:40
00:16
Verlassen
Stopuhr stoppen

(a)

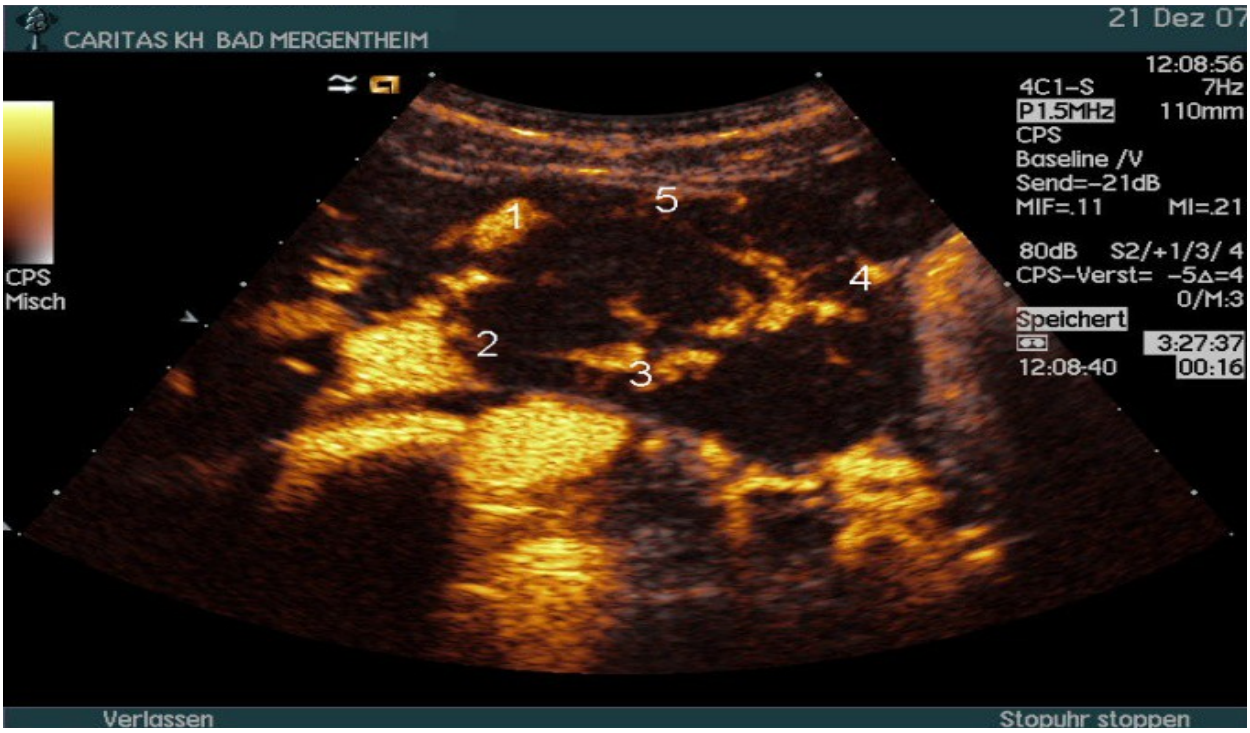
CARITAS KH BAD MERGENTHEIM
21 Dez 07
12:08:56
4C1-S
7Hz
P1.5MHz
110mm
CPS
Baseline /V
Send=-21dB
MIF=.11
MI=.21
80dB S2/+1/3/ 4
CPS-Verst= -5Δ=4
0/M:3
CPS
Misch
1
5
4
2
3
Speichert
3:27:37
12:08:40
00:16
Verlassen
Stopuhr stoppen

(b)

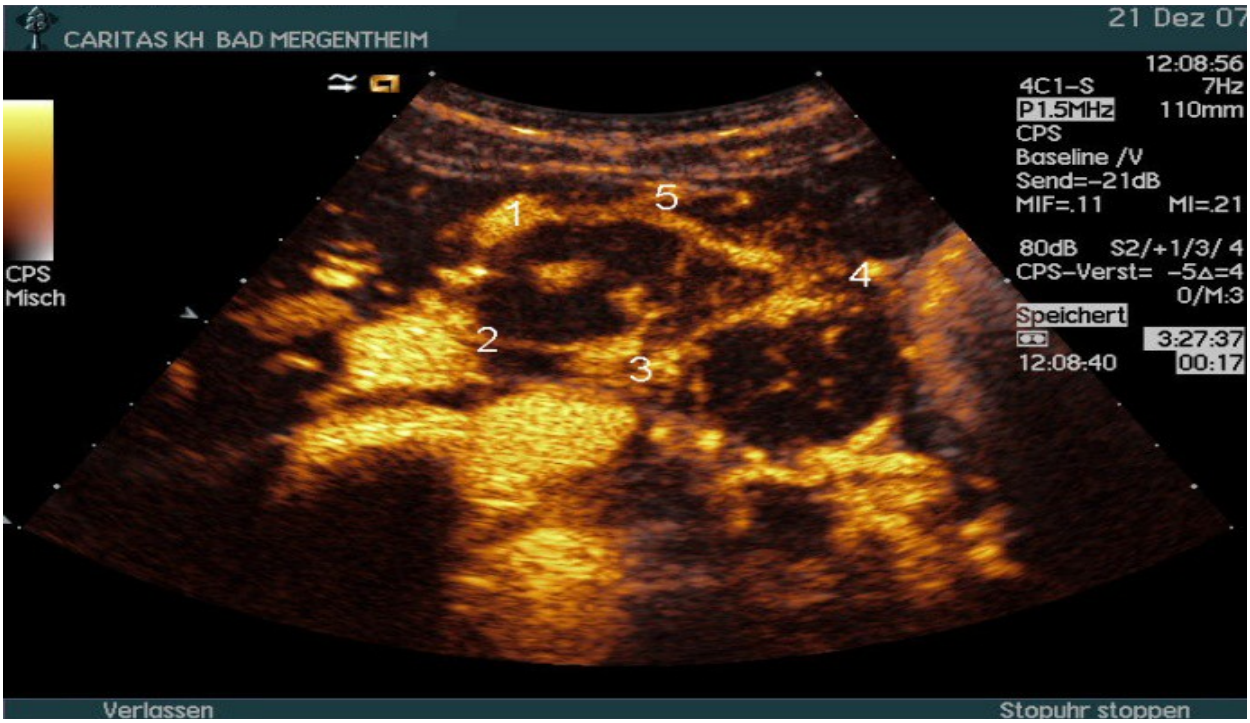
CARITAS KH BAD MERGENTHEIM
21 Dez 07
12:08:56
4C1-S
7Hz
P1.5MHz
110mm
CPS
Baseline /V
Send=-21dB
MIF=.11
MI=.21
80dB
S2/+1/3/ 4
CPS-Verst=
-5Δ=4
0/M:3
Speichert
3:27:37
12:08:40
00:17
CPS
Misch
1
2
3
4
5
Verlassen
Stopuhr stoppen

(c)

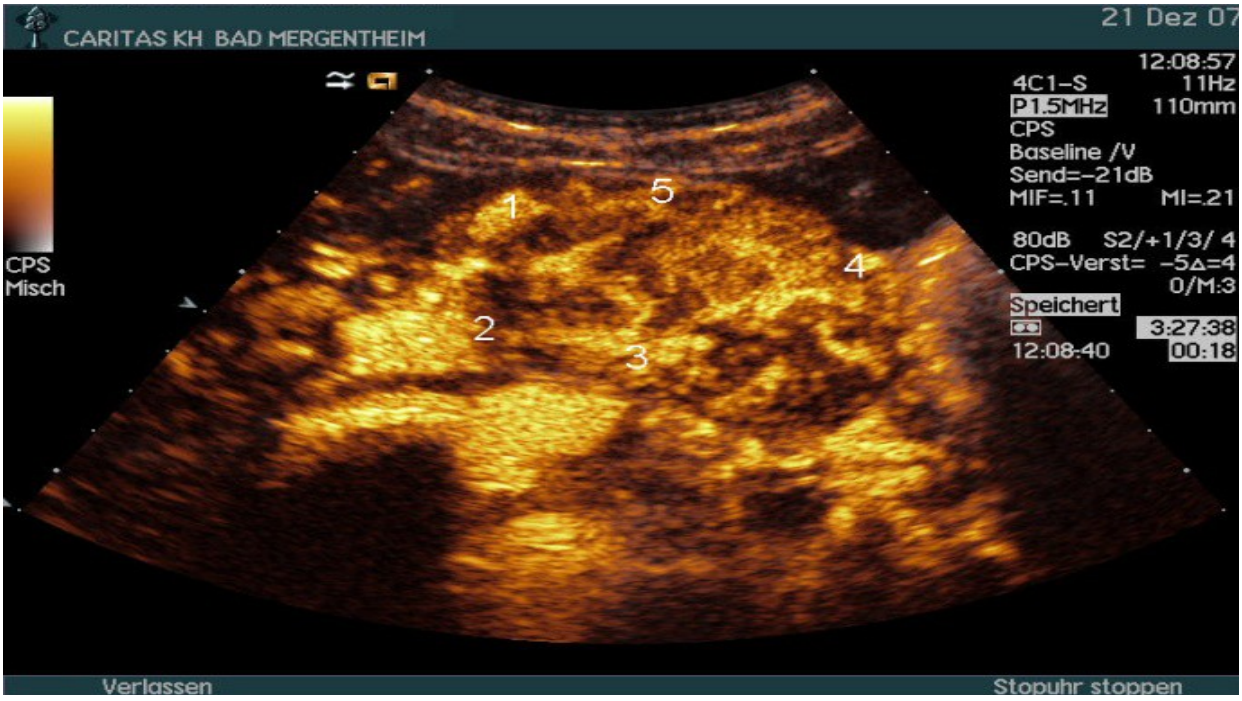
CARITAS KH BAD MERGENTHEIM
21 Dez 07
12:08:57
4C1-S
11Hz
P1.5MHz
110mm
CPS
Baseline /V
Send=-21dB
MIF=.11
MI=.21
80dB
S2/+1/3/ 4
CPS-Verst=
-5Δ=4
0/M:3
Speichert
3:27:38
12:08:40
00:18
CPS
Misch
1
2
3
4
5
Verlassen
Stopuhr stoppen

(d)

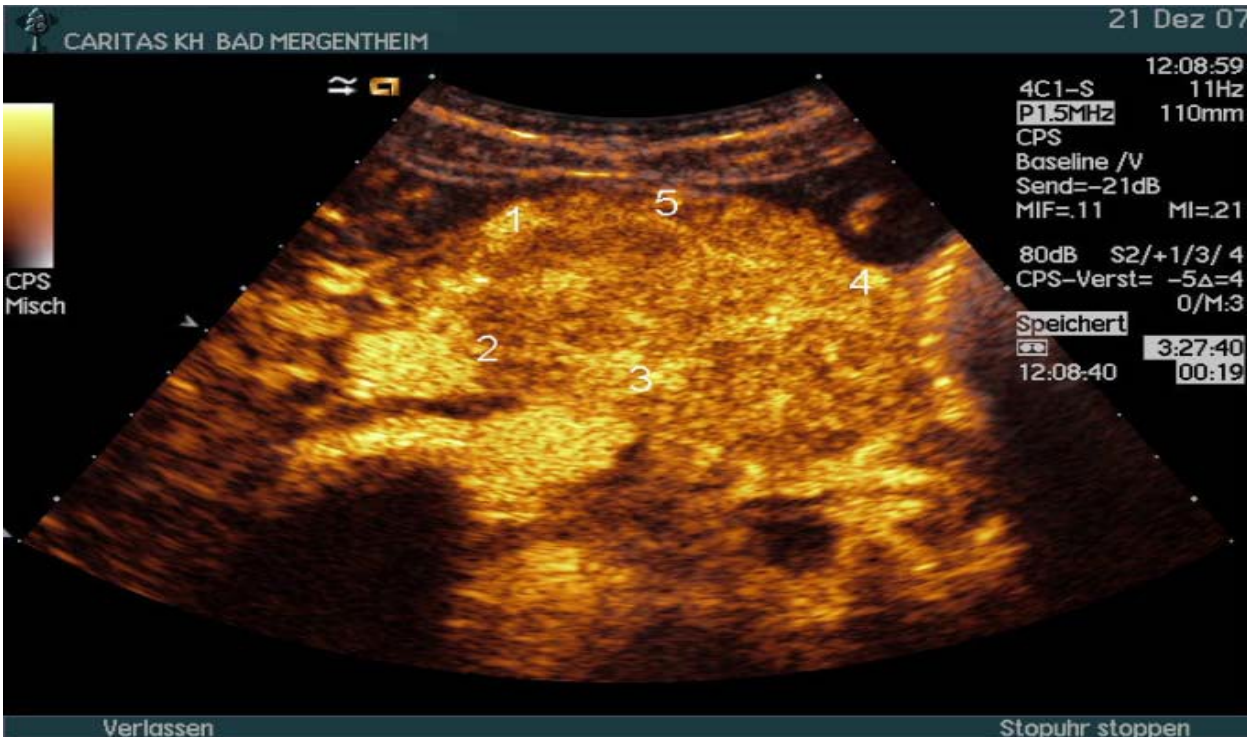
CARITAS KH BAD MERGENTHEIM
21 Dez 07
12:08:59
4C1-S
11Hz
P1.5MHz
110mm
CPS
Baseline /V
Send=-21dB
MIF=.11
MI=.21
80dB
S2/+1/3/ 4
CPS-Verst=
-5Δ=4
0/M:3
Speichert
3:27:40
12:08:40
00:19
CPS
Misch
1
2
3
4
5
Verlassen
Stopuhr stoppen

(e)

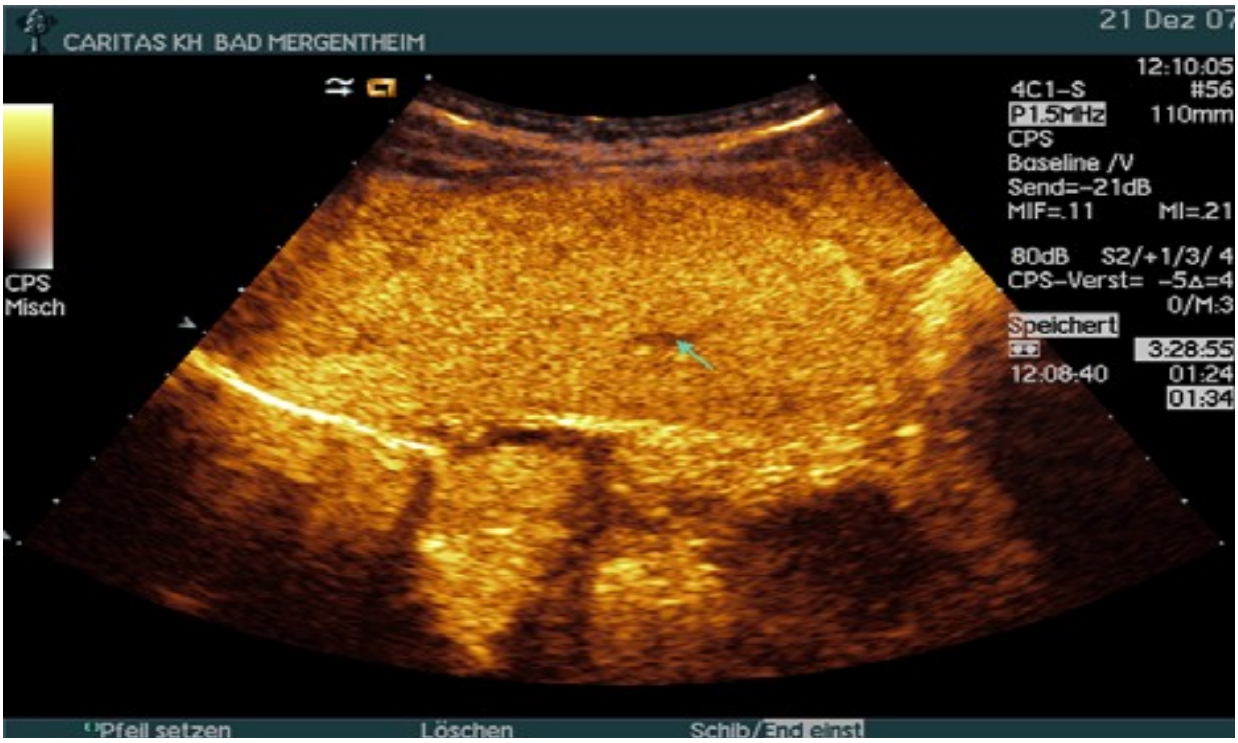
CARITAS KH BAD MERGENTHEIM
21 Dez 07
12:10:05
4C1-S
#56
P1.5MHz
110mm
CPS
Baseline /V
Send=-21dB
MIF=.11
MI=.21
80dB
S2/+1/3/ 4
CPS-Verst=
-5Δ=4
0/M:3
Speichert
3:28:55
12:08:40
01:24
01:34
CPS
Misch
Pfeil setzen
Löschen
Schib/End einst

(f)

(Figure 2.35) (a) Focal nodular hyperplasia (FNH) using B-mode ultrasound often appears as isoechoic in comparison with the surrounding liver parenchyma and can not be differentiated from malignant tumours such as hepatocellular carcinoma. (b-e) FNH in the arterial phase typically appears as a hypervascular and hyperperfused structure relative to the surrounding liver tissue demonstrating the typical central artery in up to 70% of cases, whereas in larger FNH more than one supply artery can be displayed (indicated by numbers). During the portal venous phase FNH is slightly hyperechoic in comparison with the surrounding liver parenchyma in more than 90% of lesions. The typical central scar (arrow, f) can be found in up to 70% of patients with FNH, which has been proven in autopsy studies.

2.3.19.12.Hepatocellular adenoma

2.3.19.12.1.Conventional B-mode ultrasound

In B-mode ultrasound, of an otherwise normal liver, HCA is usually isoechogenic with the surrounding liver tissue. Owing to this lack of echogenicity, an adenoma can be very difficult to differentiate from the surrounding liver tissue. In a fatty liver, adenomas may be poorly echogenic, whereas in patients with storage diseases (e.g. glycogenosis or Niemann-Pick disease) adenomas may give stronger echoes (hyperechoic). A rounded contour or a vascular impression may indicate a tumour poorly discernable from liver parenchyma. There are no other typical criteria in B-mode ultrasound (Christoph F. Dietrich.2011).

2.3.19.12.2. Colour Doppler imaging

HCA exhibit predominantly marginal arterial hypervascularity, which can be shown by CDI and CEUS. However, this vascular pattern can also be encountered in HCC and hyperperfused

metastases, and is therefore not pathognomonic. Calcifications and other regressive changes are observed depending on the size of the lesion.

2.3.19.12.3.Contrast-enhanced ultrasound

Histologically no portal veins (and in addition, no bile ducts) are present in adenomas, therefore, CEUS demonstrates only homogeneous enhancement during hepatic arterial phase (8 to 25s after injection) but no portal venous enhancement (Figure 34) resulting in slightly hypoenhancing (hypoechoic) appearance in comparison with the surrounding liver parenchyma since some overlap of the arterial and capillary phase (continuing over some minutes) may be observed (Christoph F. Dietrich.2011).

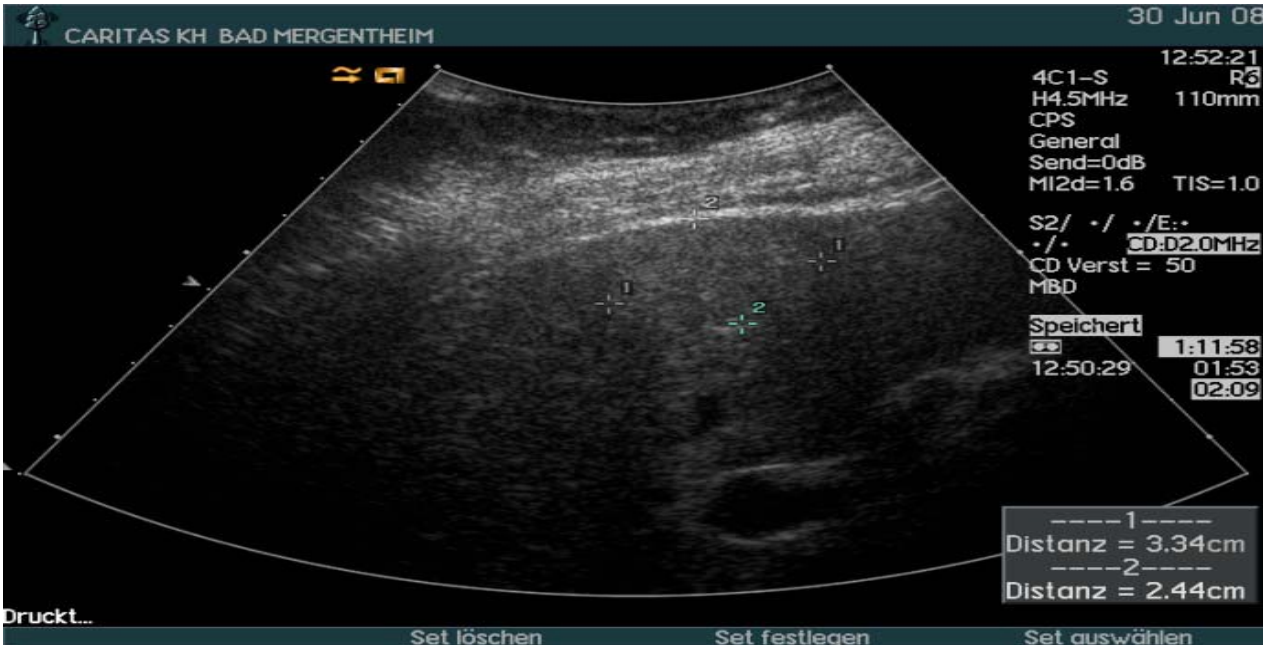

(a)

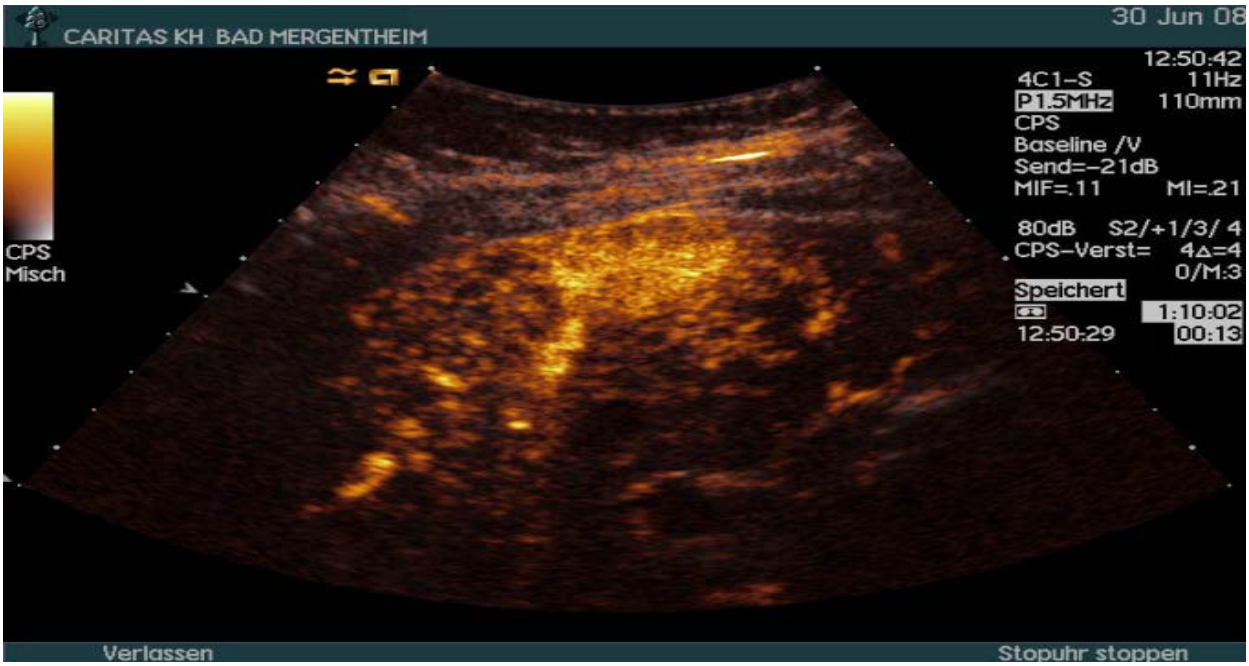
CARITAS KH BAD MERGENTHEIM
30 Jun 08
12:50:42
4C1-S
11Hz
P1.5MHz
110mm
CPS
Baseline /V
Send=-21dB
MIF=.11
MI=.21
80dB
S2/+1/3/ 4
CPS-Verst=
4Δ=4
0/M:3
Speichert
1:10:02
12:50:29
00:13
CPS
Misch
Verlassen
Stopuhr stoppen

(b)

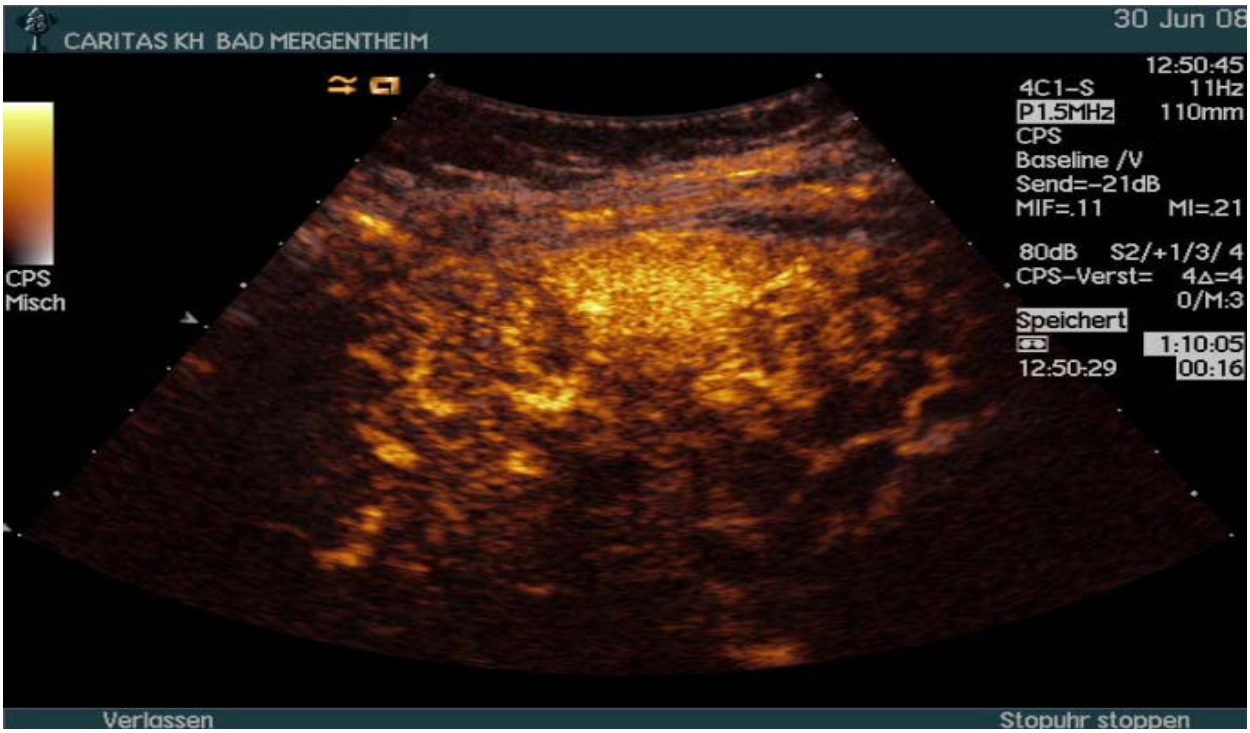
CARITAS KH BAD MERGENTHEIM
30 Jun 08
12:50:45
4C1-S
11Hz
P1.5MHz
110mm
CPS
Baseline /V
Send=-21dB
MIF=.11
MI=.21
80dB
S2/+1/3/ 4
CPS-Verst=
4Δ=4
0/M:3
Speichert
1:10:05
12:50:29
00:16
CPS
Misch
Verlassen
Stopuhr stoppen

(c)

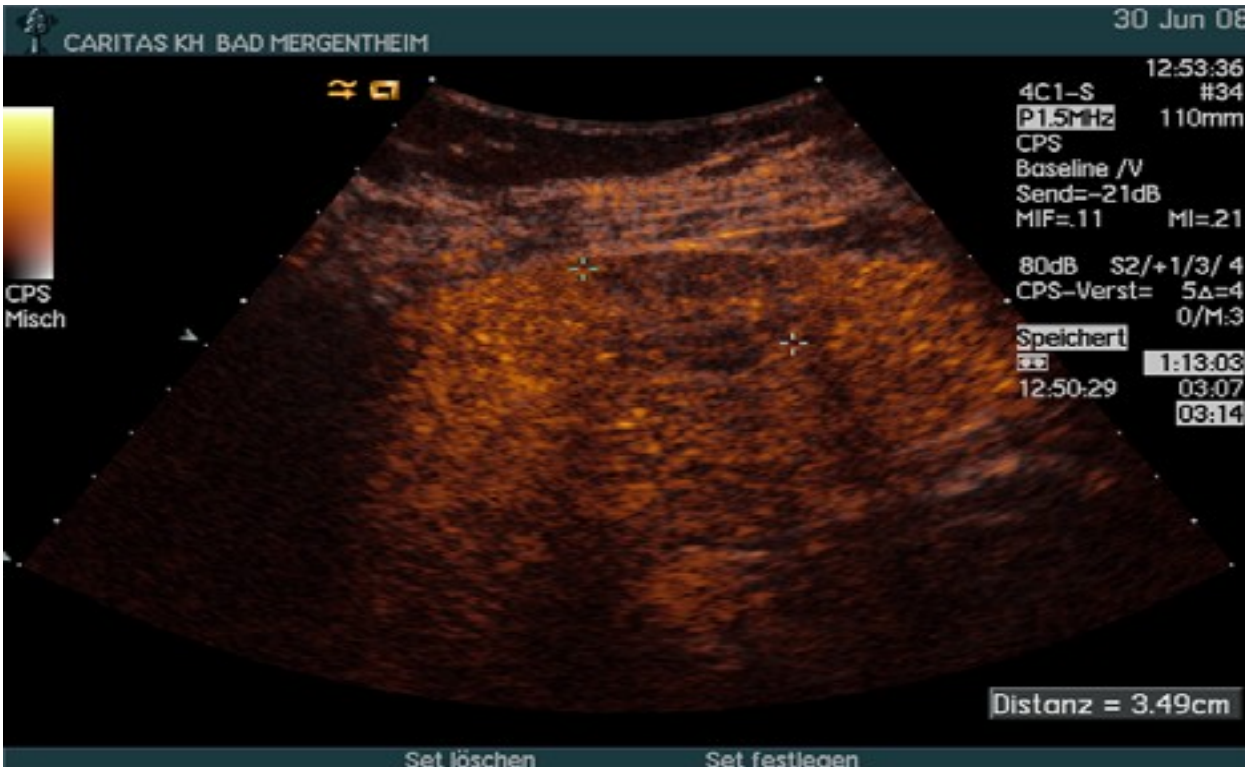

(d)

(Figure 2.36) Hepatocellular adenoma (HCA). (a) B-mode ultrasound shows an unspecific slightly hyperechoic focal liver lesion. (b, c) Contrast-enhanced ultrasound (CEUS) revealed only arterial phase enhancement after administration of SonoVue®. (d) At the end of the arterial phase (<30s after administration of SonoVue®) a hypoechoic liver tumour was detected on CEUS, which is the typical enhancement pattern of HCA in comparison with focal nodular hyperplasia (FNH), which showed more portal venous enhancement than the surrounding liver parenchyma in 96% of 300 patients with FNH [own data, not yet published].

2.3.19.13. Focal fatty lesion (regional focal fatty infiltration)

Fatty infiltration was generally considered to be a diffuse process involving the entire liver. Since Brawer and Scott identified focal hepatic fatty infiltration at autopsy and in imaging studies in 1980, focal hepatic fatty infiltration has been widely discussed. Bright focal areas in the liver

hilum occur in >40% of inflammatory bowel disease patients while taking corticosteroid medication. The histological nature of these corticosteroid derived lesions is not yet clear. Different amounts or types (large, small vacuoles) of fat deposition are likely, because a change of appearance over time can be observed. Changes in arterioportal venous perfusion have been suggested. Haemangiomas may mimic such lesions; however, not all bright lesions in the liver are haemangiomas. It is well known that the vascular supply of the hilar region in liver segment IV differs from the perfusion of liver tissue adjacent to the gallbladder. This could give a possible explanation for different reactions of liver parenchyma to fatty infiltration. In patients with focal fatty lesions, depending on the quality of the equipment used, we observed centrally located arterial blood supply and direct venous drainage into the liver hilum (Figure 2.33). (Christoph F. Dietrich.2011)

2.3.19.13.1. Conventional B-mode ultrasound

Fatty infiltration may affect the liver diffusely or focally, but it does not usually cause any mass effect or displace vessels. Sonographically, hepatic fatty infiltration appears as segmental or lobular areas of brighter echogenicity, in contrast with the echogenicity of the normal liver parenchyma. A central, perihilar location in segment IV or V is typical, other locations are rarely involved. An oval shaped hypoechoic lesion in the liver hilum is always related to a fatty liver and could represent normal liver tissue surrounded by diffuse fatty infiltration of the liver. A hypoechoic lesion in the liver hilum without signs of expansion seem to be a relevant sign of fatty liver and should not be confused with mass lesions. The typical relationship to fatty liver, location and shape are all helpful in differential diagnosis (Christoph F. Dietrich.2011)

2.3.19.13.2. Colour Doppler imaging

In colour Doppler ultrasound, both focal fatty degeneration and its focal absence appear normal; neither hyper- nor hypoperfusion is apparent, since the liver tissue is normal. Typically, central feeding and draining vessels (Figure 7) may be detected in a high percentage of patients demonstrating the pathogenetic mechanism of different vascularisation of the liver hilum.

2.3.19.13.3. Contrast-enhanced ultrasound

CEUS is helpful to rule out malignant infiltration. In the arterial and venous phase the supplying and draining vessels of the liver hilum can be imaged. In the enhanced echo-signal sequence, different fatty degeneration regions are imaged in the same way as normal liver tissue in the portal venous phase. Therefore, in the portal venous phase these lesions are indistinguishable from the background. Enhancement in the arterial phase might be slightly delayed in comparison with the surrounding liver parenchyma.

2.3.19.14. Hepatocellular carcinoma

2.3.19.14.1. Conventional B-mode ultrasound

There are no typical criteria in B-mode ultrasound in small HCC (<30mm). Echogenicity of the lesion depends on its size and the surrounding liver tissue (cirrhotic vs. non-cirrhotic) (Figure 35-36). HCC in an otherwise normal liver parenchyma is usually iso- or slightly hypoechoic compared with the surrounding liver tissue. HCC can be very difficult to identify in patients with liver cirrhosis and tumour morphology can be iso-, hypo- or hyperechoic. Dysplastic nodules are sometimes difficult to differentiate (Figure 2.38) (Christoph F. Dietrich.2011).

2.3.19.14.2. Colour Doppler imaging

HCC are, in most cases (80–90%), distinctly hypervascularised using conventional CDI (Figure 35) and are mainly peripherally located. In such cases, it is possible to confuse them with other hyperperfused liver tumours; however, these are rarely observed in a cirrhotic liver. From a differential diagnostic point of view it is then necessary to consider metastases of hyperperfused tumours, e.g. a hypernephroma, breast carcinoma, lung cancer or more typical carcinoid tumours. Metastases of primary extrahepatic tumours are, however, rare in a cirrhotic liver.

2.3.19.14.3. Contrast-enhanced ultrasound

HCC typically exhibits hyperperfusion of the tumour compared with the surrounding liver tissue at this point there is no discernible contrast effect in the surrounding liver. In the HCC a typically chaotic vascular pattern is observed, which is a sign of neovascularisation of the tumour. Regenerative nodules may also exhibit an additional arterial enrichment. Analysis of the portal venous phase makes it possible to differentiate these isoenhancing nodules from the weakly contrasting HCC.

Sonographic recognition of HCCs in liver cirrhosis can be difficult if the echo-texture is very inhomogeneous. One possible approach is to examine the liver in the early arterial phase after injection of a signal enhancer with a low mechanical index (<0.4). The use of Levovist, which has a high mechanical index (MI 1.2-1.6, 20 dB, scan rate 10-15 per second), to analyses the late phase (>3min) has been found to be helpful in improving the detection in some patients. CEUS has proven to be effective in the differential diagnosis of cirrhotic nodules (regenerative and hyperplastic nodules) (Christoph F. Dietrich.2011).

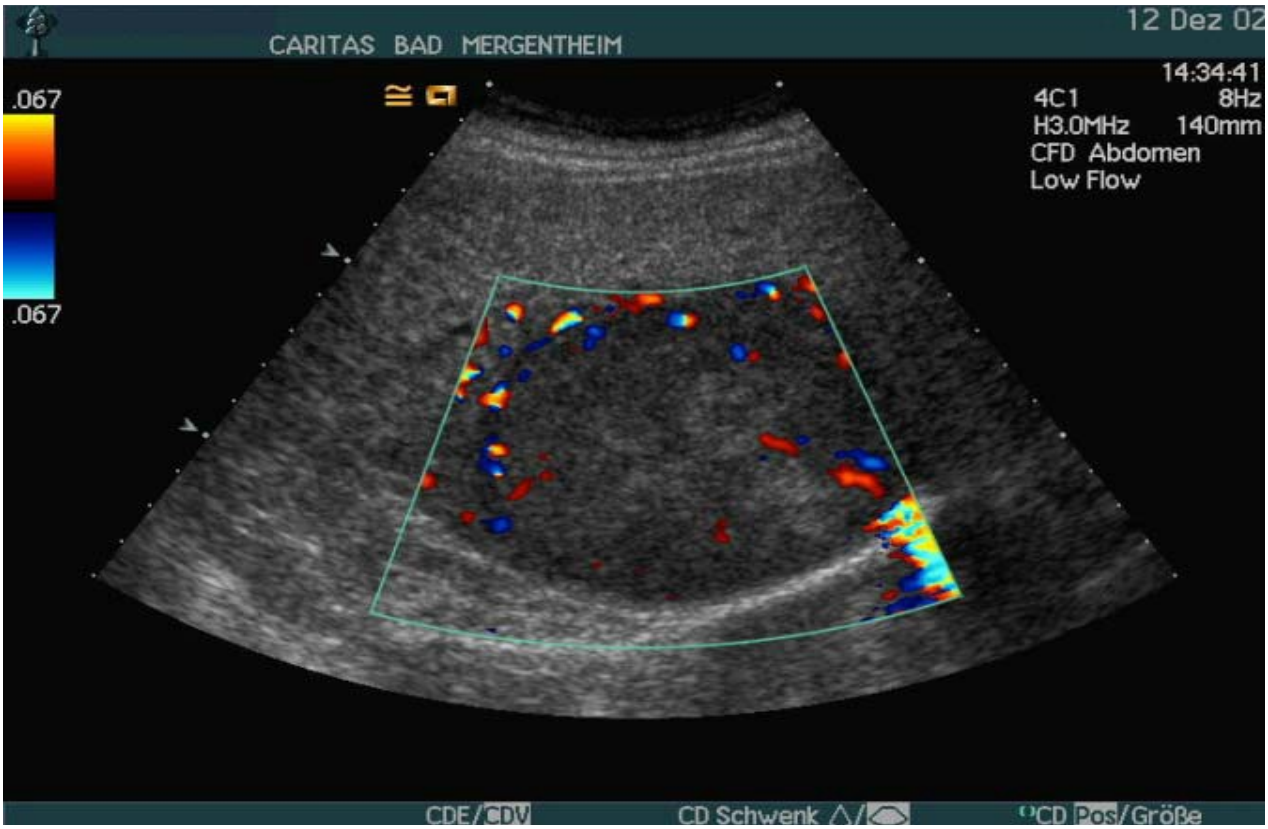

(Figure 2.37) More common, hypoechoic hepatocellular carcinoma with typically peripheral located hypervascularity using colour Doppler imaging.

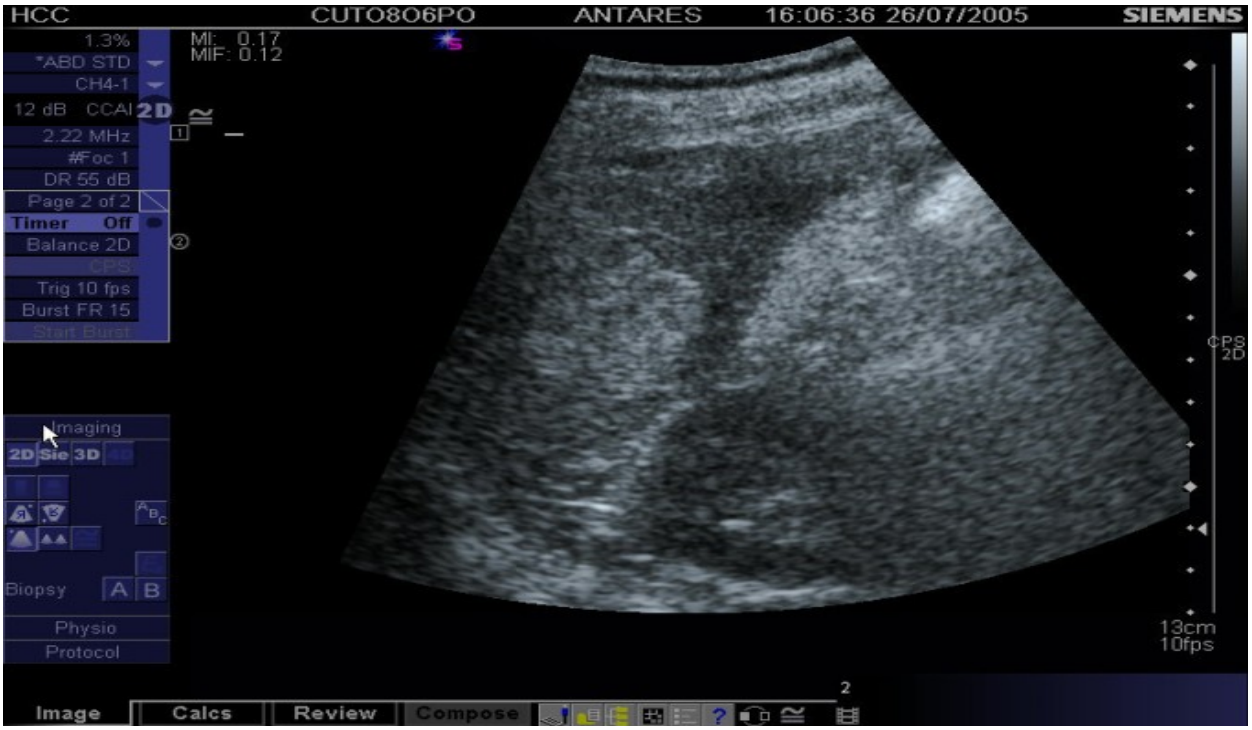
HCC
CUTO8O6PO
ANTARES
16:06:36 26/07/2005
SIEMENS
MI: 0.17
MIF: 0.12
1.3%
*ABD STD
CH4-1
12 dB CCAI
2D
2.22 MHz
#Foc 1
DR 55 dB
Page 2 of 2
Timer Off
Balance 2D
CPS
Trig 10 fps
Burst FR 15
Start Burst
Imaging
2D Sie 3D
Biopsy
A B
Physio
Protocol
CPS 2D
13cm
10fps
Image
Calcs
Review
Compose

(a)

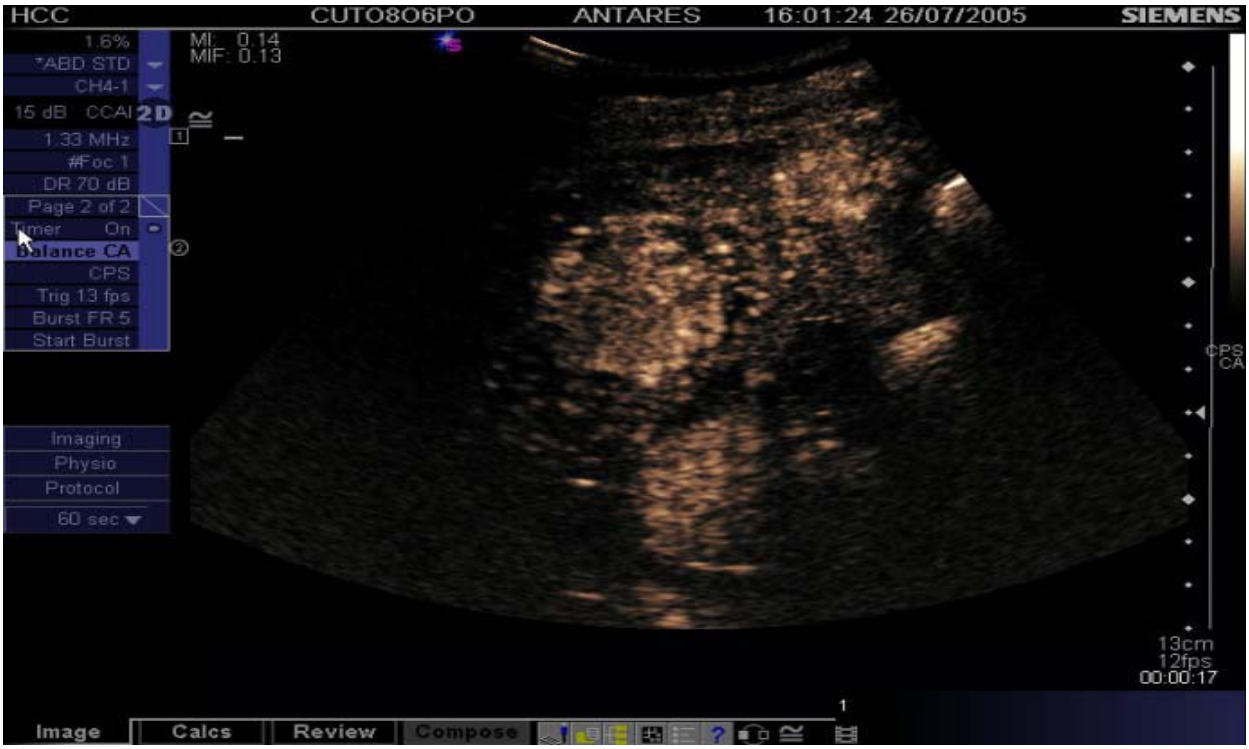
HCC
CUTO8O6PO
ANTARES
16:01:24 26/07/2005
SIEMENS
MI: 0.14
MIF: 0.13
1.6%
*ABD STD
CH4-1
15 dB CCAI
2D
1.33 MHz
#Foc 1
DR 70 dB
Page 2 of 2
Timer On
Balance CA
CPS
Trig 13 fps
Burst FR 5
Start Burst
Imaging
Physio
Protocol
60 sec
CPS CA
13cm
12fps
00:00:17
Image
Calcs
Review
Compose

(b)

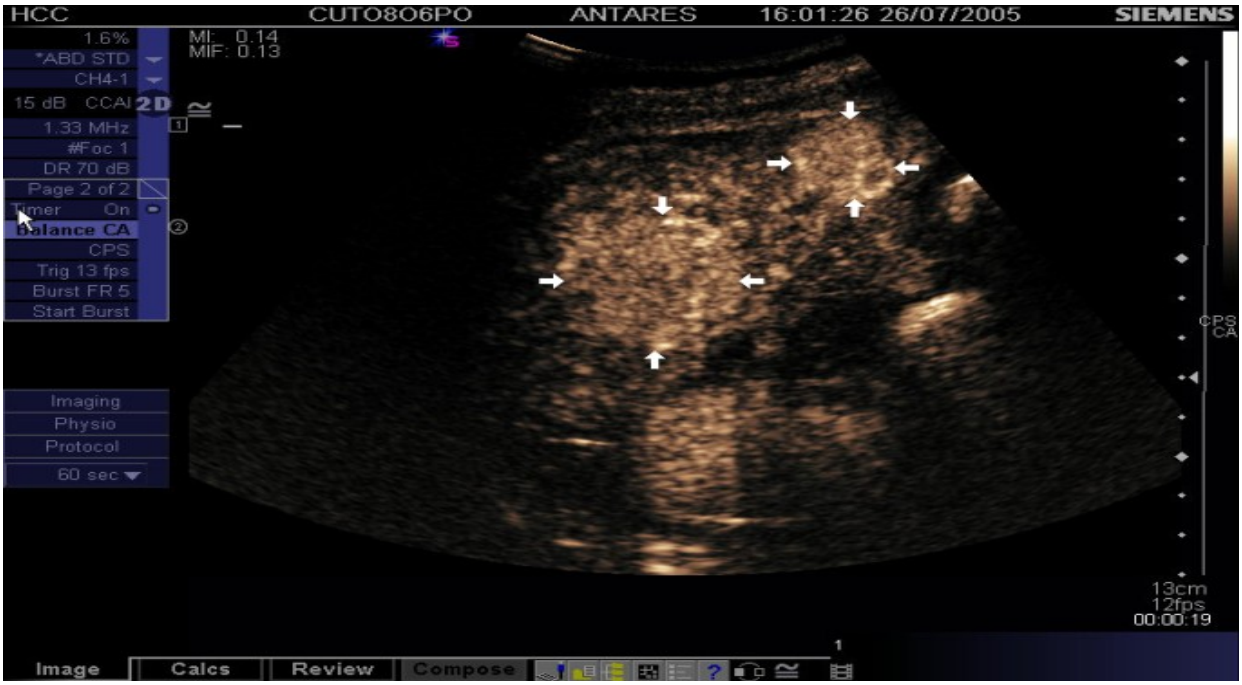
HCC
CUTO8O6PO
ANTARES
16:01:26 26/07/2005
SIEMENS
1.6%
*ABD STD
CH4-1
15 dB CCAI
2D
1.33 MHz
#Foc 1
DR 70 dB
Page 2 of 2
Timer On
Balance CA
CPS
Trig 13 fps
Burst FR 5
Start Burst
MI: 0.14
MIF: 0.13
Imaging
Physio
Protocol
60 sec
CPS
CA
13cm
12fps
00:00:19
Image
Calcs
Review
Compose

(c)

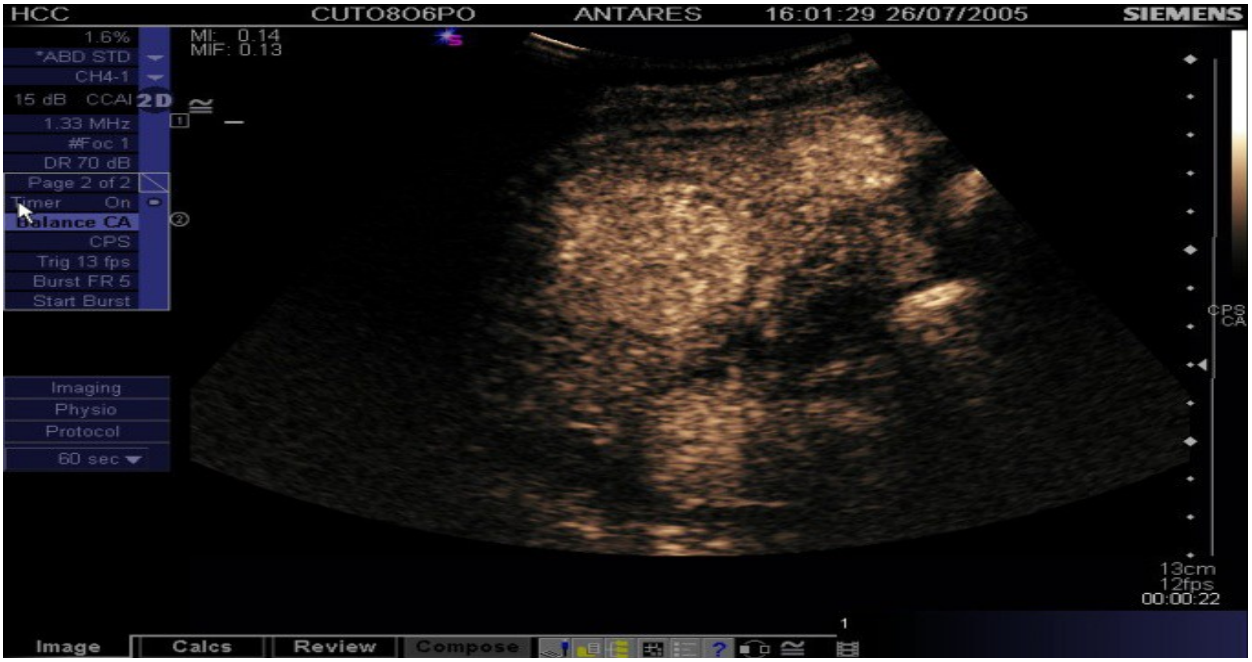
HCC
CUTO8O6PO
ANTARES
16:01:29 26/07/2005
SIEMENS
1.6%
*ABD STD
CH4-1
15 dB CCAI
2D
1.33 MHz
#Foc 1
DR 70 dB
Page 2 of 2
Timer On
Balance CA
CPS
Trig 13 fps
Burst FR 5
Start Burst
MI: 0.14
MIF: 0.13
Imaging
Physio
Protocol
60 sec
CPS
CA
13cm
12fps
00:00:22
Image
Calcs
Review
Compose

(d)

(Figure 2.38) Hyperechoic hepatocellular carcinoma (a) with arterial enhancement (b-d). A satellite is also shown (arrows) but this is not easy to recognise using B-mode ultrasound.

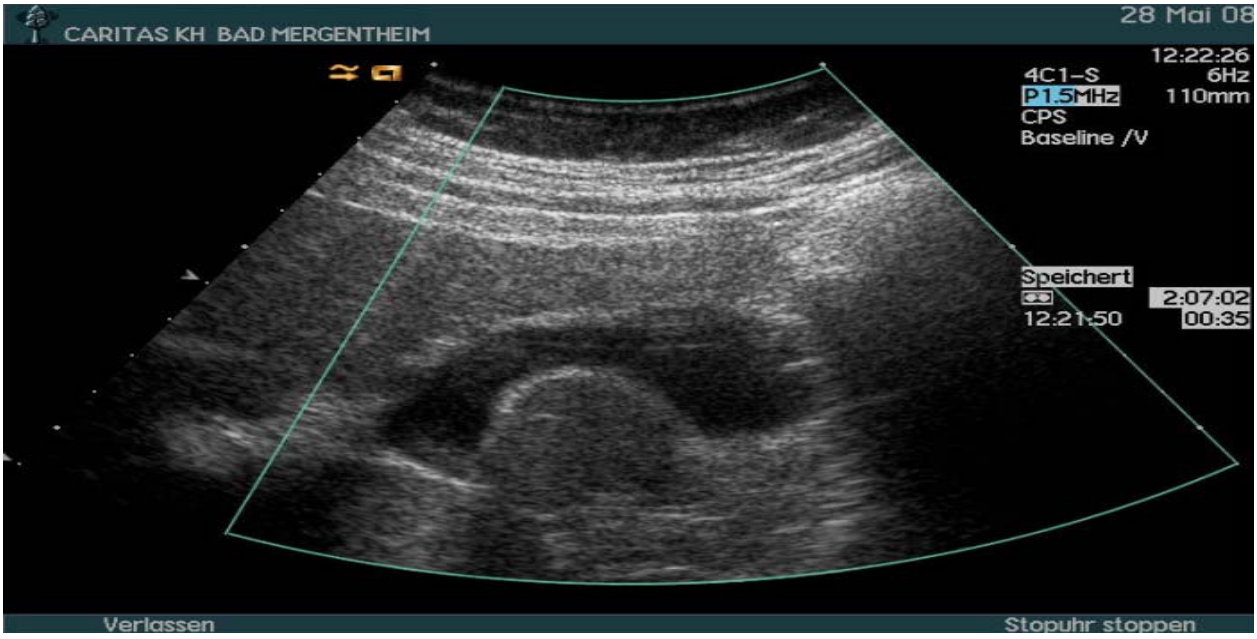

(a)

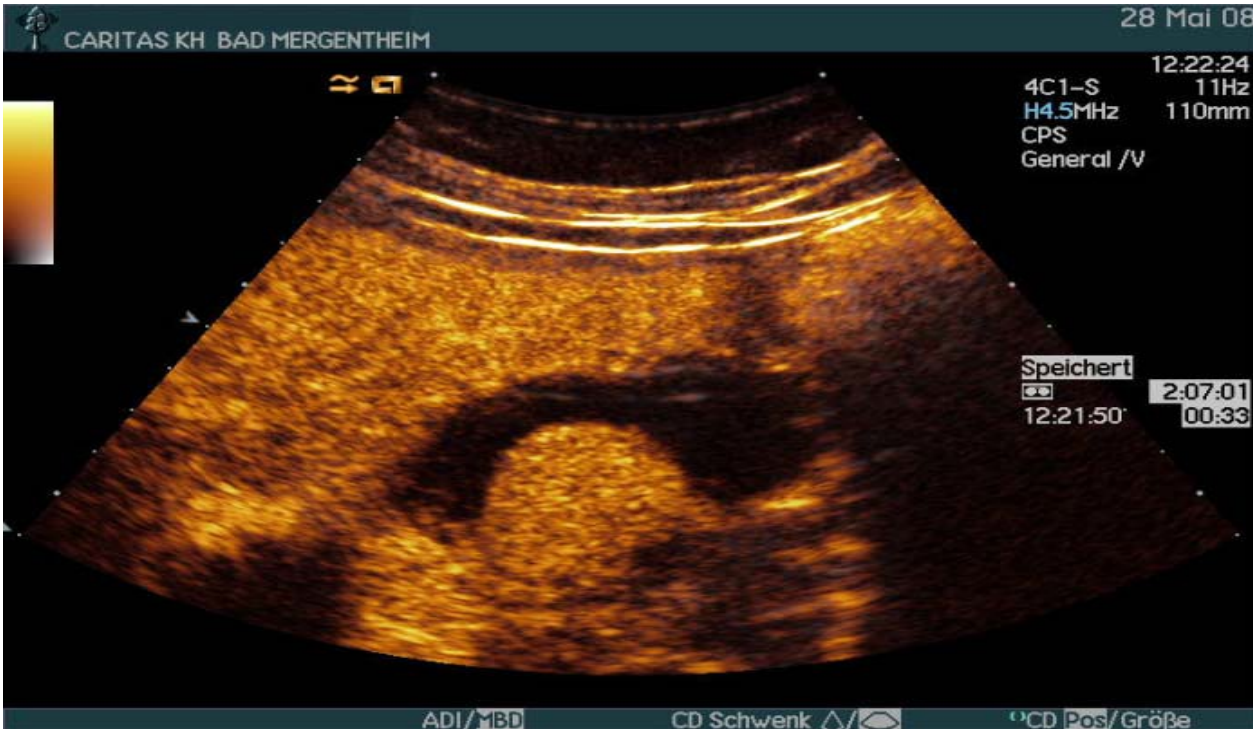

(b)

(Figure 2.39) Regenerative nodule (histologically proven and monitored over 3 years) protruding into the gall bladder lumen mimicking hepatocellular carcinoma (a, B-mode and b, contrast enhanced ultrasound).

2.3.19.15. Cholangiocellular carcinoma

2.3.19.15.1. Conventional B-mode ultrasound

CCC can occur along the bile duct in the liver hilum as so-called Klatskin tumours (the hilar CCC is the most common) (Figure 38), but they may also appear as primary solid tumours in the liver (peripheral CCC). For the peripheral type there are no typical sonographic characteristics, and the diagnosis is usually made incidentally within the framework of a biopsy of a mass found in the liver. Ultrasound examination shows a solid mass, which can have any form echogenicity and exhibits signs of a malignant growth. The liver metastases of a peripheral CCC are often situated like satellites around the primary focus (Christoph F. Dietrich.2011)

2.3.19.15.2. Colour Doppler imaging

The majority of circumscribed CCCs are slightly hyperperfused in the native colour Doppler, but CDI findings vary widely.

2.3.19.15.3. Contrast-enhanced ultrasound

In the arterial phase the perfusion picture is variable but mainly hyperperfused. In the late portal venous phase CCCs are contrasted as punched-out defects. This behaviour is not always easy to demonstrate in the case of the Klatskin tumours, which often exhibit an appreciable pericholangitic component. As far as differential diagnoses are concerned, in the case of the hilar

type of CCC, inflammatory bile duct alterations should be considered e.g. cholangitis. However, stratification of the bile ducts is then reserved, and may actually be accentuated in the sonographic image. For the detection of CCCs, the examination technique in the liver specific late phase has also proved to be diagnostically useful in patients, resulting in normal CT, MRI and MRCP, but to date there have been no conclusive studies on differential diagnosis of PSC and CCCs (Christoph F. Dietrich.2011)

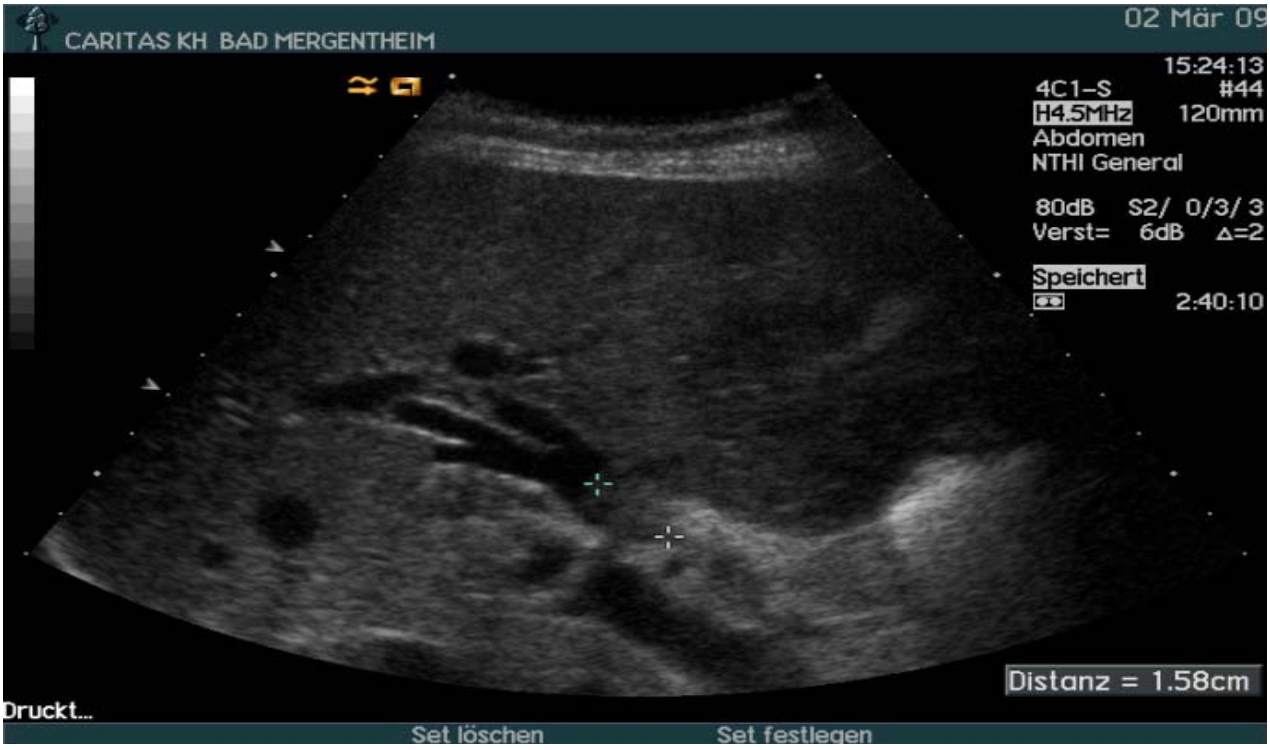

(a)

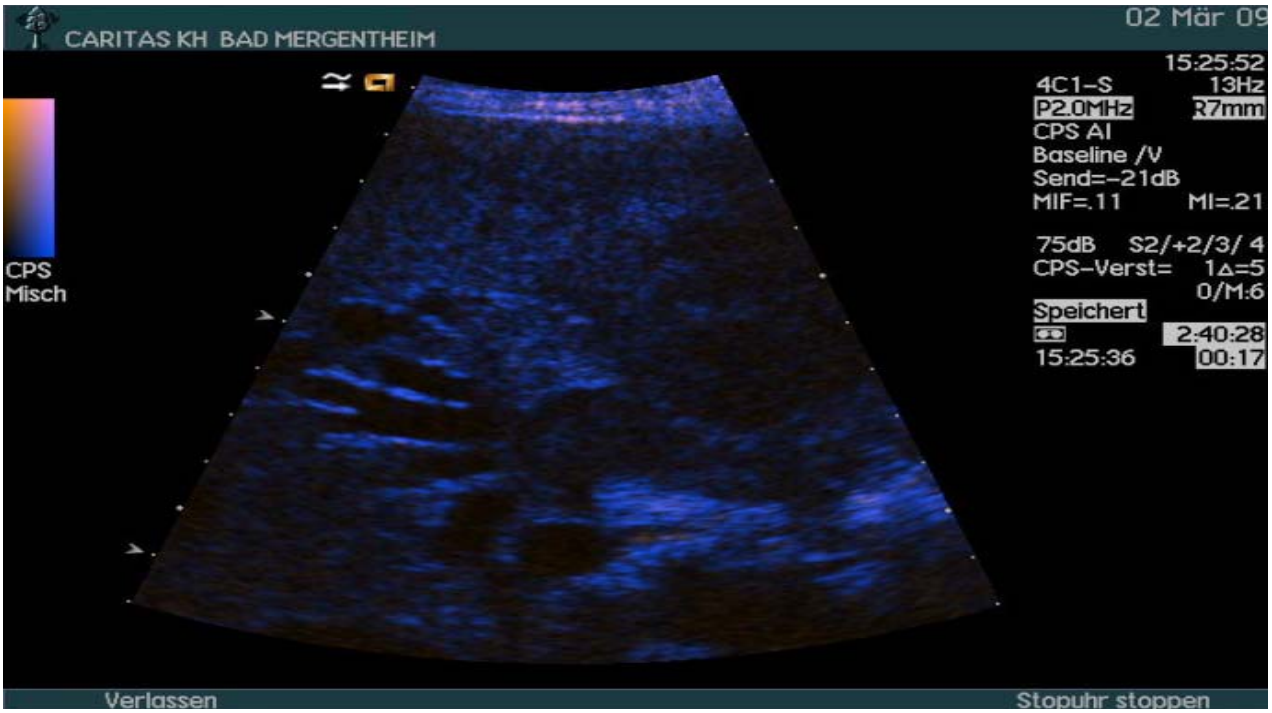
CARITAS KH BAD MERGENTHEIM
02 Mär 09
15:25:52
4C1-S
13Hz
P2.0MHz
R7mm
CPS AI
Baseline /V
Send=-21dB
MIF=.11
MI=.21
75dB S2/+2/3/ 4
CPS-Verst= 1Δ=5
0/M:6
Speichert
2:40:28
15:25:36
00:17
CPS
Misch
Verlassen
Stopuhr stoppen

(b)

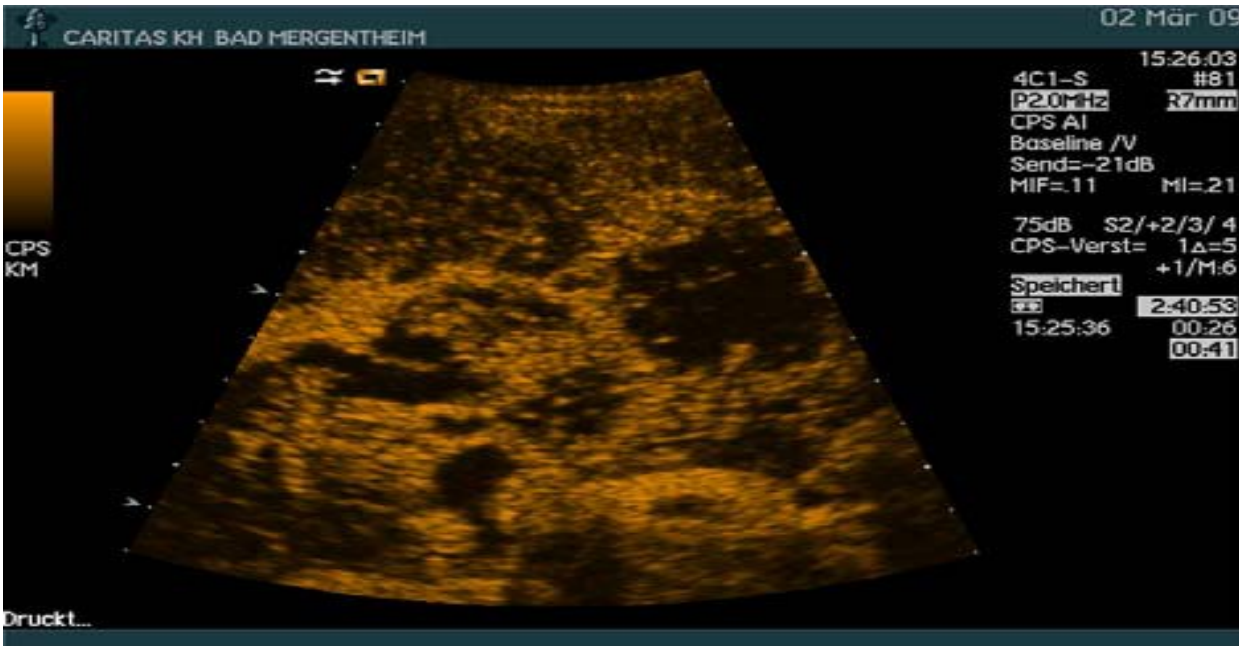
CARITAS KH BAD MERGENTHEIM
02 Mär 09
15:26:03
4C1-S
#81
P2.0MHz
R7mm
CPS AI
Baseline /V
Send=-21dB
MIF=.11
MI=.21
75dB S2/+2/3/ 4
CPS-Verst= 1Δ=5
+1/M:6
Speichert
2:40:53
15:25:36
00:26
00:41
CPS
KM
Druckt...

(c)

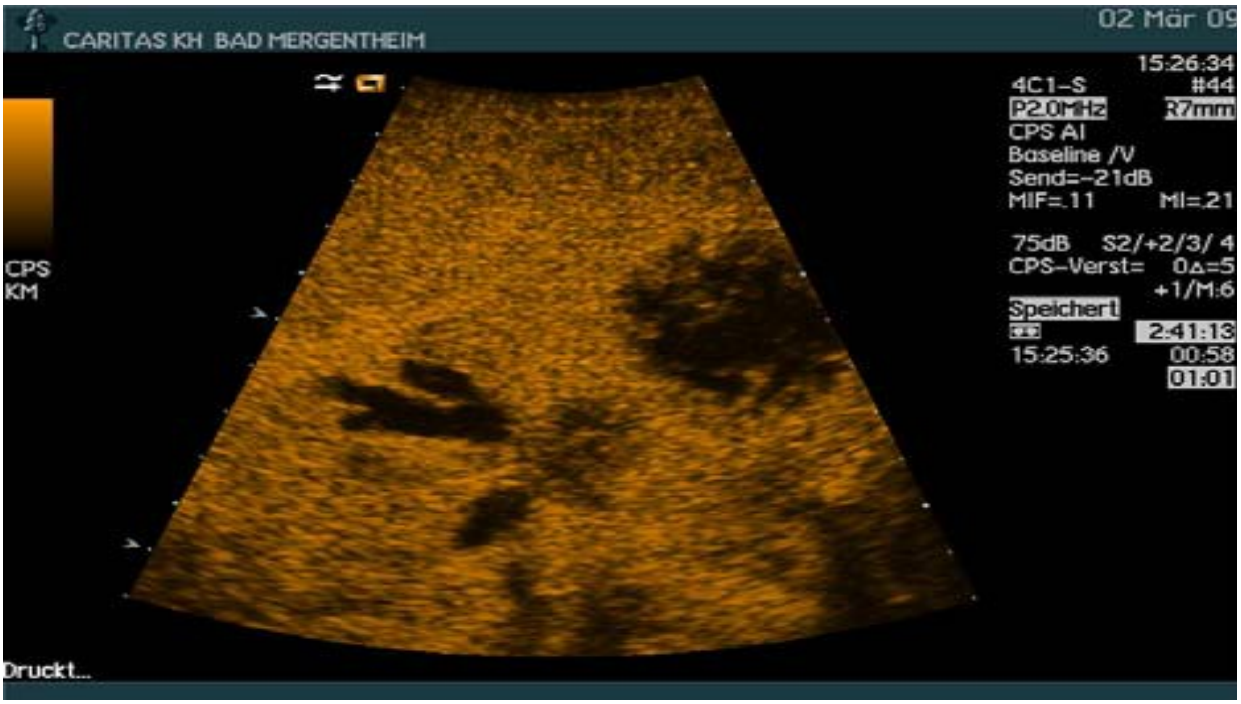

(d)

(Figure 2.40) Cholangiocellular carcinoma (CCC) (between callipers, +) can occur along the bile duct as so-called Klatskin tumours (hilar CCC is the most common), but they may also appear as primary solid tumours in the liver (peripheral CCC [(11)]). There are an abundance of different morphological patterns of CCC. B-mode (a) and contrast enhanced ultrasound (b-d) are shown.

2.3.19.16. Metastases

The liver is the parenchymatous organ in which metastases of extrahepatic tumours are usually encountered. The special features of portal vein circulation favour haematogenic metastasisation in the liver.

2.3.19.16.1. Conventional B-mode ultrasound

Size of the metastases can be anywhere between only microscopically detectable (cellular) infiltration and giant masses measuring more than 20cm; the echogenicity varies widely. Intraoperative ultrasound (IOUS) may be helpful during surgery in certain cases.

2.3.19.16.2. Colour Doppler imaging

Metastases are, as a rule, poorly vascularised and their essential characteristic is a predominantly arterial blood supply (with little or no portal venous blood supply). Like echogenicity (most often hypoechoic), the vascularisation depends on the size, biological behaviour and nature of the primary tumour. Irregular vascularisation is often observed with broken-off vessels and peripherally situated arterio(porto-)venous shunt formation. The metastases of neuroendocrine tumours (e.g. metastases of renal cell carcinomas) may be more richly vascularised than other metastases. However, no conclusions are possible about the primary tumour on the basis of the echo-texture and vascularisation pattern observed.

2.3.19.16.3. Contrast-enhanced ultrasound in metastatic disease

CEUS has markedly improved the detection rate of liver metastases. Liver metastases can be reliably diagnosed as hypoenhancing lesions during the liver specific portal venous sinusoidal phase. False-negative findings are rarely encountered whereas false-positive findings have to be ruled out by puncture and histological examination, e.g. abscess, necrosis, fibrous tissue and others. Metastases may be already contrasted in the arterial phase, even though early arterial enhancement (in less than 15s) is not typical and often the only observation is a degree of signal enhancement with a marginal emphasis (“halo sign” or “rim sign”). Contrast of the vessels proceeds from the periphery towards the centre and the vascular pattern is irregular. In poorly

vascularised metastases contrast-enhanced colour Doppler ultrasound often reveals only small blood vessels situated at the edges (or within the lesion), and in many patients vascularisation cannot be imaged at all. In the portal venous phase metastases are contrasted increasingly as signal “black spots” against the background of uniformly enhanced normal liver tissue (Figure 39). Contrast-enhanced IOUS might be helpful in certain cases to detect lesions during surgery. (Christoph F. Dietrich.2011)

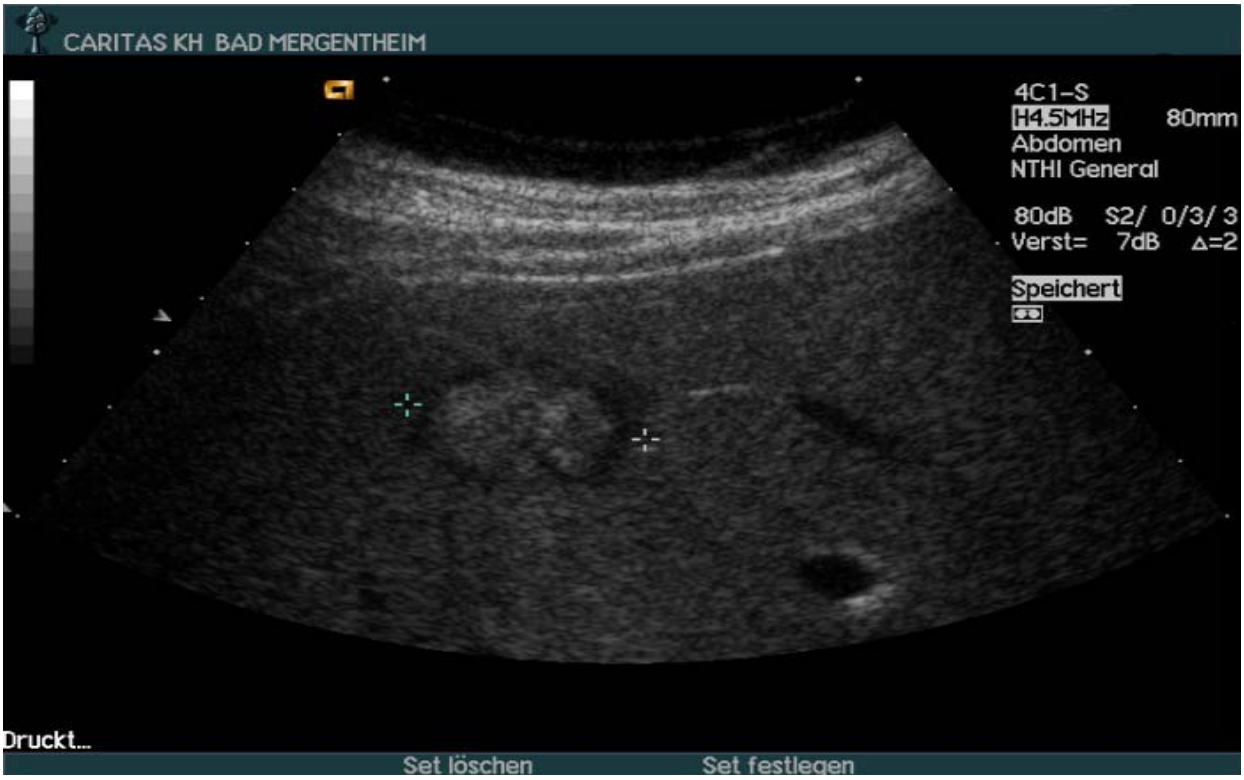

(a)

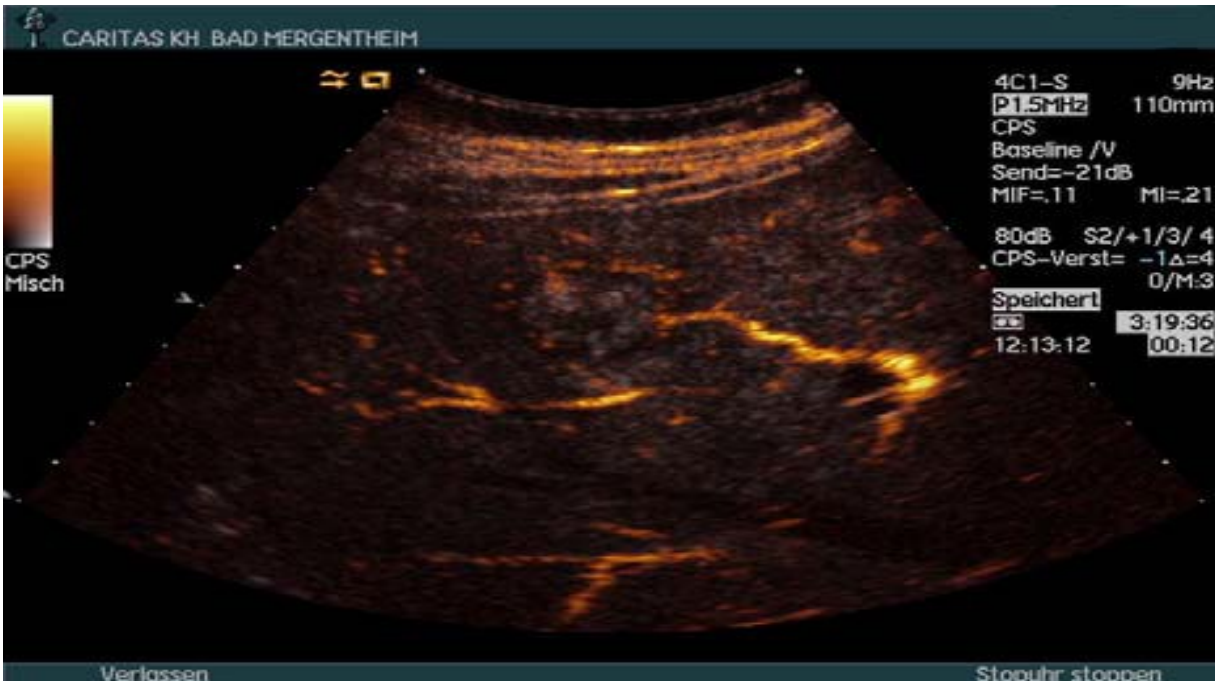
CARITAS KH BAD MERGENTHEIM
4C1-S 9Hz
P1.5MHz 110mm
CPS
Baseline /V
Send=-21dB
MIF=.11 MI=.21
80dB S2/+1/3/ 4
CPS-Verst= -1Δ=4
0/M:3
Speichert
3:19:36
12:13:12 00:12
CPS
Misch
Verlassen
Stopuhr stoppen

(b)

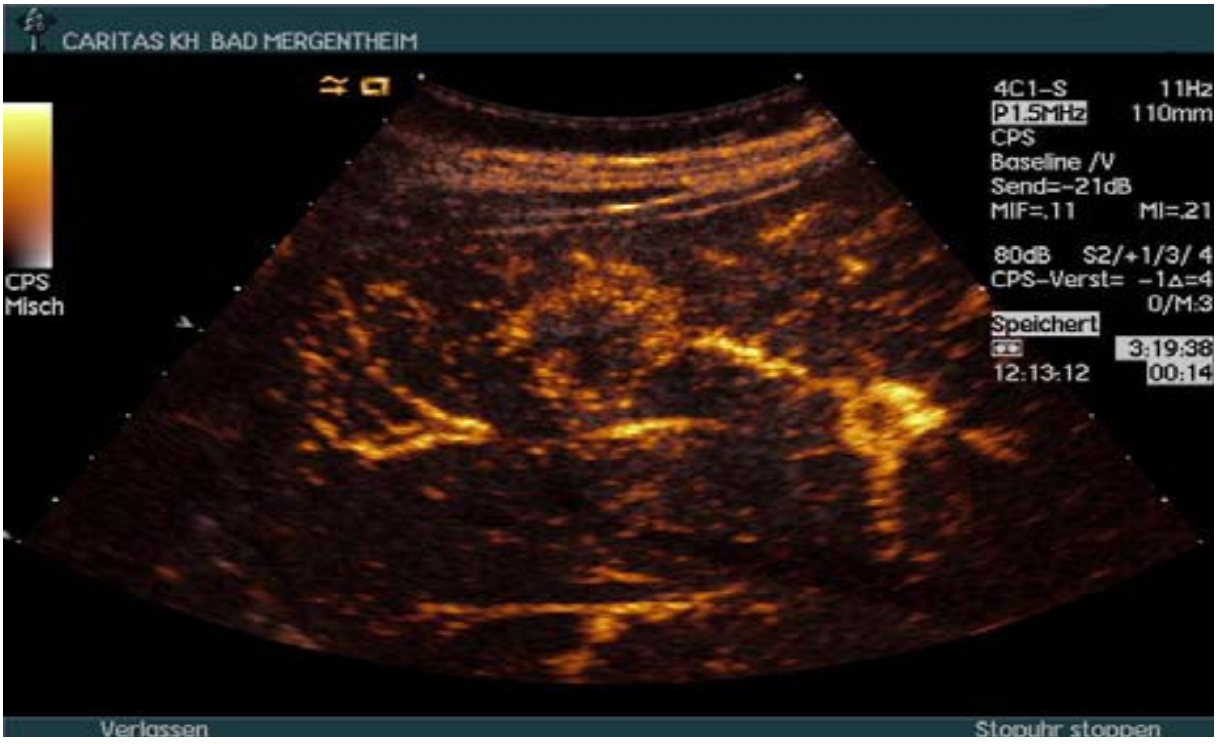
CARITAS KH BAD MERGENTHEIM
4C1-S 11Hz
P1.5MHz 110mm
CPS
Baseline /V
Send=-21dB
MIF=.11 MI=.21
80dB S2/+1/3/ 4
CPS-Verst= -1Δ=4
0/M:3
Speichert
3:19:38
12:13:12 00:14
CPS
Misch
Verlassen
Stopuhr stoppen

(c)

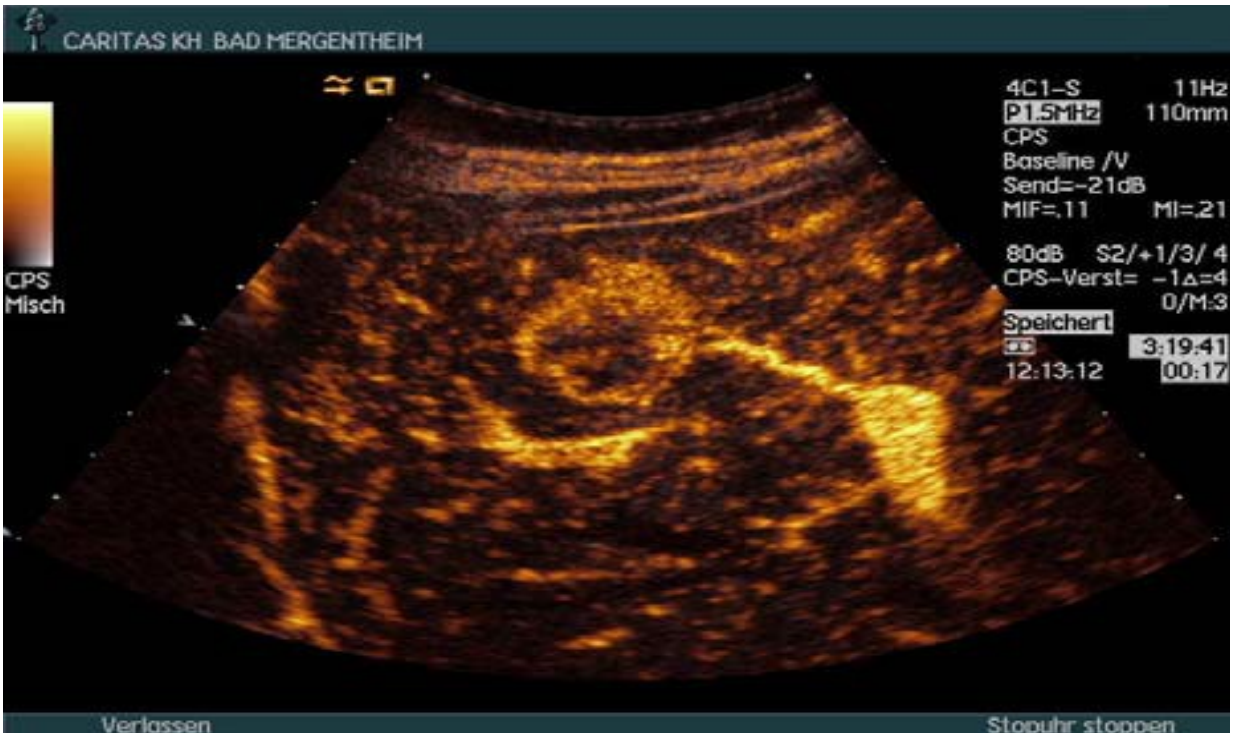
CARITAS KH BAD MERGENTHEIM
4C1-S 11Hz
P1.5MHz 110mm
CPS
Baseline /V
Send=-21dB
MIF=.11 MI=.21
80dB S2/+1/3/ 4
CPS-Verst= -1Δ=4
0/M:3
Speichert
3:19:41
12:13:12 00:17
CPS
Misch
Verlassen
Stopuhr stoppen

(d)

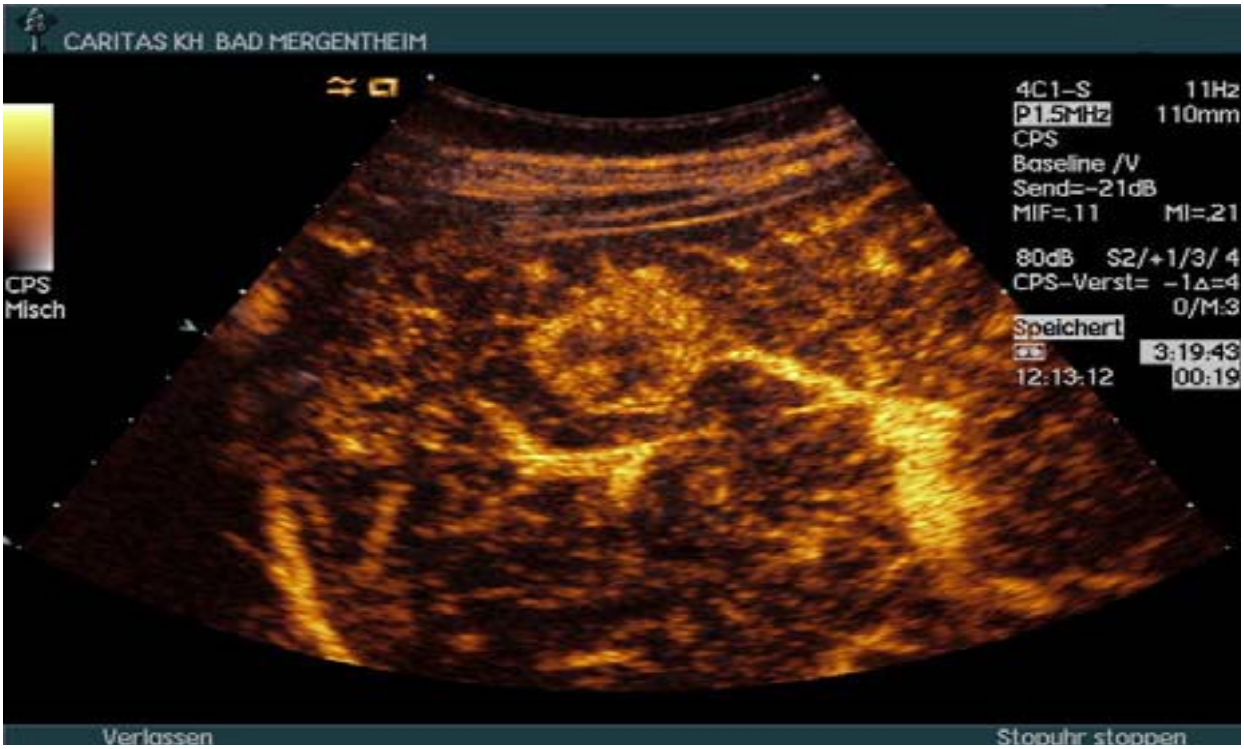
CARITAS KH BAD MERGENTHEIM
4C1-S 11Hz
P1.5MHz 110mm
CPS
Baseline /V
Send=-21dB
MIF=.11 MI=.21
80dB S2/+1/3/ 4
CPS-Verst= -1Δ=4
0/M:3
Speichert
3:19:43
12:13:12 00:19
CPS
Misch
Verlassen
Stopuhr stoppen

(e)

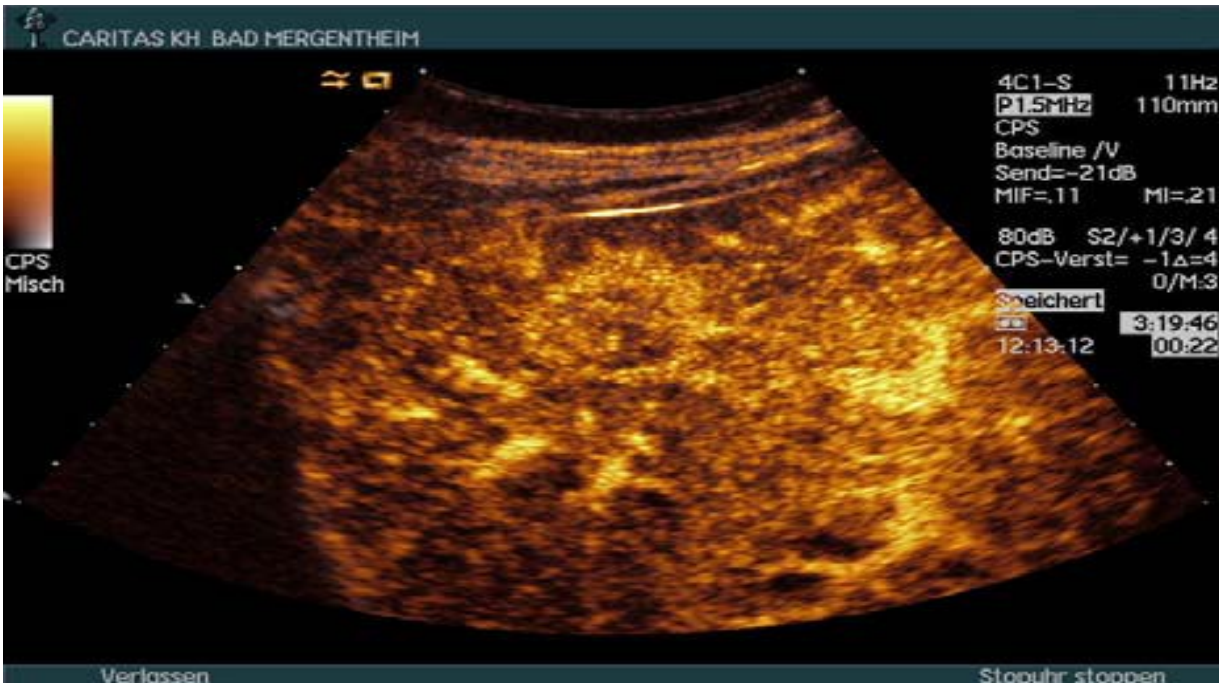

(f)

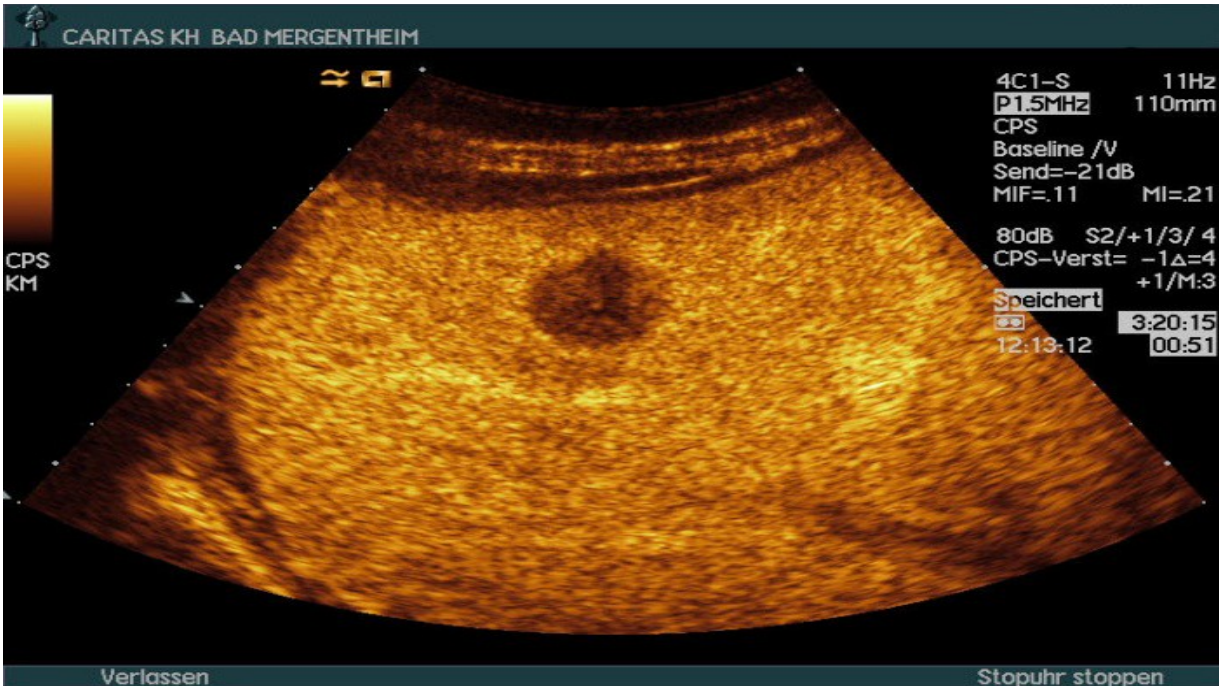

(g)

(Figure 2.41) (a) Metastases have a wide variety of B-mode ultrasound appearance and can be confused with any kind of liver lesion. Colour Doppler imaging is helpful in only few patients.

(b-f) Hypervascular metastases reveal the typical peripheral rim sign using contrast-enhanced ultrasound in the arterial phase, which can also be encountered in hepatocellular adenoma and hepatocellular carcinoma, and is, therefore, not pathognomonic. (g) Metastases typically exhibit a sharp contrast to normal liver tissue in the liver specific portal venous (sinusoidal) phase.

2.3.19.16.4. Neuro-endocrine tumour (NET)

Metastases of neuroendocrine tumours (NET) are often small and hyperechoic and therefore mimic haemangioma and occasionally metastases of other origins (e.g. gastrointestinal). With increasing size of NET, a combined hyperechoic and centrally echo-poor texture is observed as a typical sonomorphological characteristic, owing to frequent central necrosis, intra-tumoural haemorrhage, necrosis, fibrous tissue or calcifications. Therefore, visual diagnosis by B-mode ultrasound may be possible in approximately 50% of cases. NET are often hypervascularised, with a strong arterial and capillary blood supply similar to shunt haemangioma, small HCA or hypervascular tumours of other origin (Christoph F. Dietrich.2011) .

2.3.19.17. Lymphoma

2.3.19.17.1. Conventional B-mode ultrasound

Unlike the often diffuse infiltration of the liver by extranodal Hodgkin’s, and in particular non-Hodgkin’s lymphomas (approximately 50%), circumscribed alterations are only detected relatively rarely by ultrasound (in less than 10–20% of cases).

Circumscribed lymphomas can infiltrate the liver in small or large nodules or over an extended area, and depending on their rate of growth, are often very hypoechoic compared with the surrounding liver tissue. In individual cases they may in fact give no echoes at all. Characteristically, amplification of the echo distally is then observed. Depending on the

regressive changes taking place (e.g. an inward flow of blood or necroses), hyperechoic lymphomas are also not uncommon.

In our experience, lymphoma infiltrations of the liver are accompanied by sonographically detectable, but often only moderate, enlargement of the perihepatic lymph nodes (the normal lymph node size is up to 17mm (median value plus two standard deviations) and 19mm (maximum)) (Figure 40). From a differential diagnosis perspective, inflammatory liver conditions should be considered (e.g. viral hepatitis B or C, PBC, PSC, etc.), as well as lymph node metastases (Christoph F. Dietrich.2011) .

2.3.19.17.2. Colour Doppler imaging

The vascularisation of circumscribed lymphomas is often, although not always, more sparse than in healthy liver tissue. Broken-off vessel shunts are typically observed, which in Doppler wave spectral analysis can lead to the disappearance of the diastolic flow component.

2.3.19.17.3. Contrast-enhanced ultrasound

In contrast to variable arterial perfusion, characteristic lymphomas reveal reduced contrast enhancement in the portal venous phase in comparison with the surrounding liver tissue owing to the relative absence of portal veins in the lymphoma region.

By differentiation, in the liver specific late phase, inflammatory lymph nodes can be distinguished from lymph nodes with malignant infiltration because, in the early stage at least, the latter exhibit sharply demarcated malignant infiltrated areas; however, this hypothesis still needs to be tested in prospective studies.

The conditions that should be considered as differential diagnoses are complications of the underlying lymphoma (e.g. extramedullary haematopoiesis and a higher frequency of sub-capsular haematomas in the presence of coagulation disturbances) and complications of therapy (e.g. neutropenia with bacterial and/or mycotic abscesses), as well as haemophagocytosis syndrome (Christoph F. Dietrich.2011).

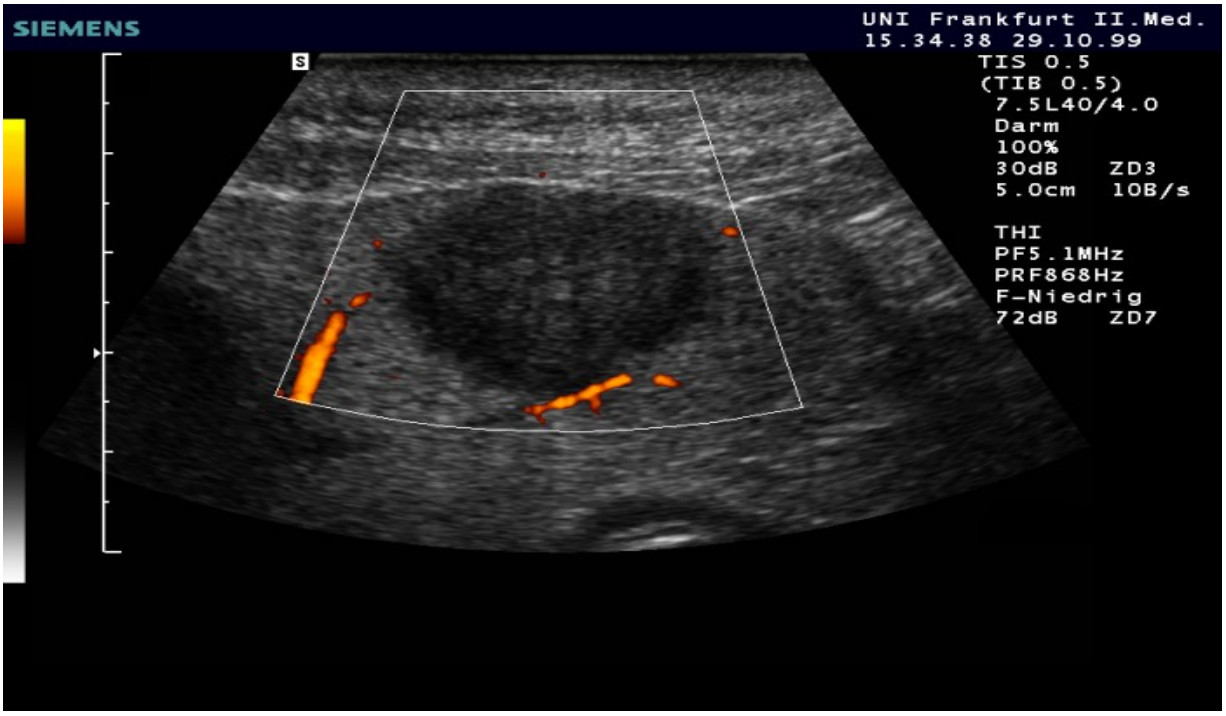

(a)

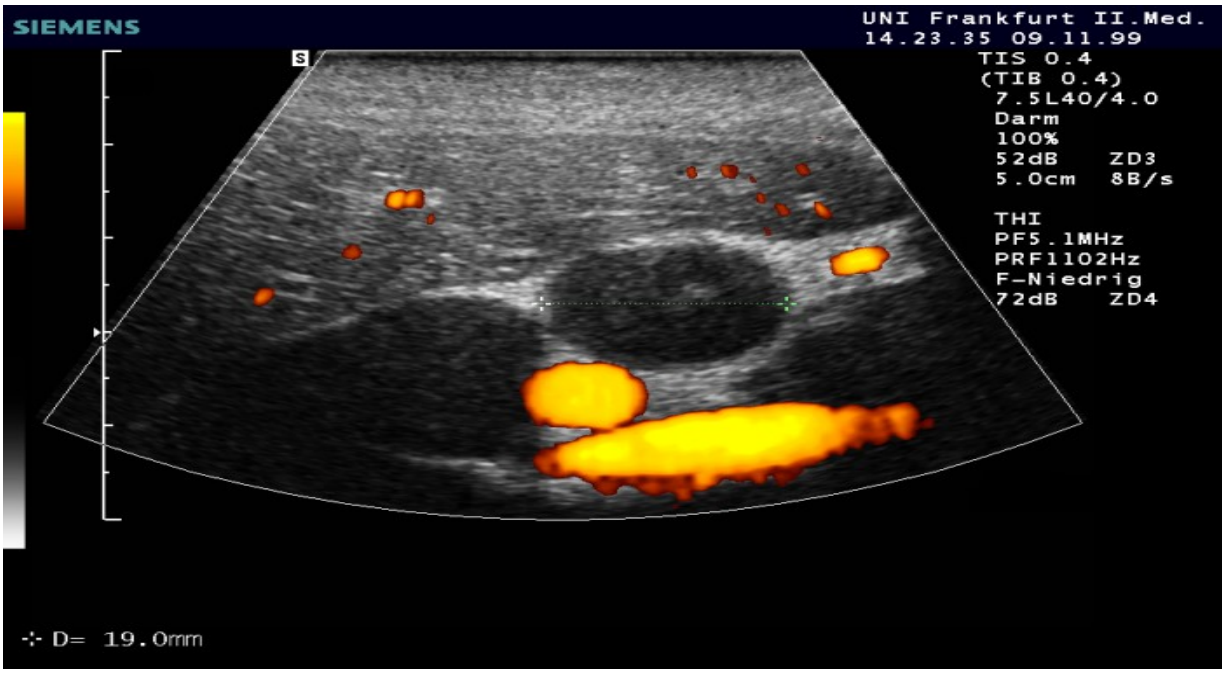

(b)

(Figure 2.42) Lymphoma. Correct diagnosis of hepatic lymphoma infiltration may be improved by also analysing the perihepatic lymph nodes. Generalised lymphoma often shows (a) intrahepatic mass lesions and (b) perihepatic lymphadenopathy.

2.3.19.18. Abscess

The patient medical history and occasionally the physical examination (febrile temperature or signs of sepsis) are the most helpful in differentiating abscesses from necrotic metastases.

Phlegmonous inflammation and abscesses demonstrate the variable and sometimes confusing change in B-mode ultrasound image over time. The initial phlegmonous inflammation is often isoechoic in comparison with the surrounding liver parenchyma and is sometimes difficult to recognise. In older (chronic) abscesses hypervascularitiy of the nodule border might be confused with a pseudotumour of the liver, even histologically. Small disseminate candida abscesses might be confused with lymphoma or circumscribed haemophagocytosis syndrome (especially in

young patients). Puncture and drainage (if necessary) are the diagnostic and therapeutic interventions. Abscesses of up to 5cm can be drained in one procedure; however, larger abscesses need to be treated over a number of days. (Christoph F. Dietrich.2011)

The initial phlegmonous inflammation is often hypervascular in comparison with the surrounding liver parenchyma, but is difficult to recognise. In older (chronic) abscesses hypervascularitiy of the nodule border is typical (Figure 41). In typical cases CEUS shows sharply delineated hypervascularity (demonstrating the pseudocapsule) and no gas bubbles inside the lesion (Christoph F. Dietrich.2011).

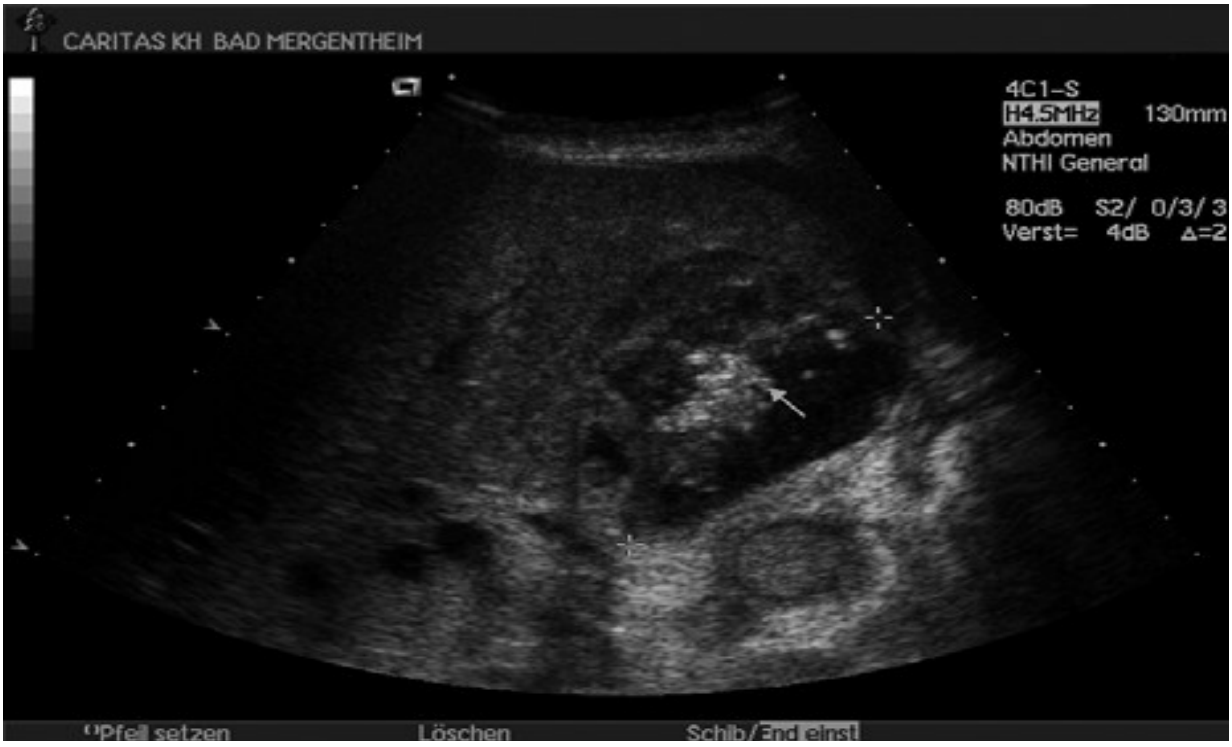

(a)

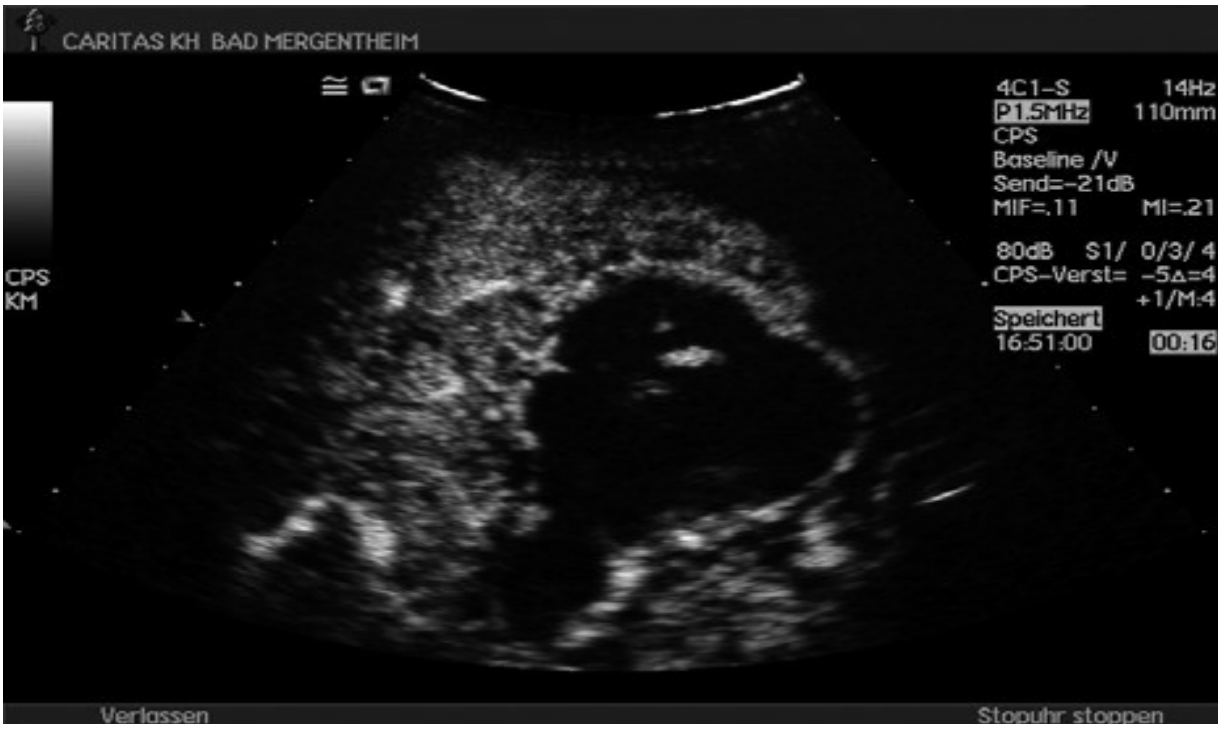
CARITAS KH BAD MERGENTHEIM
4C1-S 14Hz
P1.5MHz 110mm
CPS
Baseline /V
Send=-21dB
MIF=.11 MI=.21
80dB S1/ 0/3/ 4
CPS-Verst= -5Δ=4
+1/M:4
Speichert
16:51:00 00:16
CPS
KM
Verlassen
Stopuhr stoppen

(b)

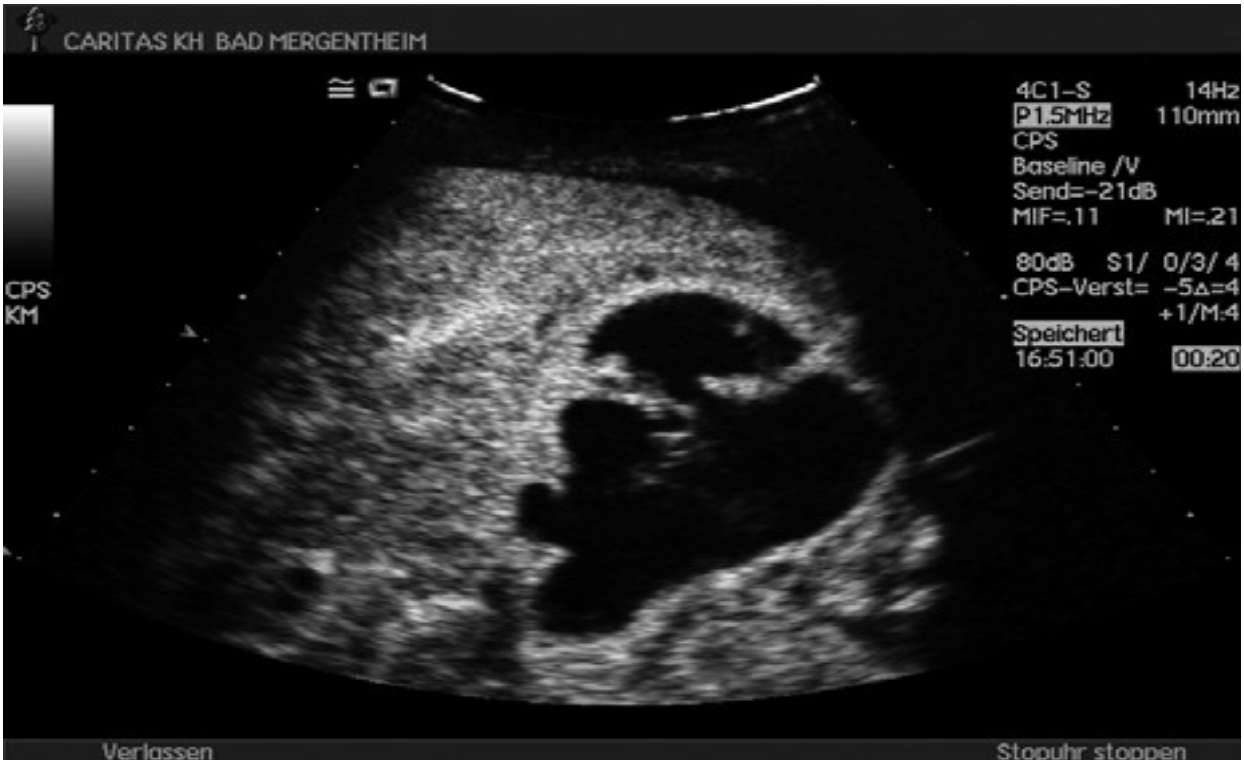
CARITAS KH BAD MERGENTHEIM
4C1-S 14Hz
P1.5MHz 110mm
CPS
Baseline /V
Send=-21dB
MIF=.11 MI=.21
80dB S1/ 0/3/ 4
CPS-Verst= -5Δ=4
+1/M:4
Speichert
16:51:00 00:20
CPS
KM
Verlassen
Stopuhr stoppen

(c)

(Figure 2.43) Liver abscess. (a) Typical liver abscesses demonstrating gas inside the lesion (arrow). (B-c) In CEUS, there will be no central signal at all, but a pronounced hyperperfusion at the abscess border. The underlying cause in this patient, choledocholithiasis, is detectable (not shown).

2.3.19.19. Haematoma

Haematoma can be clinically diagnosed in most cases. The spontaneously evolving and painful haematoma is typical for amyloidosis of the liver (Figure 2.43).

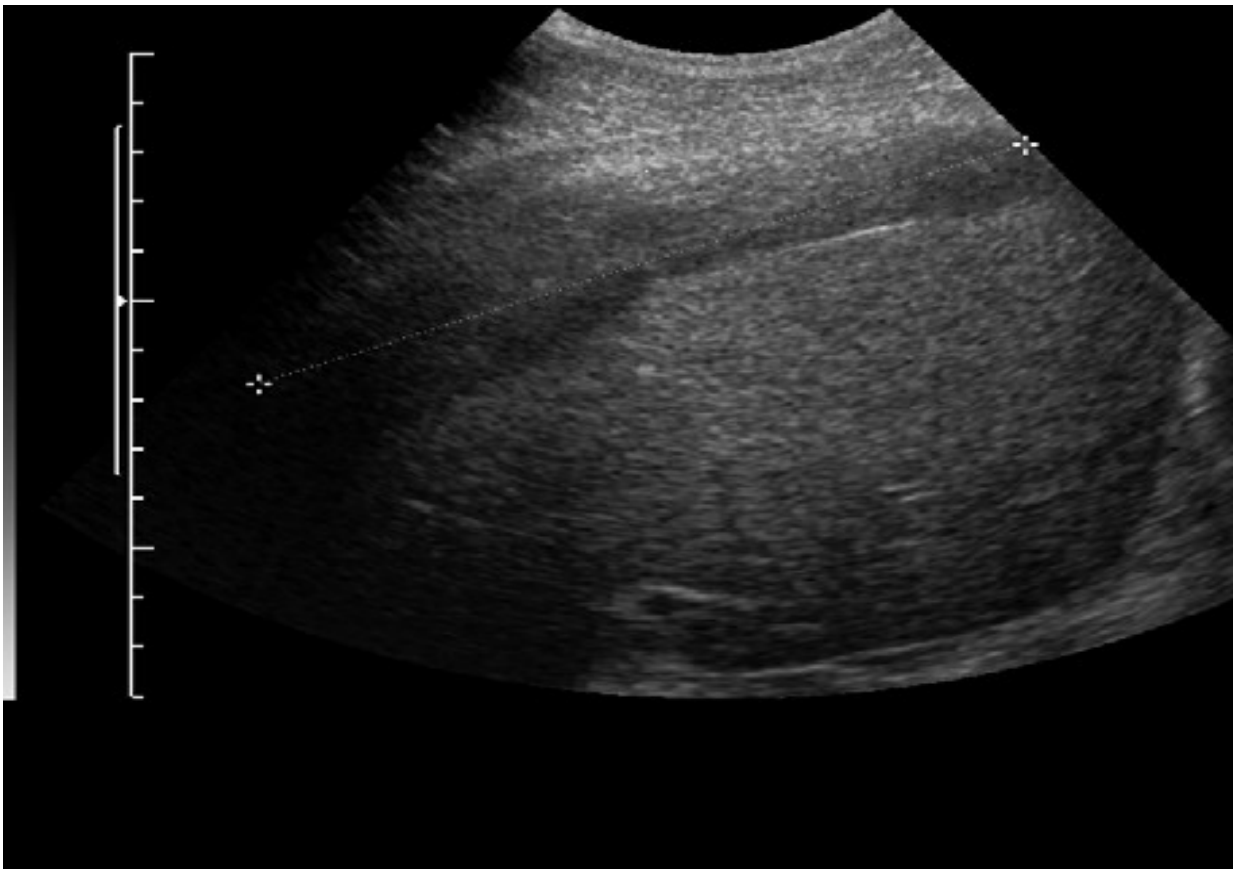

(Figure 2.44) Spontaneously evolving and painful haematoma is typical for amyloidosis of the liver.

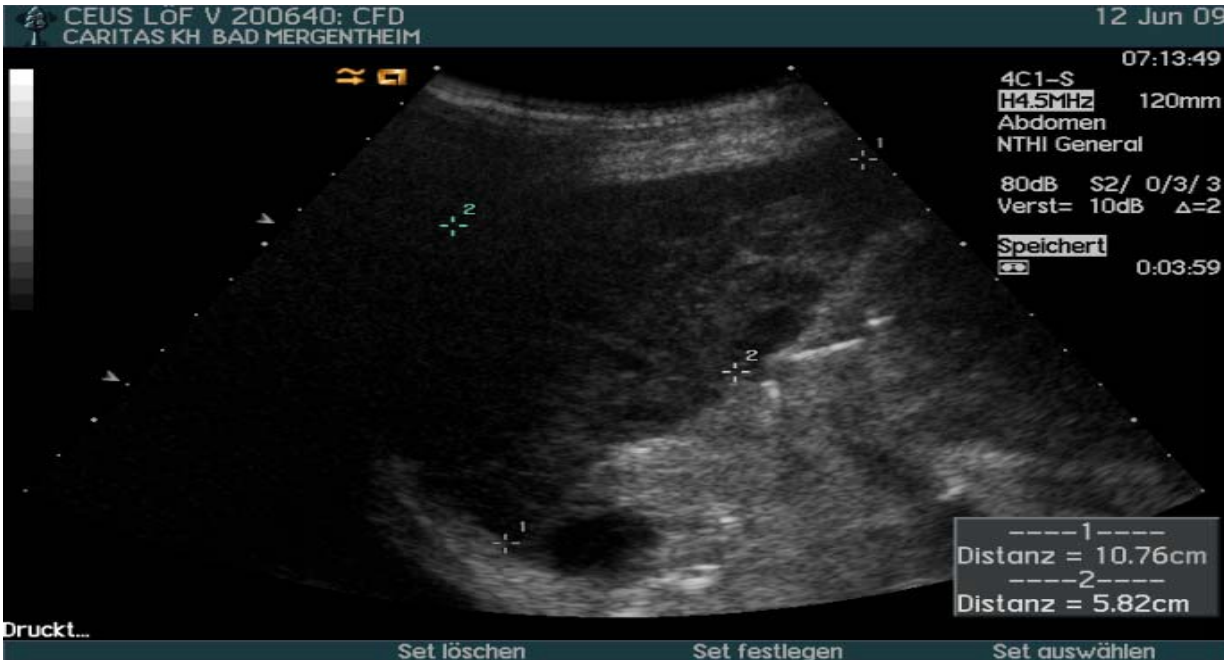

(a)

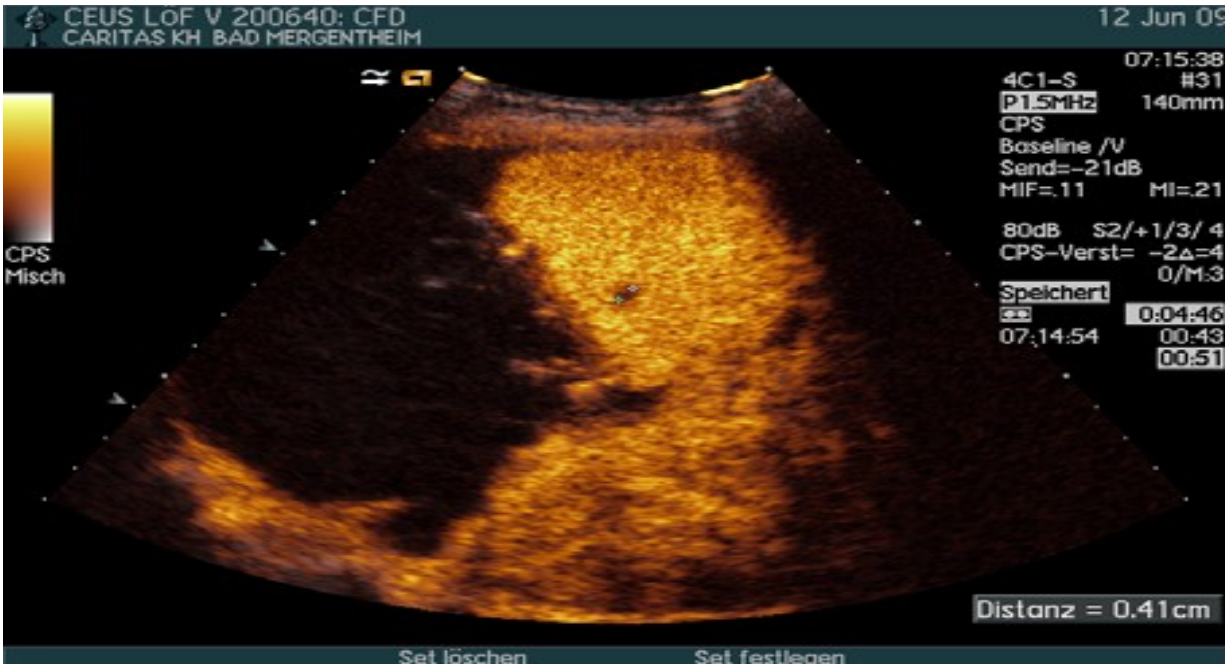

(b)

(Figure 2.45) Perihepatic haematoma using (a) B-mode ultrasound is stage dependent hypoechoic. (b) Contrast-enhanced ultrasound demonstrates early vessel invasion.

2.3.19.20. Nodular regenerative hyperplasia

Nodular regenerative hyperplasia (NRH) of the liver is a rare pathological finding, which is typically associated with haematological or autoimmune disease. The main clinical symptom is portal hypertension without underlying liver cirrhosis. NRH of the liver consists of multiple hepatic nodules resulting from periportal hepatocyte regeneration with surrounding atrophy. Typically, fibrous septa between the nodules are missing. Ultrasound typically shows multiple unspecific hepatic nodules, which are suggestive of multilocular HCC or metastatic disease of the liver. Signs of portal hypertension, and the rarer Budd-Chiari syndrome, should be carefully sought. CEUS is helpful in defining circumscribed vs diffuse infiltrating NRH. Histological assessment of the liver is necessary for diagnosis because the nodular appearance of the hepatic surface may otherwise be difficult to differentiate from cirrhosis or hepatic metastases
(Christoph F. Dietrich ..2011).

2.3.19.20. Inflammatory pseudotumour

Inflammatory pseudotumour is a rare disease that can present with fever, abdominal pain, vomiting and weight loss, which indicates, and sonographically mimics, malignancy or abscess. The definite diagnosis is often only achieved by surgery. CEUS may reveal hypoechoic contrast enhancement falsely indicating malignant disease.

2.3.20. Clinical importance of liver ultrasound in clinical practice

Ultrasound is the first and most important imaging method in suspected liver disease, both for proving (e.g. metastatic disease) and excluding pathology. It is the single best tool in the evaluation of FLL. It is unrivalled by any other imaging modality owing to its real-time, dynamic

nature, high-resolution and good safety record. It is invaluable in the differential diagnosis of jaundice, in describing liver cirrhosis complications and in any form of ultrasound guided intervention. In summary ultrasound is an indispensable tool in clinical hepatology.

Ultrasound of the liver:

- is the first and most important imaging method in suspected liver disease;
- is first line indication for the evaluation of elevated liver functions tests and cholestasis indicating enzymes; differential diagnosis of icterus (diagnosis/exclusion of cholestasis); monitoring of complications of liver cirrhosis (ascites, portal hypertension, HCC); and tumour detection, exclusion and follow-up;
- CEUS is especially helpful for tumour detection and characterization and prevents unnecessary further imaging.
- is essential for guidance of liver/biliary tree interventions such as biopsy;
- is the most important imaging method for oncological follow-up;
- Limitations include the exact measurement of the size of the liver (which is of limited value in clinical practice); and the diagnosis of early cirrhotic stages and in the differential diagnosis of diffuse parenchymal diseases.

Chapter three

Material and methods

This study were conducted in Military hospital (Omdurman) in radiology department in the period from October 2011 to April 2012 in order to characterize the ultrasound funding in patients with abnormal Liver Function Test

3-1 Material

The data in this study were collected using real time ultrasound machine GE Logic5 with 3-5 MHz and Mandarin machine with 3.5 MHz Blue aqueous gel and sterilized cotton was used for cleaning after the examination.

3-2 Methods

This is a descriptive experimental study, carried out in patients having abnormal LFT where they were scanned for liver evaluation present to the ultrasound department in military hospital (Omdurman) in the period from october2011 to April 2012.

3-2-1 Study sample

The samples size consisted of 50 cases of Sudanese population were selected randomly.

3-2-2 Data collection technique

The data was collected by directly interviewing the patients when they call in ultrasound department, asking them their history, recent complain and others investigations i.e. LFT. The patients undergoing ultrasound investigation were well prepared i.e. they must came with almost reasonably full bladder, then the patient laid in supine position on the couch. All patients were examined transabdominally, then gel was applied in abdomen area and both longitudinal and transverse views of the patient's liver were applied.

3-2-3 Data analysis

The data will be analyzed using Excel and SPSS software under windows by constructing a frequency distribution tables and cross tabulation for relationship as well as histograms portrayed the distribution of the data in each variable.

3-2-4 Ethical consideration

Ethical approval has been granted from the hospital and the department as well as a consent from the patient has been obtained that his data will be used for research purpose only and that no identification or individual details will be published, disclosed or used for other reasons than the study.

Chapter four

Result

The results of this study portrayed in tables and figures. The tables shows the frequency distribution of the patients habit, the mean and standard deviation of the variable included in the study as well as the cross-tabulation between the level of liver function test and the ultrasound findings. The graphs showed the frequency distribution of all variables as well as comparative bar graphs show the effect of liver function test values in respect to ultrasound findings.

Table 4-1 the mean and standard deviation of the age and liver dimensions

Items	mean±SD
Age	44.2±14.8
Rt. Lobe	12.4±1.8
Lt lobe	6.5±1.8
Caudate lobe	2.3±0.6
Portal vein	1.4±0.3

Figure 4-1 a bar graphs shows the distribution of the mean size of the liver lobes and portal vein for 50 patients with abnormal liver function test.

Table 4-2 a frequency distribution table show gender distribution

gender	Frequency
Male	45
Female	5
Total	50

Figure 4-2 a pie graph of gender frequency distribution of 50 patients with abnormal liver function test

Table 4-3 a frequency distribution table show ECHOGENICITY distribution

habit	Frequency	Percent
0	18	36.0
1	13	26.0
2	5	10.0
3	14	28.0
Total	50	100.0

Echogenicity	Frequency
Iso	31
Hypo	19
Total	50

Figure 4-3 a pie graph of ultrasound echogenicity distribution of 50 patients with abnormal liver function test

Table 4-4 a frequency distribution table show TEXTURE distribution

Texture	Frequency
Fine	33
Coarse	17
Total	50

Figure 4-4 a pie graph of ultrasound texture of liver distribution of 50 patients with abnormal liver function test

Table 4-5 a frequency distribution table show **LFT** distribution

LFT	Frequency	Percent
Low	41	82.0
High	9	18.0
Total	50	100.0

Figure 4-5 a pie graph show the distribution of liver function test level for 50 patients with abnormal liver function test

Table 4-6 shows means of age, RT lobe, LT lobe, caudate lobe, portal vein

Items	mean±SD
Age	44.2±14.8
Rt. Lobe	12.4±1.8
Lt lobe	6.5±1.8
Caudate lobe	2.3±0.6
Portal vein	1.4±0.3

Figure 4-6 a bar plot Shows means of age, RT lobe, LT lobe, caudate lobe, portal vein

Table 4-7 the mean size and SD of the liver lobes and portal vein in respect to liver echogenicity and the difference in means using t-test with the critical p-value shown.

Variables	echogenicity	Mean	*t*-test	*p*-value
Rt. lobe	Iso	13.1±1.4	3.47	0.001
	Hypo	11.5±1.3		
Lt lobe	Iso	5.8±1.2	3.97	0.000
	Hypo	7.7±2.1		
Caudate lobe	Iso	2.3±0.7	0.93	0.36
	Hypo	2.2±0.5		
Portal vein	Iso	1.3±0.4	2.14	0.04
	Hypo	1.5±0.3		

Figure 4-7 a bar plot of the mean liver lobes and portal vein for isoechoic and hypoechoic liver for 50 patients had abnormal liver function test.

Table 4-8 the mean size and SD of the liver lobes and portal vein in respect to liver texture and the difference in means using t-test with the critical p-value shown.

	texture	Mean	*t*-test	*p*-value
Rt. lobe	Fine	12.9±1.5	2.88	0.006
	Coarse	11.5±1.9		
Lt lobe	Fine	5.9±1.3	3.63	0.001
	Coarse	7.7±2.2		
Caudate lobe	Fine	2.3±0.7	0.60	0.55
	Coarse	2.2±0.6		
Portal vein	Fine	1.3±0.3	1.93	0.06
	Coarse	1.5±0.3		

Figure 4-8 a bar plot of the mean liver lobes and portal vein for fine and coarse texture liver for 50 patients had abnormal liver function test.

Table 4-9 the mean size and SD of the liver lobes and portal vein in respect to liver function test level and the difference in means using t-test with the critical p-value shown.

	LFT	Mean	*t*-test	*p*-value
Rt. lobe	Low	12.6±1.8	1.71	0.09
	High	11.6±1.5		
Lt lobe	Low	6.3±1.9	1.98	0.05
	High	7.6±1.3		
Caudate lobe	Low	2.4±0.7	2.23	0.03
	High	1.9±0.2		
Portal vein	Low	1.3±0.3	1.35	0.19
	High	1.5±0.3		

Figure 4-9 a bar plot of the mean liver lobes and portal vein for low and high liver function test level for 50 patients had abnormal liver function test.

Table 4-10 a cross tabulation table of gender versus liver function test

gender	LFT		Total
	Low	High	
Male	37	8	45
Female	4	1	5
Total	41	9	50

Figure 4-10 a bar plot of the gender in respect to liver function test level

Table 4-11 cross-tabulation of patient habit versus liver function test for 50 patients

habit	LFT		Total
	Low	High	
0	16	2	18
1	10	3	13
2	2	3	5
3	13	1	14
Total	41	9	50

Table 4-12 a cross-tabulation of echogenicity versus liver function test for 50 patients

echogenicity	LFT		Total
	Low	High	
Iso	29	2	31
Hypo	12	7	19
Total	41	9	50

Figure 4-11 a bar plot of the echogenecity in respect to liver function test level

Table 4-13 a cross-tabulation of texture versus liver function test for 50 patients

texture	LFT		Total
	Low	High	
Fine	29	4	33
Coarse	12	5	17
Total	41	9	50

Figure 4-12 a bar plot of the texture in respect to liver function test level

Chapter five

Conclusion, Discussion and recommendation

The main objective of this study was to evaluate the sonographic appearance of the liver in case of abnormal liver function test for 50 patients' characterized using ultrasound imaging features versus the liver function test values as high or low.

5.1 Conclusion

In conclusion, this study demonstrates that, most chronic liver disease is identified because of an incidental finding of abnormal liver function tests

(LFTs). The commonest causes of abnormal LFTs are prescribed drugs and alcohol. Significant liver disease is unlikely if alanine aminotransferase is below 100 iu/l and a chronic liver disease screen is negative Hepatic malignant infiltration should be considered with a very high alkaline phosphatase (ALP) in the absence of jaundice. Right hypochondrial pain in the presence of a high ALP is usually due to biliary obstruction. Ultrasound diagnoses of "fatty liver", "cirrhosis", diagnosed by additional signs of portal hypertension, or "cardiac congestion", yield more information. A normal ultrasound does not exclude the presence of fatty liver or cirrhosis.

5.2 Discussion

Hepatomegaly implies significant liver pathology and is an indication for further investigation even in the presence of mild LFT abnormality. Even in an asymptomatic individual a careful history may identify potential causes of abnormal LFTs such as: Alcoholic liver disease, Non-alcoholic steatohepatitis, Chronic hepatitis C or B, Drug, induced hepatotoxicity, Haemochromatosis ,Wilson’s disease, Primary biliary cirrhosis, Autoimmune hepatitis, Acute hepatitis A or E , Primary sclerosing cholangitis.

In this study the researcher obtained the mean and standard deviation of the patient age, size of the liver Rt lobe, Lt lobe, caudate lobe and mean portal vein diameter as 44.2±14.8, 12.4±1.8, 6.5±1.8, 2.3±0.6 and 1.4±0.3 respectively (Table and Figure 4-1), for a sample consisted of 50 patients (45s male and 5 females) Figure 4-2.

The echogenicity of the investigated cases were distributed between isoechoic and hypoechoic which represented 31 and 19 patients respectively (Figure4-3). The sizes of the liver lobes and portal vein diameter for isoechoic and hypoechoic were significantly using t-test at $p = 0.05$ except for caudate lobe as shown in Table 4-2 and Figure 4-6. Similarly texture goes from fine to coarse which represented 33 and 22 respectively. The sizes of the Rt and left lobe of different texture (fine and coarse) using t-test showed significant differences at $p = 0.05$; while the caudate lobe and portal diameter showed inconclusive results using t-test at $p = 0.05$ as shown in Table 4-3 and Figure 4-7.

The liver function test showed that 9 patients had high LFT and 41with low LFT (Figure 4-5). The size of the liver lobes and portal diameter showed a variable degree of differences. The difference was significant at $p = 0.05$ in case of Lt lobe and caudate lobe using t-test while the result were inconclusive incase of RT lobe and portal diameter (Table 4-4 and Figure 4-8). Where gender as shown in earlier male was predominant 45 versus 5 female; therefore generalization of result shown in table 4-5 and Figure 4-9 will be irrational due to dimensionality.

Most of the cases with high LFT had hypoechoic appearance in 77% of the cases while liver with low LFT showed isoechoic appearance and fine texture in 70% of the cases (Table 4-7&8 and Figure 4-10&11).

When ultrasound described a liver as normal, or showing "isoechoic echogenicity" or "fine texture the incidence were (66% normal). When a

definitive ultrasound diagnosis ("cirrhosis", "fatty liver" or "cardiac congestion") was made, the incidence of otherwise normal livers decreased to less than 30%.

5-3 Recommendation

- All patients with cholestatic LFTs should undergo ultrasound scanning to exclude biliary obstruction and liver metastases.
- Even if the bile ducts are not dilated on ultrasound, imaging of the biliary tree is indicated in the presence of cholangitis or pain to exclude common bile duct stones.
- If the ultasound is normal, PBC should be excluded by an antimitochondrial (AMA) antibody specific for PBC.
- A liver biopsy should be considered if the ALP is more than twice the ULN in the presence of a normal ultrasound and negative AMA.
- An endoscopic retrograde cholangiopancreatography (ERCP) is needed to exclude PSC because a liver biopsy may not be diagnostic; this should be considered, especially if there is a history of colitis.
- Large duct obstruction can be excluded non-invasively by magnetic resonance cholangiopancreatography, but resolution is not good enough to exclude abnormalities of the finer intrahepatic ducts so ERCP probably still has a diagnostic role in excluding PSC.

Reference

American Gastroenterological Association. American Gastroenterological Association medical position statement: evaluation of liver chemistry tests. Gastroenterology 2002; 123:1364.

Christoph F. Dietrich, Carla Serra, 2011. Maciej Jedrzejczyk, European Course Book, Ultrasound of the liver .11. 18:21.

Czaja A, Steinberg AS, Saldana M. 1973. Peritoneoscopy-its value in the diagnosis of liver disease. GastrointestEndosc;20:23-5.

Daniel S, Ben-Menachem T, Vasudevan G, et al. 1979. Prospective evaluation of unexplained chronic liver transaminase abnormalities in asymptomatic and symptomatic patients. Am J Gastroenterol; 94:3010.13

Wheeler PG, Theodossi A, Pickford R, Laws J, Knill-Jones RP, Williams R. 1999. Noninvasive techniques in the diagnosis of jaundice-ultrasound and computer. Gut;20:1-9.

Debognie JC, Pauls C, Fievez M, Wibin E. 1981. Prospective evaluation of the diagnostic accuracy of liver ultrasonography. Gut;22:130-5.

Dewbury KC, Clark B. The accuracy of ultrasounMd in the detection of cirrhosis of the liver. BrJ Radiol 1979;52:945-8.

Fraser A, Longnecker MP, Lawlor DA. 2007. Prevalence of elevated alanine aminotransferase among US adolescents and associated factors: NHANES 1999-2004. Gastroenterology; 133:1814.

Hultcrantz R, Glaumann H, Lindberg G, Nilsson LH. 1986. Liver investigation in 149 asymptomatic patients with moderately elevated activities of serum aminotransferases. Scand J Gastroenterol; 21:109.

Ioannou GN, Boyko EJ, Lee SP. 2006. The prevalence and predictors of elevated serum aminotransferase activity in the United States in 1999-2002. Am J Gastroenterol; 101:76.

Jane C and Maggie B, 2002. Clinical Medicine CME Gastroenterology, How to respond to abnormal liver function tests JRCPL;2:406–9.

Joseph AEA, Dewbury KC, McGuire PG. Alcohol in the detection of chronic liver disease. (The'bright' liver.) BrJ Radiol 1979;52:184-8.

Katkov WN, Friedman LS, Cody H, 1991. Elevated serum alanine aminotransferase levels in blood donors: the contribution of hepatitis C virus. Ann Intern Med; 115:882.

Kundrotas LW, Clement DJ. 1993. Serum alanine aminotransferase (ALT) elevation in asymptomatic US Air Force basic trainee blood donors. Dig Dis Sci; 38:2145.

Lawson TL. 1977. Hepatic abscess: ultrasound as an aid to diagnosis. DigDisSci;22:33-7.

Meek DR, Mills PR, Gray HW, Duncan JG, Russell RI, McKillop JH. 1984. Acomparison ofcomputer tomography, ultrasound and scintigraphy in the diagnosis of alcoholic liver disease. BrJ Radiol;57:23-7.

Piton A, Poynard T, Imbert-Bismut F. 1998. Factors associated with serum alanine transaminase activity in healthy subjects: consequences for the definition of normal values, for selection of blood donors, and for patients with chronic hepatitis C. MULTIVIRC Group. Hepatology; 27:1213.

Prati D, Taioli E, Zanella A. 2002. Updated definitions of healthy ranges for serum alanine aminotransferase levels. Ann Intern Med; 137:1.

Pratt DS, Kaplan MM. 2000. Evaluation of abnormal liver-enzyme results in asymptomatic patients. N Engl J Med; 342:1266.

Scott WW, Sanders RC, Siegelman SS. 1980. Irregular fatty infiltration of the liver-diagnosticdilemuna. AJR;134:67-71.

Taylor KJW, Rosenfield AT. 1977. Grey scale ultrasonography in the differential diagnosis of obstructive jaundice. Arch Surg;112:820-5.

Theodossi A, Spiegelhalter D, Portmann B, Eddelston AWF, Williams R. 1983. The value of clinical, biochemical, ultrasound and liver biopsy data in assessing patients with liver disease. Liver;3:315-26.

Appendices (2)

Summary of the cases collected data:

age	gender	habit	echogenicity	texture	Rt_lobe	Lt_lobe	C_lobe	Portal_vein	LFT
35	1	1	1	1	13.5	4.3	2.6	0.5	1
55	1	3	2	2	13.5	4.8	2.6	1.5	1
37	1	3	1	1	12.6	7.5	1.7	0.3	1
23	1	1	1	1	13	7.3	1.3	1.3	1
82	1	0	1	1	16.4	5.9	3.7	1.4	1
65	1	0	1	1	11.7	6.5	1.9	1.6	1
45	1	1	1	1	13.9	5	3.2	1.4	1
60	1	1	1	1	13	6.4	3.1	1.5	1
31	1	2	2	1	10.9	7.5	1.9	1.5	2
22	1	1	2	2	11	7.5	1.8	1.6	2
40	1	1	1	1	12.2	5	3	1.3	1
45	1	2	1	1	13.3	6.8	2.7	1.4	1
42	2	0	1	1	12.1	5.5	2.1	1.5	1
54	1	2	2	2	11.2	6.7	2.1	1.8	2
17	2	0	1	1	12	5.8	1.7	1.5	2
55	1	0	2	2	8.6	10.9	3.1	1.1	1
30	1	0	2	2	10.6	7.8	2	1.8	2
28	1	1	1	1	14.1	4.7	1.8	1.3	1
48	1	3	2	2	11.1	6.2	1.8	1.5	1
21	1	1	1	1	14.4	4.3	2	1	1
50	1	3	1	1	12.6	5.1	2.6	1.5	1
28	1	3	1	1	14.2	8.1	3	1.6	1
64	1	0	1	1	12.1	5.5	2.1	1.2	1
26	1	0	1	1	13.1	4.2	1.9	1	1
39	1	3	1	1	10	3.7	2.3	1.5	1

46	1	0	1	1	15.2	5.9	3.8	1.2	1
35	1	1	1	1	14.9	3.4	1.4	1.2	1
42	1	3	2	2	15.3	10.7	1.6	0.7	2
30	1	1	1	1	11.1	7.3	2	1.5	2
48	2	0	2	2	13	9.5	1.9	1.9	1
55	1	3	2	2	13.5	4.8	2.6	1.5	1
23	1	1	1	1	13	7.3	1.3	1.3	1
65	1	0	1	1	11.7	6.5	1.9	1.6	1
60	1	1	1	1	13	6.4	3.1	1.5	1
48	1	3	2	2	11.1	6.2	1.8	1.5	1
37	1	3	1	1	12.6	7.5	1.7	0.3	1
53	1	3	2	2	13.4	4.8	2.6	1.5	1
77	1	0	1	1	16.5	5.9	3.7	1.4	1
35	1	2	2	1	10.9	7.5	1.9	1.5	2
44	2	0	1	1	12	5.5	2.1	1.5	1
60	1	0	2	2	8.5	10.7	3.2	1.3	1
54	1	3	1	1	12.4	5.1	2.6	1.5	1
45	2	0	2	2	13.1	9.5	1.9	1.9	1
62	1	0	1	1	11.6	6.5	1.9	1.6	1
46	1	3	2	2	11.2	6.2	1.8	1.5	1
30	1	0	1	1	13.3	4.2	1.9	1	1
25	1	1	2	2	11.02	7.5	1.8	1.6	2
57	1	0	2	2	8.5	10.9	3.1	1.1	1
45	1	3	2	2	11.2	6.2	1.8	1.5	1
45	1	2	1	1	13.3	6.8	2.7	1.4	1

Appendices (3):RT LOBE and PV

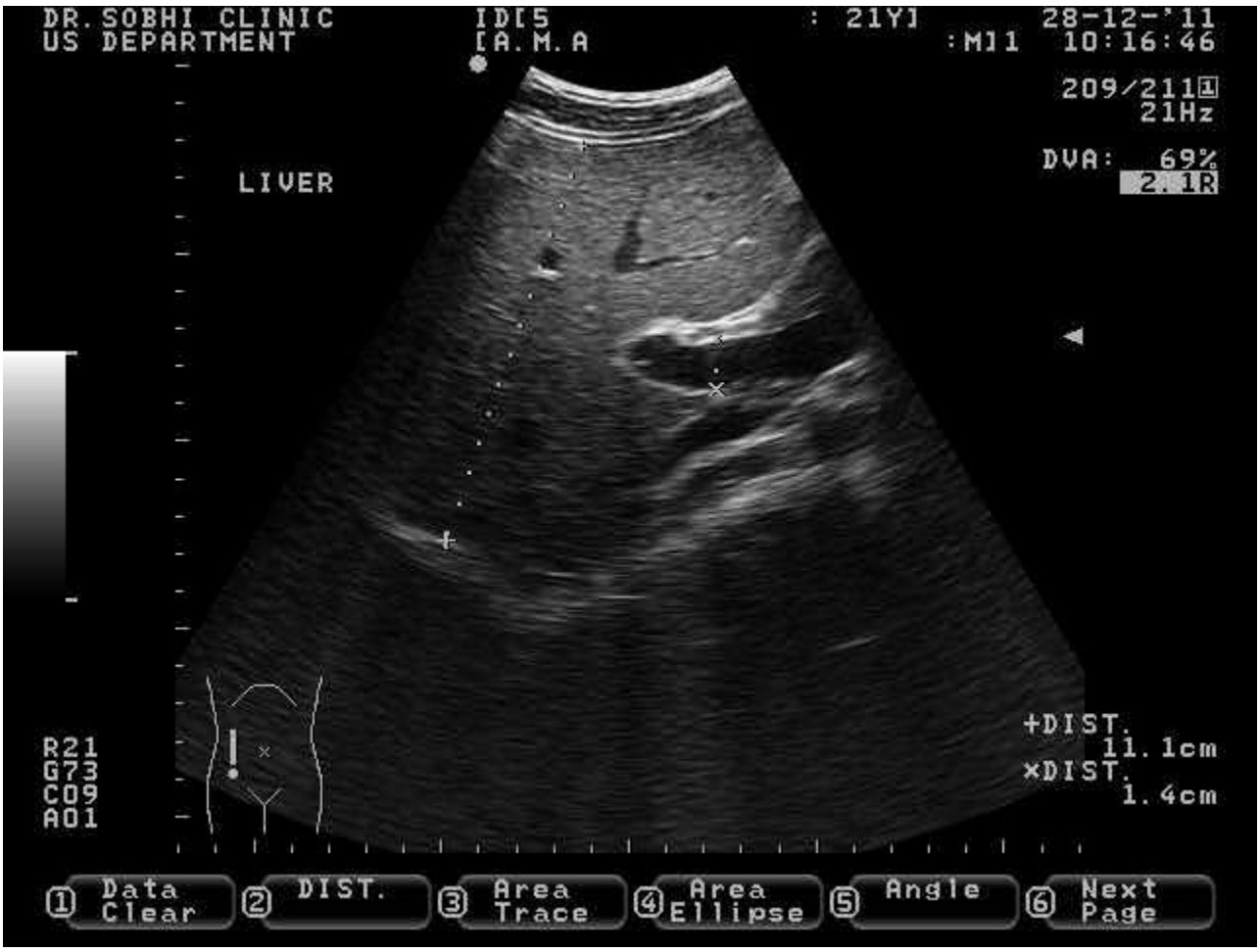

Appendices (4): RT LOBE

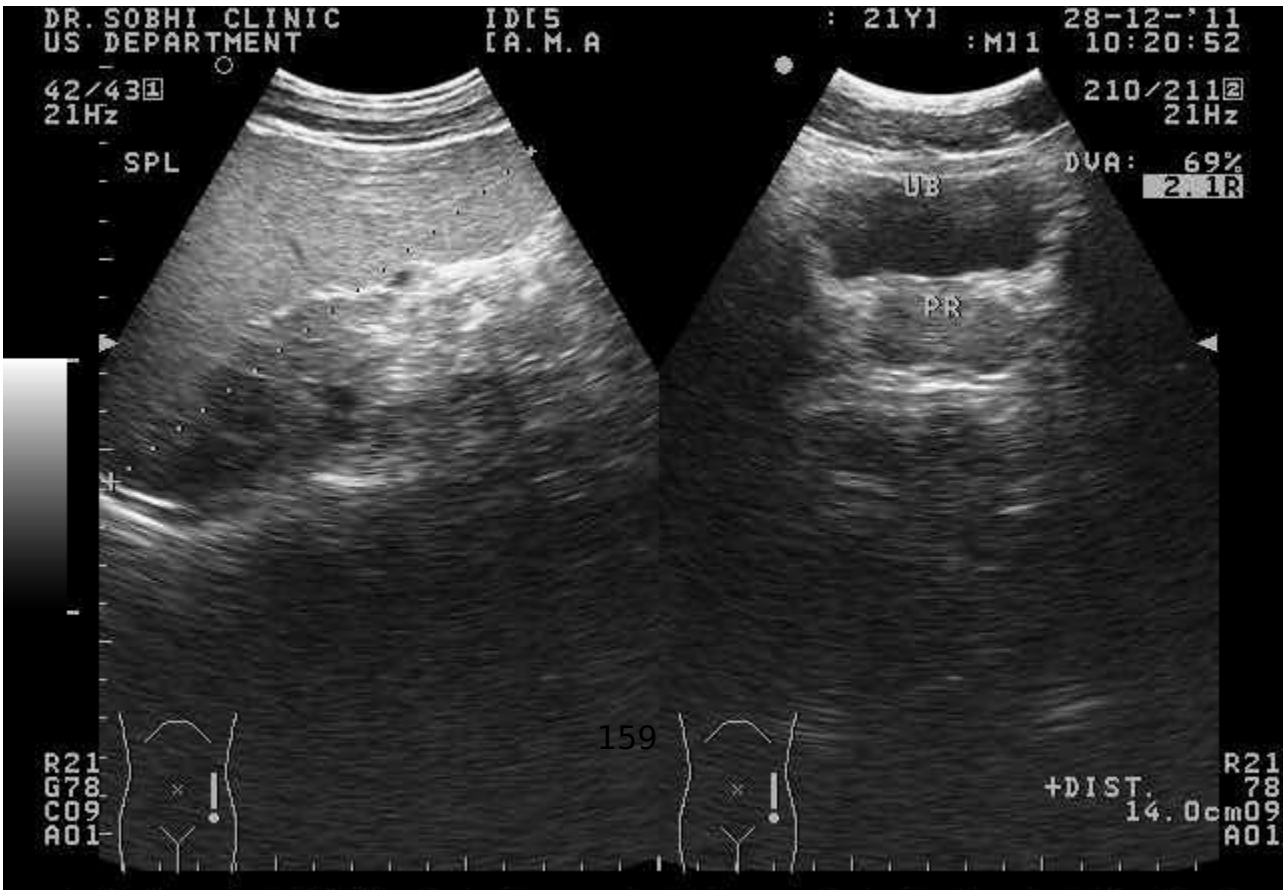

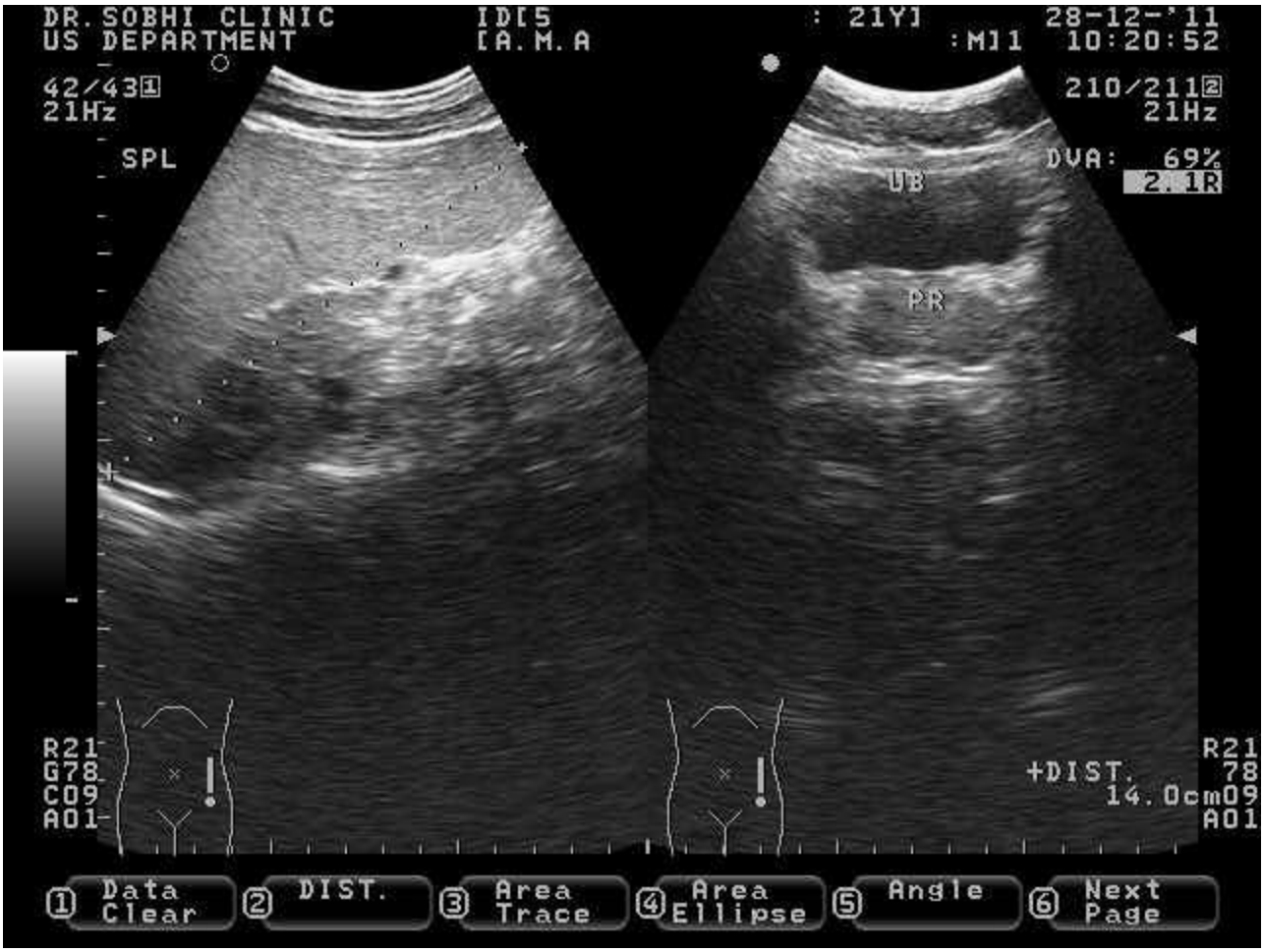
DR. SOBHI CLINIC
US DEPARTMENT
ID[5
[A.M.A
: 21Y]
:M11
28-12-'11
10:20:52
42/43
21Hz
SPL
210/211
21Hz
DVA: 69%
2.1R
UB
PR
R21
G78
C09
A01
+DIST.
14.0cm
R21
78
09
A01
1 Data Clear
2 DIST.
3 Area Trace
4 Area Ellipse
5 Angle
6 Next Page

Appendices (5): caudate lobe

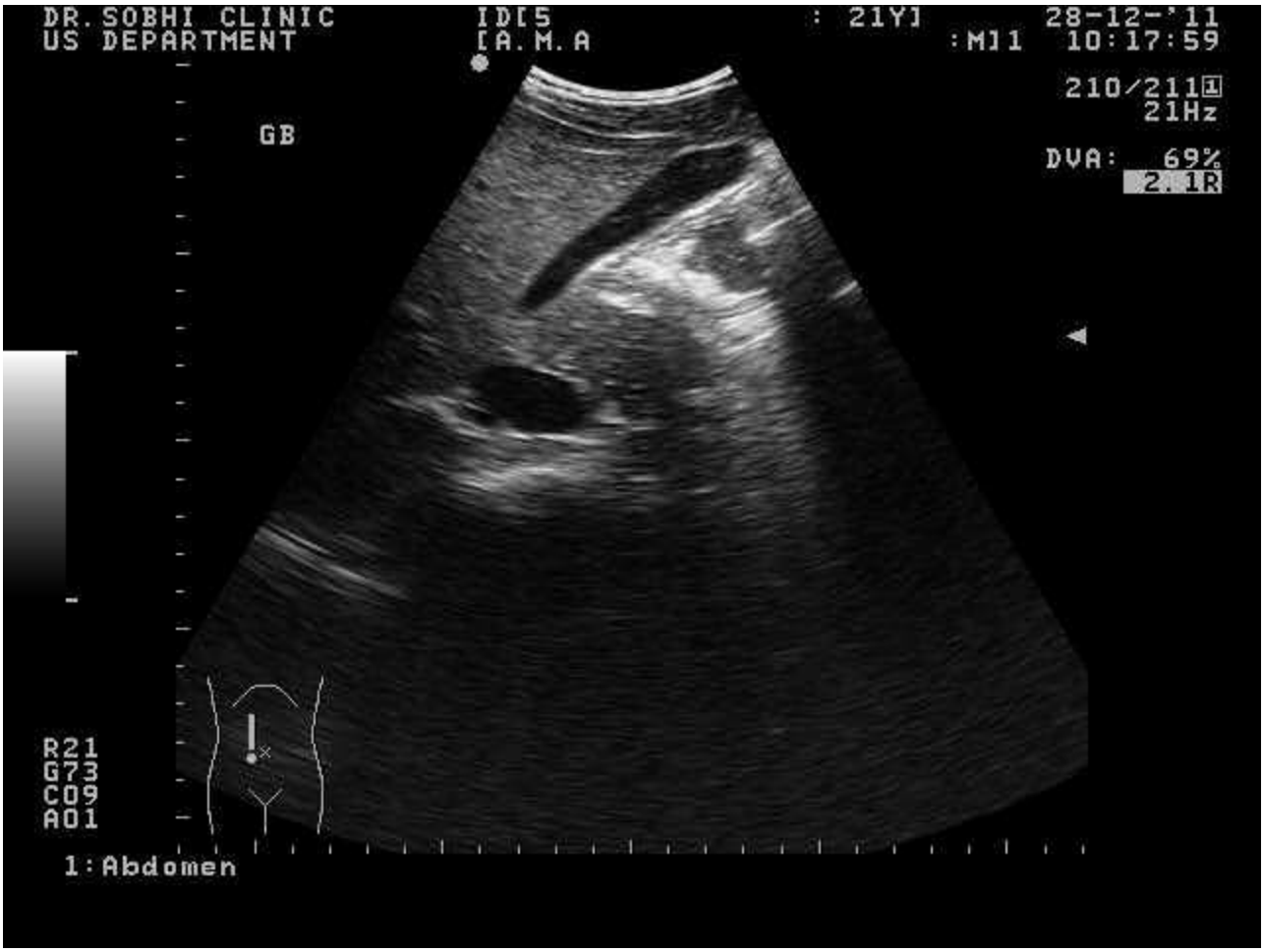
DR. SOBHI CLINIC
US DEPARTMENT
ID[5
[A.M.A
: 21Y]
:M11
28-12-'11
10:17:59
210/211
21Hz
DVA: 69%
2.1R
GB
R21
G73
C09
A01
1:Abdomen

Appendices (6): RT Lobe + ascites

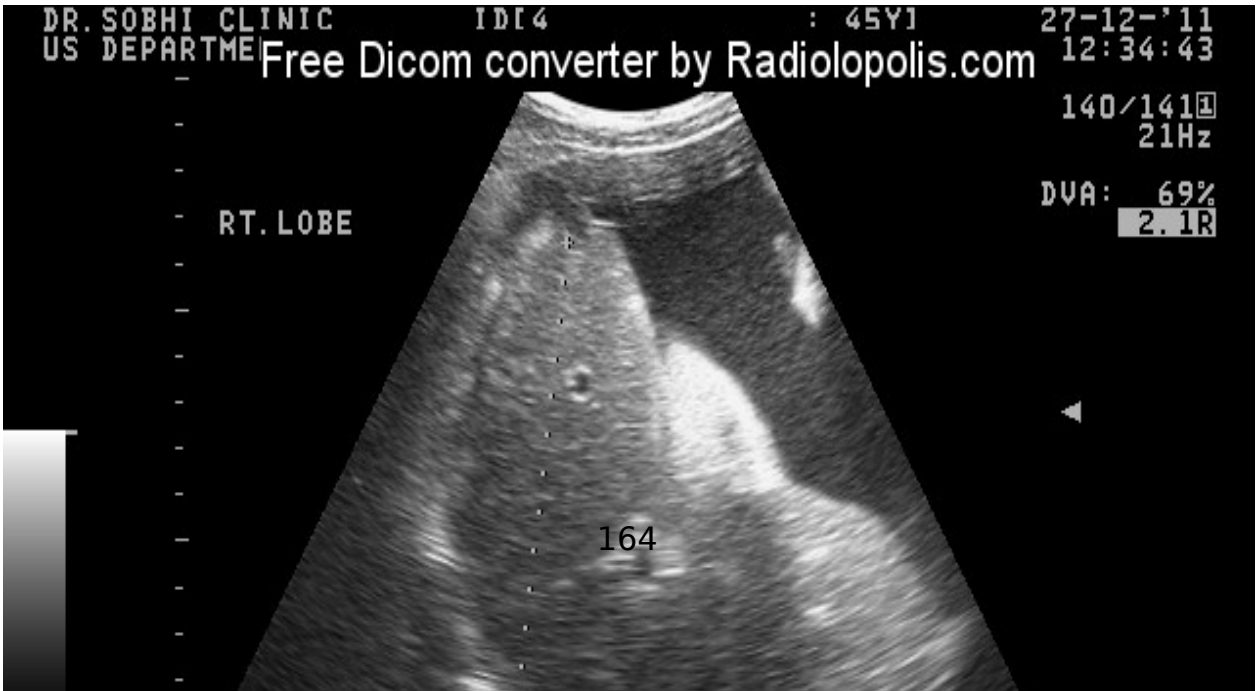

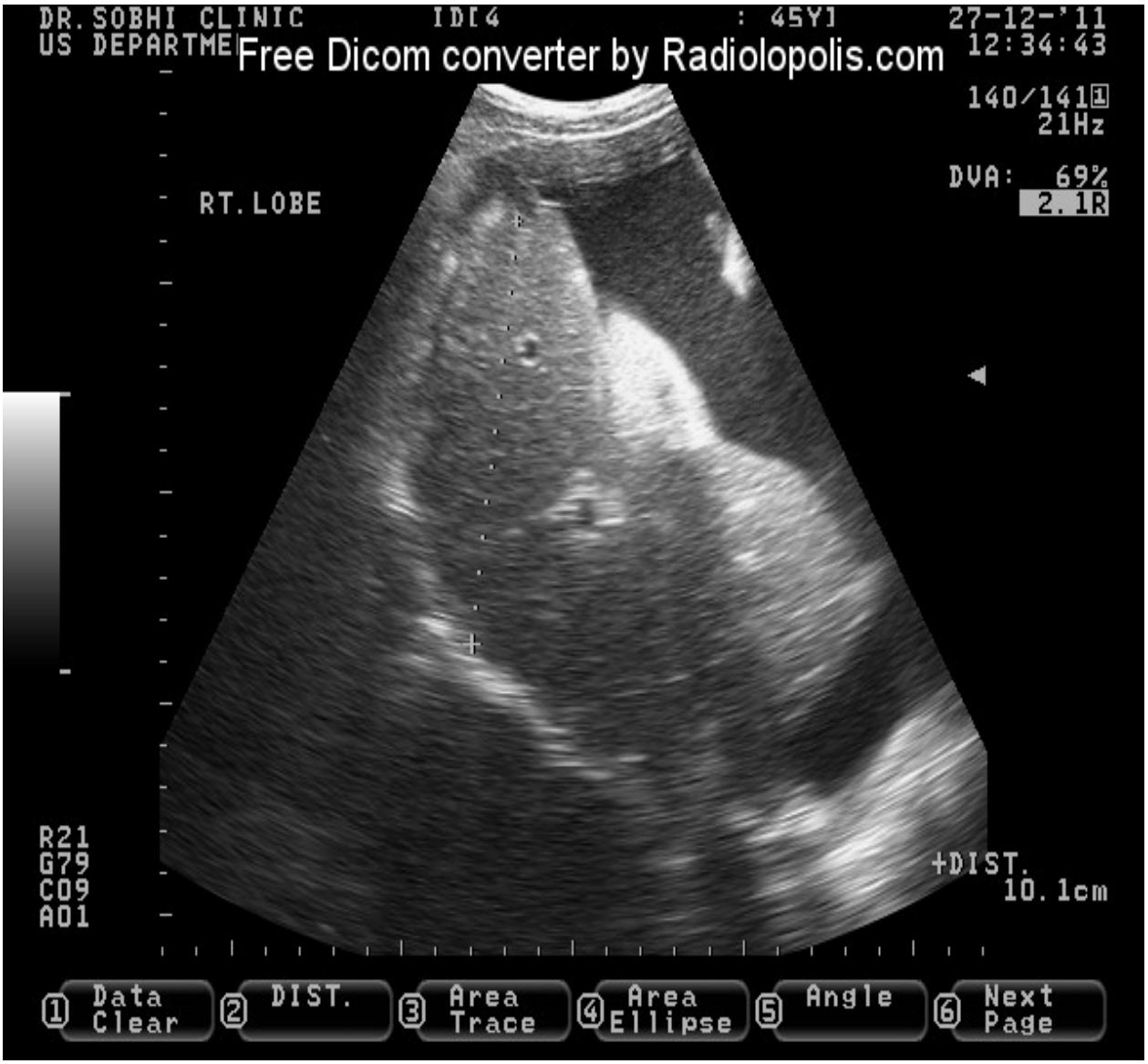
DR. SOBHI CLINIC
US DEPARTME
IDI4
: 45Y]
27-12-'11
12:34:43
Free Dicom converter by Radiolopolis.com
140/141
21Hz
DVA: 69%
2.1R
RT. LOBE
R21
G79
C09
A01
+DIST.
10.1cm
1 Data Clear
2 DIST.
3 Area Trace
4 Area Ellipse
5 Angle
6 Next Page

Appendices (7):PV

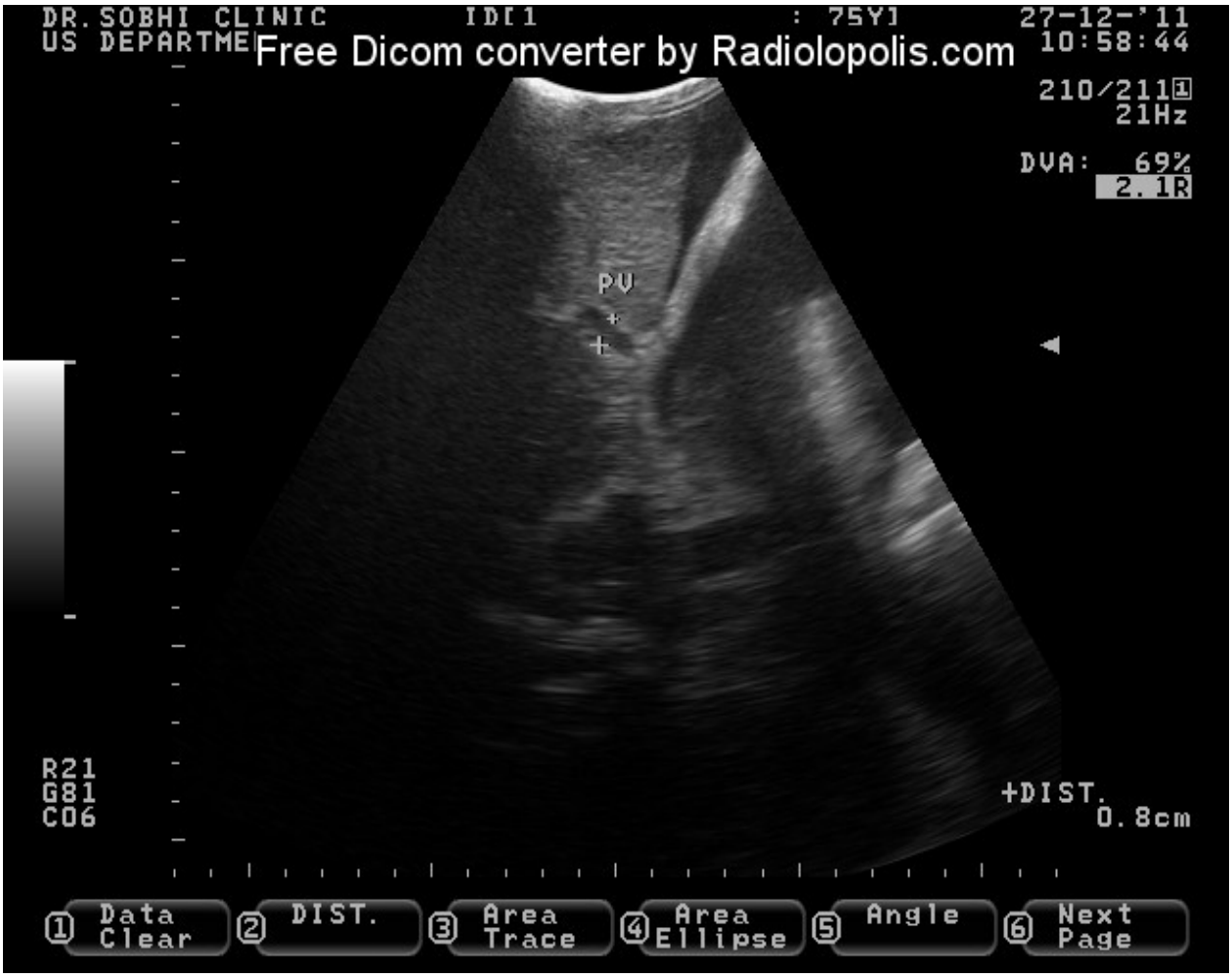
DR. SOBHI CLINIC
US DEPARTME
ID[1
: 75Y]
27-12-'11
10:58:44
Free Dicom converter by Radiolopolis.com
210/211
21Hz
DVA: 69%
2.1R
PV
R21
G81
C06
+DIST.
0.8cm
1 Data Clear
2 DIST.
3 Area Trace
4 Area Ellipse
5 Angle
6 Next Page

Appendices (8):RT Lobe

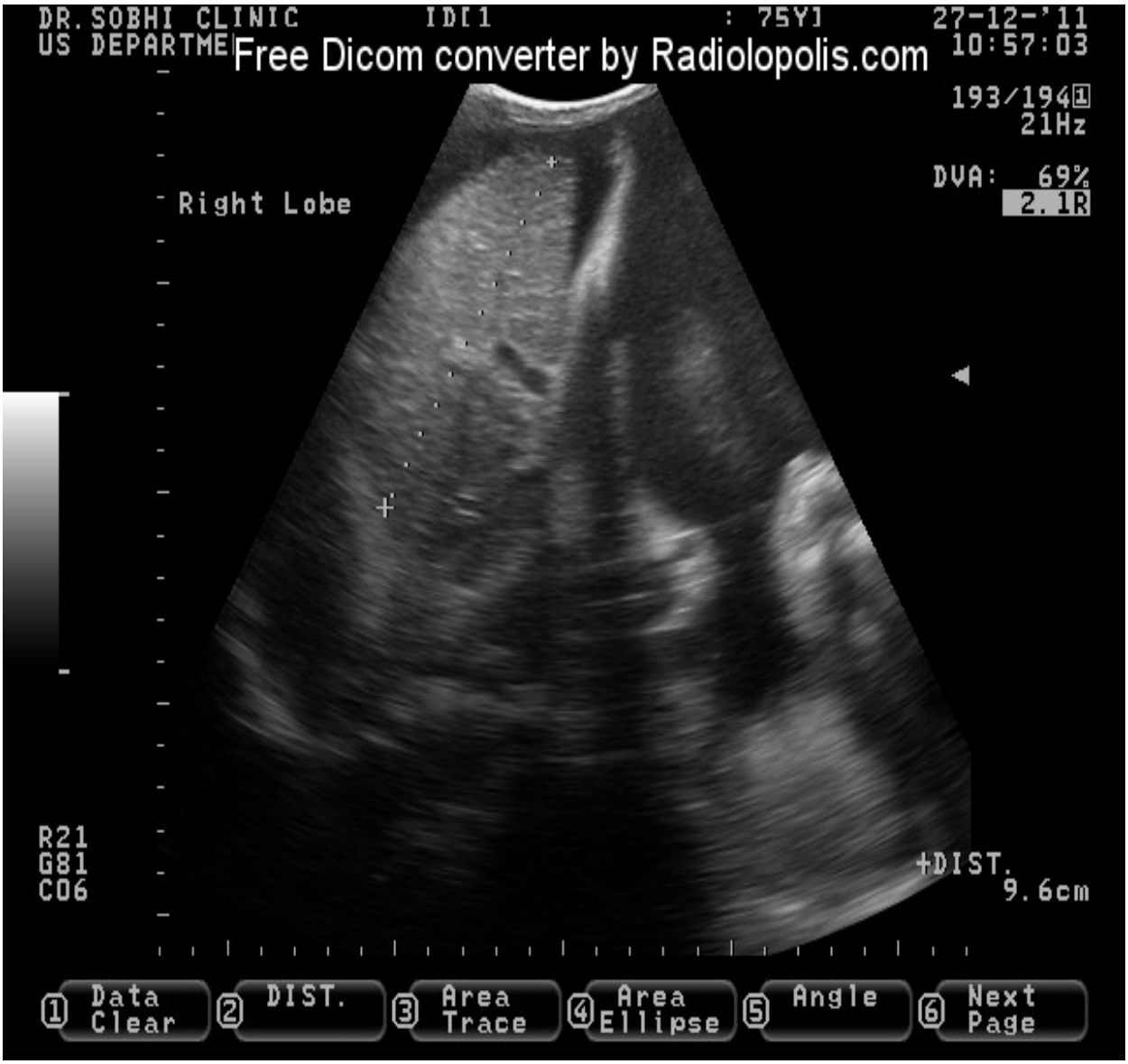
DR.SOBHI CLINIC
US DEPARTME
IDI1
: 75YI
27-12-'11
10:57:03
Free Dicom converter by Radiolopolis.com
193/194
21Hz
DVA: 69%
2.1R
Right Lobe
R21
G81
C06
+DIST.
9.6cm
1 Data Clear
2 DIST.
3 Area Trace
4 Area Ellipse
5 Angle
6 Next Page

Appendices (9): RT Lobe

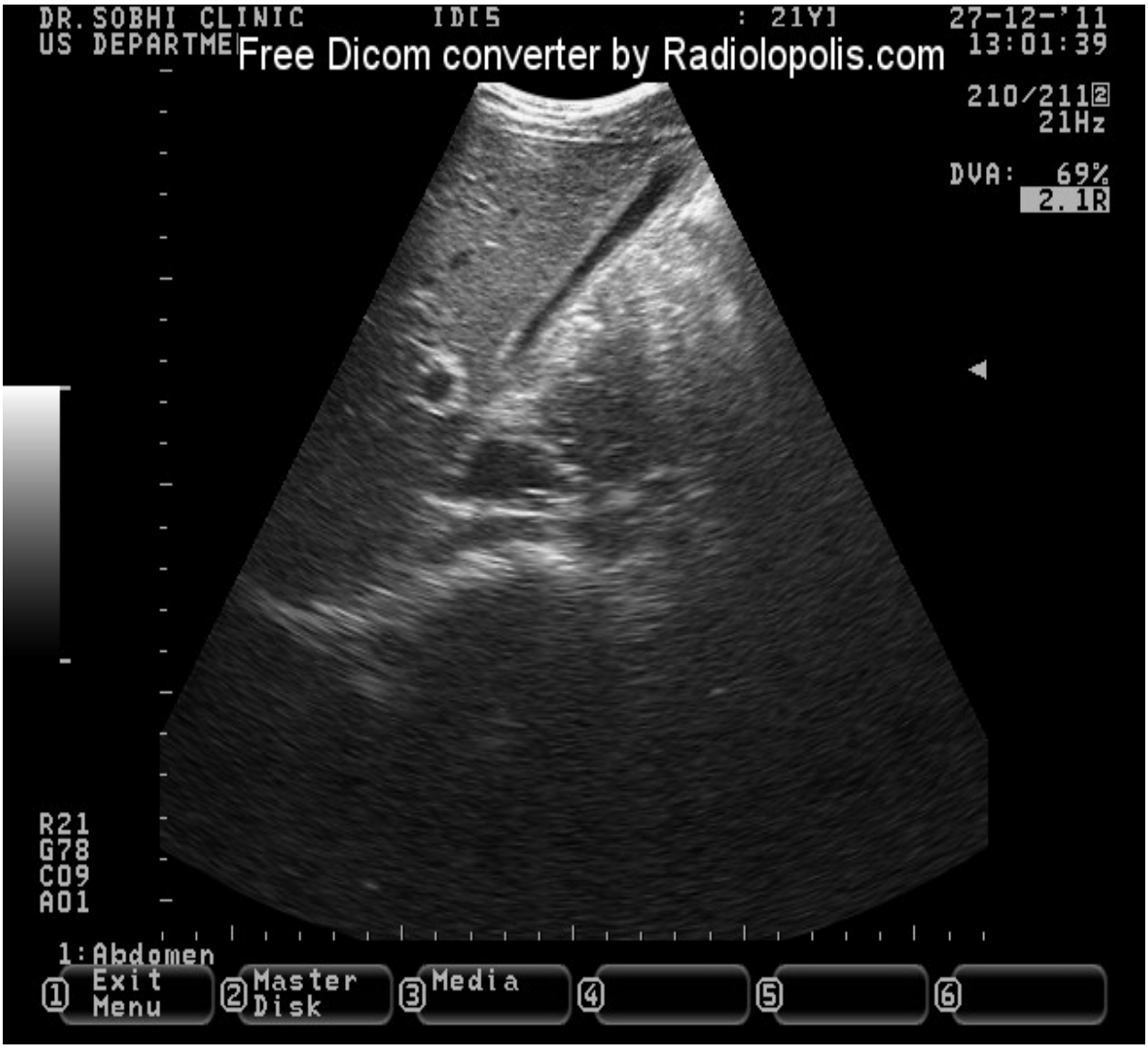

Appendices (10): caudate Lobe

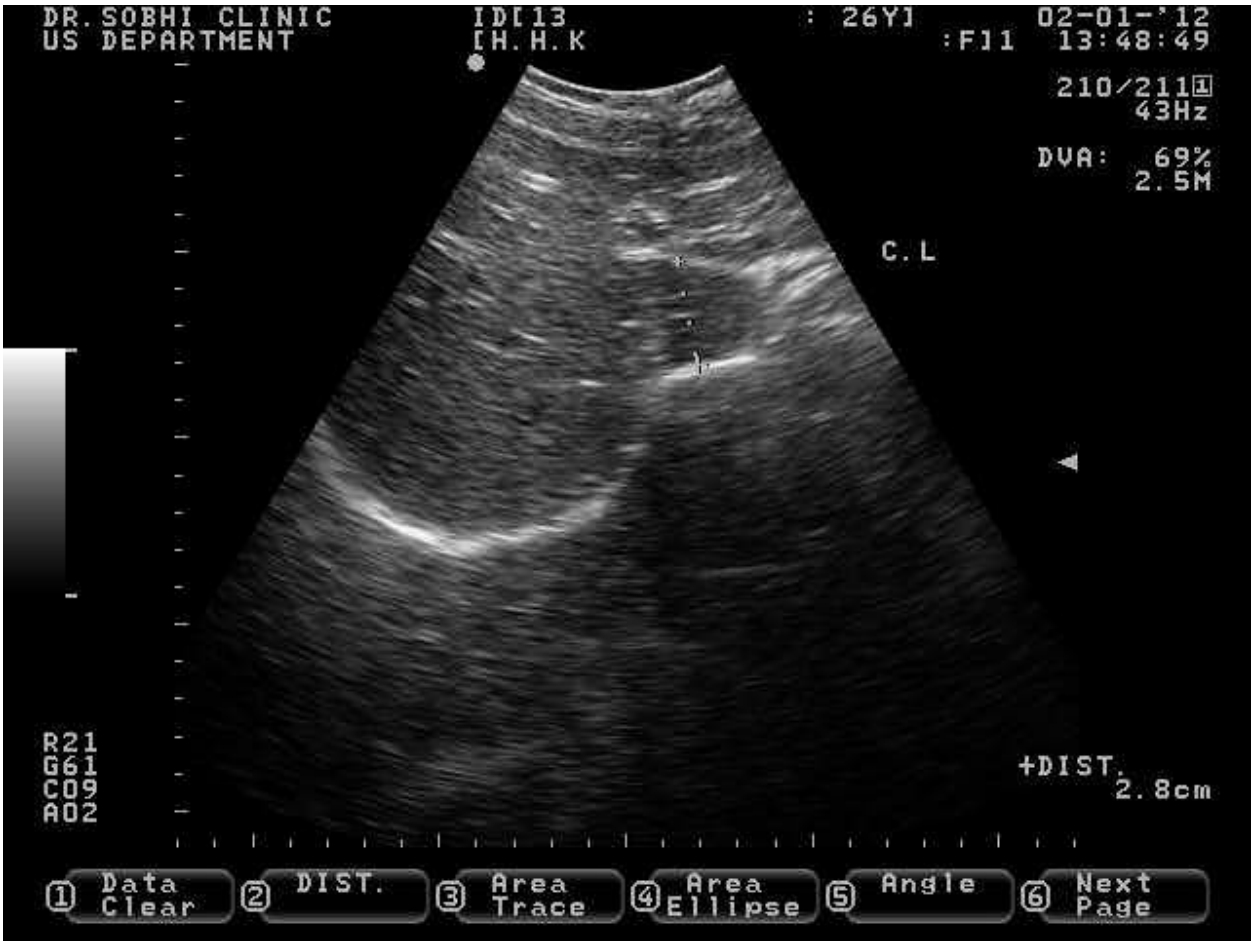

Appendices (11):PV

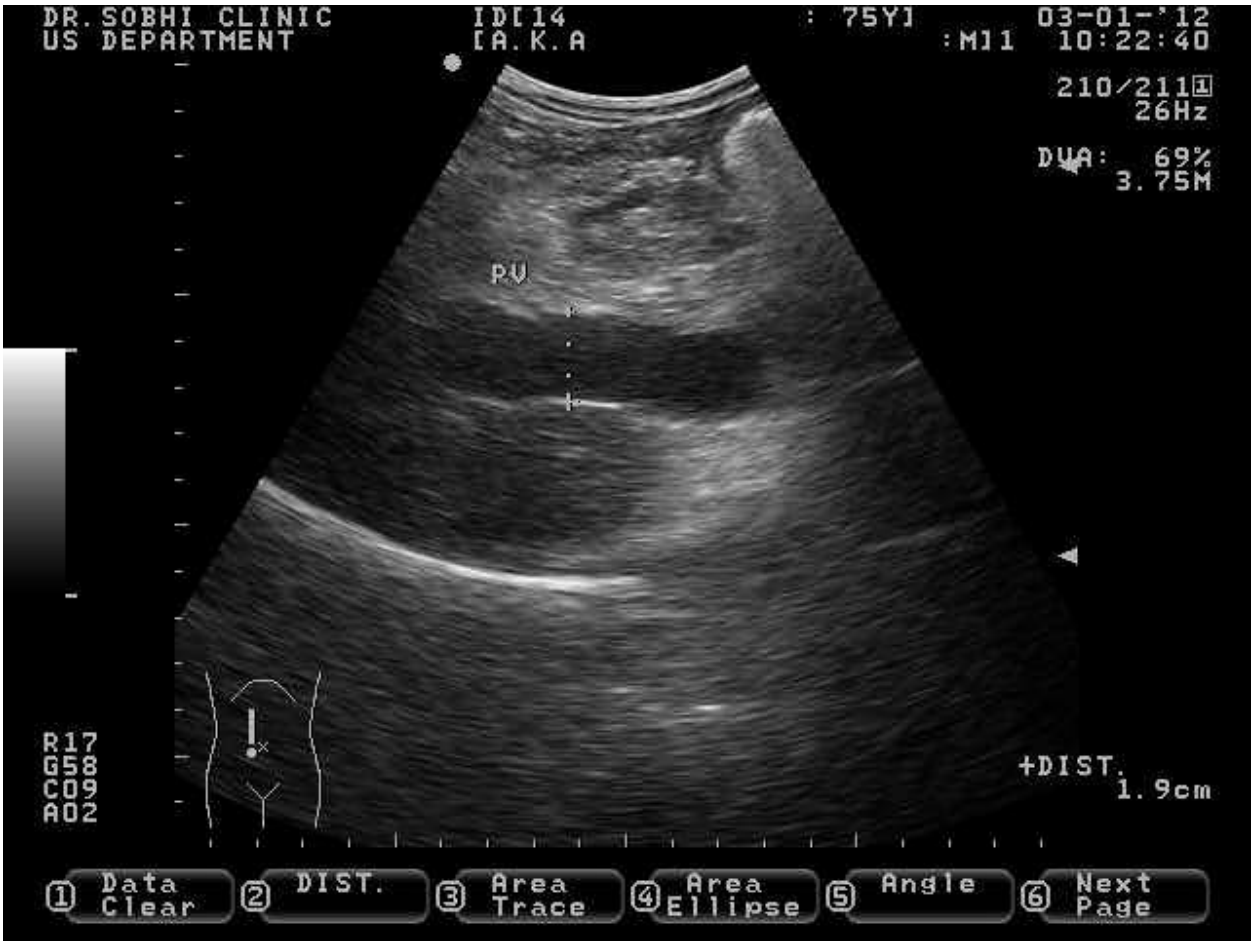

Appendices (12):caudate lobe

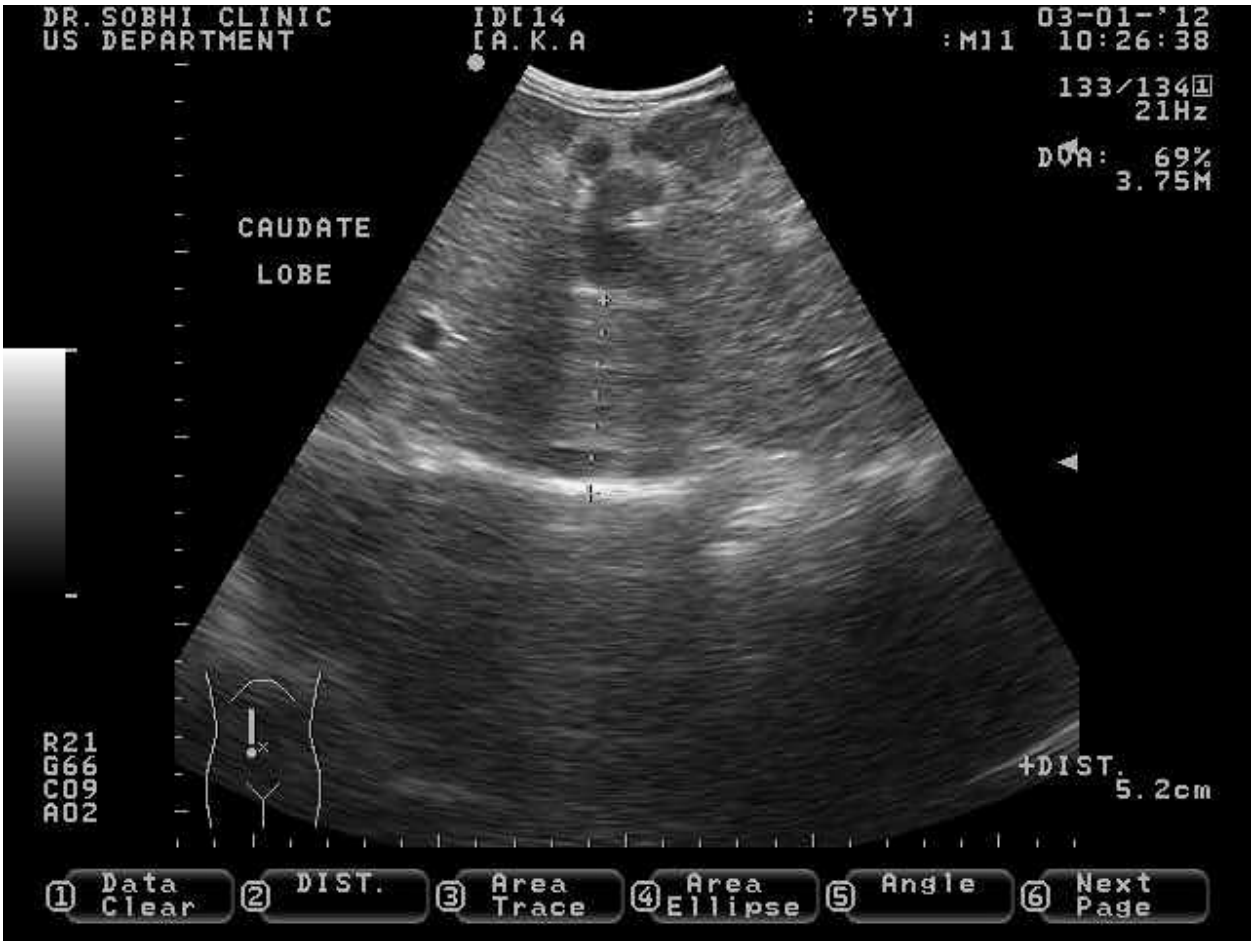

Appendices (13):RT Lobe

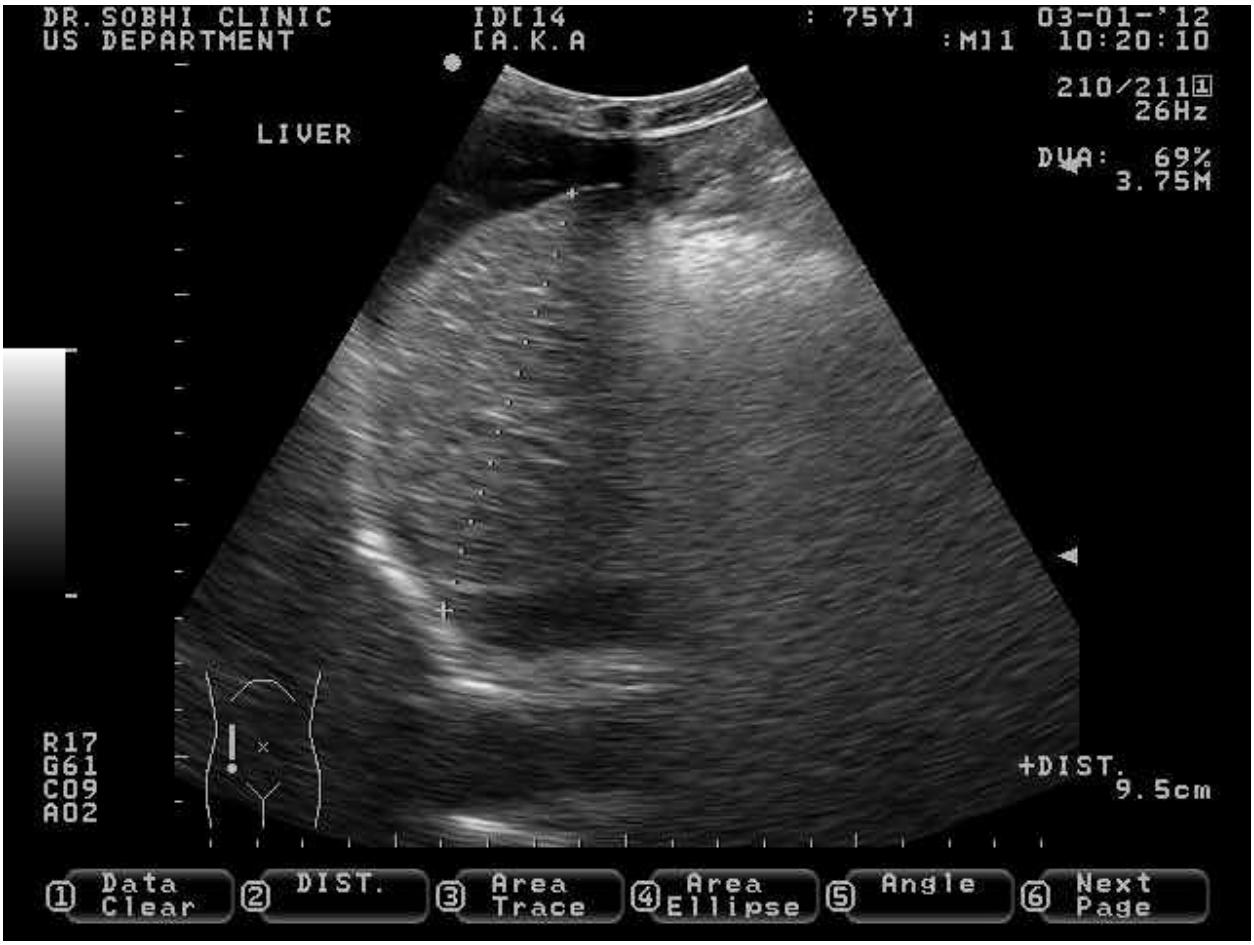

Appendices (14):RT Lobe mass

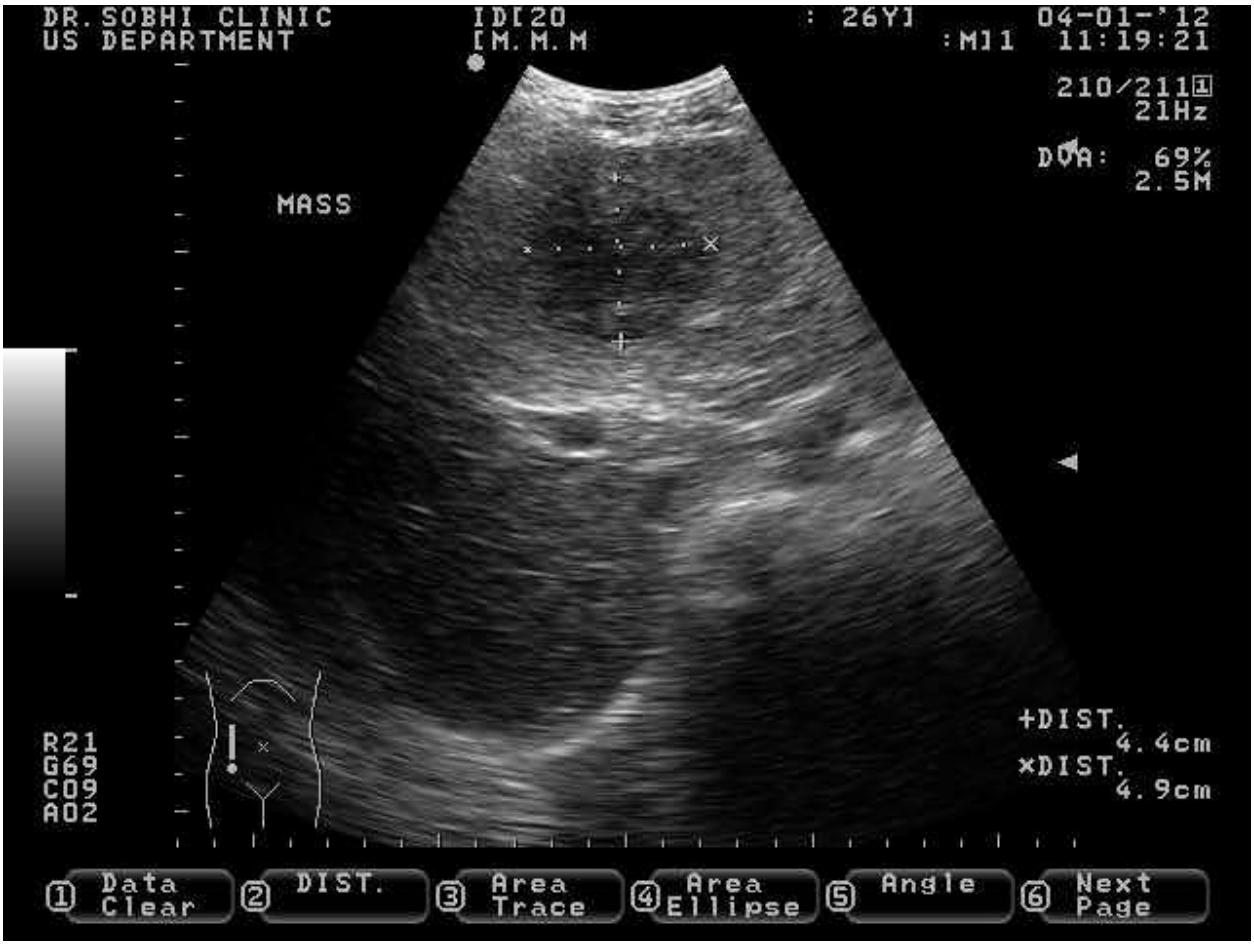

Appendices (15): Metastases

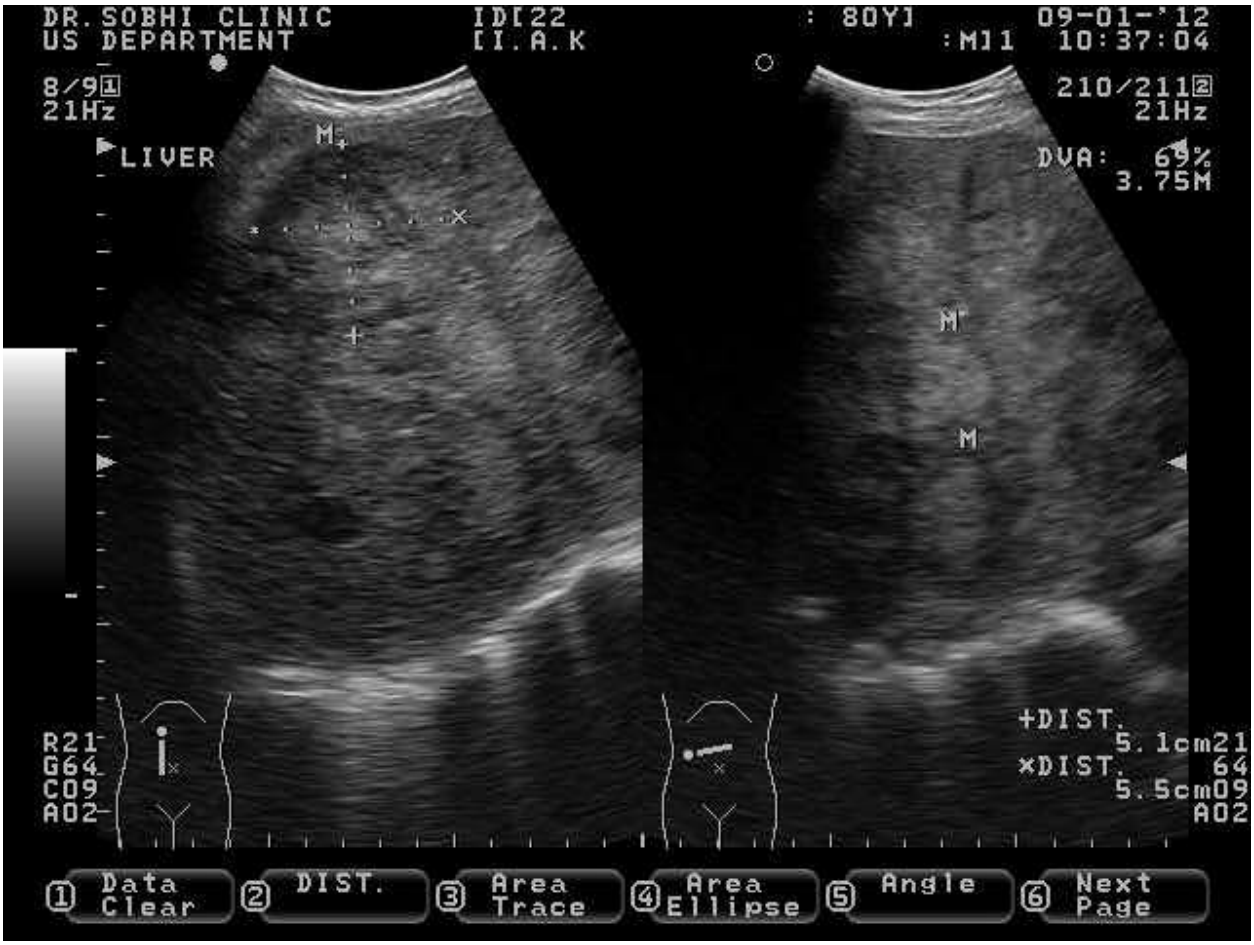

Appendices (16):LT Lobe and Cuadate lobe

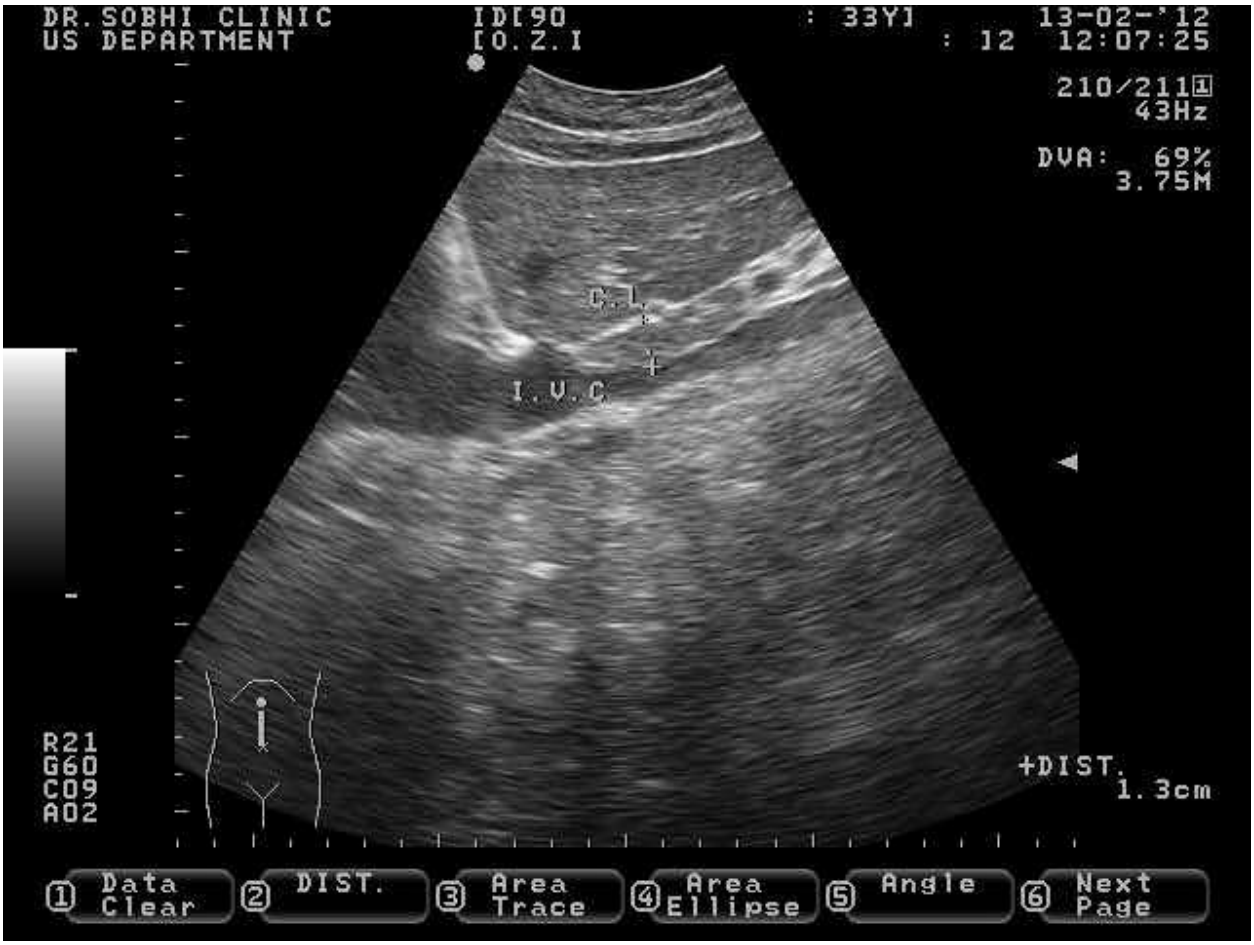

Appendices (17):LT Lobe , Caudate Lobe and ascites:

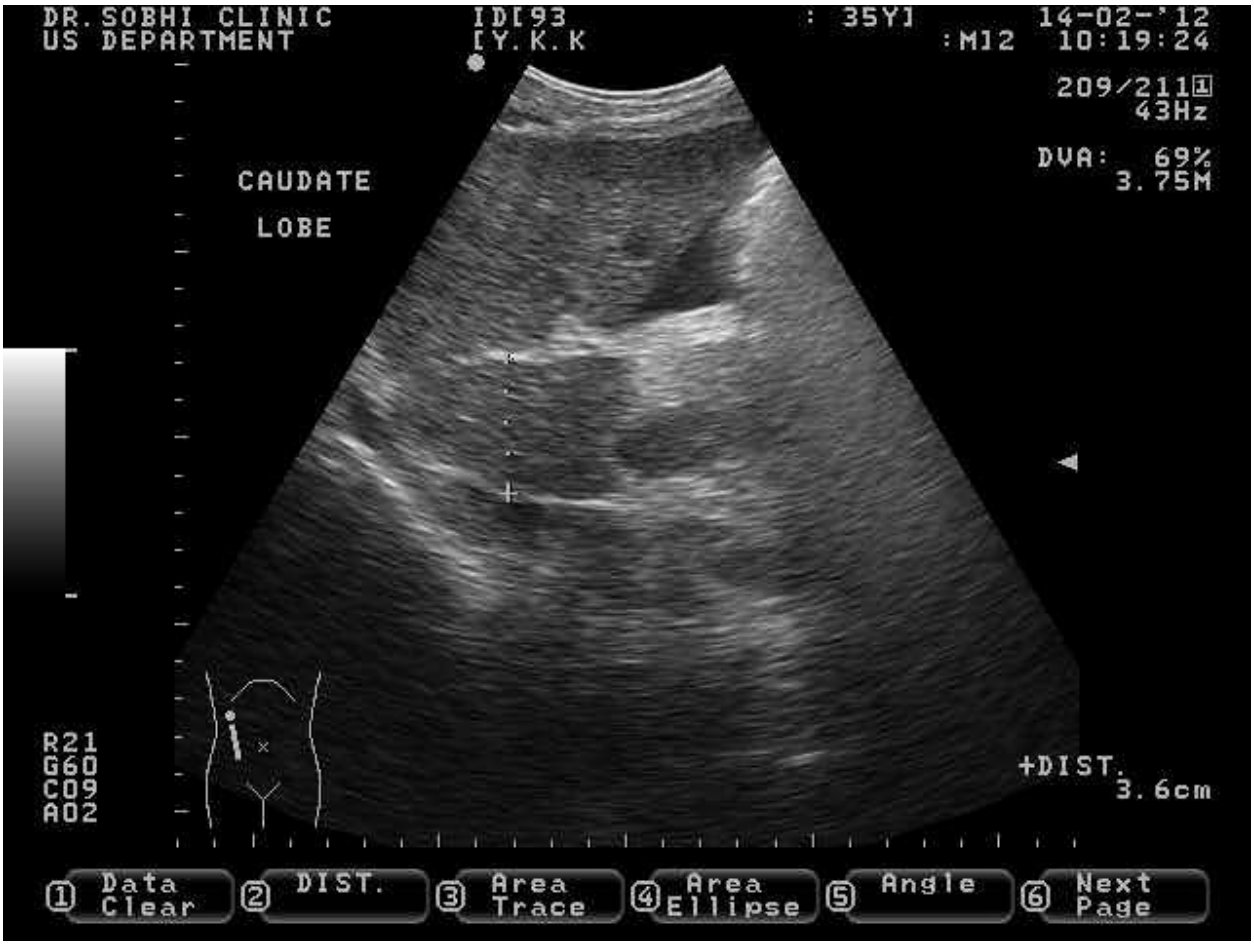

Appendices (18): shrunken liver with ascites

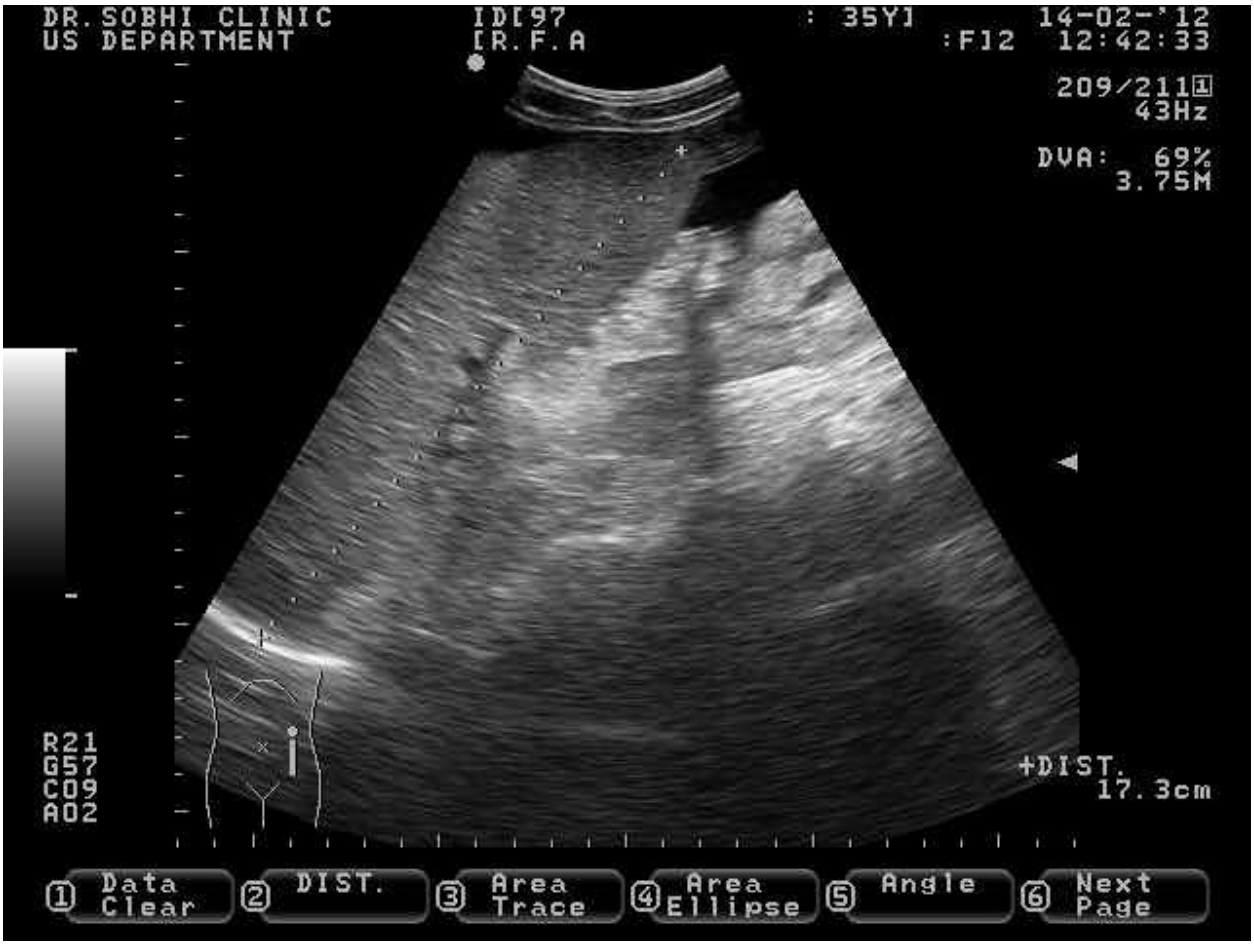

Appendices (19):PVH

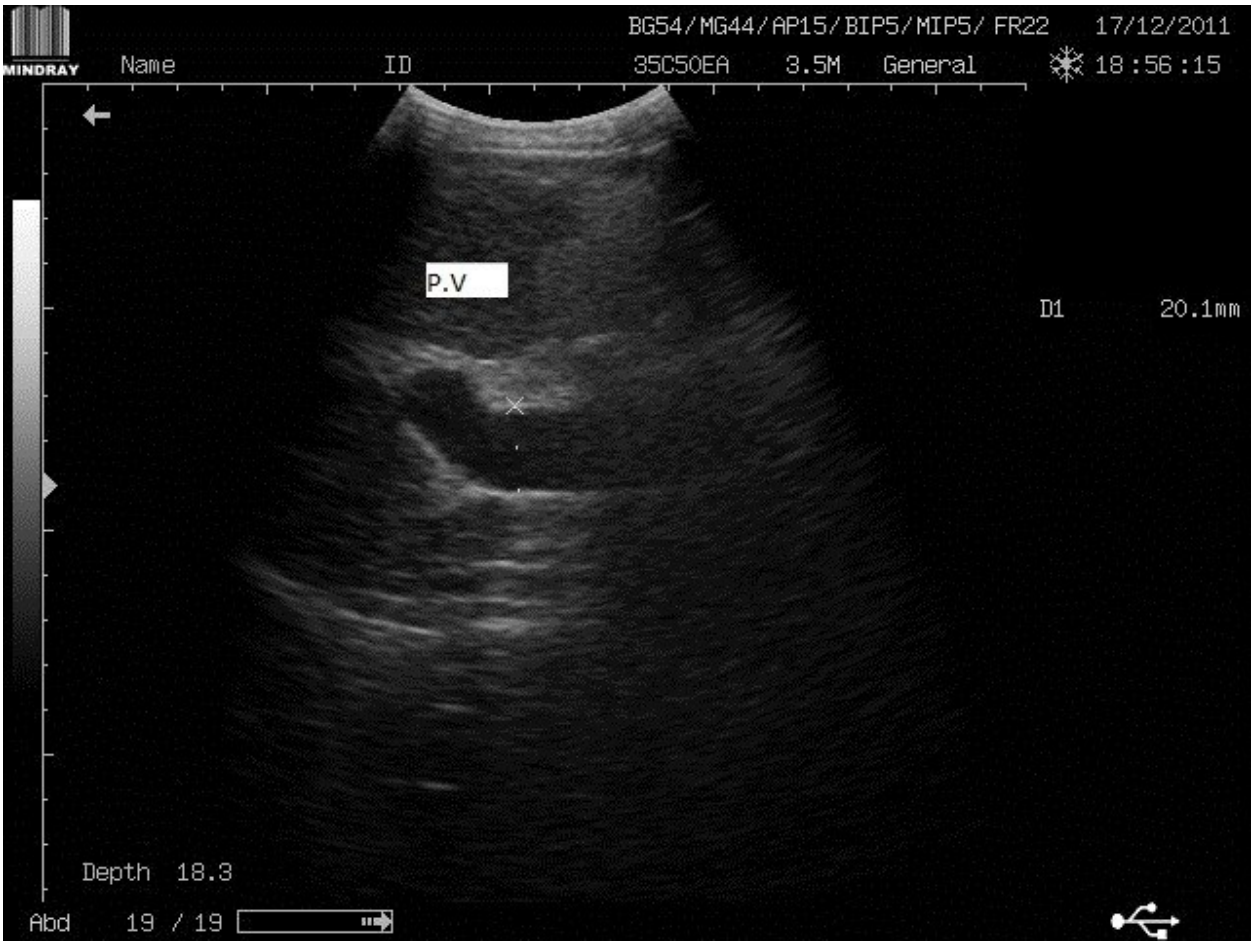

Appendices (20):LT Lobe

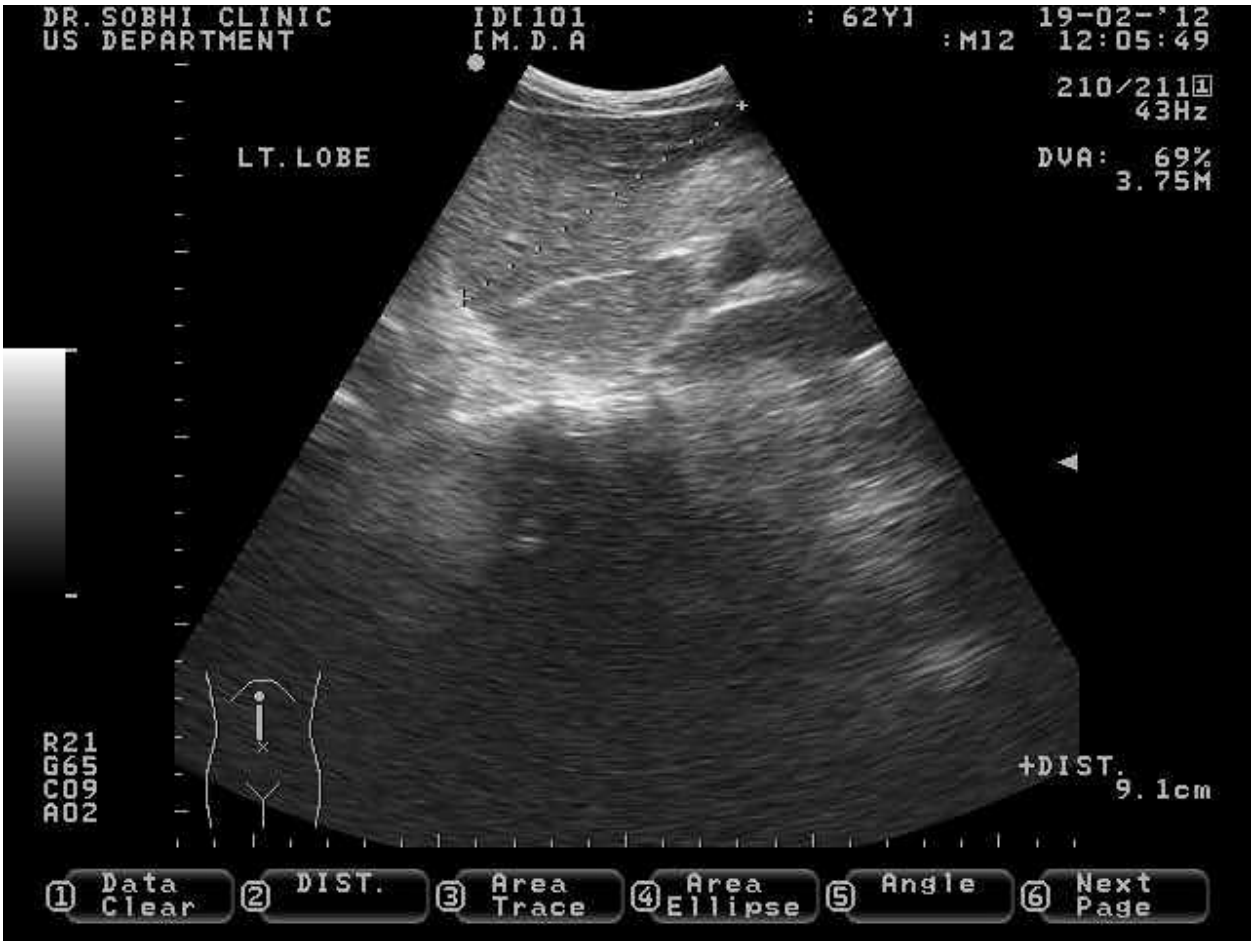
DR. SOBHI CLINIC
US DEPARTMENT
ID[101
[M.D.A
: 62Y]
:M12
19-02-'12
12:05:49
210/211
43Hz
LT. LOBE
DVA: 69%
3.75M
R21
G65
C09
A02
+DIST.
9.1cm
1 Data Clear
2 DIST.
3 Area Trace
4 Area Ellipse
5 Angle
6 Next Page